ZooKeys 996: 1–18 (2020)
doi: 10.3897/zookeys.996.54602
https://zookeys.pensoft.net

RESEARCH ARTICLE

A peer-reviewed open-access journal
ZooKeys
Launched to accelerate biodiversity research

A report of a new species and new record of *Cadlina* (Nudibranchia, Cadlinidae) from South Korea

Thinh Dinh Do[1*], Dae-Wui Jung[1,2*], Hyun-Jong Kil[3], Chang-Bae Kim[1]

1 *Department of Biotechnology, Sangmyung University, Seoul 03016, South Korea* **2** *Korea Marine-Bio Lab, Daejeon 34130, South Korea* **3** *Genetic Resources Information Center, National Institute of Biological Resources, Incheon 22689, South Korea*

Corresponding author: Chang-Bae Kim (evodevo@smu.ac.kr)

Academic editor: N. Yonow | Received 22 May 2020 | Accepted 19 October 2020 | Published 24 November 2020

http://zoobank.org/8315A0E8-D820-454C-B2AA-5C6B5D003D86

Citation: Do TD, Jung D-W, Kil H-J, Kim C-B (2020) A report of a new species and new record of *Cadlina* (Nudibranchia, Cadlinidae) from South Korea. ZooKeys 996: 1–18. https://doi.org/10.3897/zookeys.996.54602

Abstract

Of the four species in the genus *Cadlina* present in the northwestern Pacific region, *C. japonica* has been the only species recorded from South Korea. For the purpose of investigating *Cadlina* in Korean waters, specimens were collected from the Korean East Sea (Sea of Japan) by scuba diving. The radula and morphology of these specimens were examined by stereoscopic and scanning electron microscopy. Based on morphology, three species were identified in Korean waters, including the new species, *Cadlina koreana* **sp. nov.**, *C. umiushi* (first record in South Korea), and *C. japonica*. *Cadlina koreana* **sp. nov.** somewhat resembles *C. umiushi* but differs in both its morphology as well as the structure of its radula. The background color of *Cadlina koreana* **sp. nov.** is translucent white, tubercles on the dorsum are opaque white and the yellow marginal band is absent. The radular formula of *Cadlina koreana* **sp. nov.** is 57 × 23.1.23 with a rectangular rachidian tooth. In addition, mitochondrial cytochrome c subunit 1 (COI), 16S ribosomal RNA (16S rRNA), and nuclear 28S ribosomal RNA (28S rRNA) gene sequences were generated and used for analysis of Automatic Barcode Gap Discovery (ABGD) and reconstruction of the phylogenetic tree. Morphological distinction and genetic analyses confirm that three *Cadlina* species are present in Korean waters of which *Cadlina koreana* is a new species.

Keywords

Cadlina koreana sp. nov., description, northwestern Pacific region, morphology, phylogeny

* Contributed equally as the first authors.

Introduction

Cadlina Bergh, 1879 is a genus of slow-moving and flattened dorid nudibranchs (Korshunova et al. 2020). *Cadlina* species are reported as common dorid nudibranchs in northern temperate waters but become remarkably scarcer in tropical regions (Schrödl 2000). Recently, the genus was extensively reviewed by Korshunova et al. (2020). In that study, the authors described four new species and re-described *C. umiushi* Korshunova et al., 2015 and *C. kamchatica* Korshunova et al., 2015. Their findings increase the understanding of *Cadlina* species in the northern seas, especially in the northwestern Pacific region. To date, there have been four *Cadlina* species recorded in the northwestern Pacific region: *C. japonica* Baba, 1937, *C. kamchatica*, *C. umiushi*, and *C. paninae* Korshunova et al., 2020. Of these, only *C. japonica* was previously recorded from South Korea by Choe and Lee (1994). Potentially, there are more *Cadlina* species present in Korean waters awaiting discovery.

Members of the nudibranch genus *Cadlina* generally have similar body shapes and coloration so it is a difficult task to distinguish them based on their morphology (Korshunova et al. 2020). DNA barcoding is widely reported as an effective tool for both the identification of known species and the discovery of new species (Hebert et al. 2003). Because of the difficulty in identifying *Cadlina* species from morphology only, molecular markers have been analyzed to improve the accuracy of species discrimination (Korshunova et al. 2020). Mitochondrial and nuclear markers such as COI, 16S rRNA, and 28S rRNA genes are often selected for analysis. In previous studies of nudibranchs, these markers were used in combination with a morphological examination to discover new species and separate species complexes (Lindsay and Valdés 2016; Korshunova et al. 2020).

This study aimed to investigate *Cadlina* species in Korean waters. For this purpose, eight specimens were collected for species identification. In addition, fragments of COI, 16S rRNA, and 28S rRNA genes from these specimens were sequenced and analyzed to compare with the morphological examinations.

Materials and methods

Sample collection and morphological examination

Cadlina species were collected from the Korean East Sea (Sea of Japan) by scuba diving. Upon collection, specimens were preserved in 10% neutral buffered formalin for morphological examination. In addition, small sample of tissue from the foot was stored in 95% ethanol for DNA extraction. Sample collection data and depositories are presented in Suppl. material 1: Table S1. A stereoscopic microscope (Nikon SMZ800N) was used to examine the specimens. The buccal mass was extracted under a stereo microscope for radula extraction. The buccal mass was placed in 10% KOH for two days at room temperature to dissolve muscle. The radula was then carefully removed from

the solution and placed in deionized water for 20 minutes to remove excess KOH. The radulae were examined under a JEOL JSM-6390LV scanning electron microscope (Jeol Inc., USA). The reproductive systems were dissected under a stereoscopic microscope and drawn with a camera lucida. Morphological comparison and species descriptions were prepared following previous guidelines (Schrödl 2000; Chichvarkhin 2016; Korshunova et al. 2020).

Molecular analysis

Total DNA was extracted from the foot of each specimen using E.Z.N.A. Mollusc DNA Kit (Omega Bio-tek, USA). The quality and concentration of the extracted DNA were checked using a MaestroNano spectrophotometer (Maestrogen, Taiwan). Polymerase chain reaction (PCR) analysis was performed for two mitochondrial markers (COI and 16S rRNA) and one nuclear marker (28S rRNA). The primer set for each marker is listed in Table 1.

The 20 µl PCR reaction mixture contained 10 µl of 2X TOPsimple DyeMIX-Tenuto (Enzynomics, South Korea), 1 µl of each primer (10 pmoles/µl), 100 ng of DNA, and distilled water. The amplification protocol was as follows: initial denaturation at 95 °C for 5 minutes, followed by 35 cycles of denaturation at 95 °C for 45 seconds, variable annealing temperature for each primer set as listed in Table 1 for 45 seconds, extension at 72 °C for 1 minute, and final elongation at 72 °C for 5 minutes. The PCR products were checked by electrophoresis in 1% agarose gels in 1× TAE buffer. Sequencing was performed by an ABI 3730 DNA Analyzer (Applied Biosystems, USA).

Consensus sequences were generated from the forward and reverse sequences with Geneious software version 9.1.8 (Kearse et al. 2012). The obtained sequences were submitted to GenBank and the sequence accession numbers are listed in Suppl. material 1: Table S1. The sequences were compared with sequences in GenBank using the BLAST tool to search for related species. Additionally, sequences of the genus *Cadlina* were obtained from GenBank for Automatic Barcode Gap Discovery (ABGD) analysis and phylogenetic reconstruction. The ABGD webtool (https://bioinfo.mnhn.fr/abi/public/abgd/abgdweb.html) was applied to delineate putative species based on COI and 16S rRNA sequences (Puillandre et al. 2012). The distance matrices for COI and 16S rRNA were built in MEGA X software using the Kimura 2-parameter model (Kumar et al. 2018). The default settings used for analysis were Pmin = 0.001, Pmax =

Table 1. Primer sets of COI and 16S rRNA and 28S rRNA genes used in this study.

Primer	Gene	Sequence (5'-3') genes	Annealing temperature	Reference
LCO1490	COI	GGTCAACAAATCATAAAGATATTGG	45°	Folmer et al. 1994
HCO2198		TAAACTTCAGGGTGACCAAAAAATCA		
16Sar-L	16S rRNA	CGCCTGTTTATCAAAAACAT	48°	Palumbi 1996
16S R		CCGRTYTGAACTCAGCTCACG		Puslednik and Serb 2008
28S C1	28S rRNA	ACCCGCTGAATTTAAGCAT	48°	Hassouna et al. 1984
28S C2		TGAACTCTCTCTTCAAAGTTCTTTTC		Le et al. 1993

0.1, Steps = 10, X = 1.5, Nb bins = 20. All three different distance models are available from the ABGD webtool: Simple Distance, Jukes-Cantor (JC69), and Kimura (K80) TS/TV were tested (Puillandre et al. 2012).

Phylogenetic reconstruction of *Cadlina* species was conducted based on the concatenation of three markers (COI, 16S rRNA, and 28S rRNA) or two markers (COI and 16S rRNA) because there were no 28S rRNA sequences for some species. Two species of the genus *Aldisa*, *A. sanguinea* and *A. smaragdina*, in the family Cadlinidae were used as the outgroup. Before concatenation, each marker was aligned using the ClustalW method in MEGA X software (Kumar et al. 2018) and poorly aligned regions were trimmed by GBlocks 0.91b (Castresana 2000). The Akaike Information Criterion in jModelTest 2.1.10 was used to search for the best model for phylogenetic tree reconstruction (Darriba et al. 2012). The phylogenetic trees were reconstructed using both the Maximum Likelihood (ML) and Bayesian Inference (BI) methods. The ML phylogenetic tree was constructed using the GTR+G+I model with 1000 bootstrap replicates in MEGA X software (Kumar et al. 2018). The BI tree was reconstructed in MrBayes ver. 3.2.7a with two runs for 10 million generations and a sampling interval of 1000 generations (Ronquist et al. 2012).

Results

Morphological results

***Cadlina koreana* sp. nov.**
http://zoobank.org/BDAF5119-92FB-499A-BD02-63EB7077ABED
Figures 1, 4A

Type material. ***Holotype*.** NIBRIV0000865970; South Korea, Gangwon-do, Goseong-gun, Jugwang-myeon, Munamjin-ri; 38°18'14.75"N, 128°34'1.05"E; collected on 02 June 2013 (COI GenBank number: MT420429). ***Paratype*.** NIBRIV0000865971; South Korea, Gangwon-do, Goseong-gun, Jugwang-myeon, Munamjin-ri; 38°18'14.75"N, 128°34'1.05"E; collected on 02 June 2013 (COI GenBank number: MT420430).

Other material. Voucher: SMU00051; South Korea, Gangwon-do, Goseong-gun, Jugwang-myeon, Munamjin-ri; 38°18'14.75"N, 128°34'1.05"E; collected on 02 June 2013 (COI GenBank number: MT420431).

Diagnosis. Ground color translucent white (Fig. 1A). Rhinophores and gills opaque white to translucent yellow. Entire dorsum covered by small rounded tubercles with white coloration. Radula formula 57 × 23.1.23. Rachidian tooth rectangular with four main sharp cusps (Fig. 1B). Innermost lateral teeth massive, wide base; cusp strong, slightly curved; two inner denticles and three to four outer denticles (Fig. 1C). Outer lateral teeth hamate, well-defined denticles (Fig. 1D).

Description. Body elongated ovate; body lengths 10.3 mm (holotype), 14 mm (paratype), and 9 mm (additional specimen). Ground color translucent white

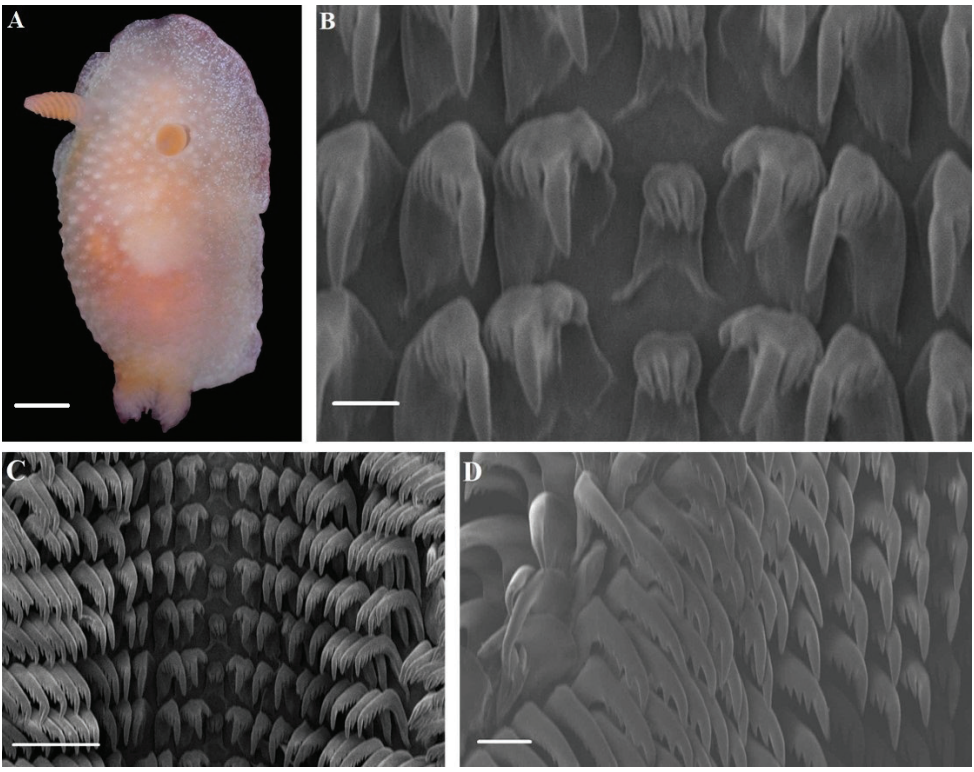

Figure 1. *Cadlina koreana* **A** body; Radula **B** rachidian teeth **C** central and lateral region **D** outer lateral region. Scale bars: 2 mm (**A**); 10 μm (**B**); 50 μm (**C**); 20 μm (**D**).

(Fig. 1A). Dorsum broad in front and posteriorly. Mantle broad and wider than foot; thin at the edge. Numerous white specks present at mantle edge, lacking a yellow marginal band. Dorsum covered with numerous small white tubercles. Rhinophores opaque white to translucent yellow; clavus lamellate; cylindrical stalk smooth. Rhinophoral sheath smooth. Gills opaque white to yellow, six multi-pinnate branchial leaves, retractable into gill cavity. Gill sheath bears small nodules. Oral veil forms triangular, lateral sides. Foot anteriorly rounded and thickened. Radula formula: 57 × 23.1.23. Rachidian tooth rectangular with four sharp denticles; two central denticles slightly longer than two lateral denticles (Fig. 1B). Innermost lateral tooth massive with one large, slightly curved cusp; two short, inner denticles; and three to four outer denticles. Second lateral tooth with one cusp, no inner denticle and four or five outer denticles. Middle lateral tooth hamate with one large cusp and up to seven denticles (Fig. 1C). Outer lateral teeth hamate, comb-shaped with 5–7 clearly visible denticles (Fig. 1D). Reproductive system triaulic (Fig. 4A). Ampulla moderate, convoluted, and connects with female gland and prostate. Prostate long and narrow. Seminal vesicle slightly more swollen than prostate. Vas deferens narrow, smooth, and distinct. Penis armed with spines. Vagina relatively narrow and connects with bursa copulatrix. Bursa copulatrix ovate and ca. 1.5 × larger than

receptaculum seminis. Uterine duct short and narrow, bifurcates into female gland and receptaculum seminis.

Remarks. A comparison of *Cadlina* species recorded in the northwestern Pacific region is presented in Table 2. *Cadlina koreana* sp. nov. is most similar externally to *C. paninae*, differing in color variation of the rhinophores and gills as well as the structure of the radula. In *C. paninae*, the color of the rhinophores and gills are opaque white while in *Cadlina koreana*, color of the rhinophores can vary from opaque white to translucent yellow and that of the gills can vary from opaque white to yellow. *Cadlina koreana* also has fewer rows and fewer denticles on both the rachidian tooth and its lateral tooth compared to those of *C. paninae*. In addition, the rachidian tooth of *C. paninae* is often bifurcated at the tips while the rachidian tooth of *Cadlina koreana* is not bifurcated at the tips.

The external morphology of *Cadlina koreana* is relatively similar to *C. umiushi*, which also has small-sized tubercles on the dorsum. However, clear differences between these two species can be observed by comparing their coloration. The color pattern of *Cadlina koreana* is white without yellow tubercles or a yellow marginal band. In contrast, *C. umiushi* is semi-transparent white with yellow tubercles and a yellow marginal band. The rachidian tooth of *Cadlina koreana* is rectangular while it is trapezoid in *C. umiushi*. The inner denticles of the first lateral tooth of *C. umiushi* are half the length of the tooth body, but in *Cadlina koreana* it is less than half the length of the tooth body. Moreover, the outer lateral teeth of *Cadlina koreana* are hamate with clearly visible denticles. In contrast, the outer lateral teeth of *C. umiushi* are almost straight with inconspicuous denticles.

Cadlina japonica is distinguished from *Cadlina koreana* sp. nov. by brownish patches on the dorsum and an elongate rachidian tooth with lobe-like denticles. *Cadlina kamchatica* clearly differs from *Cadlina koreana* by its yellowish body color and the higher number of denticles on the rachidian tooth and lateral tooth. The common *Cadlina* species in the northeastern Pacific, *C. luteomarginata* MacFarland, 1966, differs from *Cadlina koreana* by yellow dots on the dorsum and a yellow rim to the mantle. The other species in this region, *C. flavomaculata* MacFarland, 1905, also has yellow dots on the dorsum that are not present in *Cadlina koreana*. The color of *C. modesta* MacFarland, 1966 is light yellowish to light brown while it is translucent white in *Cadlina koreana*. Compared to *Cadlina koreana*, three *Cadlina* species recently described by Korshunova et al. (2020), *C. klasmalmbergi*, *C. jannanicholsae*, and *C. sylviaearleae* have yellow mantle bands and yellow tubercles. In *Cadlina koreana*, the yellow mantle band is absent and the color of the tubercles is white. The maximum intraspecific distances in *C. koreana* are 0% for the COI marker and 0.23% for the 16S rRNA marker (Suppl. material 1: Table S3). The lowest COI interspecific distance of 5.78% is found between *C. koreana* and *C. umiushi*. The lowest 16S rRNA interspecific distance of 4.56% is found between *C. koreana* and *C. paninae*.

Etymology. The species is named after the country of its type locality.

Distribution. *Cadlina koreana* sp. nov. is currently known only from Munamjin-ri, South Korea.

Table 2. Morphological comparison among *Cadlina* species in the northwestern Pacific region.

Species	Locality	Size	Morphology	Radular formula	Rachidian tooth	First lateral teeth	Mid-lateral teeth	Outer lateral teeth	Ampulla	Vas deferens	Vagina	Bursa copulatrix and receptaculum seminis	Source of information
Cadlina koreana	Munamjin-ri, South Korea	9–14 mm	Translucent white; dorsum covered with small white tubercles; small white specs present on mantle edge. No yellow marginal band	57 × 23.1.23	Rectangular, hook-shaped, 2 longer central denticles, and 2 shorter lateral denticles	1 cusp, 2 short inner denticles, and 3–4 outer denticles.	Hamate, comb-shaped, up to 7 denticles	Hamate, comb-shaped, 5–7 denticles.	Moderate and convoluted	Long and narrow	Relatively long and narrow	Ovate and ca. 1.5 × larger than receptaculum seminis	This study
Cadlina umiushi	Munamjin-ri, South Korea	8–9 mm	White background; numerous small yellow tubercles; yellow marginal band	55 x 16.1.16	Trapezoid, hook-shaped, 2 central denticles, and 2 lateral denticles	1 cusp, 2 inner denticles, and 3 outer denticles	Hamate, rather comb-shaped, 6–8 distinct outer denticles.	Hamate to straight, up to 10 inconspicuous denticles	Long and convoluted	Relatively short	Relatively short and broad	Ovate and ca. 2 × larger than receptaculum seminis	This study
Cadlina japonica	Munamjin-ri and Yeonji-ri, South Korea	48–55 mm	Yellowish with dark brown patches; small scattered yellow spots; yellow marginal band	88 x 71.1.71	Elongate, 2–4 lobe-like denticles	1 bigger cusp, 3–4 inner denticles, and 4–6 outer denticles	Hook-shaped, no inner denticle and 3–5 outer denticles	Hook-shaped, bearing up to 6 denticles	Moderate and convoluted	Long, narrow and distinct	Relatively short and narrow	Almost rectangular in shape, ca. 5 × larger than receptaculum seminis	This study
Cadlina kamchatica	Kamchatka, Starichkov Island, Russia	37 mm	Creamy to dark yellow/light brown; small, low rounded yellow tubercles	82 × 35.1.35	Moderately high, trapezoid, 5–6 denticles, 2 middle usually larger than outer ones	1 cusp, 4–6 large inner denticles, 5–6 distinct outer denticles	Hamate, comb-shaped, up to 17 distinct outer denticles only	Hamate reduced, up to 19 sharp denticles	Long and convoluted	Relatively short	Long and narrow	Pear-shaped, 2 × larger than receptaculum seminis	Korshunova et al. (2020)
Cadlina paninae	Matua Islands, Middle Kurile Islands, Russia	29 mm	Opaque whitish, sometimes with some yellowish shadow; low indistinct tubercles	90 × 38.1.38	Low rectangular, 3–5 distinct cusps, often bifurcated at tips	1 cusp, 2–3 inner denticles and 3–4 outer denticles	Elongate hook-shaped, up to 20 comb-shaped denticles	Hook-shaped, up to 20 comb-shaped denticles	Relatively short and slightly convoluted	Long and narrow	Long and narrow	Ovate, 1.5 × larger than receptaculum seminis	Korshunova et al. (2020)

***Cadlina umiushi* Korshunova, Picton, Sanamyan & Martynov, 2015**
Figures 2, 4B

Cadlina umiushi Korshunova, Picton, Sanamyan & Martynov, 2015 in Martynov et al. 2015: 65, fig. 1; Korshunova et al. 2020: 15, 29, figs 7, 15B.
Cadlina olgae Chichvarkhin, 2016: 12–14, fig. 4.

Material examined. One individual, voucher NIBRIV0000865972; South Korea, Gangwon-do, Goseong-gun, Jugwang-myeon, Munamjin-ri; 38°18'14.75"N, 128°34'1.05"E; collected on 02 June 2013 (COI GenBank number: MT420435). One individual, voucher SMU00060; South Korea, Gangwon-do, Goseong-gun, Jugwang-myeon, Munamjin-ri; 38°18'14.75"N, 128°34'1.05"E; collected on 02 June 2013 (COI GenBank number: MT420436).

Description. Body ovate, 8 mm and 9 mm long. Living specimens with a translucent white dorsum (Fig. 2A). Small yellow glands are present on both sides of the dorsum margin. Thin yellow marginal band present. Dorsum broad, rounded anteriorly and posteriorly. Small yellow tubercles cover the entire dorsum. Rhinophores long and broad. Six multipinnate gills connected by a membrane into circle around anus. Gills retractable into gill cavity. Foot broad, anteriorly thickened. Radula formula: 55 × 16.1.16. Rachidian tooth moderately high, trapezoid, and bearing four denticles (Fig. 2B). Innermost lateral tooth massive with one cusp, two inner denticles, and three outer denticles. Second lateral tooth with one cusp, no inner denticles and three outer denticles. Mid-lateral tooth hamate, 6–8 distinct outer denticles (Fig. 2C). Outer lateral tooth almost straight, denticles small, inconspicuous (Fig. 2D). Reproductive system triaulic (Fig. 4B). Ampulla long, wide, convoluted. Prostate moderate in length and wide, transiting to vas deferens. Vas deferens relatively short. Penis armed with spines. Vagina relatively short and broad, connecting with oval bursa copulatrix. Bursa copulatrix ca. 2 × larger than receptaculum seminis. Uterine duct short and narrow, connecting from female gland mass to base of ovate receptaculum seminis.

Remarks. *Cadlina umiushi* was first described in Martynov et al. (2015) from the holotype specimen collected in Peter the Great Bay, Russia. *Cadlina olgae* Chichvarkhin, 2016, described from specimens collected in south of Rudnaya Bay, Russia is considered a junior synonym of *C. umiushi* by Korshunova et al. (2020). This study records the presence of *C. umiushi* in Korean waters for the first time. Even though there were slight differences in the number of denticles of the rachidian and the first lateral tooth, and in the ampulla compartments of specimens collected from South Korea compared to the specimens collected from Russia, other morphological characteristics are similar. It should be noted that this difference is also observed between specimens in Russia collected by Chichvarkhin (2016) and Korshunova et al. (2020). The differences could be explained by the geographical distribution or maybe a different stage of development. The maximum intraspecific distances in *C. umiushi* are 1.56% for the COI marker and 1.37% for the 16S rRNA marker (Suppl. material 1: Table S3). The

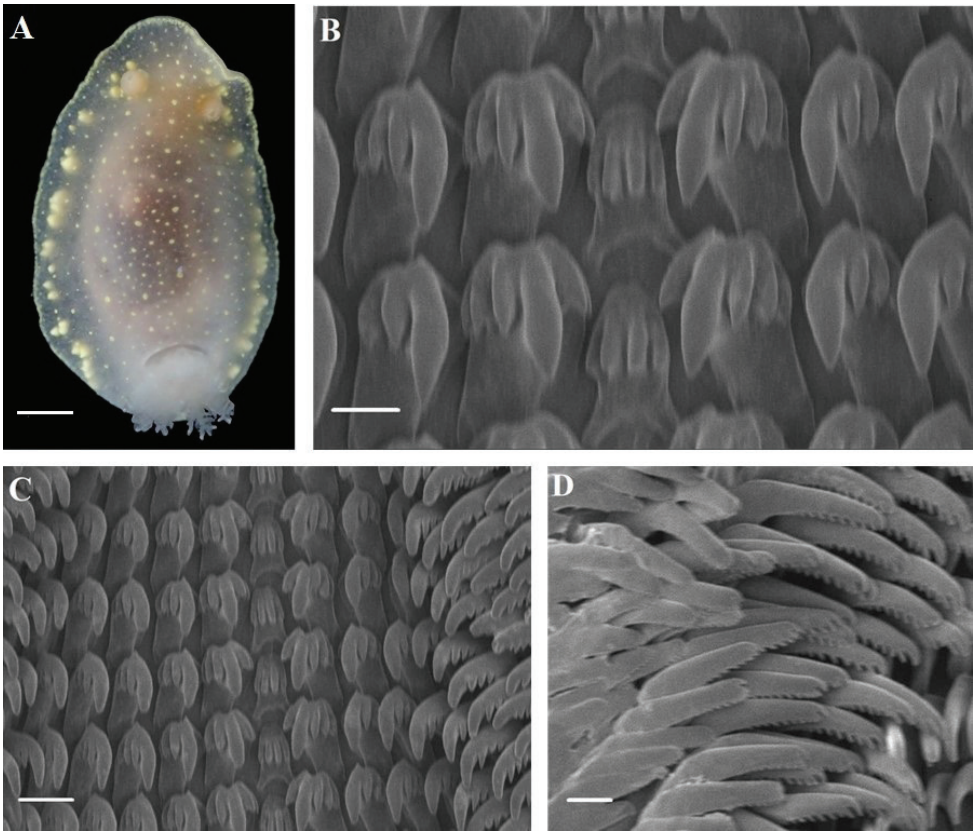

Figure 2. *Cadlina umiushi* **A** body; Radula **B** rachidian teeth **C** central and lateral region **D** outer lateral region. Scale bars: 2 mm (**A**); 10 μm (**B**); 50 μm (**C**); 20 μm (**D**).

lowest COI interspecific distance of 4.33% is found between *C. umiushi* and *C. laevis* (Linnaeus, 1767). The lowest 16S rRNA interspecific distance of 1.37% is found between *C. umiushi* and *C. kamchatica*.

Distribution. Northern part of Sea of Japan (Russia) to Munamjin-ri (South Korea).

Cadlina japonica Baba, 1937

Figures 3, 4C

Cadlina japonica Baba, 1937: 76–78, fig. 1; Baba 1949: 57, pl. XXI, figs 75–77, text fig. 67; Choe and Lee 1994: 362, fig. 2; Nakano 2018: 275; Korshunova et al. 2020: 36–39, figs 11, 12.

Material examined. Two individuals, vouchers: NIBRIV0000865973 and NIBRIV0000865974; South Korea, Gangwon-do, Goseong-gun, Jugwang-myeon,

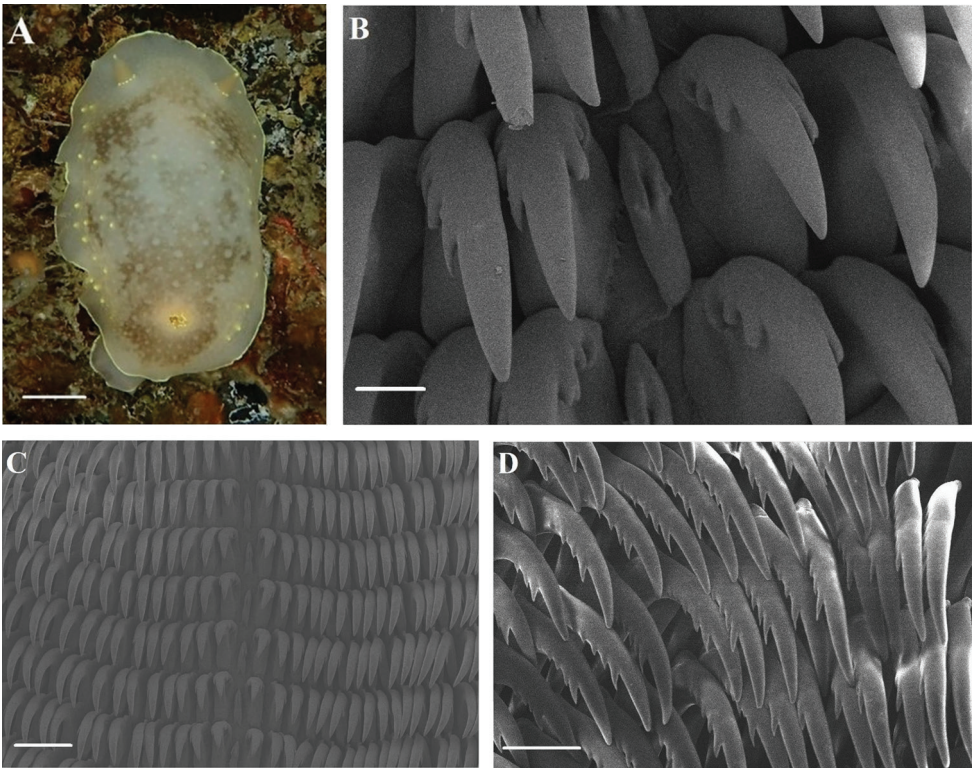

Figure 3. *Cadlina japonica* **A** body; Radula **B** rachidian teeth **C** central and lateral region **D** outer lateral region. Scale bars: 1 cm (**A**); 20 μm (**B**); 100 μm (**C**); 50 μm (**D**).

Munamjin-ri; 38°18'14.75"N, 128°34'1.05"E; collected on 02 June 2013 and 20 July 2019 (COI GenBank numbers: MT420432 and MT420433). One individual, voucher NIBRIV0000865975; South Korea, Gyeongsangbuk-do, Uljin-gun, Uljin-eup, Yeonji-ri; 37°00'0.59"N, 129°26'1.89"E; collected on 25 August 2011 (COI GenBank number: MT420434).

Description. Size up to 55 mm long. Live specimens commonly opaque white with a yellowish ground color and several dark brownish patches present on the dorsum (Fig. 3A). Rhinophores yellowish like the ground color with bright yellow tips. Rhinophoral sheath bears small tubercles and yellow dots. Six multipinnate, translucent white gills with yellow tips. Yellow dots present irregularly on the dorsum, but often concentrated near the mantle margin. Continuous yellow band present on mantel edge. Oral tentacles short and triangular. Foot broad, anteriorly thickened to form a double edge. Radula formula: 88 × 71.1.71. Rachidian tooth elongate and bears 2–4 distinct lobe-like cusps (Fig. 3B). Innermost lateral tooth hamate with a relatively narrow base and short, strong cusp; three or four inner denticles and 4–6 outer denticles (Fig. 3B). Middle lateral teeth hook-shaped, no inner denticle and 3–5 outer denticles (Fig. 3C). Outer lateral teeth bear up to six denticles (Fig. 3D). Reproductive system

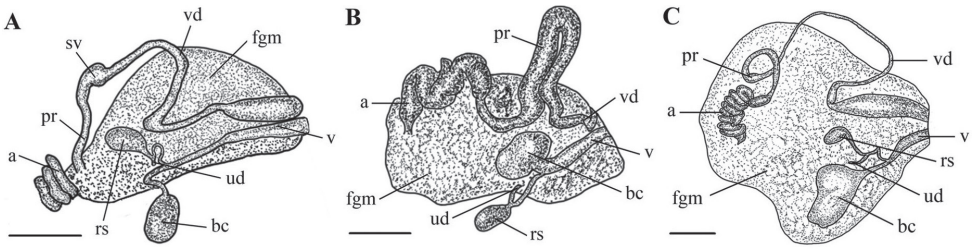

Figure 4. Reproductive systems of *Cadlina* species **A** *Cadlina koreana* sp. nov. **B** *Cadlina umiushi* **C** *Cadlina japonica*. Abbreviations: a, ampulla; bc, bursa copulatrix; fgm, female gland mass; rs, receptaculum seminis; pr, prostate; sv, seminal vesicle; ud, uterine duct; v, vaginal duct; vd, vas deferens. Scale bars: 0.5 mm (**A, B**); 2 mm (**C**).

triaulic (Fig. 4C). Ampulla is moderate and convoluted. Prostate long and narrow. Vas deferens long, narrow, convoluted. Penial spines absent. Vagina relatively short, narrow and connects with bursa copulatrix. Bursa copulatrix almost rectangular in shape, ca. 5 × larger than receptaculum seminis. Uterine duct short and narrow.

Remarks. *Cadlina japonica* was first described by Baba (1937). Recently, this species was thoroughly reviewed by Korshunova et al. (2020). Morphologically, the *C. japonica* specimens collected in this study are consistent with *C. japonica* described in previous studies (Baba 1937; Choe and Lee 1994; Korshunova et al. 2020). *Cadlina japonica* is completely distinguishable from other species of the genus by several characteristics. Irregular brownish patches are present on the mantle, but these patches are absent on several small individuals. Its rachidian tooth is elongate and its first lateral tooth is hamate. In addition, compared to other *Cadlina* species in the region, *C. japonica* is large, with the sample in this study measuring up to 55 mm. The maximum intraspecific distances in *C. japonica* are 0.78% for the COI marker and 0.23% for the 16S rRNA marker (Suppl. material 1: Table S3). The lowest COI interspecific distance of 7.97% is found between *C. japonica* and *C. jannanicholsae* Korshunova et al., 2020. The lowest 16S rRNA interspecific distance of 1.87% is found between *C. japonica* and *C. klasmalmbergi*.

Distribution. Southern Hokkaido to southern Honshu (Japan) and East Sea, South Korea (Sea of Japan).

Molecular analyses

Analyses of the three molecular markers also demonstrated differences between *Cadlina koreana* sp. nov. and other *Cadlina* species recorded in GenBank. The BLAST results showed that *C. umiushi* is the closest species to *Cadlina koreana* with 93.8% and 95.3% similarity in the COI and 16S rRNA genes, respectively. The number of taxonomic groups based on ABGD analysis for COI varied from 11 to 13, depending on the intraspecific divergence prior (p) value (Suppl. material 1: Table S4). In the 11-groups partition, all input species including three species in this study and spe-

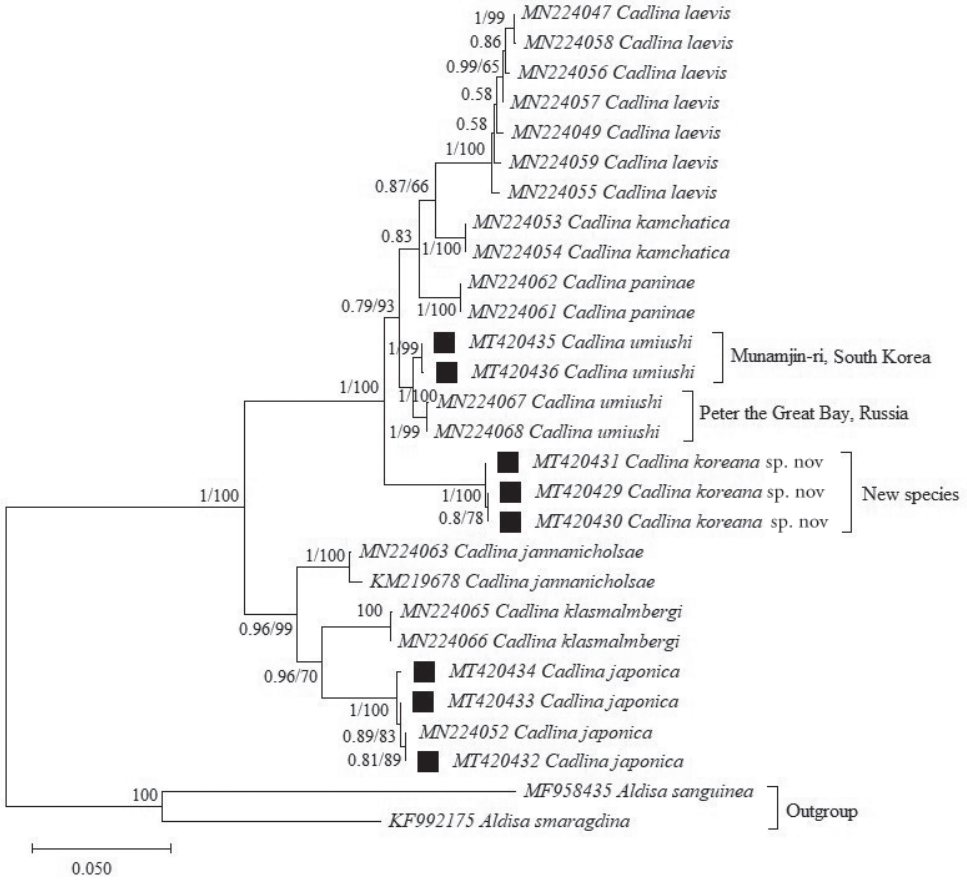

Figure 5. Phylogenetic tree based on concatenation of COI, 16S rRNA, and 28S rRNA markers. Sequences generated in this study are marked with back squares; the remaining sequences were obtained from GenBank. Accession numbers of COI sequences appear in front of species names to identify specific specimens as in Suppl. material 1: Tables S1, S2. The tree was constructed using the Maximum Likelihood method with 1000 bootstrap replicates in MEGA X software and Bayesian Inference in MrBayes software. *Aldisa sanguinea* and *A. smaragdina* were used as the outgroup. Numbers at each node indicated bootstrap (right) and posterior probability (left) values. The values > 50 (BS) and 0.5 (PP) are provided.

cies in Suppl. material 1: Table S3 were recovered, and each species corresponded to a distinct group. In the 12- and 13-groups partition, *Cadlina koreana* sequences were always clustered together. The same pattern was also observed for *C. japonica*. Meanwhile, *C. umiushi* sequences were partitioned into two or three groups, depending on the p value. ABGD analysis for 16S rRNA revealed 9–5 groups (Suppl. material 1: Table S5). Similar to the COI analysis, in the 11-group partition, all input species were recovered. *Cadlina koreana* sequences always formed a distinct group for all partitions. Similarly, *C. japonica* sequences also formed a group, except in the 15-group partition. In this partition, the p value was minimum and two groups of *C. japonica* were

observed. In the 9-group partition, *C. umiushi* was grouped with *C. kamchatica* and *C. paninae*. When the p value decreased, the total number of groups increased to 15 and *C. umiushi* sequences were divided into three groups.

A phylogenetic tree of three concatenated markers (COI, 16S rRNA, and 28S rRNA) was reconstructed to determine the positions of the three species of *Cadlina* found in South Korea (Fig. 5) while the phylogenetic tree of two concatenated markers (COI and 16S rRNA) was reconstructed to resolve the relationship of as many species in the genus *Cadlina* as possible (Suppl. material 2: Fig. S1). The ML and BI trees based on the three concatenated markers show a similar pattern (Fig. 5). The phylogenetic tree of the three concatenated markers indicates that *Cadlina koreana* specimens form an independent branch that is sister to a group that includes *C. umiushi*, *C. kamchatica*, *C. paninae*, and *C. laevis*. Moreover, the *C. umiushi* specimens were clustered together and formed two groups, a Russian group from Peter the Great Bay and a South Korean group from Munamjin-ri. Meanwhile, *C. japonica* was clustered with sequences from the same species available in GenBank (Fig. 5). The ML and BI trees of two concatenated markers (COI and 16S rRNA) had slightly different topology patterns (Suppl. material 2: Fig. S1A, S1B). However, both trees showed a separated position of *Cadlina koreana*. In the tree from three concatenated markers, the *C. umiushi* specimens from south of Rudnaya, Russia were added for analysis due to the availability of COI and 16S rRNA sequences. As a result, *C. umiushi* formed three branches according to geographical distributions, including two Russian branches (Peter the Great Bay and south of Rudnaya Bay) and one South Korean branch (Munamjin-ri). Both trees of two concatenated markers and three concatenated markers showed that *C. japonica* specimens were clustered with sequences from GenBank, and no clear separated groups were observed (Fig. 5; Suppl. material 2: Fig. S1).

Discussion

Species of the genus *Cadlina* are widely distributed in the northern temperate regions. *Cadlina japonica*, the first species of this genus reported from the northwestern Pacific region (Baba 1937), was described based on specimens collected in Japan; this species was also recorded in South Korea (Baba 1937; Choe and Lee 1994). Compared to other the *Cadlina* species, *C. japonica* is easily recognized by its distinct brownish patches on the mantle and distinct morphology of the rachidian and lateral teeth; the specimens examined in this work are similar to previous descriptions. The second and third species found in the region, *C. umiushi* and *C. kamchatica*, were described by Martynov et al. (2015). The latest species, and most similar to our new species, *C. paninae*, was recently described by Korshunova et al. (2020). With unambiguous evidence from morphological and molecular analyses, the present study identified three species in Korean waters: *C. japonica*, *C. umiushi*, and a new species named *Cadlina koreana*.

Cadlina koreana is the fifth species recorded in the northwestern Pacific region. The new species can be differentiated from all previously described species by a combination of morphological and molecular markers. Similar to most *Cadlina* species,

the ground color of *Cadlina koreana* is white. However, the distinct characteristics of *Cadlina koreana* are the absence of both the yellow tubercles on the dorsum and a yellow marginal band, two features present in most *Cadlina* species found in the northern Pacific (Korshunova et al. 2020). The observations of radulae by SEM also support the distinction of *Cadlina koreana*: the shape of the rachidian and lateral teeth as well as the radula formula distinguishes it from the other species.

Moreover, the presence of *C. umiushi* in Korean waters is described for the first time. The morphology of *C. umiushi* collected in the present study resembled that of other specimens described in previous studies (Chichvarkhin 2016; Korshunova et al. 2020). Similar to those reports, the dorsum of *C. umiushi* in this study was broad with small yellow tubercles. Also, there was a yellow mantle band on the specimens. The radula of specimens collected from Munamjin-ri, South Korea showed almost perfect resemblance with those of specimens described by Chichvarkhin (2016) and Korshunova et al. (2020), except for slight differences in the radular formulae and the numbers of denticles in the rachidian and first lateral teeth (Table 2). The radula formula (55 × 16.1.16) in this study was closer to the specimens from Chichvarkhin (2016) (55–60 × 13.1.13) than the specimen from Korshunova et al. (2020) (70 × 30.1.30). For the rachidian tooth of the radula, both Chichvarkhin (2016) and Korshunova et al. (2020) reported five or six denticles while there were four denticles in the specimens collected from South Korea. For the first lateral tooth, the specimens in this study included two inner denticles, a distinct cusp, and three outer denticles that were closest to the specimens reported by Korshunova et al. (2020) with two or three inner denticles, a distinct cusp, and 4–6 outer denticles. Also, the morphology of the reproductive system of the specimens collected from the three sites was similar except for the ampulla: even though all specimens showed long and convoluted ampullae, the specimens from Munamjin-ri and south of Rudnaya Bay had two folds, while several compartments were seen in the specimens from Peter the Great Bay (Chichvarkhin 2016; Korshunova et al. 2020).

It is challenging to identify *Cadlina* species based on morphology because of similar characteristics and morphological conservatism. Molecular markers are well known as a useful tool to support the identification of this group (Korshunova et al. 2020). In this study, three molecular markers COI, 16S rRNA, and 28S rRNA were used together with morphological examination. Our molecular analysis confirmed the findings of our morphological study: *Cadlina koreana* sp. nov. and *C. japonica* are distinct species based on ABGD analyses. For both markers, *C. umiushi* sequences were partitioned into a distinct group at a specific p value. For the COI marker, *C. umiushi* sequences were not grouped with any other species. All COI sequences of *C. umiushi* were grouped together or partitioned into two or three groups when the p value decreased. For the 16S rRNA marker, *C. umiushi* sequences can be partitioned into up to three groups, depending on the p value. When the p value was high, all *C. umiushi* sequences formed a group with *C. kamchatica* and *C. paninae*. This finding showed a high intraspecific distance within *C. umiushi* and low interspecific distances between *C. umiushi*, *C. kamchatica* and *C. paninae*. Our results are concordant with a previous study that observed a small gap between the maximum intraspecific distance and the minimum interspecific distance

of 16S rRNA sequences of *C. umiushi* (Korshunova et al. 2020), which were 1.18% and 1.41%, respectively. In the present study, when more 16S rRNA sequences from Korean waters were added for estimation, the intraspecific distance within *C. umiushi* became larger (1.37%) and comparable to the distance between *C. umiushi*, *C. kamchatica*, and *C. paninae*. In contrast, even though the COI sequences from our *C. umiushi* specimens were added, *C. umiushi* were not grouped with other *Cadlina* species. In a previous study of aeolid nudibranchs, the COI gene was proven to be better than 16S rRNA gene in resolving the relationship at the species level (Cella et al. 2016).

According to the phylogenetic tree, *Cadlina koreana* sp. nov., *C. japonica*, and *C. umiushi* formed independent clusters. Interestingly, three separate groups of *C. umiushi* were observed that corresponded with the three geographical collection sites. The ABGD and phylogenetic analyses showed some distances within *C. umiushi* among the collection sites. This result was congruent with the morphological examination discussed above and could indicate a possible hidden diversity within this species. It is worth noting that the number of specimens in this study as well as in the surveys of Martynov et al. (2015), Chichvarkhin (2016), and Korshunova et al. (2020) are limited. More *C. umiushi* specimens from different geographical localities must be collected to further elucidate the population structure and speciation of this species.

Based on morphology and analyses of three molecular markers, three *Cadlina* species are identified from South Korea: *Cadlina koreana* sp. nov., *C. umiushi* (a new record for South Korea), and *C. japonica*. These results demonstrate the usefulness of the combination of morphological examination and molecular analyses in species identification, termed integrative taxonomy by Dayrat (2005). This approach should be applied for any future works that deal with the taxonomy of *Cadlina* species. Further studies are necessary to investigate the taxonomy and distribution of *Cadlina* species in the region. This is fundamental to improving our understanding of *Cadlina* diversity and systematics.

Acknowledgments

This work was supported by a National Research Foundation of South Korea (NRF) grant funded by the South Korean Government (MSIP) (No. NRF-2018R1D-1A1B07042858) and a grant from the National Institute of Biological Resource (NIBR) funded by the Ministry of Environment (MOE) of South Korea (NIBR No. 2016-02-001). We thank Mr. Jung-il Kim (Department of Biotechnology, Sangmyung University) for his support in the preparation and examination of radulae.

References

Baba K (1937) Two new species of the nudibranchiate genus *Cadlina* from Sagami Bay, Japan. Venus, Japanese Journal of Malacology 7: 75–80.

Baba K (1949) Opisthobranchia of Sagami Bay Collected by His Majesty the Emperor of Japan. Iwanami Shoten, Tokyo, 207 pp.

Castresana J (2000) Selection of conserved blocks from multiple alignments for their use in phylogenetic analysis. Molecular Biology and Evolution 17: 540–552. https://doi.org/10.1093/oxfordjournals.molbev.a026334

Cella K, Carmona L, Ekimova I, Chichvarkhin A, Schepetov D, Gosliner TM (2016) A radical solution: the phylogeny of the nudibranch family Fionidae. PLoS ONE 11: e0167800. https://doi.org/10.1371/journal.pone.0167800

Chichvarkhin A (2016) Shallow water sea slugs (Gastropoda: Heterobranchia) from the northwestern coast of the Sea of Japan, north of Peter the Great Bay, Russia. PeerJ 4: e2774. https://doi.org/10.7717/peerj.2774

Choe BL, Lee JR (1994) Opisthobranchs (Mollusca: Gastropoda) from Ullung and Dog-do Islands, Korea. Korean Journal of Zoology 37: 352–376.

Darriba D, Taboada GL, Doallo R, Posada D (2012) jModelTest 2: more models, new heuristics and parallel computing. Nature Methods 9(8): e772. https://doi.org/10.1038/nmeth.2109

Dayrat B (2005) Towards integrative taxonomy. Biological Journal of the Linnean Society 85: 407–415. https://doi.org/10.1111/j.1095-8312.2005.00503.x

Folmer O, Black M, Hoeh W, Lutz R, Vrijenhoek R (1994) DNA primers for amplification of mitochondrial cytochrome c oxidase subunit I from diverse metazoan invertebrates. Molecular Marine Biology and Biotechnology 3: 294–299.

Hassouna N, Michot B, Bachellerie JP (1984) The complete nucleotide sequence of mouse 28S rRNA gene. Implications for the process of size increase of the large subunit rRNA in higher eukaryotes. Nucleic Acids Research 12: 3563–3583. https://doi.org/10.1093/nar/12.8.3563

Hebert PD, Ratnasingham S, de Waard JR (2003) Barcoding animal life: cytochrome c oxidase subunit 1 divergences among closely related species. Proceedings of the Royal Society of London B: Biological Sciences 270: S96–S99. https://doi.org/10.1098/rsbl.2003.0025

Kearse M, Moir R, Wilson A, Stones-Havas S, Cheung M, Sturrock S, Buxton S, Cooper A, Markowitz S, Duran C, Thierer T, Ashton B, Meintjes P, Drummond A (2012) Geneious Basic: an integrated and extendable desktop software platform for the organization and analysis of sequence data. Bioinformatics 28: 1647–1649. https://doi.org/10.1093/bioinformatics/bts199

Korshunova TA, Fletcher K, Picton B, Lundin K, Kashio S, Sanamyan N, Sanamyan K, Padula V, Schrödl M, Martynov A (2020) The Emperor's *Cadlina*, hidden diversity and gill cavity evolution: new insights for the taxonomy and phylogeny of dorid nudibranchs (Mollusca: Gastropoda). Zoological Journal of the Linnean Society 20: 1–66. https://doi.org/10.1093/zoolinnean/zlz126

Kumar S, Stecher G, Li M, Knyaz C, Tamura K (2018) MEGA X: molecular evolutionary genetics analysis across computing platforms. Molecular Biology and Evolution 35: 1547–1549. https://doi.org/10.1093/molbev/msy096

Le HLV, Lecointre G, Perasso R (1993) A 28S rRNA based phylogeny of the Gnathostomes: First steps in the analysis of conflict and congruence with morphologically based cladograms. Molecular Biology and Evolution 2: 31–51. https://doi.org/10.1006/mpev.1993.1005

Lindsay T, Valdés Á (2016) The model organism *Hermissenda crassicornis* (Gastropoda: Heterobranchia) is a species complex. PLoS ONE 11: e0154265. https://doi.org/10.1371/journal.pone.0154265

Martynov AV, Sanamyan NP, Korshunova TA (2015) Review of the opisthobranch mollusc fauna of Russian Far Eastern seas: Pleurobranchomorpha, Doridida and Nudibranchia. Bulletin of Kamchatka State Technical University 34: 62–87. https://doi.org/10.17217/2079-0333-2015-34-62-87

Nakano R (2018) Field Guide to Sea Slugs and Nudibranchs of Japan. Bun-ichi Co. Ltd., Tokyo, 544 pp.

Palumbi SR (1996) Nucleic acids II: The polymerase chain reaction. In: Hillis DM, Moritz C, Mable BK (Eds) Molecular Systematics. Sinauer Associates, Sunderland, 205–247.

Puillandre N, Lambert A, Brouillet S, Achaz G (2012) ABGD, Automatic Barcode Gap Discovery for primary species delimitation. Molecular Ecology 21: 1864–1877. https://doi.org/10.1111/j.1365-294X.2011.05239.x

Puslednik L, Serb JM (2008) Molecular phylogenetics of the Pectinidae (Mollusca: Bivalvia) and effect of increased taxon sampling and outgroup selection on tree topology. Molecular Biology and Evolution 48: 1178–1188. https://doi.org/10.1016/j.ympev.2008.05.006

Ronquist F, Teslenko M, van der Mark P, Ayres D, Darling A, Hohna S, Larget B, Liu L, Suchard MA, Huelsenbeck JP (2012) MrBayes 3.2: Efficient Bayesian phylogenetic inference and model choice across a large model space. Systematic Biology 61: 539–542. https://doi.org/10.1093/sysbio/sys029

Schrödl M (2000) Revision of the nudibranch genus *Cadlina* (Gastropoda: Opisthobranchia) from the Southern Ocean. Journal of the Marine Biological Association of the United Kingdom 80: 299–309. https://doi.org/10.1017/S0025315499001873

Supplementary material 1

Tables S1–S3

Authors: Thinh Dinh Do, Dae-Wui Jung, Hyun-Jong Kil, Chang-Bae Kim

Data type: molecular data

Explanation note: **Table S1.** Collection information and Genbank accession numbers of samples. **Table S2.** Sequences obtained from GenBank used in the present study. **Table S3.** Intraspecific and interspecific distances (%) of *Cadlina* species based on COI and 16S rRNA sequences. Species with multiple sequences available for each marker were targeted for analysis. **Table S4.** ABGD analysis for COI sequences of *Cadlina* species. **Table S5.** ABGD analysis for 16S rRNA sequences of *Cadlina* species.

Link: https://doi.org/10.3897/zookeys.996.54602.suppl1

Supplementary material 2

Figure S1

Authors: Thinh Dinh Do, Dae-Wui Jung, Hyun-Jong Kil, Chang-Bae Kim

Data type: molecular data

Explanation note: Phylogenetic tree based on concatenation of COI and 16S rRNA markers. Sequences generated in this study are marked with black squares; the remaining sequences were obtained from GenBank. Accession numbers of COI sequences appear in front of species names to identify specific specimens listed in Table S1 and Table S2. The tree was constructed using the Maximum Likelihood method with 1000 bootstrap replicates in MEGA X software (**A**) and Bayesian Inference in MrBayes software (**B**). *Aldisa sanguinea* and *A. smaragdina* were used as the outgroup. Numbers at nodes indicate bootstrap and posterior probability values. The values > 50 (BS) and 0.5 (PP) are provided.

Link: https://doi.org/10.3897/zookeys.996.54602.suppl2

ZooKeys 996: 19–35 (2020)
doi: 10.3897/zookeys.996.55034
https://zookeys.pensoft.net

RESEARCH ARTICLE

A peer-reviewed open-access journal
ZooKeys
Launched to accelerate biodiversity research

A new species of *Psammonitocrella* Huys, 2009 (Copepoda, Harpacticoida, Ameiridae) from California (USA), with a discussion of the relationship between *Psammonitocrella* and Parastenocarididae

Paulo Henrique Costa Corgosinho[1], Terue Cristina Kihara[2], Pedro Martínez Arbizu[2]

1 *Department of General Biology, Universidade Estadual de Montes Claros, 39401-089, Montes Claros, Brazil*
2 *Senckenberg am Meer Wilhelmshaven, Abt. Deutsches Zentrum für Marine Biodiversität, DZMB, German Centre for Marine Biodiversity Research, Südstrand 44, 26382, Wilhelmshaven, Germany*

Corresponding author: Paulo Henrique Costa Corgosinho (pcorgo@gmail.com)

Academic editor: Kai Horst George | Received 3 June 2020 | Accepted 11 September 2020 | Published 24 November 2020

http://zoobank.org/8DF77B56-E942-41B5-8A5F-66E377118357

Citation: Corgosinho PHC, Kihara TC, Arbizu PM (2020) A new species of *Psammonitocrella* Huys, 2009 (Copepoda, Harpacticoida, Ameiridae) from California (USA), with a discussion of the relationship between *Psammonitocrella* and Parastenocarididae. ZooKeys 996: 19–35. https://doi.org/10.3897/zookeys.996.55034

Abstract

The freshwater harpacticoid *Psammonitocrella kumeyaayi* **sp. nov.** from the Nearctic Region (California; USA) is proposed. The position of the genus within Harpacticoida and its relationship with the Parastenocarididae is discussed. The new species can be included within *Psammonitocrella* on account of a) the cylindrical furca, longer than the telson, b) the unmodified inner spine on the basis of the male first leg, c) loss of the outer spine on the second exopodal segment of the first leg, d) loss of the outer spine of the third exopodal segment of the second, third, and fourth legs, e) loss of the inner apical seta on the third exopodal segment of the second and third legs, f) transformation of the inner apical seta of the third exopodal segment of the fourth leg into a spine, and g) loss of the endopodite of the fourth leg. The new species differs remarkably from *P. boultoni*, and *P. longifurcata* in the loss of the outer spine of the second exopodal segment of the fourth leg, in the presence of a one-segmented fifth leg exopodite, and in the presence of an outer seta on the basis of the first and second legs. Both *Psammonitocrella* and the known species of Parastenocarididae have a one-segmented endopod on the fourth leg, and the endopods of the second and third legs are reduced to one or two segments. *Psammonitocrella* is currently allocated into the Ameiridae, and evidence suggesting a sister-group relationship with Parastenocarididae—both share the loss of the inner seta on the first endopodal segment of the first leg—indicates that the Parastenocarididae should be included into the Ameiridae. In an evolutionary context, Parastenocarididae could have evolved from a lineage of freshwater ameirids that became interstitial in continental waters and colonized aquifers and groundwaters.

Keywords
fresh water, groundwater diversity, meiofauna, phylogeny, *Psammonitocrella kumeyaayi* sp. nov., San Clemente Canyon, systematics

Introduction

The family Ameiridae Boeck, 1865 is composed of about 300 species accommodated in 47 marine and freshwater genera (Walter and Boxshall 2020), excluding *Anoplosomella* Strand, 1929 and *Malacopsyllus* Sars, 1911, transferred to Argestidae Por, 1986 by Corgosinho and Martínez Arbizu (2010). Nowadays, with 150 freshwater species, this is one of the most species-rich families in fresh water. It is especially diverse in subterranean waters (Rouch 1986; Galassi 2001), and is dominated by the group of genera related to *Nitokra* and *Nitocrella* (Boxshall and Jaume 2000; Boxshall and Defaye 2008). The freshwater species of Ameiridae are found worldwide, with the highest diversity recorded from the Palearctic Region (Boxshall and Defaye 2008).

Psammonitocrella Huys, 2009 is known only from the USA, and is represented by *P. boultoni* Rouch, 1992 and *P. longifurcata* Rouch, 1992. The taxonomic position of this genus was debated in the last decades. In their analysis of a wide range of ameirid-like taxa, Martínez Arbizu and Moura (1994) revealed the sister-group relationship between *Psammonitocrella* and Parastenocarididae Chappuis, 1940, and concluded, that, if the family rank of Parastenocarididae is to be maintained, *Psammonitocrella* could not be maintained within Ameiridae. Lee and Huys (2002) proposed to return *Psammonitocrella* to Ameiridae, and Karanovic and Hancock (2009) considered the genus as a derived group within a clade of freshwater ameirids—with one-segmented, reduced or without a P4 enp—closely related to *Eduardonitocrella mexicana* (Suárez-Morales & Iliffe, 2005) and *Stygonitocrella orghidani* (Petkovski, 1973) *incertae sedis* (Karanovic and Hancock 2009). None of these authors discussed the position of Parastenocarididae, but by excluding this family from their analyses, and including *Psammonitocrella* into Ameiridae, they implicitly disagreed with the sister-group relationship between Parastenocarididae and *Psammonitocrella*.

In this work we describe *Psammonitocrella kumeyaayi* sp. nov from the historical collection of late Professor W. Noodt, collected by himself in the state of California, USA, in 1974. An amended diagnosis is offered for the genus, and the position of the new species within the genus *Psammonitocrella* is briefly addressed. Here we discuss an alternative hypothesis for the position of Parastenocarididae within Harpacticoida.

Material and methods

A single male specimen of the new species was sorted from a sample collected by Prof. Wolfram Noodt on 29/03/1974 at a locality identified as San Clemente Canyon (California, USA). The sampling locality is described in Noodt's field notebook and in the sample identification as "wenig fließendes stehendes Wasser", an almost lotic or

a standing water environment or with very low current. After an extensive toponymic search we concluded that Prof. Noodt was referring to the San Clemente Canyon in San Diego County. The San Clemente Canyon is nowadays included in the Marian Bear Memorial Park in the city of San Diego, a linear open space park along a canyon rich in temporary water bodies.

The habitus was drawn from the whole specimen temporarily mounted onto one slide with glycerin as mounting medium; adhesive plastic discs were used to support the cover slip and prevent destruction of the specimen (Kihara and Rocha 2009). Total length of the only specimen available was measured from the tip of the rostrum to the posterior rim of the furca. Once the habitus was drawn, the specimen was dissected under a Leica MZ12.5 microscope (Leica, Wetzlar, Germany). The dissected parts were mounted on slides using glycerin as mounting medium, and preparations were sealed with transparent nail varnish. Drawings were made at 400× and 1000× magnification with a Leica DM 2500 microscope (Leica, Wetzlar, Germany) equipped with Nomarsky interference contrast and a drawing tube.

The terms 'furca' and 'telson' are used according to Schminke (1976). Terminology and homologization of maxillary and maxillipedal structure follow Ferrari and Ivanenko (2008). Therefore, by the application of serial homology, the nomenclature of Huys and Boxshall (1991) for the maxilla (fig. 1.5.5, p. 26) is modified as follows: the praecoxa of the maxilla is hereafter recognized as the syncoxa (praecoxa and coxa fused), the coxa is considered as the basis, and the basis is recognized as the first endopodal segment with claw. Other morphological terms follow Huys and Boxshall (1991).

The diagnosis represents the reconstructed ground pattern of *Psammonitocrella*. It is amended from Karanovic and Hancock (2009: 46). The term "ground pattern" is used in the sense of "Grundmuster" (Ax 1984: 156), and refers to all plesiomorphies and autapomorphies present in the stem species of the genus**.**

Abbreviations used in the text and figures: A1= antennule, A2 = antenna, aes = aesthetasc, ap= apomorphy, benp(s)= basendopod(s), cph = cephalothorax, DAS= distal apical seta; DOS= distal outer seta; enp= endopod, exp(s)= exopod(s), enp1–3 = endopodal segments 1–3, exp1–3 = exopodal segments 1–3, Fu= furca, GF = genital field, IAS= inner apical seta/spine; ms= modified spine, md = mandible, mx1 = maxillule, mx2 = maxilla, mxp = maxilliped, P1–P6= legs 1 to 6, pl= plesiomorphy, Ur1 to 5= first to fifth urosomites.

Results

Order Harpacticoida Sars, 1903
Family Ameiridae Boeck, 1865
Genus *Psammonitocrella* Huys, 2009

Diagnosis amended. Ameiridae. Body small, slender, and cylindrical, without distinct demarcation between prosome and urosome. Integument weakly chitinized, with or without lateral cuticular windows on P2–P3-bearing somites (presence of

these cuticular windows is uncertain for *P. longifurcata* and *P. boultoni*); hyaline posterior fringe of all somites smooth. First pedigerous somite incorporated into cephalosome. Prosome ornamented only with sensilla; Ur ornamented with rows of small spinules. Genital (Ur2) and Ur3 separated in female; GF with single large copulatory pore, wide copulatory duct, and two small semicircular seminal receptacles; single small genital aperture covered by fused reduced P6, without armature or ornamentation. Telson unornamented or ornamented with small spinules and tube pores. Anal operculum unornamented or ornamented with small spinules, wide and convex, not reaching or reaching posterior end of anal somite. Fu slender, tapering distally or cylindrical, slightly divergent, longer than anal somite, with long tube pores in *P. kumeyaayi* sp. nov.; seta VII inserted subdistally, close to inner margin, less than half the ramus length; outer setae I and II inserted on the proximal half of Fu; seta III on the same plane as seta VII; seta VI minute; seta V without breaking plane; seta IV longer, as long as or shorter than ramus. A1 long and slender, eight-segmented in female, 10-segmented, haplocer, and geniculate in male; without seta on short first segment in female, with a seta on the first segment in male. A2 composed of coxa, basis, two-segmented enp and one-segmented exp; exp armed with three setae. Md with narrow cutting edge and two-segmented uniramous palp; basis unarmed; enp with three to five apical setae. Mx1 with praecoxal arthrite armed with three distal claws, one or two minute oral setae, and one or two accessory aboral setae; coxa with two or three apical setae; basis with two to four apical setae; enp present or absent. Mx2 with syncoxal endite armed with a single element, or endite absent; basal endite armed with three elements; enp1 drawn out into a claw, with an accessory seta; remaining endopodal segment represented by one or two setae. Basis of P1 with unmodified inner spine in male, and with or without outer seta; without any other sexual dimorphism in swimming legs; basis of P2 with or without outer seta. Enp of P1 three-segmented; enp of P2 and P3 one- or two-segmented, of P4 reduced to small knob or completely absent; P1 enp1 unarmed, long, reaching distal margin of exp2 or nearly as long as exp1; P1 enp2 unarmed, longer than enp3; P1 enp3 with outer seta, with or without geniculation, inner seta probably geniculated in all species; if enp of P2 and P3 two-segmented, then first segment unarmed, second segment with one apical seta. All swimming legs with three-segmented exps; exopodal segments of P2–P4 subequal in length; P1–P4 exp1 without inner seta; exp2 of P1 without outer spine and with inner seta; exp2 of P2 and P3 with inner seta and outer spine; exp2 of P4 with or without outer spine and with inner seta; exp3 of P1 with two outer spines, two geniculate distal setae, and without inner armature; P2–P4 exp3 without outer spine; P2–P3 exp3 with or without inner apical seta; inner apical seta of P4 exp3 may be transformed into a spine. P5 similar in both sexes; fused to somite or free; with or without recognizable endopodal lobe, and with recognizable exopodal lobe, or exp one-segmented; endopodal lobe (if present) armed with one or two elements; exopodal lobe or exp with four, three, two or only one seta.

Type species. *Psammonitocrella boultoni* Rouch, 1992.

Other species. *Psammonitocrella longifurcata* Rouch, 1992; *P. kumeyaayi* sp. nov.

Table 1. Setal formulae of the swimming legs as hypothesized to occur in the ground pattern of the genus. Roman numerals represent spines; Arabic numerals represent setae.

Legs	Basis	Exopod	Endopod
P1	1-I	I-0, 0-1, II-2-0	0-0, 0-0, 0-I+1*-0
P2	1-0	I-0, I-1, 0-I+2**-0	0-0, 0-1-0+
P3	1-0	I-0, I-1, 0-I+1-0	0-0, 0-1-0+
P4	1-0	I-0, I-1++, 0-I+1-I#	Knob##

*2 setae in *P. kumeyaayi* sp. nov; distal outer seta geniculate.
**I+1 in *P. boultoni* and *P. kumeyaayi* sp. nov. +one-segmented in *P. longifurcata;* 0-1-0.
++0-1 in *P. kumeyaayi* sp. nov. #0-I+1-0 in *P. longifurcata*.
##Absent in *P. kumeyaayi* sp. nov. and in *P. longifurcata*.

Psammonitocrella kumeyaayi sp. nov.

Figs 1–4
http://zoobank.org/16622CED-8D1F-4F39-9132-E7C66AD3A972

Material examined. ***Holotype:*** One male dissected and mounted onto 7 slides (reg. no. SMF 37256/1-7; 1-7 refers to the number of slides).

Type locality: San Clemente Canyon, San Diego, California, USA (32.8446°N, 117.1949°W).

Description of male. Total length 302 µm, measured from rostrum to end of furca. Rostrum not fused to cph, with two sensilla on tip (Fig. 1A). First and second free prosomal segments with large oval window on each side of the body (Fig. 1A). Ur4 and 5 weakly ornamented with small spinules. Pattern of sensilla and pores as depicted (Fig. 1A). Telson weakly ornamented with small spinules on anal operculum; laterally with few spinules and three long tube pores (Fig. 1A; tube pores marked with arrowheads). Fu (Fig. 1A, E) cylindrical, tapering distally, approximately 2.5 times longer than wide, 1.4 times longer than telson, with dorsal pore subdistally and three long tube pores –two on outer margin, one on inner margin (marked with asterisk on Fig. 1E) armed with seven setae; setae I and II inserted dorsally on proximal half, seta I shorter; seta III (Fig. 1A, broken in Fig. 1E) on distal third, longer than seta I, shorter than seta II; seta IV inserted distally on outer margin, longer than seta II; seta V longest (broken in Fig. 1A and E); seta VI inserted distally on inner margin, almost as long as seta I; seta VII broken (Fig. 1A and E), tetra-articulated at basis, inserted dorsally at the same level as seta III. Spermatophore (Fig. 1A, B) occupying almost the whole length of Ur4 and 5 combined.

A1 haplocer (Fig. 2A–C), 10-segmented; armature and ornamentation as follows: 1(1)/2(7)/3(5)/4(2)/5(1ms+4+(1+ae))/6(1ms)/7(3+ms)/8(4ms +1)/9(4)/10(4+acrothek). Acrothek consisting of two setae fused to aesthetasc.

A2 (Fig. 2D, E) basis without abexopodal armature; one-segmented exp with long unipinate seta and two spines with comb tip; enp1 rectangular and smooth; enp2 with two inner marginal spines, four apical geniculated setae, and one geniculate outer seta fused basally to small seta.

Md (Fig. 2 F, G) with oral bulge (marked with asterisk), opposite to md palp. Gnathobase smooth, elongate (Fig. 2F; depicted as shorter in 2G due to a different viewing

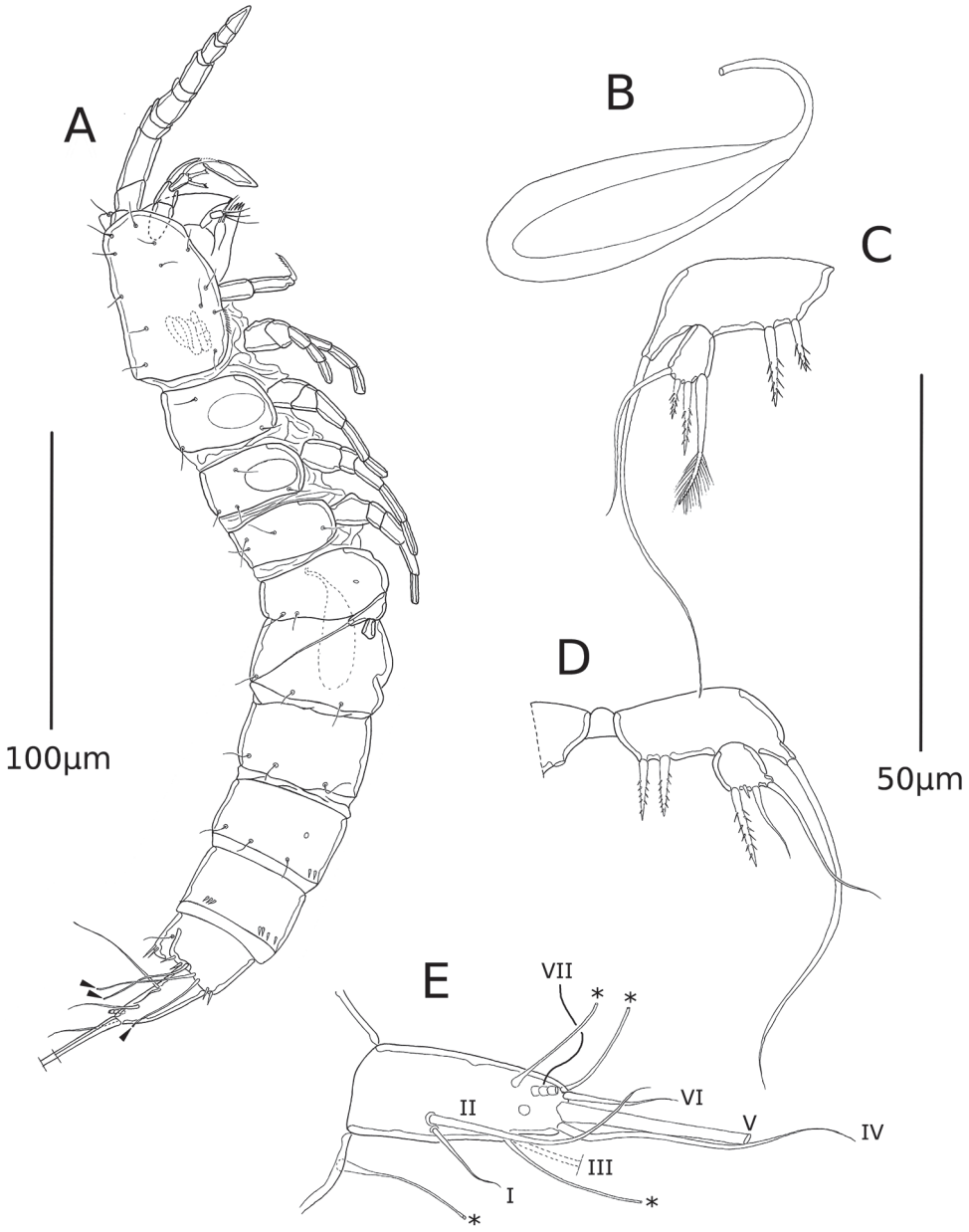

Figure 1. *Psammonitocrella kumeyaayi* sp. nov., male. **A** Lateral habitus of male **B** spermatophore **C** right P5 **D** left P5 **E** furca. Arrowheads on (**A**) and asterisks on (**E**) mark tube pores. Roman numerals indicate each seta on (**E**).

angle) with weakly developed cutting edge; oral margin without distal seta. Palp uniramous, comprising smooth basis and one-segmented enp with five distal setae.

Mx1 (Fig. 2H). Praecoxa, coxa and basis fused. Praecoxal arthrite rectangular; with row of proximal spinules close to the insertion site of the coxal and basal endites; with

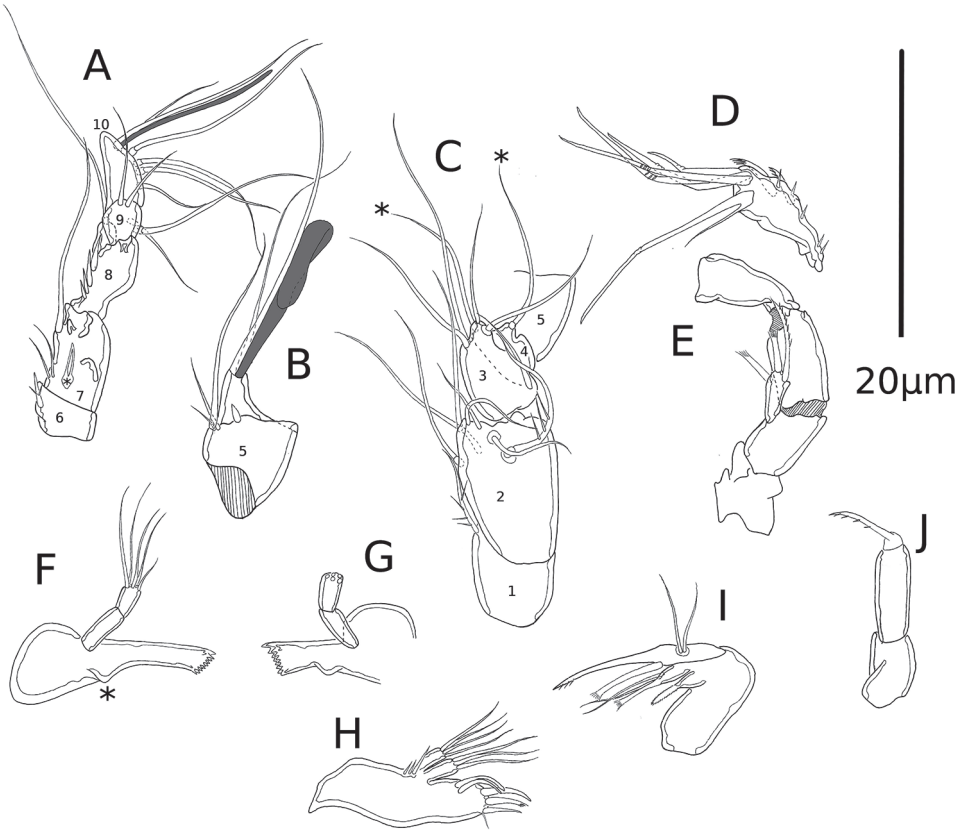

Figure 2. *Psammonitocrella kumeyaayi* sp. nov., male. **A** 6th to 10th A1 segments **B** 5th A1 segment **C** 1st to 5th A1 segments **D** enp2 of A2 **E** A2 with unarmed enp2 **F** md **G** md with unarmed palp **H** mx1 **I** mx2 **J** mxp. Asterisk mark the setae of the 4th A1 segment, and the md oral bulge.

three distal spines, a minute oral seta and two surface aboral setae. Coxal endite with three long apical setae. Basis approximately of the same length of coxal endite, with four long apical setae. Enp and exp absent.

Mx2 (Fig. 2I). Syncoxal endite with modified finely bipinnate spine with rounded tip. Basal endite with spine with comb-like tip and fused to endite, and two setae. Enp1 drawn into claw, proximally with accessory spine with comb-like tip; enp2 represented by two setae.

Mxp (Fig. 2J) prehensile, with smooth syncoxa and basis, the former slightly shorter than the latter. Enp represented by long and slightly curved claw, ornamented with medial-distal row of spinules along concave side.

P1 (Fig. 3A). Intercoxal sclerite smooth, sub-rectangular, wider than long. Coxa with anterior rows of medial, medial-distal, and inner small spinules. Basis with rows of spinules close to insertion site of exp and enp, and at base of outer element; with inner spine and outer seta, the former not sexually dimorphic. Exp three-segmented; exp1 with outer row of spinules and outer unipinnate spine; exp2 without outer spine,

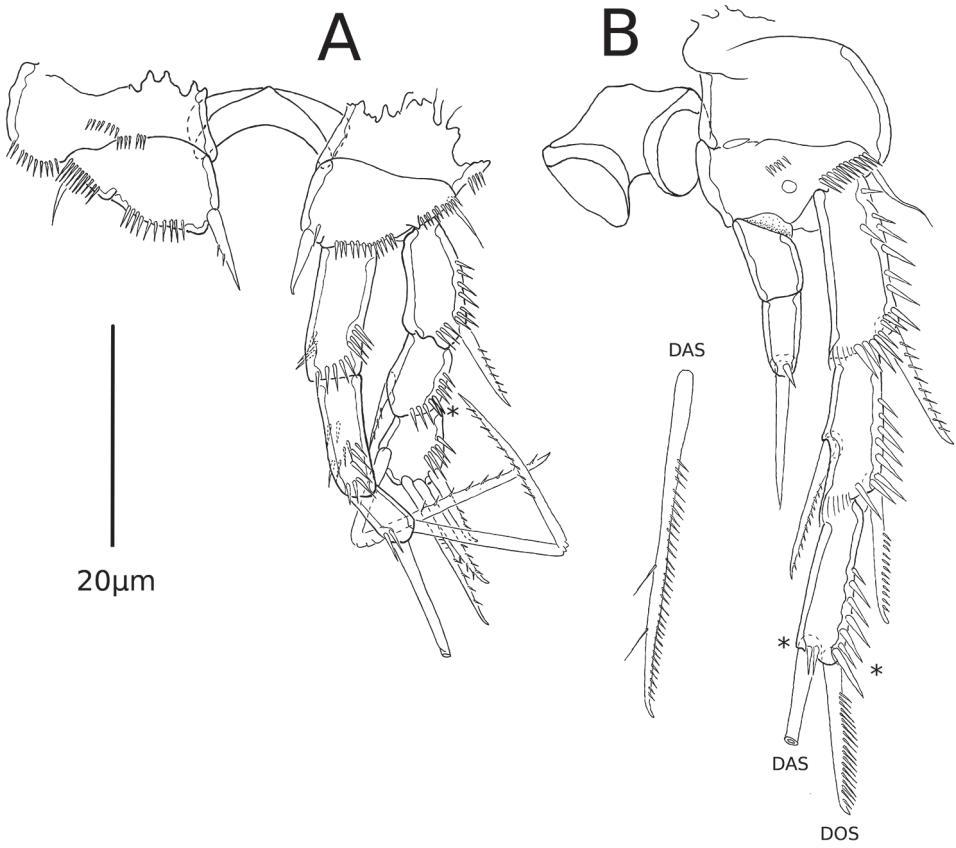

Figure 3. *Psammonitocrella kumeyaayi* sp. nov., male. **A** P1 **B** P2. Asterisks mark the position of apomorphies represented by the loss of spines or setae. DAS= Distal apical seta; DOS= distal outer seta.

with outer row of spinules and with short unipinnate inner seta; exp3 with outer row of spinules, two unipinnate outer spines and two unipinnate and geniculate distal setae. Enp three-segmented; enp1 unarmed, slightly longer than exp1, reaching middle of exp2, with inner, distal and outer rows of spinules; enp2 unarmed, shorter than enp1, with inner, distal, outer and posterior rows of spinules; enp3 shortest, with inner row of spinules, one distal inner and one geniculate distal outer seta, the latter unipinnate distally.

P2 (Fig. 3B). Intercoxal sclerite almost as wide as long, with proximal hump, outer distal extensions rounded, medial-distal part concave. Coxa unornamented. Basis with medial row of spinules, with transverse spinular row close to insertion of exp and at base of outer short seta; with medial pore. Exopodal segments subequal in size; exp1 with outer and distal rows of spinules, with inner distal hyaline frill and unipinnate outer spine; exp2 ornamented as in exp1, with unipinnate outer spine and unipinnate inner spiniform seta; exp3 with outer and distal rows of spinules, with outer unipinnate spine and inner spiniform seta, the latter with pinnate outer

margin and with two inner setules. Enp two-segmented, slightly longer than exp1; enp1 unornamented, unarmed; enp2 with small spinule and spiniform distal seta.

P3 (Fig. 4A) with intercoxal sclerite as in P2. Triangular praecoxa and square coxa unornamented. Basis with row of spinules near insertion of enp, with row of spinules between exp and outer long seta, with proximal outer pore. Exp three-segmented, exp1–3 subequal in size; exp1 with outer and distal rows of spinules, with inner hyaline frill, and outer unipinnate spine; exp2 ornamented as in exp1, with unipinnate outer spine and unipinnate inner spiniform seta; exp3 with outer row of spinules, outer unipinnate spine and inner unipinate seta. Enp two-segmented, almost as long as exp1; enp1 unornamented, unarmed; enp2 with small spinule and spiniform seta distally.

P4 (Fig. 4B). Intercoxal sclerite wider than long, outer distal extensions short, with proximal and distal-medial parts concave. Coxa unornamented. Basis without

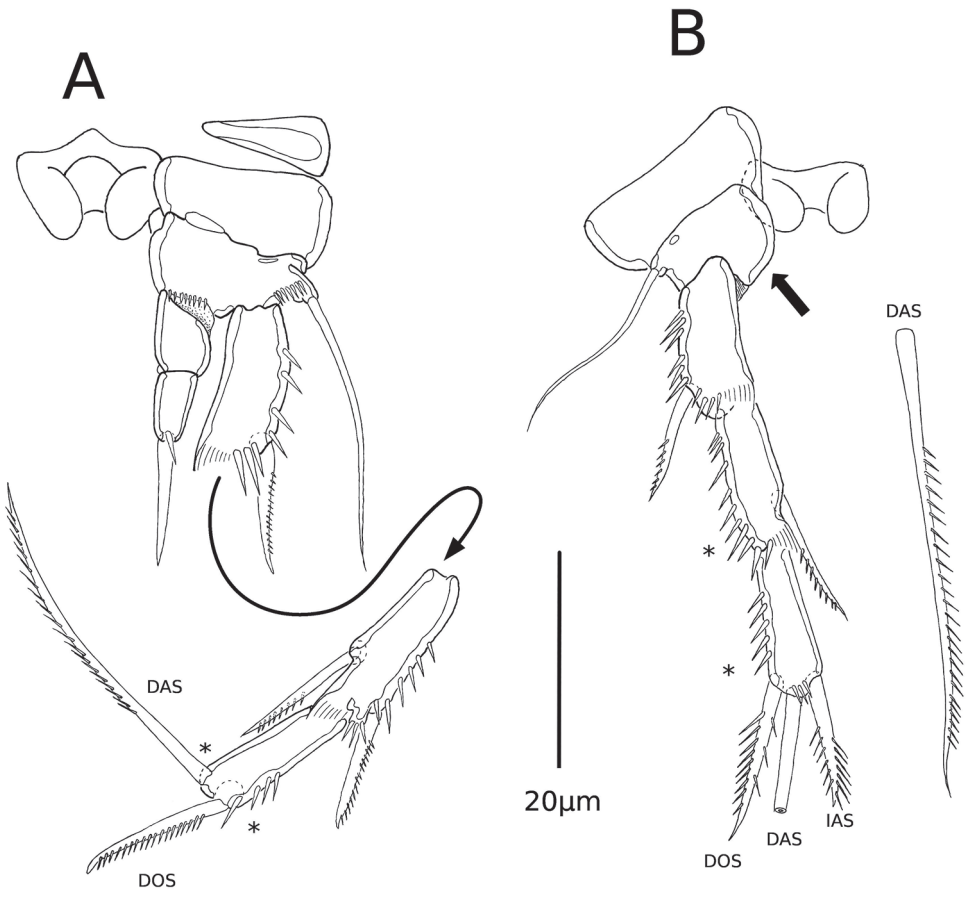

Figure 4. *Psammonitocrella kumeyaayi* sp. nov., male. **A** P3 with detached exp2 and exp3 **B** P4. Asterisks mark the position of apomorphies represented by the loss of spines or setae. Arrow indicates the absence of the enp. DAS= Distal apical seta; DOS= distal outer seta; IAS= inner apical seta.

Table 2. Setal formulae of the swimming legs. Roman numerals represent spines; Arabic numerals represent setae and spiniform setae.

Legs	Basis	Exopod	Endopod
P1	1-I	I-0, 0-1, II-2-0	0-0, 0-0, 0-2-0
P2	1-0	I-0, I-1, 0-I+1-0	0-0, 0-1-0^{+}
P3	1-0	I-0, I-1, 0-I+1-0	0-0, 0-1-0^{+}
P4	1-0	I-0, 0-1, 0-I+1-I	absent

ornamentation, with proximal outer pore, and outer long seta. Exp three-segmented; exp1–3 subequal in size; exp1 with outer and distal spinules, with inner hyaline frill, and outer unipinnate spine; exp2 ornamented as in exp1, without outer spine, with unipinnate inner spiniform seta; exp3 with outer row of spinules, with outer bipinnate spine, distal long unipinnate seta, and inner bipinnate spine. Enp absent.

P5 (Fig. 1C, D). Rectangular benps united by small intercoxal sclerite, with long outer basal seta, and two small bipinnate spines on endopodal lobe. Exp one-segmented, square, with four elements (setae and spines) of variable shape, size and ornamentation in left (Fig. 1C) and right limbs (Fig. 1D); right exp (Fig. 1C) with long and smooth outer seta, short bipinnate distal spine, and comparatively longer bipinnate distal spine, and inner seta, the latter with tuft of setules distally on both sides; left exp (Fig. 1D) with long and smooth outer seta (shorter than in the right limb), distal seta smooth, a distal tiny element probably representing a reduced spine, and an inner bipinnate seta.

P6 (not shown) represented by unarmed cuticular flap.

Etymology. The specific epithet "*kumeyaayi*" refers to the Kumeyaay native American people, who inhabited the area of San Diego County for 10,000 years. Evidence of their presence still remains in San Clemente Canyon.

Remarks. Female unknown. The presence of integumental windows on the third and fourth pedigerous somites was reported by Karanovic and Hancock (2009: 11, table 2; character 2) for most species analyzed by them, including *Eduardonitocrella mexicana*, *S. orghidani*, and their closely related species *Psammonitocrella boultoni* and *P. longifurcata*. This character was, however, never mentioned by Rouch (1992) or illustrated in the original description, and Karanovic and Hancock (2009) did not mention whether they inspected the type material of *Psammonitocrella*. However, it is possible that integumental windows are present on some pedigerous somites within the genus *Psammonitocrella*, as indicated by the presence of lateral integumental windows on the second and third pedigerous somites of *Psammonitocrella kumeyaayi* sp. nov. The probable loss of lateral integumental windows in *Psammonitocrella boultoni* and *P. longifurcata* should be considered as derived. The presence of lateral integumental windows is a potential synapomorphy for a larger group of groundwater ameirids as proposed by Karanovic and Hancock (2009). The absence of the outer spine of the P4 exp2 is an autapomorphy for the new species.

Discussion

According to Karanovic and Hancock (2009), the genus *Psammonitocrella* would have fitted nicely into the original diagnosis of the genus *Stygonitocrella* as defined by Petkovski (1976). However, Petkovski's (1976) diagnosis is too inaccurate and many other taxa would fit that diagnosis. The careful comparison of the species included within *Stygonitocrella* before Karanovic and Hancock's (2009) revisionary work, and the species included here in *Psammonitocrella* revealed that both genera differ in the armature of P1 exp2, P2–P4 exp3, and shape of the furca, with major reductions in the armature of P1–P4 and furca elongation in *Psammonitocrella*. However, one could still assume that *Psammonitocrella* is a junior synonym of *Stygonitocrella*, and that the constituent taxa of the former belong to a derived group within the latter. This assumption is not supported by Karanovic and Hancock (2009). They (Karanovic and Hancock 2009) analyzed the phylogenetic affinities among the species previously attributed to *Stygonitocrella*, and concluded that the generic diagnosis of the genus should be emended and the genus rearranged to include only four species: the type species *S. montana* (Noodt, 1965) from Argentina, *S. dubia* (Chappuis, 1937) and *S. guadalfensis* Rouch, 1985 from Spain, and *S. sequoyahi* Reid, Hunt & Stanley, 2003 from the USA. Other species previously included within *Stygonitocrella* were reallocated into *Eduardonitocrella* Karanovic & Hancock, 2009, *Reidnitocrella* Karanovic & Hancock, 2009, and *Megastygonitocrella* Karanovic & Hancock, 2009. If the hypothesis proposed by Karanovic and Hancock (2009) is accepted, *Psammonitocrella* should be considered as monophyletic and closely related to the monotypic genera *Inermipes* Lee & Huys, 2002, *Neonitocrella* Lee & Huys, 2002, and *Eduardonitocrella* (*Stygonitocrella orghidani* was relegated to *incertae sedis* by Karanovic and Hancock 2009, but appears as the sister group of *Eduardonitocrella* in the same publication). It is our opinion that Karanovic and Hancock (2009) restricted too much the ingroup, including in their analysis only freshwater ameirids with one-segmented P4 enp, and one- or two-segmented P2 and P3 enp. However, both reductions are known to occur in the Parastenocarididae, and the reduction of the P2–P4 enp to a two-segmented structure occurs in or within some interstitial genera of ameirids (i.e., *Leptameira* Huys, 2009; *Parevansula* Guille & Soyer, 1966; *Pseudoleptomesochrella* Lang, 1965; *Psyllocamptus* Scott, 1899) and in some genera assigned to the Leptopontiidae Lang, 1948 (i.e. P2-P4 enp, *Bereraia* Huys, 2009; *Leptopontia* Scott, 1902; *Parasewellina* Cottarelli, Saporito & Puccetti, 1986; *Prosewellina* Mielke, 1987; *Psammopsyllus* Nicholls, 1945; *Sewellina* Krishnaswamy, 1956; *Syrticola* Willems & Claeys, 1982).

In fact, the 250+ species of the Parastenocarididae would code in the cladistic analysis of Karanovic and Hancock (2009) with exactly the same character states as in *Psammonitocrella*—Karanovic and Hancock (2009) ignored this taxon—forming a cluster with *Psammonitocrella*, and evidencing their sister-group relationship.

One important achievement of Martínez Arbizu and Moura (1994) was the discovery and justification of the sister-group relationship between the Parastenocarididae and *Psammonitocrella*. In an evolutionary context this is relevant because this evidenced

that the Parastenocarididae—one of the largest continental groundwater family of the Harpacticoida—did not evolve from pre-adapted marine interstitial ancestors, but from freshwater interstitial (groundwater) ancestors. This has deep implications for the understanding of the colonization and evolution of groundwater fauna. Because both the Parastenocarididae and Ameiridae had a family rank at that time, placing *Psammonitocrella* as sister group of the Parastenocarididae unequivocally implies its exclusion from the Ameiridae. Martínez Arbizu and Moura (1994) however refrained from giving a full family rank to *Psammonitocrella*, but also from including this genus into the Parastenocarididae, waiting for more robust evidence.

Lee and Huys (2002) listed *Psammonitocrella* as belonging to the Ameiridae without properly discussing Martínez Arbizu and Moura's (1994) hypothesis or proposing synapomorphies for the inclusion of *Psammonitocrella* into the Ameiridae. However, Lee and Huys (2002) were uncritically followed by subsequent researchers (see Reid et al. 2003; Boxshall and Halsey 2004; Karanovic 2004, 2006; Karanovic and Hancock 2009), and *Psammonitocrella* was considered to belong to the Ameiridae without proper phylogenetic analyses.

The simple removal of a genus from one family to another without proper discussion is naive, and it does not solve the real problem. The phylogenetic position of *Psammonitocrella* cannot be solved without discussing the position of its sister group, Parastenocarididae, nor without including in the discussion the Ameiridae as a whole. Note that also Martínez Arbizu and Moura (1994) did not include all the Ameiridae in their discussion. They just defined the Ameiridae as displaying the synapomorphic modification of the basal inner seta of P1 in the males. It is interesting to note that all Ameiridae discussed by Karanovic and Hancock (2009) display this characteristic sexually dimorphic seta in the males, but this seta is not modified in the Parastenocarididae and *Psammonitocrella*. Martínez Arbizu and Moura (1994) argued consequently for the retention of the plesiomorphic state of this character in the Parastenocarididae and *Psammonitocrella*, rather than a secondary reduction.

The sister-group relationship between the Parastenocarididae and *Psammonitocrella* allows for only two systematic scenarios.

1) Parastenocarididae + *Psammonitocrella* are the sister group of the Ameiridae (or any other family). In this case, a new family should be proposed for *Psammonitocrella*, and the Parastenocarididae would be composed only by those species with the synapomorphic characters proposed by Corgosinho et al. (2007), Ranga-Reddy et al. (2014), and Corgosinho et al. (2017) (e.g., grasping male P3; one-segmented male and female P2-P4 enp; absence of outer spine on the P2 and P4 exp2 of both male and female, etc.).

   or

2) Parastenocarididae + *Psammonitocrella* is a monophyletic group within the Ameiridae. In this case the family rank of the Parastenocarididae would be

compromised. "Parastenocarididae" would be a junior subjective synonym of "Ameiridae", and the Parastenocarididae + *Psammonitocrella* would be a derived group within the Ameiridae.

In an evolutionary context, it would make sense that the Parastenocarididae evolved from a lineage of freshwater ameirids that became interstitial in continental waters and colonized aquifers and groundwaters. The analysis offered by Karanovic and Hancock (2009) convincingly places *Psammonitocrella* as phylogenetically related to a group of freshwater interstitial ameirids, but they unfortunately ignored the Parastenocarididae.

We advocate for the consideration of alternative 2 as the most realistic evolutionary working scenario.

If we accept that *Psammonitocrella* is an Ameiridae, the evidence suggesting its sister-group relationship with the Parastenocarididae—both sharing the loss of the inner seta on the enp1 of the P1—indicates that the Parastenocarididae should be included into the Ameiridae. But the relationships to marine taxa as discussed by Martínez Arbizu and Moura (1994) would remain unresolved. *Psammonitocrella*, Parastenocarididae and Leptopontiidae share the loss of the inner seta of the enp2 of P1 and most importantly, the loss of the outer spine of the exp2 of P1—which is a rare reduction within Harpacticoida (Martínez Arbizu and Moura 1994)—and could indicate that the Leptopontiidae should also be incorporated into the Ameiridae.

According to Boxshall and Jaume (2000), to treat the freshwater ameirids as the product of a single independent colonization event probably represents an underestimate. Therefore, future phylogenetic studies should include both freshwater and marine ameirids, especially those interstitial marine genera with reduced P2–P4 enp and reduced inner and outer armature of P2–P4 exp3, to test the hypothesis that some freshwater taxa are more related to marine ones, and that the invasion of the fresh water by this family followed multiple waves. In addition, the position of the Parastenocarididae and Leptopontiidae within the ameirid-like harpacticoids should be tested.

The family Parastenocarididae can be easily accommodated within the Ameiridae as the sister group of *Psammonitocrella*. Within the Parastenocarididae the P1 enp is reduced to a two-segmented enp [three-segmented P1 enp in *Psammonitocrella*], and the inner seta of P1 exp2 is lost [present in *Psammonitocrella*]; the enp of P2 and P3 is one-segmented [probably two-segmented in the ground pattern of *Psammonitocrella*], and the exp2 of P2 and P4 lost the inner and outer elements [present in *Psammonitocrella*]. The outer spine of the P4 exp2 is absent in the Parastenocarididae and in *P. kumeyaayi* sp. nov. For the mouthparts, the md has a uniramous palp in both *Psammonitocrella* and the Parastenocarididae (two-segmented in the former, without armature on the proximal segment, and one-segmented in the latter), and the mx1 has a reduced distal armature of three spines on the praecoxal arthrite of both taxa. Except for *E. mexicana*, the distal rim of the anal operculum of the species studied by Karanovic and Hancock (2009) reaches the posterior margin of the telson as in the Parastenocarididae.

Taking this into account, future studies are necessary to unfold the relationship between the Ameiridae and Parastenocarididae. We believe that only a phylogenetic

analysis of the Ameiridae and Parastenocarididae, with a large taxonomic coverage based on both traditional morphological and multi-gene datasets is suitable to undisputedly determine which one of the two hypotheses mentioned above is better supported by the data. Unfortunately, within the Harpacticoida the taxon sampling for molecular work is still in its infancy.

The monophyly of *Psammonitocrella* can be supported by some reductions of the armature of P1 to P4, and the length of the furca. Of remarkable importance is the cylindrical furca which is also longer than the telson (ap), the basis of P1 in male with unmodified inner spine (ap), loss of the outer spine on the P1 exp2 (ap), loss of the outer spine of the exp3 of P2 (ap), P3 (ap) and P4 (ap), loss of the inner apical seta (IAS) on the exp3 of P3 (ap) (Karanovic and Hancock 2009), transformation of the IAS of the P4 exp3 into a spine (ap), reduction of the P4 enp to a small knob or its complete loss (ap).

Nowadays the genus *Psammonitocrella* is composed of *P. boultoni* and *P. longifurcata* from Sycamore creek (Arizona, USA), and *P. kumeyaayi* sp. nov. from the San Clemente Canyon, San Diego (California, USA). The new species differs remarkably from *P. boultoni*, and *P. longifurcata* in the loss of the outer spine of the P4 exp2 (ap), in the presence of a one-segmented P5 exp (pl), and in the presence of an outer seta of the basis of P1 (pl) and P2 (pl). The one-segmented exp of the P5 of *P. kumeyaayi* sp. nov. closely resembles that of *P. boultoni*. In the former species it is armed with four elements —one very reduced spine on the left limb—, and three setae are present in the exopodal lobe of the P5 of *P. boultoni*. However, the benp of *P. kumeyaayi* sp. nov. is armed with two spines, but it is armed with only one spine in *P. boultoni*. The enp of the P2 and P3 is two-segmented in both *P. boultoni* and *P. kumeyaayi* sp. nov., whereas the P2 and P3 enp is one-segmented in *P. longifurcata*. The shape and length of the furca is similar in *P. boultoni* and *P. kumeyaayi* sp. nov., and it is much longer in *P. longifurcata*.

The two-segmented P2 and P3 enps of *P. boultoni* and *P. kumeyaayi* sp. nov. are definitely plesiomorphic within the genus. The one-segmented P5 exp and the presence of two spines on the benp of P5 of *P. kumeyaayi* sp. nov are also considered plesiomorphic. The long furca of *P. longifurcata* seems to be an apomorphic condition within the genus. The presence of the outer seta on the basis of the P1 and P2 are plesiomorphic for *P. kumeyaayi* sp. nov. Considering this, it seems possible that *P. longifurcata* and *P. boultoni* forms a monophyletic group within *Psammonitocrella*, sharing the absence of the outer basal seta of P1 and P2, what could be also supported by the fact that *P. longifurcata* and *P. boultoni* occur in sympatry. The absence of the outer seta on the basis of P1 and P2 is uncommon within Harpacticoida, whilst the reduction or loss of the enp may have occurred convergently many times. Appendage reductions, character losses, and miniaturization (i.e., the evolution of extremely small adults) are common denominators of the 'darkness syndrome' of many stygobionts (Galassi 2009). Consequently, the loss of the enp could be a convergent event in both *P. longifurcata* and *P. kumeyaayi* sp. nov. Alternatively, the absence of the P4 enp could be the ancestral con-

dition for *Psammonitocrella*, and the small knob representing the P4 enp of *P. boultoni* could be attributed to secondary expression, i.e., it is an autapomorphy for this species. However, although reductions such as the loss of an enp could occur convergently within monophyletic groups, without a proper phylogenetic analysis and observation of the types studied by Rouch (1992), it is difficult to establish how the three species of *Psammonitocrella* are related to each other.

Key to the species of *Psammonitocrella*

1 Enp2 of P4 with outer spine **2**

– Exp2 of P4 without outer spine; enp two-segmented in the P2 and P3; enp of P4 absent; armature of the exp3 of P2–P3 (0-I+1-0); armature of the exp-3 of P4 (0-I+1-I); P5 with an outer seta, benp with two spines, exp one-segmented, with asymmetric armature; telson and furca with long tube pores; furcal ramus about 2.5 longer than wide..... ***P. kumeyaayi* sp. nov.**

2 Two-segmented enp of P2 and P3; enp P4 reduced to a knob; armature P2 and P3 exp3 (0-I+1-0); armature P4 exp3 (0-I+1-I); P5 with an outer seta, benp with a single seta, expopodal lobe fused to benp and armed with 3 setae; furcal ramus about 4 times longer than wide..... ***P. boultoni***

– One-segmented enp of P2 and P3; enp P4 absent; armature of P2 exp3 (0-I+2-0); armature of P3–P4 exp3 (0-I+1-0); P5 with an outer seta, reduced into a small plate, with asymmetric armature; furcal ramus almost 7 times longer than wide..... ***P. longifurcata***

Conclusions

1) A new species of the freshwater ameirid genus *Psammonitocrella* is proposed for California (USA). The new species can be clearly distinguished from its congeners by the absence of the outer spine on P4 exp2 and the presence of a one-segmented P5 exp.
2) *P. kumeyaayi* sp. nov. is probably the sister group of a monophylum formed by *P. boultoni* and *P. longifurcata*. However, without the study of the species described by Rouch (1992), it is difficult to establish how the three species are related to each other.
3) If *Psammonitocrella* is an Ameiridae, the evidence suggesting its sister-group relationship with the Parastenocarididae indicates that the Parastenocarididae should be included into the Ameiridae.
4) Future phylogenetic studies should include both freshwater and marine ameirids, to test the hypothesis that some freshwater taxa are more related to marine ones, and that the invasion of the fresh water by this family followed multiple waves. In addition, the position of the Parastenocarididae and Leptopontiidae within the ameirid-like harpacticoids should be tested.

Acknowledgements

We would like to thank the CeDAMar (Census of Diversity of Abyssal Marine Life), which have supported the first author, granting him with a postdoctoral scholarship from 2004 to 2008. We are also indebted to the DZMB (Senckenberg am Meer, Wilhelmshaven, Germany) for the logistic support during this work. This study would not have been possible without the study of Noodt´s collection. We express our special gratitude to Dr Ahmed Ahnert who curated Noodt´s material after he passed away and put it at our disposal for the present study at the DZMB. The work of the first author was supported by FAPEMIG (CRA–BPV-00393-16 and CRABPV-00547-17). We would like to thank Dr Thomas Glatzel, Professor Dr Samuel Gómez and an anonymous reviewer for their valuable comments and corrections of the manuscript.

References

Ax P (1984) Das Phylogenetische System. Gustav Fischer Verlag, Stuttgart, 349 pp.

Boxshall GA, Defaye D (2008) Global diversity of copepods (Crustacea: Copepoda) in freshwater. In: Freshwater Animal Diversity Assessment. Hydrobiologia 595(1): 195–207. https://doi.org/10.1007/s10750-007-9014-4

Boxshall GA, Jaume D (2000) Making waves: The repeated colonization of fresh water by copepod crustaceans. Advances in Ecological Research 31: 61–79. https://doi.org/10.1016/S0065-2504(00)31007-8

Boxshall GA, Halsey SH (2004) An Introduction to Copepod Diversity. The Ray Society, London, 966 pp.

Corgosinho, PHC, Martínez Arbizu P (2010) Ameiridae Boeck and Argestidae Por revisited, with establishment of Parameiropsidae, a new family of Harpacticoida (Crustacea, Copepoda) from deep-sea sediments. Helgoland Marine Research 64(3): 223–255. https://doi.org/10.1007/s10152-009-0185-4

Corgosinho PHC, Martínez Arbizu P, Santos-Silva EN (2007) Three new species of *Remaneicaris* Jakobi, 1972 (Copepoda, Harpacticoida, Parastenocarididae) from the Ribeirão do Ouro River, Minas Gerais, Brazil, with some remarks on the groundpattern of the Parastenocarididae. Zootaxa 1437: 1–28.

Corgosinho PHC, Schizas NV, Previattelli D, Rocha CEF, Santos-Silva EN (2017) A new genus of Parastenocarididae (Copepoda, Harpacticoida) from the Tocantins River basin (Goiás, Brazil), and a phylogenetic analysis of the Parastenocaridinae. Zoosystematics and Evolution 93(1): 167–187. https://doi.org/10.3897/zse.93.11602

Ferrari FD, Ivanenko VN (2008) The identity of protopodal segments and the ramus of maxilla 2 of copepods (Copepoda). Crustaceana 81: 823–835. https://doi.org/10.1163/156854008784771702

Galassi DMP (2001) Groundwater copepods: diversity patterns over ecological and evolutionary scales. Hydrobiologia 453/454: 227–253. https://doi.org/10.1023/A:1013100924948

Galassi DMP (2009) Diversity, ecology and evolution of groundwater copepods. Freshwater Biology 54: 691–708. https://doi.org/10.1111/j.1365-2427.2009.02185.x

Huys R, Boxshall GA (1991) Copepod Evolution. The Ray Society, London, 468 pp.

Karanovic T (2004) Subterranean Copepoda from Arid Western Australia. Crustaceana Monographs 3, Brill, Leiden, 366 pp.

Karanovic T (2006) Subterranean copepods (Crustacea, Copepoda) from the Pilbara region in Western Australia. Records of the Western Australian Museum, Supplement 70: 1–239. https://doi.org/10.18195/issn.0313-122x.70.2006.001-239

Karanovic T, Hancock P (2009) On the diagnostic characters of the genus *Stygonitocrella* (Copepoda, Harpacticoida), with descriptions of seven new species from Australian subterranean waters. Zootaxa 2324: 1–85. https://doi.org/10.11646/zootaxa.2324.1.1

Kihara TC, Rocha CEF (2009) Técnicas para estudo taxonômico de copépodes harpacticóides da meiofauna marinha. Asterisco, Porto Alegre, 96 pp.

Lee W, Huys R (2002) A new genus of groundwater Ameiridae (Copepoda, Harpacticoida) from boreholes in Western Australia and the artificial status of *Stygonitocrella* Petkovski, 1976. Bulletin of the Natural History Museum, London (Zoology) 68: 39–50. https://doi.org/10.1017/S0968047002000055

Martínez Arbizu P, Moura G (1994) The phylogenetic position of the Cylindropsyllinae Sars (Copepoda, Harpacticoida) and the systematic status of the Leptopontiinae Lang. Zoologische Beiträge 35: 55–77

Petkovski TK (1976) Drei neue *Nitocrella*-Arten von Kuba, zugleich eine Revision des Genus *Nitocrella* Chappuis (s. restr.) (Crustacea, Copepoda, Ameiridae). Acta Musei Macedonici Scientiarum Naturalium 15: 1–26.

Ranga Reddy Y, Totakura VR, Corgosinho PHC (2014) *Himalayacaris alaknanda* n. gen., n. sp. (Copepoda: Harpacticoida: Parastenocarididae) from the hyporheic zone of a himalayan river, Northern India. Journal of Crustacean Biology 34: 801–819. https://doi.org/10.1163/1937240X-00002281

Reid JW, Hunt GW, Stanley EH (2003) A new species of *Stygonitocrella* (Crustacea: Copepoda: Ameiridae), the first report of the genus in North America. Proceedings of the Biological Society of Washington 116: 996–1006.

Rouch R (1986) Copepoda: les Harpacticoïdes souterrains des eaux douces continentales. In: Botosaneanu L (Ed.) Stygofauna Mundi: A Faunistic, Distributional and Ecological Synthesis of the World Fauna Inhabiting Subterranean Waters (Including the Marine Interstitial). Brill, Leiden, 321–355.

Rouch R (1992) Un nouveau genre d'Ameiridae (Copepoda, Harpacticoida) dans le milieu hyporhéique d'un cours d'eau de l'Arizona. Stygologia 7: 149–157.

Schminke HK (1976) The ubiquitous telson and the deceptive furca. Crustaceana 30: 292–300. https://doi.org/10.1163/156854076X00657

Walter TC, Boxshall G (2020) World of Copepods database. Ameiridae Boeck, 1865. World Register of Marine Species http://www.marinespecies.org/aphia.php?p=taxdetails&id=115135 [Accessed on 2020-10-17]

ZooKeys 996: 37–58 (2020)
doi: 10.3897/zookeys.996.54187
https://zookeys.pensoft.net

RESEARCH ARTICLE

A peer-reviewed open-access journal
ZooKeys
Launched to accelerate biodiversity research

Descriptions of four new dextral land snails of the genus *Camaena* (Gastropoda, Eupulmonata, Camaenidae) from south China

Pei Wang[1], Mei-Ling Hu[1], Jun-Hong Lin[1,2], Hai-Fang Yang[3], Xiao-Jing Li[1], Wei-Chuan Zhou[1]

1 *Key Laboratory of Molluscan Quarantine and Identification of GACC, Fuzhou Customs District, Fujian 350001, China* **2** *College of Plant Protection, Fujian Agriculture and Forestry University, Fuzhou, Fujian 350002, China* **3** *National Wetland Museum of China, Hangzhou, Zhejiang, 310013, China*

Corresponding author: Wei-Chuan Zhou (wczhou@163.com); Mei-Ling Hu (93770092@qq.cn)

Academic editor: M.Schilthuizen | Received 12 May 2020 | Accepted 6 November 2020 | Published 24 November 2020

http://zoobank.org/CF98F8DE-F863-419E-B904-183D85779CAB

Citation: Wang P, Hu M-L, Lin J-H, Yang H-F, Li X-J, Zhou W-C (2020) Descriptions of four new dextral land snails of the genus *Camaena* (Gastropoda, Eupulmonata, Camaenidae) from south China. ZooKeys 996: 37–58. https://doi.org/10.3897/zookeys.996.54187

Abstract

In this study, four new dextral camaenid from China are reported, based on shell morphology, reproductive system anatomy, and molecular phylogenetic analyses: *Camaena funingensis* Zhou, Wang & Lin, **sp. nov.**, *Camaena gaolongensis* Zhou, Wang & Lin, **sp. nov.**, *Camaena maguanensis* Zhou, Wang & Hu, **sp. nov.**, and *Camaena yulinensis* Zhou, Wang & Hu, **sp. nov.** Detailed descriptions of the morphological characteristics including shells and genitalia, DNA sequences, and living environments of the four new species are provided, with further comparisons with congeners.

Keywords

Anatomy, *Camaena*, molecular biology, shell morphology, terrestrial snail

Introduction

The genus *Camaena* was established by Albers (1850). It is the speciose type genus in the family Camaenidae, with the type species *Helix cicatricosa* Müller, 1774. The species in this genus are mainly distributed throughout southern China, Indochina, and

beyond in Southeast Asia, and most are locally endemic (Pilsbry 1894; Zilch 1959–1960, 1964; Richardson 1985; Chen and Gao 1987; Ding et al. 2016; Inkhavilay et al. 2019). The genus was divided into five subgenera (*Camaena* Albers, 1850, *Camaenella* Pilsbry, 1893, *Pseudobba* Moellendorff, 1891, *Pancala* Kuroda & Habe, 1949, *Miyakoia* Minato, 1980) on the basis of classifications by Pilsbry (1894), Kuroda and Habe (1949), Zilch (1959–1960), and Vaught (1989). A recent molecular phylogeny (Hoso et al. 2010) and anatomical study (Hwang 2012) suggested that *Pancala* and *Miyakoia* should be synonyms of the confamilial genus *Satsuma*.

There are 24 species of the genus distributed in southern China belonging to two subgenera, *Camaena* and *Camaenella*. Twenty-three species belong to *Camaena* (Yen 1939; Chen and Zhang 1999; Schileyko 2003; Ai et al. 2016; Ding et al. 2016), and only one species is in *Camaenella* (Pilsbry 1894; Yen 1939; Chen and Zhang 1999). The subgenus *Camaenella* was treated as a synonym of *Camaena* or as a genus in its own right by some scholars (Chen and Gao 1987; Chen and Zhang 1999). In this article, *Camaenella* will be considered as a valid subgenus.

Camaena species are divided into a sinistral group and a dextral one. They are usually characterized by a moderately solid shell with scar-like protrusions or malleations, 4.5–5.5 slightly convex whorls, a brown or yellow surface with red or puce spiral bands, and reflexed aperture margins (Schileyko 2003; Ai et al. 2016). The classification of *Camaena* has mainly relied on the shell features. Anatomical and molecular studies of *Camaena* are rare, except for the sinistral and the newly described species (Chen and Zhang 1999; Ai et al. 2016; Ding et al. 2016; Páll-Gergely et al. 2016; Wu et al. 2019). Historically, the classification of this genus is rather confused. For the sinistral group, the taxonomic status has always been controversial, and scientific names have been revised repeatedly. Ding et al. (2016) revised *C. cicatricosa* as four species, *C. cicatricosa*, *C. inflata* (Möllendorff, 1885), *C. obtecta* (Fischer, 1898), and *C. connectens* (Dautzenberg & Fischer, 1906), and described one new species *C. poyuensis* Zhou, Wang & Ding, 2016 using morphological and molecular studies. In the same year, Ai et al. (2016) described two new species *C. lingyunensis* Zhou & Lin, 2016 and *C. detianensis* Zhou & Lin, 2016 according to shell morphology, reproductive system and molecular biology. Thus, the sinistral *Camaena* group contains 12 species or subspecies to date (Schileyko 2003; Ai et al. 2016; Ding et al. 2016). The dextral group can be divided into three informal subgeneric groups according to the morphological characteristics of the shell, especially the shape and location of the carina.

1. Group I possesses an acute and moderate carina on the body whorl. This group could be further divided into two categories by shell height i.e., a relatively low and flat spire, which includes *C. longsonensis* (Morlet, 1891), *C. jinpingensis* Chen, Zhang & Li, 1990 and *C. vorvonga* (Bavay & Dautzenberg, 1900); a relatively high spire, e.g., *C. vayssierei* (Bavay & Dautzenberg, 1909).
2. Group II possesses a blunt carina, which is placed on the higher or middle parts of the body whorl, such as *C. vulpis* (Gredler, 1887), *C. leonhardti* (Möllendorff, 1888), and *C. choboensis* (Mabille, 1889).

3. Group III possesses a smooth periphery, e.g., *C. hainanensis* (Adams, 1870) and *C. xanthoderma* (Möllendorff, 1882).

In this study, the authors have examined many specimens collected in Guangxi and Yunnan in southern China between 2013 and 2015, and discovered four new dextral species on the basis of morphological, anatomical, and molecular evidence, and living environments.

Materials and methods

Specimens were collected by the authors from several sites in China (Fig. 1). The longitude and latitude were recorded using a GPS. The map was established by MapInfo Professional 15.0. The live adults were drowned in water for 12–24 hours, and then killed in hot water. Soft bodies were preserved in 95% ethanol and stored at -20 °C. Empty shells were cleaned and preserved at room temperature in the Key Laboratory of Molluscan Quarantine and Identification of Fuzhou Customs District, Fujian, China (**GACC**).

Shells were measured to 0.1 mm using electronic calipers. Standard shell parameters were taken following Dillon (1984). All adult specimens of each species were measured. Live sexually mature specimens were dissected for the examination of reproductive system under a dissecting microscope (ZEISS Stemi 2000). Terminology for reproductive system follows Gómez (2001). The basal direction starts from the reproductive opening while that of verge starts from the epiphallus following Hwang et al. (2018).

Approximately 30 mg of the foot muscle was used for DNA extraction. The foot muscle was bathed in sterile water for 3–6 hours to remove residual alcohol. Genomic DNA was isolated using Qiagen DNeasy Blood & Tissue kit (Qiagen, Beijing), examined by agarose gel electrophoresis and ultra-micro spectrophotometer (Implen NP80, Germany), then stored at -20 °C for further use. The partial mitochondrial cytochrome c oxidase subunit 1 (COI) was amplified by PCR using apt primer pairs, reaction system, and amplification condition listed in Table 1. The PCR products were analyzed using 1.2% agarose gel electrophoresis.

After sequencing, raw sequences were proof-read on chromatograms and aligned into contigs using BioEdit 7.2 (Hall 1999). Sequence alignments were generated using ClustalW implemented in MEGA6 (Tamura et al. 2013). A total of 35 sequences were used in this study, 23 sequences of which were newly generated and deposited in GenBank (Table 2), and the remainder referenced in Wu et al. (2008), Ding et al. (2016), Ai et al. (2016), and Hu et al. (2019). Pairwise *p*-distances between taxa were calculated using MEGA6 (Tamura et al. 2013) and were compared with the currently known intra and inter- specific differentiation values (p-distances) of Camaenidae (Criscione and Köhler 2014; Ai et al. 2016; Ding et al. 2016). Neighbor-Joining and Minimum-Evolution analyses based on COI sequences were performed using MEGA6 (Tamura et al. 2013). *Amphidromus atricallosus* (Gould, 1843) (Camaenidae) was used

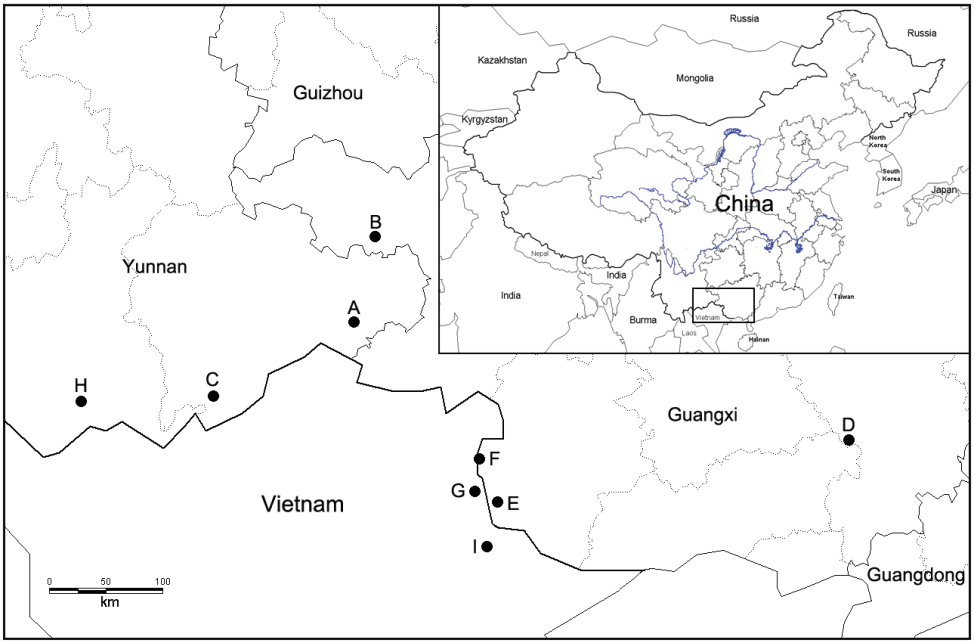

Figure 1. Map of locations of *Camaena* species. *C. funingensis* sp. nov. **A** Laolida, Funing, Wenshan, Yunnan, China. *C. gaolongensis* sp. nov. **B** Dayao, Gaolong, Tianlin, Guangxi, China. *C. maguanensis* sp. nov. **C** Huazhige, Maguan, Wenshan, Yunnan, China. *C. yulinensis* sp. nov. **D** Longquan cave, Yulin, Guangxi, China. *C. vorvonga* **E** Pingxiang, Guangxi, China **F** Longzhou, Guangxi, China **G** That-khe, Vietnam (Type locality). *C. jinpingensis* **H** Jinping, Yunnan, China. *C. longsonensis* **I** Lang-Son, Vietnam.

Table 1. Primer pairs and PCR conditions used in the analyses of the COI gene of *Camaena*.

Gene	COI
Primer pairs (5'-3')	LCO:GGTCAACAAATCATAAAGATATTGG
	HCO:TAAACTTCAGGGTGACCAAAAAATCA
Reaction systems	25 μl Taq PCR MasterMix × 2; 1 μl each primer; 2 μl DNA; 16 μl ddH_2O
Cycling conditions	94 °C: 30 s; 94 °C: 10 s, 45 °C: 50 s, 72 °C: 1 min, 40 cycles; 72 °C: 10 min.
Reference	Folmer et al. 1994

as outgroup. The node support values were assessed by bootstrap resampling using 1000 replicates (Felsenstein 1985).

Abbreviations used in this work:

AG albumen gland;
AH aperture height;
AW aperture width;
BC bursa copulatrix;
COI cytochrome c oxidase subunit 1gene;
E epiphallus;
F flagellum;
FJIQBC Original Fujian Entry-Exit Inspection & Quarantine Bureau, Fuzhou, Fujian, China;
GACC General Administration of Customs, People's Republic of China;

HD	hermaphroditic duct;	**PBC**	pedunculus of bursa copulatrix;
ME	Minimum-Evolution;	**PR**	penis retractor muscle;
MNHN	Muséum national d'Histoire naturelle, Paris, France;	**SH**	shell height;
		SW	shell width;
NJ	Neighbor-Joining;	**V**	verge;
O	oviduct;	**Va**	vagina;
P	penis;	**VD**	vas deferens.

Results

Molecular analysis

In this study, a total of 35 sequences of COI from 28 species were used, including eleven sequences from *C. funingensis* sp. nov., *C. gaolongensis* sp. nov., *C. maguanensis* sp. nov., and *C. yulinensis* sp. nov., 8 sequences from sinistral *Camaena* (*C. cicatricosa*, *C. obtecta*, *C. inflata*, *C. connectens*, *C. hahni*, *C. detianensis*, *C. lingyunensis*, *C. poyuensis*), 16 sequences from dextral *Camaena* and one outgroup (*A. atricallosus* Family Camaenidae) listed in Table 2.

Table 2. Sampling GenBank accession numbers used in phylogenetic analysis.

Species	COI accession numbers	References
Camaena funingensis sp. nov.	MT449465, MT449466, MT449467	Present study
Camaena gaolongensis sp. nov.	MT449468, MT449469, MT449470	Present study
Camaena maguanensis sp. nov.	MT449471, MT449472	Present study
Camaena yulinensis sp. nov.	MT449473, MT449474, MT449475	Present study
Camaena vorvonga	MT984239	Present study
Camaena xanthoderma	MT984235	Present study
Camaena xanthoderma polyzona	MT984236	Present study
Camaena hainanensis	MT984234	Present study
Camaena choboensis	MT984240	Present study
Camaena gabriellae	MT984241	Present study
Camaena gabriellae platytaenia	MT984242	Present study
Camaena longsonensis	EF057379	Wu et al. 2008
Camaena jinpingensis	KU586503	Ding et al. 2016
Camaena menglunensis	KU586506	Ding et al. 2016
Camaena inflata	KU586524	Ding et al. 2016
Camaena obtecta	KU055610	Ding et al. 2016
Camaena hahni	KX621263	Ai et al. 2016
Camaena connectens	KU586518	Ding et al. 2016
Camaena poyuensis	KU061273	Ding et al. 2016
Camaena lingyunensis	KX345077	Ai et al. 2016
Camaena cicatricosa	KU061276	Ding et al. 2016
Camaena detianensis	KX345074	Ai et al. 2016
Camaenella platyodon	MH362759	Hu et al. 2019
Camaena leonhardti	MT984237	Present study
Camaena vulpis	MT984238	Present study
Camaena hemiclista	MT984243	Present study
Camaena haematozona	MT984244	Present study
Amphidromus atricallosus	MT984245	Present study

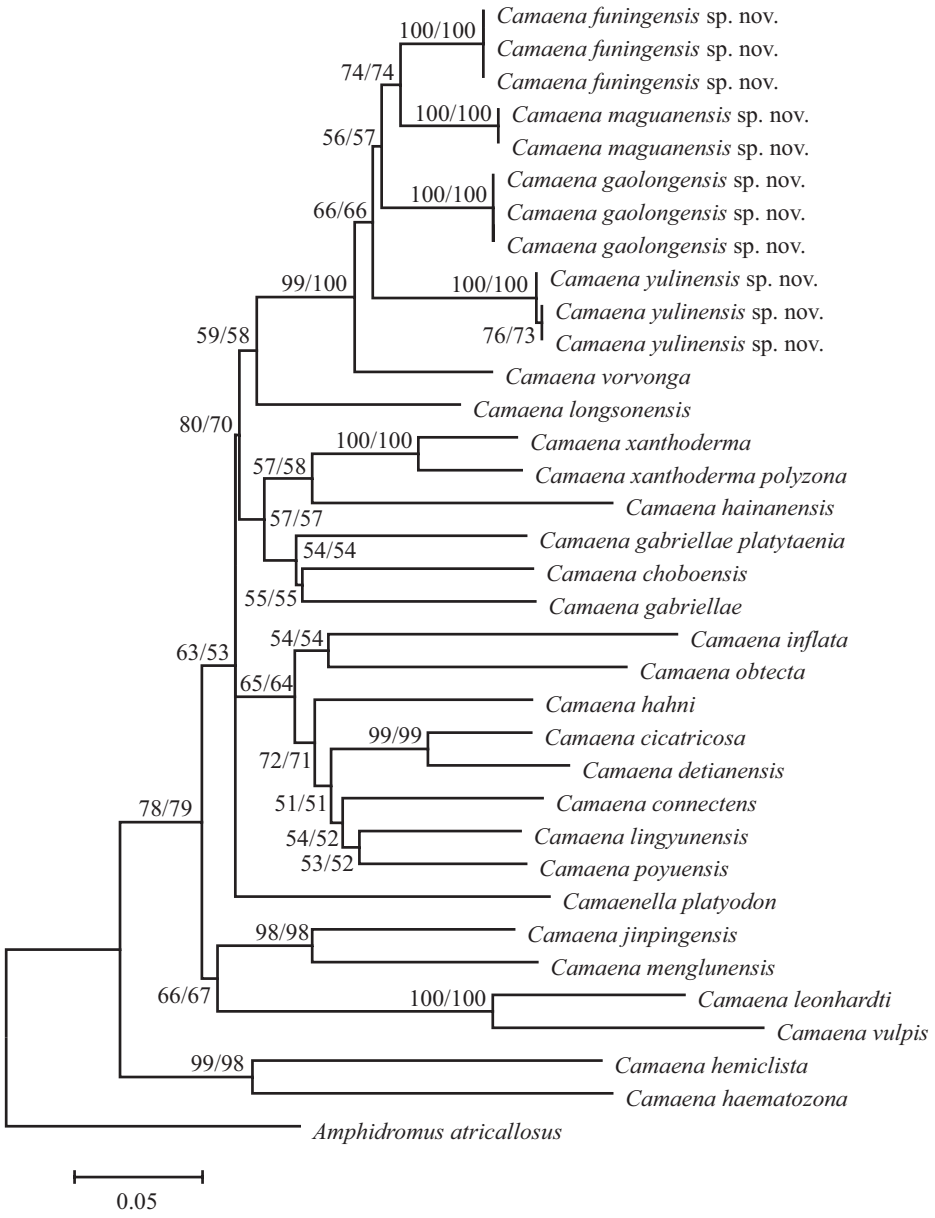

Figure 2. Neighbor-Joining and Minimum-Evolution trees based on analysis of the COI sequences. Numbers beside nodes indicate bootstrapping support (%) for the main clades, based on 1000 replicates.

Inter and intra-specific *P*-distances from COI gene of seven species were calculated and are listed in Table 3. According to the results of the target gene COI, the *p*-distances between *C. funingensis* sp. nov., *C. gaolongensis* sp. nov., *C. maguanensis* sp. nov., and *C. yulinensis* sp. nov. and other dextral *Camaena* were 0.068–0.200, 0.075–0.203, 0.068–0.198 and 0.092–0.202 respectively.

Table 3. Inter and intra-specific *P*-distances of the COI sequences on dextral *Camaena* species.

Sampling	P-distances	
	Within	Between
Camaena funingensis sp. nov.	0.000	0.068–0.200
Camaena gaolongensis sp. nov.	0.000	0.075–0.203
Camaena maguanensis sp. nov.	0.000	0.068–0.198
Camaena yulinensis sp. nov.	0.000–0.002	0.092–0.202
Camaena vorvonga	0.000–0.002	0.089–0.209
Camaena jinpingensis	0.000–0.002	0.196–0.209
Camaena longsonensis	0.000	0.153–0.211

For phylogenetic analysis, results showed that Neighbor-Joining and Minimum-Evolution trees had mostly the same topological structure (Fig. 2), and indicated that phylogenic analyses were relatively correct and reliable. The bootstrap support of each species exceeds 50%. The sinistral camaenids were clearly clustered together. The four dextral new species have the closest phylogenetic relationship to each other and are sister species with *C. vorvonga*. From the tree structure, branch length and comparison of the known species, the phylogenetic trees supported *C. funingensis* sp. nov., *C. gaolongensis* sp. nov., *C. maguanensis* sp. nov., and *C. yulinensis* sp. nov. as new species. Moreover, the four new species all had a closer genetic relationship with each other than with any other *Camaena* species studied here.

Systematics

Camaenidae Pilsbry, 1895

***Camaena* Albers, 1850**

Type species. *Helix cicatricosa* Müller, 1774, subsequent designation by Martens 1860.

***Camaena funingensis* Zhou, Wang & Lin, sp. nov.**
http://zoobank.org/E94E735E-BAD1-4D8C-AC91-5D50DF90AFE5
Figures 3A, 4, 5A, 6, Tables 3–5

Type material. ***Holotype*.** [FJIQBC 19340] Shell height 21.0 mm, shell width 41.0 mm, height of aperture 14.0 mm, width of aperture 18.7 mm, 22 October 2014, collected from the type locality.

***Paratype*.** [FJIQBC 19341–19343] 3 live specimens: 2 adults, 1 juvenile.

Type locality. Laolida, Funing, Wenshan, Yunnan, China (23°31'48.88"N, 105°32'59.70"E).

Etymology. The name of the new species refers to the type locality.

Diagnosis. ***Shell*.** Shell dextral, large, thin, fragile and lucent, low, and flat conical. 4.5 whorls, the front whorls increasing slowly. Spire relatively low. Body whorl rapidly

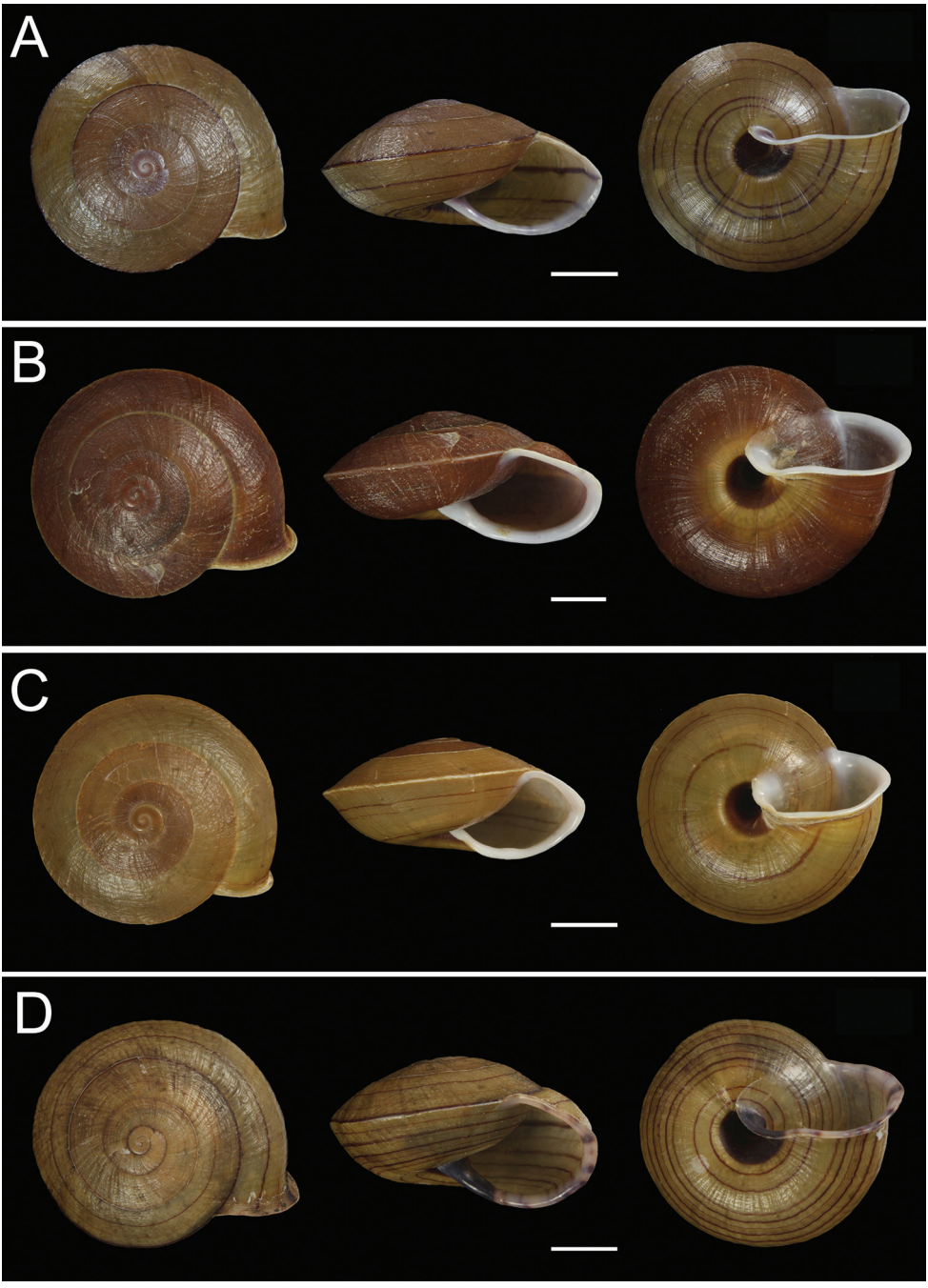

Figure 3. Photographs of the four new species **A** *Camaena funingensis* sp. nov. (holotype, FJIQBC 19340, Laolida, Funing, Yunnan, China) **B** *Camaena gaolongensis* sp. nov. (holotype, FJIQBC 19353, Dayao, Gaolong, Guangxi, China) **C** *Camaena maguanensis* sp. nov. (FJIQBC 19405, Huazhige, Maguan, Yunnan, China) **D** *Camaena yulinensis* sp. nov. (FJIQBC 19460, Longquan cave, Yulin, Guangxi, China). Scale bars: 10 mm.

expanded. Shell light yellowish brown with clear growth lines and spiral bands on the surface. Apex quite blunt. Suture shallow. The protoconch surface smooth, and some short clear growth lines near the inner side of suture under 32 × stereomicroscope. Body whorl with carinate periphery, and a thin reddish brown band on the carina and several sparse bands below the carina. Aperture lunate, slightly descending. Peristome reflected, white, thin, sharp. Columellar lip reflected. Umbilicus reddish brown, large, only 1/5 covered. Inner lip attached to the body whorl, forming translucent callus.

Soft body. Yellowish brown with irregular black lines and spots. Tentacles dark.

Reproductive system. Bursa copulatrix oval and large with long and tapering pedunculus, expanded at the base. Flagellum long, tapering distally. Vas deferens short and thin. Epiphallus long, slightly thick. Penis retractor muscle medium length and slender, becoming wider at the end. Penis swollen and long, with longitudinal, slightly corrugated, strong and widely spaced pilasters internally. Verge ovate, opened terminally, and one clear crack on the verge surface extending from the terminal to the base.

Habitat. The species was found on limestone.

Distribution. Only known from the type locality.

Remarks. *Camaena funingensis* sp. nov. is characterized by a more oblate shape, lower spire, thin and fragile shell, and yellowish brown coloration, which are clearly different from the other dextral camaenids except *C. longsonensis* (Morlet, 1891), *C jinpingensis* Chen, Zhang & Li, 1990, and *C. vorvonga* (Bavay & Dautzenberg, 1900) (Chen et al. 1990; Schileyko 2011). The shells of the above four species are distinct from *C. funingensis* in the following ways:

(1) The umbilicus of *C. funingensis* sp. nov. is only 1/5 covered, while that of *C. longsonensis* is almost covered by reflected columellar lip leaving only a narrow slit, and that of *C. jinpingensis* is fully covered.
(2) *C. funingensis* sp. nov. has several reddish brown bands at the bottom of the body whorl in addition to those on the carina, while only one thin reddish brown band is present on the carinate periphery of *C. vorvonga*.
(3) For *C. funingensis* sp. nov., the verge is ovate and has one clear crack on the surface extending to the base, which makes it stand out other dextral camaenids.

Camaena gaolongensis sp. nov. is distinguishable from *C. funingensis* sp. nov. in having no spiral band. For *C. maguanensis* sp. nov., there is no band on the carinate periphery of the body whorl except for several below the carina. Moreover, the verge of *C. maguanensis* sp. nov. is small and circular. *Camaena yulinensis* sp. nov. differs to *C. funingensis* sp. nov. in having a conical verge and flesh-colored peristome.

P-distances of the COI gene between *C. funingensis* sp. nov. and the other camaenids are 0.068–0.200 (Table 3), and those between *C. funingensis* sp. nov. and *C. gaolongensis* sp. nov., *C. maguanensis* sp. nov. and *C. yulinensis* sp. nov. are 0.075, 0.068 and 0.094 respectively. All of these *P*-distances exceed the maximum intra-specific value 0.059 in the family Camaenidae. On the phylogenetic tree, these four new species are adjacent, hence it is reasonable to designate this as a new species.

***Camaena gaolongensis* Zhou, Wang & Lin, sp. nov.**
http://zoobank.org/1B657A19-59B9-46D2-B874-9DB7120730E9
Figures 3B, 4, 5B, 7, Tables 3–5

Type material. ***Holotype*.** [FJIQBC 19353] Shell height 23.8 mm, shell width 49.0 mm, height of aperture 14.0 mm, width of aperture 19.2 mm, 11 April 2015, collected from the type locality.

***Paratype*.** [FJIQBC 19354] 1 live juvenile, 20 October 2014; [FJIQBC 19355–19356] 2 live adults, 11 April 2015.

Type locality. Dayao, Gaolong, Tianlin, Guangxi, China (24°11'52.33"N, 105°43'40.56"E).

Etymology. The name of the new species refers to the type locality.

Diagnosis. ***Shell*.** Shell dextral, large, thick, strong, low, and flat conical. 4.5 whorls, the front whorls increasing slowly. Spire relatively low. Body whorl rapidly expanded. Shell dark brown with clear and dense growth lines on the surface. Apex quite blunt. Suture shallow. The protoconch surface smooth with scale marks, and some short growth lines clear near the outer side of suture under 32 × stereomicroscope. Body whorl with acute and carinate periphery, but no spiral band. Aperture U-shaped. Peristome reflected, white and thick. Columellar lip reflected. Umbilicus reddish brown, open, large, and only 2/5 covered. Inner lip attached to the body whorl, forming translucent callus.

***Soft body*.** Brown with irregularly black lines and spots. Tentacles dark.

***Reproductive system*.** Bursa copulatrix oval and medium sized with long pedunculus, expanded at the base, becoming thinner at the distal end. Flagellum long and smooth, tapering distally. Vas deferens long and thin. Epiphallus medium length and thick. Penis retractor muscle short, slender basally but wide and flat distally. Penis thick and medium length. Inner penial wall supporting longitudinal, stronger, and more widely spaced pilasters, smooth basally, curved distally. Verge irregularly conical, opened basally, extending from the base to the end, with several slanted wrinkles on the surface.

Habitat. It is common in primary forest and loess areas, but it has not been found on the reclaimed lands outside the primary forest.

Distribution. Only known from the type locality.

Remarks. *Camaena gaolongensis* sp. nov. is clearly different from other dextral camaenids by its quite thick, low, flat, and dark brown conical shell resembling a flying saucer (Chen et al. 1990, Schileyko 2011). Additionally, the longitudinal pilasters on the inner penial wall are stronger and more widely spaced, as well as smooth at the base but curved at the end, which are also distinct from the other dissected *Camaena* snails (Ding et al. 2016, Ai et al.2016).

P-distances of the COI gene between *C. gaolongensis* sp. nov. and other dextral *Camaena* species are 0.075–0.203 (Table 3), and those between *C. gaolongensis* sp. nov., *C. maguanensis* sp. nov., and *C. yulinensis* sp. nov. are 0.085 and 0.104 respectively. Combining the topological structure of the phylogenetic tree, the new species *C. gaolongensis* sp. nov. is distinct from other dextral *Camaena* species.

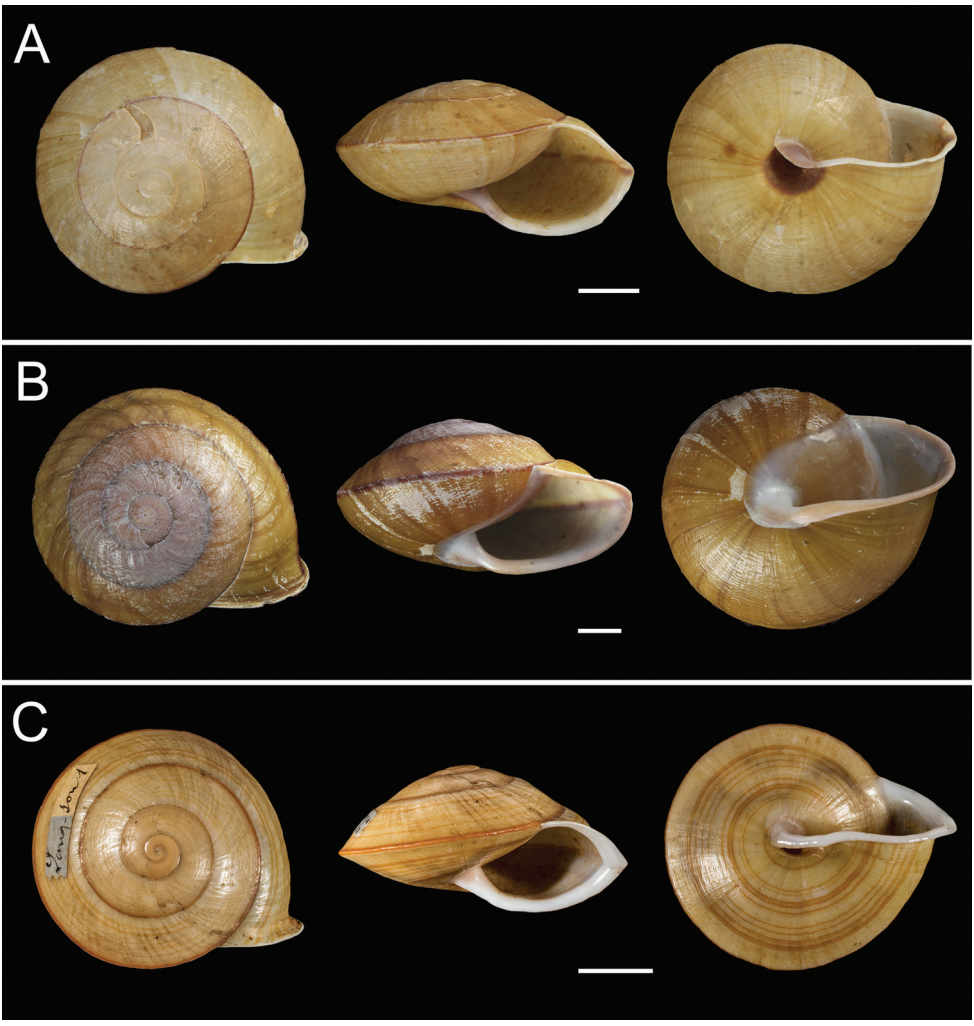

Figure 4. Photographs of three camaenids **A** *Camaena vorvonga* (Pingxiang, Guangxi, China) **B** *Camaena jinpingensis* (Jinping, Yunnan, China) **C** *Camaena longsonensis* (Lang-Son, Vietnam). Scale bars: 10 mm.

***Camaena maguanensis* Zhou, Wang & Hu, sp. nov.**
http://zoobank.org/EC5431C5-CFB6-4309-80C1-0CF8F3C9BE0E
Figures 3C, 4, 5C, 8, Tables 3–5

Type material. ***Holotype.*** [FJIQBC 19405] Shell height 19.2 mm, shell width 39.0 mm, height of aperture 12.0 mm, width of aperture 16.5 mm, 16 April 2015, collected from the type locality.

Paratype. [FJIQBC 19406] 1 live adult; [FJIQBC 19407–19413] 7 empty shells: 5 adults, 2 juveniles.

Type locality. Huazhige, Maguan, Wenshan, Yunnan, China (22°57'24.48"N, 104°21'12.96"E).

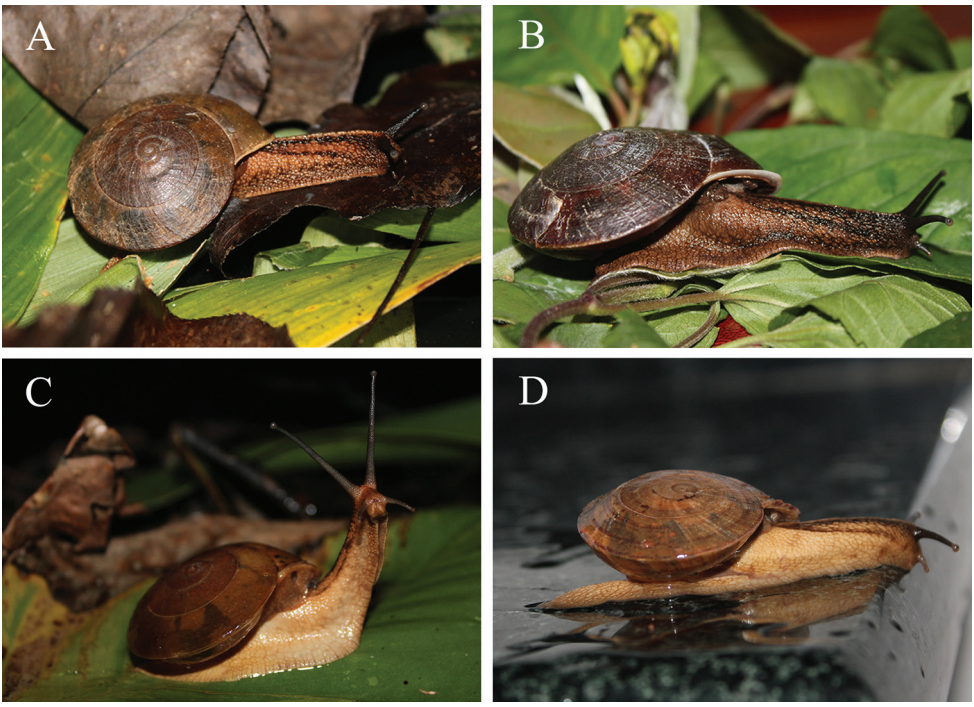

Figure 5. Ecological photographs of snails **A** *Camaena funingensis* sp. nov. (Laolida, Funing, Yunnan, China) **B** *Camaena gaolongensis* sp. nov. (Dayao, Gaolong, Guangxi, China) **C** *Camaena maguanensis* sp. nov. (Huazhige, Maguan, Yunnan, China) **D** *Camaena yulinensis* sp. nov. (Longquan cave, Yulin, Guangxi, China).

Table 4. Adult shell dimensions (mm).

Species	*C. funingensis* sp. nov.	*C. gaolongensis* sp. nov.	*C. maguanensis* sp. nov.	*C. yulinensis* sp. nov.
Voucher	FJIQBC19340–19342	FJIQBC19353 FJIQBC19355–19356	FJIQBC19405–19411	FJIQBC19460–19466 FJIQBC19468–19470
Sample size	3	3	7	10
SH	19.5–21.0 (20.17±0.62)	23.5–24.5 (23.93±0.42)	19.2–22.0 (20.36±0.90)	19.8–23.0 (21.35±1.05)
SW	39.2–41.0 (40.23±0.76)	47.0–50.0 (48.67±1.25)	38.0–40.5 (39.24±0.74)	37.0–42.6 (40.54±1.58)
SW/SH	1.95–2.03 (2.00±0.03)	2.00–2.06 (2.03±0.02)	1.84–2.03 (1.93±0.06)	1.84–1.96 (1.90±0.03)
AH	13.4–14.0 (13.63±0.26)	13.8–14.2 (14.00±0.16)	12.0–13.1 (12.64±0.34)	13.0–14.6 (13.76±0.48)
AW	18.0–18.7 (18.30±0.29)	19.0–19.4 (19.20±0.16)	16.5–18.1 (17.22±0.56)	17.5–21.6 (19.11±1.46)
AW/AH	1.34–1.35 (1.34±0.01)	1.37–1.38 (1.37±0.00)	1.33–1.39 (1.36±0.02)	1.33–1.48 (1.39±0.06)

Etymology. The name of the new species refers to the type locality.

Diagnosis. ***Shell.*** Shell dextral, large, thin, fragile, and glossy, low and flat conical. 4.5 whorls, the front whorls increasing slowly. Spire relatively low. Body whorl rapidly expanded. Shell yellowish with unclear growth lines and spiral bands on the surface.

Apex quite blunt. Suture shallow. The protoconch surface smooth, some short growth lines visible near the two sides of suture under 32 × stereomicroscope. Last whorl with quite acute carina at periphery and a shallow groove-like depression above and below the carina. No band on the carina, but several reddish brown and sparse spire bands below the carina. Aperture crescent-shaped. Peristome reflected, white and thick. Columellar lip reflected. Umbilicus reddish brown, open, large and only 2/5 covered. Inner lip attached to the body whorl, forming translucent callus.

***Soft body*.** Light yellowish brown with black lines. Tentacles dark.

***Reproductive system*.** Bursa copulatrix oval, small, with quite long and tapering pedunculus. Flagellum long, tapering distally. Vas deferens long and thin. Epiphallus medium thickness and length. Penis retractor muscle very short and slender. Penis long with a short protrusion at the middle. Inner penial wall with longitudinal, slightly straight and smooth pilasters. Verge circular, somewhat small, opened basally, extending from the base to the end.

Habitat. The species was found on limestone in Maguan county of Yunnan province, China.

Distribution. Only known from the type locality.

Remarks. *Camaena maguanensis* sp. nov. is clearly different from other dextral camaenids with a lower conical shell. In particular, *C. maguanensis* sp. nov. has a large and open umbilicus, which distinguishes it from *C. longsonensis* and *C. jinpingensis*. Although the umbilicus of *C. maguanensis* sp. nov. is similar to that of *C. vorvonga*, some differences are obvious. For example, *C. maguanensis* sp. nov. has no spiral band on the carinate periphery of the body whorl but some spaced bands at the base. The shell of *C. maguanensis* sp. nov. is yellowish, but that of *C. gaolongensis* sp. nov. is dark brown. On the other hand, *C. maguanensis* sp. nov. has a circular and slightly smaller verge.

P-distances of the COI gene between this new species and the other dextral species are 0.068–0.198 (Table 3), and that between *C. maguanensis* sp. nov. and *C. yulinensis* sp. nov. is 0.108, also exceeding 0.059 (currently the maximum differentiation value (p-distance) of Camaenidae) (Criscione and Köhler 2014), and the topology of the phylogenetic tree also supports the new species.

Camaena yulinensis Zhou, Wang & Hu, sp. nov.

http://zoobank.org/3038DBDB-A3B2-4364-B2D3-CB7E694EA8ED
Figures 3D, 4, 5D, 9, Tables 3–5

Type material. ***Holotype*.** [FJIQBC 19460] Shell height 21.0 mm, shell width 40.5 mm, height of aperture 13.5 mm, width of aperture 18.2 mm, 21 September 2014, collected from the type locality.

***Paratype*.** [FJIQBC 19461–19466] 6 specimens: 3 live adults, 3 empty adult shells, 4 November 2013; [FJIQBC 19468–19472] 5 specimens: 3 live adults, 2 empty juvenile shells, 21 September 2014.

Type locality. Longquan cave, Yulin, Guangxi, China (22°36'41.24"N, 109°45'21.36"E).

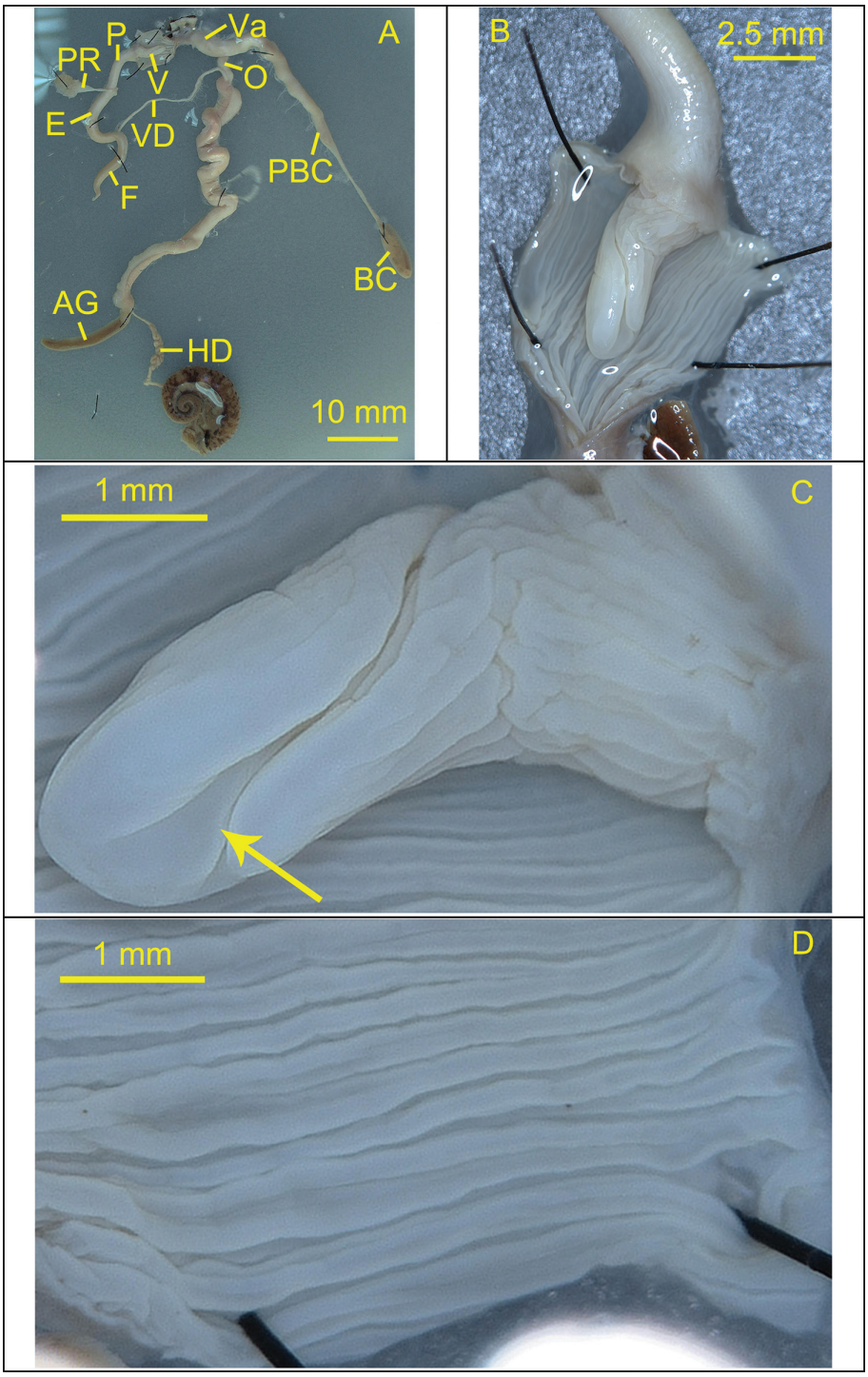

Figure 6. Reproductive system of the snail *Camaena funingensis* sp. nov. (holotype, FJIQBC 19340, Laolida, Funing, Yunnan, China) **A** reproductive organ **B** penis **C** verge **D** inner penial wall. The arrow indicates opening position of the verge.

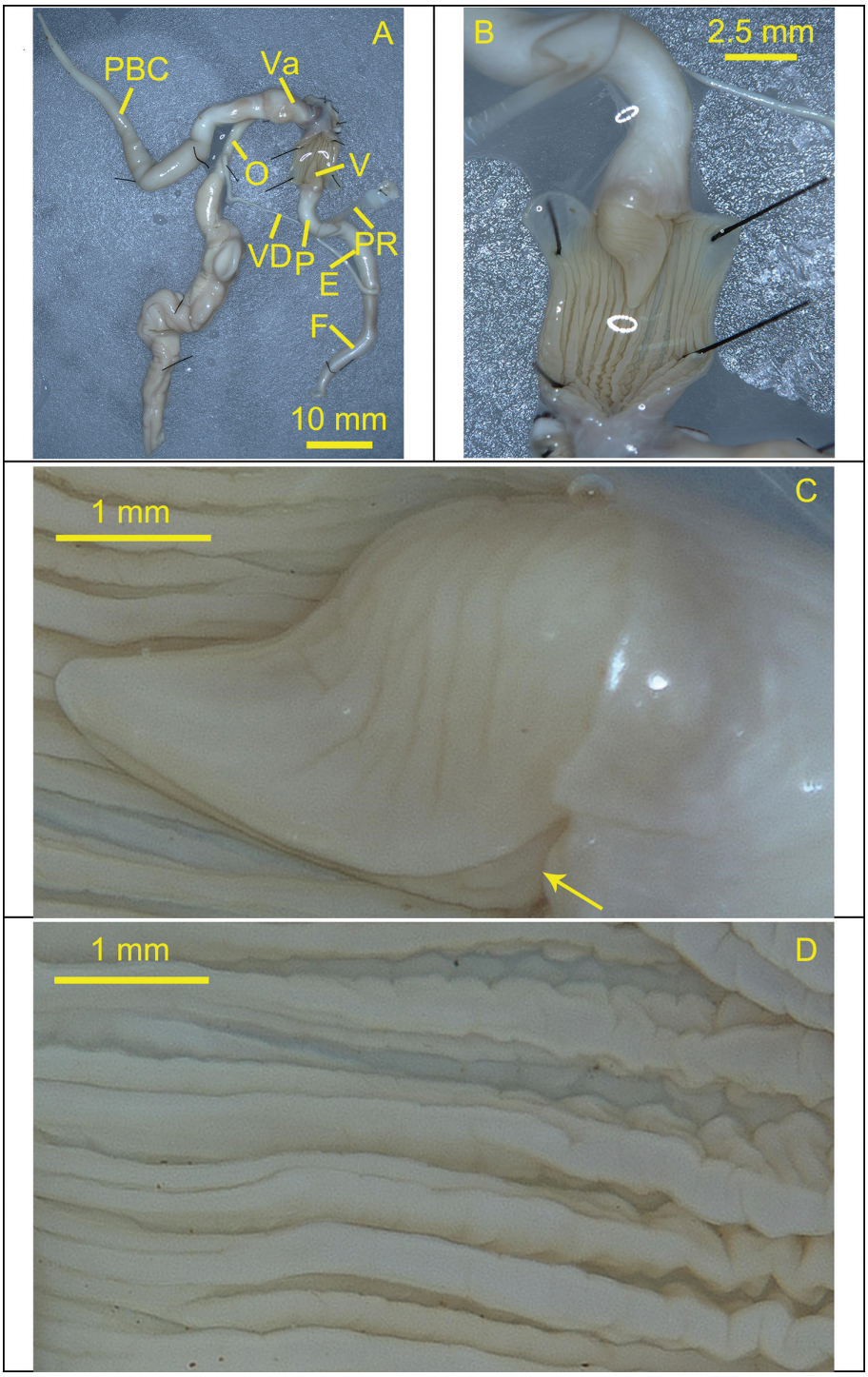

Figure 7. Reproductive system of the snail *Camaena gaolongensis* sp. nov. (holotype, FJIQBC 19353, Dayao, Gaolong, Guangxi, China) **A** reproductive organ **B** penis **C** verge **D** inner penial wall. The arrow indicates opening position of the verge.

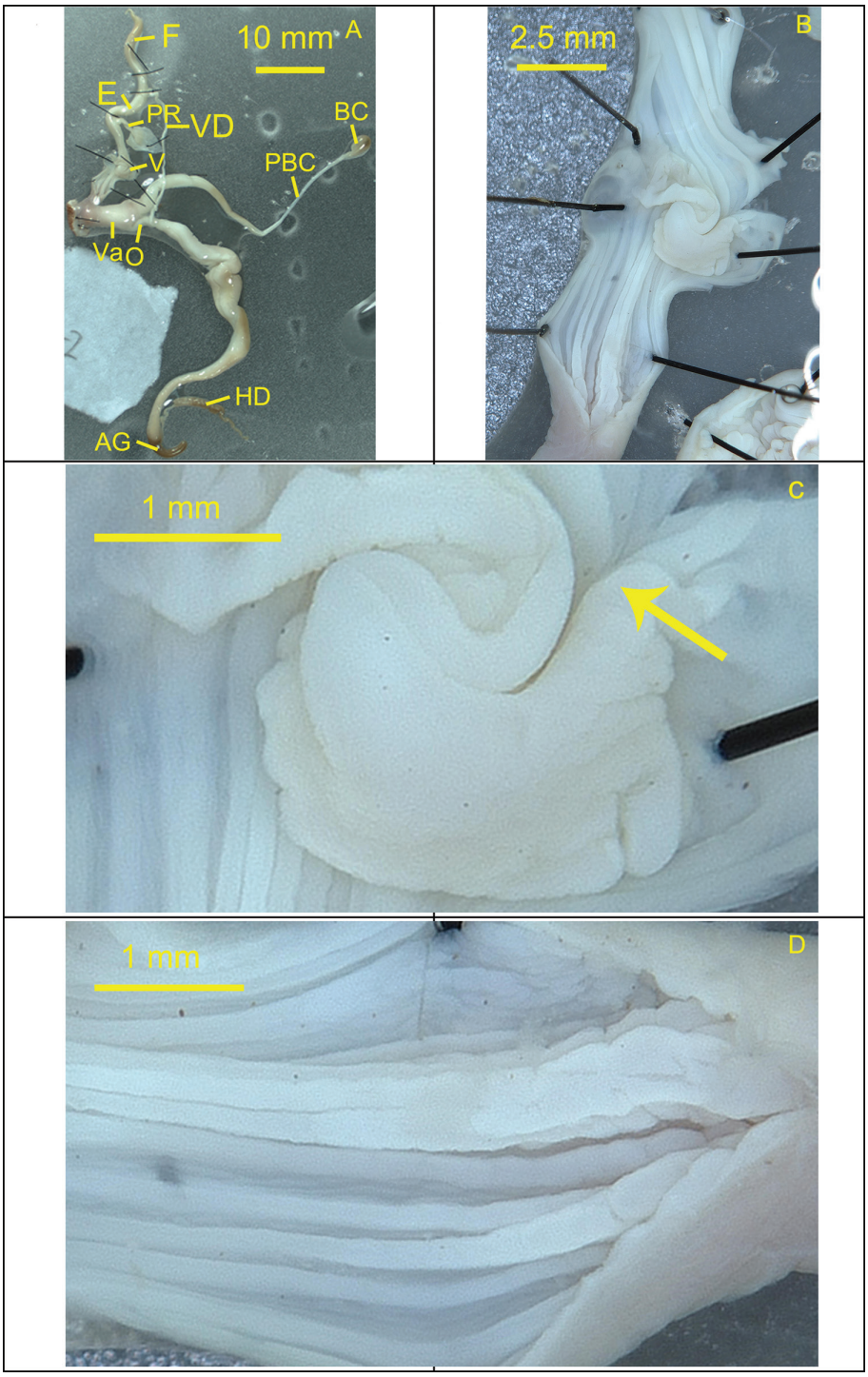

Figure 8. Reproductive system of the snail *Camaena maguanensis* sp. nov. (FJIQBC 19405, Huazhige, Maguan, Yunnan, China) **A** reproductive organ **B** penis **C** verge **D** inner penial wall. The arrow indicates opening position of the verge.

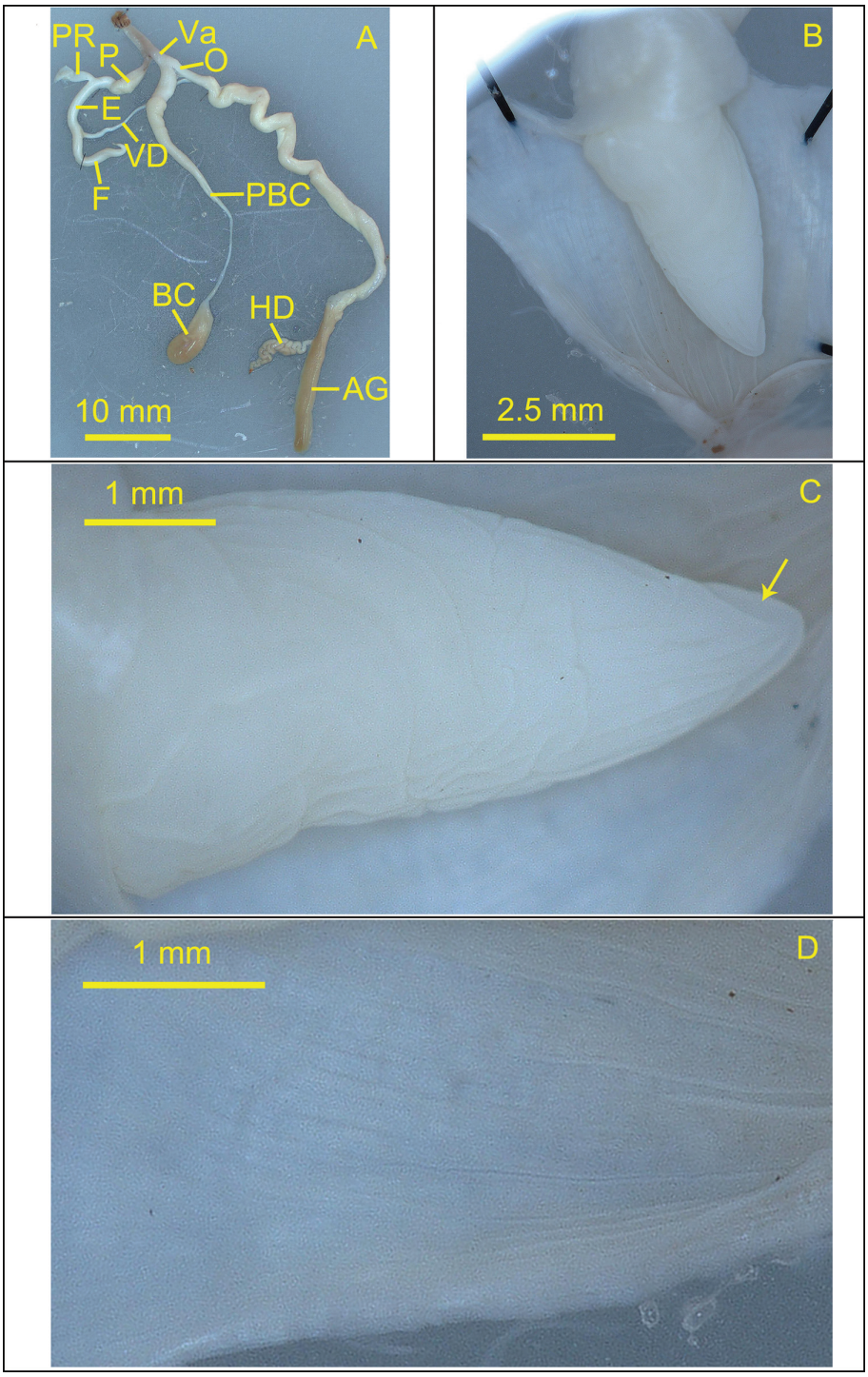

Figure 9. Reproductive system of the snail *Camaena yulinensis* sp. nov. (FJIQBC 19460, Longquan cave, Yulin, Guangxi, China) **A** reproductive organ **B** penis **C** verge **D** inner penial wall. The arrow indicates opening position of the verge.

Table 5. Diagnostic comparisons of morphological characters of the four new species.

Character	*C. funingensis* sp. nov.	*C. gaolongensis* sp. nov.	*C. maguanensis* sp. nov.	*C. yulinensis* sp.nov.
Shell thickness	thin	quite thick	thin	thin
Shell color	light yellowish brown	dark brown	yellowish	light yellowish
Periphery	carinate	acute and carinate	acute and carinate	carinate
Growth lines	clear	clear and dense	unclear	clear and dense
Umbilicus	only 1/5 covered	only 2/5 covered	only 2/5 covered	1/3 covered
Verge	ovate	short conic	circular and small	long conic
Verge opening	terminally, one clear crack on the surface extending from the end to the base	basally, one crack on the side surface extending from the base to the end	basally, one crack on the surface extending from the base to the end	terminally

Etymology. The name of the new species refers to the type locality.

Diagnosis. ***Shell.*** Shell dextral, large, thin, fragile, and slightly lucent, low and flat conical. 4.5 whorls, the front whorls increasing slowly. Spire relatively low. Body whorl rapidly expanded. Shell light yellowish with clear and dense growth lines and spiral bands on the surface. Apex quite blunt. Suture shallow. The protoconch surface smooth for most individuals, but a few are rough. Growth lines clear near the outer side of suture under 32 × stereomicroscope. Last whorl with carinate periphery, a thin reddish brown spiral band on the carina, and many reddish brown spiral bands of different thickness on the upper and lower parts. Aperture lunate. Peristome reflected, flesh-colored, thin, sharp. Columellar lip reflected. Umbilicus reddish brown, open, large, and only 1/3 covered. Inner lip attached to body whorl, forming translucent callus.

Soft body. Pale yellow with irregular black lines. Tentacles dark brown.

Reproductive system. Bursa copulatrix oval, large, with long and tapering pedunculus. Flagellum long and slightly thick, tapering distally. Vas deferens short and thin. Epiphallus medium length and slightly thick. Penis retractor muscle short and wide. Penis short and swollen at distal 1/3, with longitudinal, thin, smooth pilasters internally. Verge conical, large, opened terminally, with some irregular wrinkles on the surface.

Habitat. The species was found on limestone in Yulin city, Guangxi province.

Distribution. Only known from the type locality.

Remarks. *Camaena yulinensis* sp. nov. differs from *C. longsonensis* and *C. jinpingensis* in the key characteristic of large open umbilicus. This new species not only has spiral bands with different thickness on the body whorl but also has a flesh-colored peristome compared to *C. vorvonga*. The differences between this species and the other three new *Camaena* species herein have already been described above.

P-distances of the COI gene between *C. yulinensis* sp. nov. and the other dextral congeners ranges from 0.092 to 0.202 (Table 3) and the phylogenetic topology tree supports the establishment of this new species.

Discussion

We describe four new species of dextral *Camaena* snails, namely *C. funingensis* sp. nov., *C. gaolongensis* sp. nov., *C. maguanensis* sp. nov. and *C. yulinensis* sp. nov., which

are distinguished from their congeners by their shell morphologies, especially the low and flat shell shape, the large open umbilicus, the acute and carinate periphery of the body whorl, as well as features in their reproductive systems and molecular characteristics. Among the first three new species, the differences of shells and genitals are obvious. Although *C. funingensis* sp. nov. and *C. yulinensis* sp. nov. are similar in shell morphology except size, color and umbilicus, the former has an ovate and terminally opened verge and one clear crack on the surface extending from the end to the base, as well as strong and widely spaced penis pilasters, that distinguish it from *C. yulinensis* sp. nov. with a conical verge, thin penial inner pilasters and without crack on the surface (Figs 3, 5–9). Nonetheless, the two similar-shaped species are relatively distantly related genetically (Fig. 2).

Some scholars have considered genetic distance as one of the more important pieces of evidence used for identifying new species and revising species; for example, in the Asian camaenids *Luchuhadra* (Kameda et al. 2007) and *Satsuma* (Wu et al. 2008), the Australian camaenid *Kimberleytrachia* (Criscione and Köhler 2014), and *Camaena* (Ai et al. 2016; Ding et al. 2016). In the present study, the *p*-distances between *C. funingensis* sp. nov., *C. gaolongensis* sp. nov., *C. maguanensis* sp. nov., *C. yulinensis* sp. nov., and the other dextral *Camaena* was substantial: 0.068–0.200, 0.075–0.203, 0.068–0.198, and 0.092–0.202 respectively for the mitochondrial COI barcoding region (Table 3). These numbers exceed the intra-specific differentiation values (*p*-distances) of Camaenidae (for *Camaena*, minimum 0.00, maximum 0.018 in Ding et al. (2016), minimum 0.00, maximum 0.019 in Ai et al. (2016), for *Kimberleytrachia*, minimum 0.00, maximum 0.059, mean 0.026 in Criscione and Köhler (2014). Based on these considerations, inter-specific differentiation supports the recognition of the four new species.

In the phylogenetic analyses, *C. vorvonga* and *C. longsonensis*, which were placed in informal subgeneric group I, have a close relationship, while they are distant from *C. jinpingensis* that originally also belonged to group I. In the future, more species and sequences will be needed for a more robust analysis of camaenid phylogeny.

During our long-term field investigations, we observed that most *Camaena* species have a narrow distribution and a low population density, and only inhabit primary forests. An exception to this is *C. cicatricosa*, which is widespread and has high population densities (Ai et al. 2016; Ding et al. 2016). In recent years, with the development of the Chinese economy, areas of primary forest have been decreasing and the habitats of *Camaena* species are becoming increasingly restricted and threatened. Therefore, it is necessary to maximize forest protection, prevent deforestation, and prevent excessive tourist development to preserve the biodiversity of these terrestrial mollusks and other animals and plants.

Acknowledgements

We gratefully acknowledge the assistance of Chung-Chi Hwang (National University of Kaohsiung) in the field work, and the Muséum national d'Histoire naturelle, Paris,

France, for open access to the digitized photograph of type specimens. This research is supported by National Natural Science Foundation of China (31801960, 31372162), Agricultural Science and Technology Major Project Funds of Fujian (2017NZ0003-1) and National Key Research and Development Program of China (2017YFF0210304).

References

Adams H (1870) Descriptions of a new genus, and of eighteen new species of Molluscs. Proceedings of the Zoological Society of London 1870: 5–9.

Albers JC (1850) Die Heliceen, Nach Natürlicher Verwandtschaft Systematisch Geordnet. T. C. F. Enslin, Berlin, 262 pp. https://www.biodiversitylibrary.org/page/11965983

Ai HM, Lin JH, Wang P, Zhou WC, Hwang CC (2016) Descriptions of two new species of the genus *Camaena* from Guangxi, China (Gastropoda, Stylommatophora, Camaenidae). ZooKeys 634: 29–45. https://doi.org/10.3897/zookeys.634.10236

Bavay A, Dautzenberg P (1900) Diagnose de nouveaux mollusques d'Indo-Chine. Journal de Conchyliologie 48: 108–122.

Bavay A, Dautzenberg P (1909) Description de coquilles nouvelles de l'Indo-Chine. Journal de Conchyliologie 57: 163–206.

Chen DN, Gao JX (1987) Economic Fauna Sinica of China (Terrestrial Mollusca). Science Press, Beijing, 186 pp.

Chen DN, Zhang GQ (1999) Studies on the genus *Camaena* from China, with description of two new species (Gastropoda: Camaenidae). Transactions of the Chinese Society of Malacology 8: 28–43.

Chen DN, Zhang QG, Li BH (1990) A new terrestrial snail species from China. Zoological Systematics 2(6): 33–35.

Criscione F, Köhler F (2014) Molecular phylogenetics and comparative anatomy of *Kimberleytrachia* Köhler, 2011 – a genus of land snail endemic to the coastal Kimberley, Western Australia with description of new taxa (Gastropoda, Camaenidae). Contributions to Zoology 83(4): 245–267. https://doi.org/10.1163/18759866-08304003

Dautzenberg PH, Fischer H (1906) Liste de mollusques récoltés par M. H. Mansuy en Indochine et au Yunnan, et description d'espèces nouvelles. Journal de Conchyliologie, Paris 53: 343–471.

Dillon RT (1984) What shall I measure on my snails? Allozyme data and multivariate analysis used to reduce the nongenetic component of morphological variance in *Goniobasis proxima*. Malacologia 25: 503–511.

Ding HL, Wang P, Qian ZX, Lin JH, Zhou WC, Hwang CC, Ai HM (2016) Revision of sinistral land snails of the genus *Camaena* (Stylommatophora, Camaenidae) from China based on morphological and molecular data, with description of a new species from Guangxi, China. ZooKeys 584: 25–48. https://doi.org/10.3897/zookeys.584.7173

Eddy S (1998) Profile hidden Markov models. Bioinformatics 14: 755–763. https://doi.org/10.1093/bioinformatics/14.9.755

Felsenstein J (1985) Confidence limits on phylogenies: an approach using the bootstrap. Evolution 39: 783–791. https://doi.org/10.2307/2408678

Fischer H (1898) Notes sur la faune du Haut Tonkin. III. Liste des mollusques recueillis par le Dr A. Billet. Bulletin scientifique de la France et de la Belgique 28: 310–338.

Folmer O, Black M, Hoeh W, Lutz R, Vrijenhoek R (1994) DNA primers for amplification of mitochondrial cytochrome c oxidase subunit I from diverse metazoan invertebrates. Molecular Marine Biology and Biotechnology 3: 294–299.

Gómez BJ (2001) Structure and functioning of the reproductive system. In: Baker GM (Ed.) The Biology of Terrestrial Molluscs. CABI Publishing, Oxon, 307–330. https://doi.org/10.1079/9780851993188.0307

Gould AA (1843) Description of land mollusks from the province of Tavoy, in British Burmah. Proceedings of the Boston Society of Natural History 1843: 137–141.

Gredler V (1888) Zur Conchylien-Fauna von China. XIII. Stück. Jahrbücher der deutschen malakozoologischen Gesellschaft, 14: 343–373.

Hall TA (1999) BioEdit: a user-friendly biological sequence alignment editor and analysis program for Windows 95/98/NT. Nucleic Acids Symposium Series 41: 95–98. https://doi.org/10.1021/bk-1999-0734.ch008

Hoso M, Kameda Y, Wu SP, Asami T, Kato M, Hori M (2010) A speciation gene for left–right reversal in snails results in anti-predator adaptation. Nature Communications 1: e133. https://doi.org/10.1038/ncomms1133

Hu ML, Wang P, Chen Y, Zhang MZ, Yang SP, Lin JH, Zhou WC (2019) The mitochondrial genome of the land snail *Camaenella platyodon* (Pfeiffer, 1846) (Stylommatophora, Camaenidae), Mitochondrial DNA Part B 4: 2753–2754. https://doi.org/10.1080/23802359.2019.1644559

Hwang CC (2012) Anatomy and taxonomy of *Satsuma succincta* (Adams, 1866) and *Satsuma batanica pancala* (Schmacker & Boettger, 1891) (Gastropoda: Camaenidae) from southern Taiwan. Bulletin of Malacology 35: 1–11.

Hwang CC, Okuba K, Tada A (2018) *Satsuma jinlunensis*– a new species from Taiwan (Stylommatophora: Camaenidae). Molluscan Research 38: 1–6. https://doi.org/10.1080/13235818.2017.1358340

Inkhavilay K, Sutcharit C, Bantaowong U, Chanabun R, Siriwut W, Srisonchai R, Polyotha A, Jirapatrasilp P, Panha S (2019) Annotated Checklist of the Terrestrial Molluscs from Laos (Gastropoda: Neritimorpha, Caenogastropoda and Heterobranchia). ZooKeys 834: 1–166. https://doi.org/10.3897/zookeys.834.28800

Kameda Y, Kawakita A, Kato M (2007) Cryptic genetic divergence and associated morphological differentiation in the arboreal land snail *Satsuma* (*Luchuhadra*) *largillierti* (Camaenidae) endemic to the Ryukyu Archipelago, Japan. Molecular Phylogenetics and Evolution 45: 519–533. https://doi.org/10.1016/j.ympev.2007.03.021

Koetschan C, Förster F, Keller A, Schleicher T, Ruderisch B, Schwarz R, Müller T, Wolf M, Schultz J (2010) The ITS2 Database III – sequences and structures for phylogeny. Nucleic Acids Research 38: 275–279. https://doi.org/10.1093/nar/gkp966

Kuroda L, Habe T (1949) Helicacea. Osaka, 129 pp. [1 pl.]

Mabille J (1889) Contribution à la faune malacologique du Tonkin. A. Masson, Meulan, 20 pp.

Minato H (1980) Land snail fauna of Miyako Islands, the southern Ryukyu, Japan. Venus 39: 83–99.

Möllendorff OF von (1882) Diagnoses specierum novarum Chinae meridionalis. Jahrbücher der Deutschen Malakozoologischen Gesellschaft 9: 179–188.

Möllendorff OF von (1885) Materialien zur Fauna von China. Die Auriculaceen. Jahrbücher der Deutschen Malakozoologischen Gesellschaft 12: 349–398.

Möllendorff OF von (1888) Mittheilungen aus dem Gebiete der Malakozoologie. Diagnoses specierum novarum sinensium. Nachrichtsblatt der deutschen malakozoologischen Gesellschaft 20(2/3): 38–44.

Morlet L (1891) Diagnoses Molluscorum novorum, in Indo-Chinâ collectorum. Journal de Conchyliologie, Paris 39: 25–28.

Müller OF (1774) Vermivm terrestrium et fluviatilium, v.2. Havni.apud Heineck et Faber, 214 pp.

Páll-Gergely B, Hunyadi A, Otani JU, Asami T (2016) An impressive new camaenid, *Entadella entadiformis* gen. & sp. n. from Guangxi, China (Gastropoda: Pulmonata). Journal of Conchology 42(4): 167–179.

Palumbi S, Martin A, Romano S, Mcmillan WO, Stice L, Grabowwski G (1991) The Simple Fool's Guide to PCR. Department of Zoology, University of Hawaii, Honolulu, 46 pp.

Pilsbry HA (1893) Preliminary outline of a new classification of the helices. Academy of Natural Sciences of Philadelphia, Philadelphia, 44: 387–404.

Pilsbry HA (1894) Manual of Conchology. Series 2, vol.9. Academy of Natural Sciences, Philadelphia, 302 pp.

Richardson L (1985) Camaenidae: catalog of species. Tryonia 12: 1–479.

Schileyko AA (2003) Treatise on recent terrestrial pulmonate molluscs. Part 11. Trigonochlamydidae, Papillodermidae, Vitrinidae, Limacidae, Bielziidae, Agriolimacidae, Boettgerillidae, Camaenidae. Ruthenica Suppl 2: 1510–1621.

Schileyko AA (2011) Check-list of land pulmonate molluscs of Vietnam (Gastropoda: Stylommatophora). Ruthenica 21(1): 1–68.

Tamura K, Stecher G, Peterson D, Filipski A, Kumar S (2013) MEGA6: Molecular Evolutionary Genetics Analysis version 6.0. Molecular Biology and Evolution 30(12): 2725–2729. https://doi.org/10.1093/molbev/mst197

Vaught KC (1989) A Classification of the Living Mollusca. Melbourne, 189 pp.

Wall-Palmer D, Hegmann M, Goetze E, Peijnenburg KTCA (2019) Resolving species boundaries in the Atlanta brunnea species group (Gastropoda, Pterotracheoidea). ZooKeys 899: 59–84. https://doi.org/10.3897/zookeys.899.38892

Wu M, Chen ZY, Zhu XR (2019) Two new camaenid land snails (Eupulmonata) from Central China. ZooKeys 861: 129–144. https://doi.org/10.3897/zookeys.861.35430

Wu SP, Hwang CC, Lin YS (2008) Systematic revision of the arboreal snail *Satsuma* albida species complex (Mollusca: Camaenidae) with descriptions of fourteen new species from Taiwan. Zoological Journal of the Linnean Society 154: 437–493. https://doi.org/10.1111/j.1096-3642.2008.00415.x

Yen TC (1939) Die chinesischen Land-und Süsswasser Gastropoden des Natur-Museums Senckenberg. Vittorio Klostermann, Frankfurt-am-Main. Abhandlungen der Senckenbergischen Naturforschenden Gesellschaft 444: 1–235.

Zilch A (1959–1960) Gastropoda. Teil 2: Euthyneura. Handbuch der Paläozoologie, Band 6. Berlin-Nikolassee, Gebrüder Borntraeger, 834 pp.

Zilch A (1964) Die Typen und Typoid des Natur-Museums Senckenberg, 29: Mollusca, Camaenidae (3). Archiv für Molluskenkunde 93: 243–262.

ZooKeys 996: 59–91 (2020)
doi: 10.3897/zookeys.996.57411
https://zookeys.pensoft.net

RESEARCH ARTICLE

A peer-reviewed open-access journal
ZooKeys
Launched to accelerate biodiversity research

A new micropolydesmoid millipede of the genus *Eutrichodesmus* Silvestri, 1910 from Cambodia, with a key to species in mainland Southeast Asia (Diplopoda, Polydesmida, Haplodesmidae)

Ruttapon Srisonchai[1], Natdanai Likhitrakarn[2], Chirasak Sutcharit[1], Ekgachai Jeratthitikul[3], Warut Siriwut[3], Phanara Thrach[4,5], Samol Chhuoy[4,5], Peng Bun Ngor[4,5], Somsak Panha[1,6]

1 *Animal Systematics Research Unit, Department of Biology, Faculty of Science, Chulalongkorn University, Phayathai Road, Patumwan, Bangkok 10330, Thailand* **2** *Division of Plant Protection, Faculty of Agricultural Production, Maejo University, San Sai, Chiang Mai 50290, Thailand* **3** *Animal Systematics and Molecular Ecology Laboratory, Department of Biology, Faculty of Science, Mahidol University, Bangkok 10400, Thailand* **4** *Inland Fisheries Research and Development Institute (IFReDI), Fisheries Administration, No. 86, Norodom Blvd., PO Box 582, Phnom Penh, Cambodia* **5** *Wonders of the Mekong Project, c/o IFReDI, No. 86, Norodom Blvd., PO Box 582, Phnom Penh, Cambodia* **6** *Academy of Science, The Royal Society of Thailand, Bangkok 10300, Thailand*

Corresponding author: Somsak Panha (somsak.pan@chula.ac.th)

Academic editor: P. Stoev | Received 9 August 2020 | Accepted 15 October 2020 | Published 24 November 2020

http://zoobank.org/EAA3A8D2-0AC1-422B-A2CD-5A491958C6F7

Citation: Srisonchai R, Likhitrakarn N, Sutcharit C, Jeratthitikul E, Siriwut W, Thrach P, Chhuoy S, Ngor PB, Panha S (2020) A new micropolydesmoid millipede of the genus *Eutrichodesmus* Silvestri, 1910 from Cambodia, with a key to species in mainland Southeast Asia (Diplopoda, Polydesmida, Haplodesmidae). ZooKeys 996: 59–91. https://doi.org/10.3897/zookeys.996.57411

Abstract

The micropolydesmoid millipede family Haplodesmidae is here recorded from Cambodia for the first time through the discovery of the first, new species of the genus *Eutrichodesmus* Silvestri, 1910: *E. cambodiensis* **sp. nov.** This new species is described from two limestone habitats in Kampot Province, based on abundant material. It is easily distinguished from all related congeners by the following combination of characters: body greyish-brown; limbus roundly lobulate; solenomere partially divided from acropodite by a digitiform lobe, but without hairpad. Brief remarks on the previously-proposed "*pecularis*-group"

are provided and a second group, the "*demangei*-group", is established and discussed on the basis of morphological evidence, updating the number of recognised species groups of *Eutrichodesmus* to two. Detailed morphological illustrations, photographs and a distribution map, as well as remarks on its habitat and mating behaviour of the new species are presented. Furthermore, the current distributions of all 55 presently-known species of *Eutrichodesmus* are provided and a key to all 23 species that occur in mainland Southeast Asia is given.

Keywords
Karst, new species, Southeast Asia, taxonomy

Introduction

Previous and recent studies on millipedes in the Kingdom of Cambodia have revealed at least 23 species from 17 genera, 12 families and eight orders (Likhitrakarn et al. 2015, 2020; Golovatch 2018). Although the Polydesmida Pocock, 1887 is the most diverse order of Diplopoda worldwide, only two polydesmidan families have hitherto been reported from Cambodia: Cryptodesmidae and Paradoxosomatidae. The Cryptodesmidae is typically considered as "micropolydesmoid" due to small body sizes of its species. The group is represented in Cambodia by only two species: *Trichopeltis kometis* (Attems, 1938) and *Circulocryptus kompantsevi* Golovatch, 2018. The former species was originally described from Kratié Province (Attems 1938), but it has since been recorded from Vietnam and Laos as well (Golovatch and Akkari 2016). *Circulocryptus kompantsevi* has recently been described from a rain–and-cloud forest at about 1,000 m above sea-level (AMSL) in the Phnom Bokor National Park, Kampot Province (Golovatch 2018). Surprisingly, no other micropolydesmoid families (e.g. Haplodesmidae or Pyrgodesmidae), both quite diverse and common in Indochina, have been recorded from Cambodia yet. Not only the micropolydesmoids, but also the genera *Desmoxytes* Chamberlin, 1923, *Antheromorpha* Jeekel, 1968 and *Tylopus* Jeekel, 1968, all in the family Paradoxosomatidae and all quite diverse and common in the neighbouring countries, also appear to be poorly represented in Cambodia. This strongly contrasts with the adjacent parts of Indochina where more than 20 micropolydesmoid species have been discovered in Laos, Thailand and Vietnam over the last few years (Golovatch et al. 2015; Liu et al. 2017; Golovatch 2018; Likhitrakarn et al. 2019). Amongst these micropolydesmoids, many are quite rare and most are known only from their original descriptions.

The micropolydesmoid genus *Eutrichodesmus* Silvestri, 1910 is amongst the most speciose not only in Haplodesmidae, but also in the entire order Polydesmida. Its distribution ranges from southern Japan in the north, through Taiwan, continental China and mainland Southeast Asia, to Indonesia and Vanuatu in the south (Liu and Wynne 2019; Golovatch and Liu 2020). *Eutrichodesmus* currently comprises 54 recognised species (Sierwald and Spelda 2019), of which over half are known from continental China alone, whereas 22 species are restricted to mainland Southeast Asia. Golovatch

et al. (2009a, 2009b) provided the most thorough and basic treatment of the group. However, since then, the number of known species has increased almost three-fold (Golovatch et al. 2009b, 2010, 2015, 2016; Makhan 2010; Liu et al. 2013, 2017; Liu and Wynne 2019). This invites an update and a modern key.

We have recently conducted surveys in southern Cambodia with emphasis on the biodiversity of limestone karsts. A considerable amount of material has been collected and become available for study. As a result, several new species from different millipede groups have been revealed and mostly already described: *Plusioglyphiulus* Silvestri, 1923 and *Trachyjulus* Peters, 1864 (Cambalopsidae, Spirostreptida), as well as *Tylopus* and *Orthomorpha* Bollman, 1893 (Paradoxosomatidae, Polydesmida). The present paper is devoted to the description of a new *Eutrichodesmus*, the first Haplodesmidae to be recorded from Cambodia. We also provide an identification key to and update the distributions of all known species of *Eutrichodesmus*.

Material and methods

The material for this contribution was collected during surveys on freshwater and terrestrial invertebrates in Cambodia, conducted jointly by researchers from the Inland Fisheries Research & Development Institute of Cambodia (IFReDI) and several Thai specialists. Since the expeditions started (from 2018 until now), large collections of millipedes have become available, also representing the first reference collections in Cambodia.

Specimen collecting and preservation

All specimens were hand-collected from limestone habitats in Cambodia. Live animals were photographed using a Nikon D700, equipped with an AF-S VR Micro-Nikkor 105 mm lens in the field. Some mating pairs were observed at the type locality and some were brought back to the laboratory for further behavioural observations. Specimens were euthanised, based on AVMA guidelines for the euthanasia of animals (American Veterinary Medical Association 2020) and then mostly stored in 70% (v/v) ethanol for morphological study and, partly, in 95% (v/v) ethanol for molecular analysis. Latitude, longitude and elevation were obtained from a Garmin GPSMAP 60 CSx and all coordinates and elevations were double-checked with Google Earth to confirm the precise location.

Morphological descriptions

All specimens of the new species were carefully examined for non-gonopodal and gonopodal characteristics using stereo and compound light microscopes. For some male specimens, the gonopods were carefully dissected and then mounted on a slide with DPX/ balsam. The morphological terminology used in this study follows that of

previous publications (Golovatch et al. 2009a, 2009b, 2010, 2015, 2016; Hoffman 1977a, 1977b; Liu and Tian 2013; Liu et al. 2017). Details of gonopodal terminology are shown in the section "Abbreviations used in descriptions" below.

The holotype and some paratypes are deposited in the Chulalongkorn University Museum of Zoology (CUMZ–hpd0001 and CUMZ–hpd0002). Some paratypes are housed in the collections of the Inland Fisheries Research and Development Institute (CIFI), Cambodia and the Zoological Reference Collection (ZRC) of the Lee Kong Chian Natural History Museum, Singapore.

All available literature sources, especially the original descriptions, were critically accessed in order to compare morphological characters to all known species. Positional and directional terms for gonopod descriptions follow Srisonchai et al. (2018).

Illustrations

Drawings were sketched under a stereomicroscope and a light microscope. All plates of figures were generated and edited using Adobe Photoshop CS6 to adjust the colour and brightness. The distribution map was modified from Willett et al. (2015).

Abbreviations used in descriptions

As the previous studies of gonopods from different authors are quite variable, ranging from a brief description to several deeply detailed ones, we chose to follow the comprehensive gonopod terminology from Golovatch et al. (2009b, 2015), Hoffman (1977a, 1977b) and Liu et al. (2017).

Abbreviations: cn = cannula, cx = coxa, dp = distofemoral process, sg = seminal groove; acropodite = the apical part of gonopod that starts from a prominent cingulum (the end of the femorite); solenomere = an independent part of the gonopod acropodite that carries the seminal groove, with or without hairpad, completely or partly fused to the acropodite; telopodite = the main part of the gonopod pivoting on the coxa, including the prefemur, femorite and acropodite.

Other abbreviations used

AMSL above mean sea level;
ca. about, around, circa;
CIFI the collection of the Inland Fisheries Research and Development Institute, Cambodia;
CUMZ Chulalongkorn University Museum of Zoology, Bangkok, Thailand;
IFReD Inland Fisheries Research and Development Institute, Cambodia;
SEM Scanning electron microscopy;
ZRC Zoological Reference Collection of the Lee Kong Chian Natural History Museum, National University of Singapore, Singapore.

Results

Taxonomy

Order Polydesmida Pocock, 1887
Suborder Polydesmidea Pocock, 1887
Family Haplodesmidae Cook, 1895

Genus *Eutrichodesmus* Silvestri, 1910

Type species. *Eutrichodesmus demangei* Silvestri, 1910

All species included. The genus *Eutrichodesmus* currently contains 55 species, including the new one described herein, see Table 1.

Recorded distributions of all known species. Based on all the recent literature and excluding the newly-described species, the genus *Eutrichodesmus* is widely distributed in southern Japan, Taiwan, southern China, mainland Southeast Asia (Malaysia, Laos, Thailand and Vietnam), Indonesia (Sulawesi) and Melanesia (Vanuatu) (Golovatch et al. 2009a, 2009b, 2015, 2016; Liu et al. 2017; Golovatch and Liu 2020; see Table 1). No *Eutrichodesmus* species have hitherto been reported from Cambodia.

Updated diagnosis of the genus *Eutrichodesmus* Silvestri, 1910. Golovatch et al. (2009a, 2009b) provided a complete diagnosis of the genus, as well as the main structural details of all genera in the family Haplodesmidae. It is therefore relatively easy to provide a morphological overview of *Eutrichodesmus*. However, as the genus shares some characters with certain confamilial genera, i.e. *Cylindrodesmus* Pocock, 1889; *Doratodesmus* Cook *in* Cook and Collin, 1985; and *Helodesmus* Cook, 1896, a refined diagnosis seems to be warranted. The more so as, since 2009, 18 further species of *Eutrichodesmus* have been described, adding a number of morphological traits across the genus (Makhan 2010; Golovatch et al. 2010, 2015, 2016; Liu et al. 2017; Liu and Wynne 2019). The amended diagnosis of *Eutrichodesmus* is chiefly based on that by Golovatch et al. (2009a, 2009b).

The genus *Eutrichodesmus* differs from all other Haplodesmidae by showing the following combination of characters. Body small (ca. 3.5–14 mm in length), with 19–20 rings; usually "doratodesmid" (= capable of volvation); conglobation usually complete, but sometimes incomplete. Tegument: collum and metaterga usually microgranulate and microvillose; prozonae often alveolate. Metaterga with or without mid-dorsal projections (outgrowths); usually with two or three rows of conspicuous tubercles (seldom four or more), often arranged mixostictic (irregular in axial direction) or, sometimes, isostictic (regular in axial direction). Paraterga short or long, usually lobulate. Ozopores usually present on rings 5, 7, 9, 10, 12, 13, 15–19, rarely reduced or absent; with or without porosteles. Gonopod: Coxae often microgranulate; usually abundantly setose, sometimes with a distolateral outgrowth. Telopodite usu-

Table 1. Known distribution of all *Eutrichodesmus* species. Note that the species are listed, based on the appearance of mid-dorsal projections on metaterga due to the simpliest way for their examination.

No.	Species	Type locality	Distribution	References
Species with conspicuous mid-dorsal projections on metaterga				
1	*E. anisodentus* (Zhang, 1995)	China, Fujian Province, Mt Wuyi	South-eastern China	Zhang 1995b; Golovatch et al. 2010, 2015
2	*E. aster* Golovatch et al., 2009	Vietnam, Yen Bai Province, Nghia Lo: Xa Som a, Tham Han Cave	North-western Vietnam	Golovatch et al. 2009b
3	*E. asteroides* Golovatch et al., 2009	Vietnam, Quang Binh Province, Cha Noi: Hang Cha Noi Cave	Central Vietnam	Golovatch et al. 2009b
4	*E. astriproximus* Golovatch et al., 2016	Vietnam, Quang Binh Province, Thuong Hoa, Cave Hang Mo O	Central Vietnam	Golovatch et al. 2016
5	*E. astrisimilis* Golovatch et al., 2016	Vietnam, Quang Binh Province, Hoan Son, Cave Hang Cha Ra	Central Vietnam	Golovatch et al. 2016
6	*E. cavernicola* (Sinclair, 1901)	Thailand, Yala Province, Mueang Yala District, Wat Khuhapimuk (Gua Glaf = Gua Galp = Dark Cave) (exact location based on Huber et al. (2015))	Southern Thailand	Sinclair 1901; Hoffman 1977b; Golovatch et al. 2009a, 2009b
7	*E. deporatus* Liu & Wesener, 2017	Laos, Luang Prabang Province, Northeast of Luang Prabang, Nam Ou, Nong Khiao, Cave Tham Pathok	Northern Laos	Liu et al. 2017
8	*E. dorsiangulatus* (Zhang *in* Zhang & Wang, 1993)	China, Yunnan Province, Mengla County, Baoniujiao Cave	South-western China	Zhang and Wang 1993; Golovatch et al. 2009a, 2009b, 2015
9	*E. lipsae* Golovatch et al., 2015	China, Guangxi Province, Guilin County, Grotte des Squelettes	Southern China	Golovatch et al. 2015
10	*E. macclurei* (Hoffman, 1977)	Malaysia, Selangor State, near Kuala Lumpur, Batu Caves	Peninlular Malaysia	Hoffman 1977a; Golovatch et al. 2009a, 2009b
11	*E. nodulosus* (Verhoeff, 1939)	Japan, Ryukyu Island of "Fukafuguza", a cave (Fukafuguza not known to exist in the Ryukyu Island)	Southern Japan	Verhoeff 1939; Omine 1982; Omine and Ito 1998; Golovatch et al. 2010
12	*E. paraster* Liu & Wesener, 2017	Laos, Huaphan Province, Xop, Cave Tham Long Puang	Eastern Laos	Liu et al. 2017
13	*E. pectinatidentis* (Zhang, 1995)	China, Zhejiang Province, Lin'an County, Mt. Tianmu	East-central China	Zhang 1995a; Golovatch et al. 2010, 2015
14	*E. reclinatus* (Hoffman, 1977)	Malaysia, Selangor State, near Kuala Lumpur, Gua Anak Takun at Templer Park	Peninsular Malaysia	Hoffman 1977b; Golovatch et al. 2009a, 2009b
15	*E. soesilae* Makhan, 2010	China, Chongqing Municipality, Beibei District, Mt. Jinyun	South-western China	Makhan 2010; Golovatch et al. 2010, 2015
16	*E. steineri* Liu & Wesener, 2017	Laos, Luang Prabang Province, Phou Khoun District, Cave Tham Deu	Northern Laos	Liu et al. 2017
17	*E. subasteroides* Golovatch et al., 2016	Vietnam, Quang Binh Province, Hoan Son, Cave Hang Da Voi	Central Vietnam	Golovatch et al. 2016
Species without mid-dorsal projections on metaterga				
18	*E. apicalis* Golovatch et al., 2015	China, Hubei Province, Yishang Yichang County, Grotte des Araignées	Central China	Golovatch et al. 2015
19	*E. arcicollaris* Zhang *in* Zhang & Wang, 1993	China, Yunnan Province, Hekou County, near Laofanzhai Village, Huayu Cave	South-western China	Zhang and Wang 1993; Golovatch et al. 2009a, 2009b, 2015
20	*E. armatocaudatus* Golovatch et al., 2009	Vietnam, Thanh Hoa Province, Pu Luong, Lung Cao, Hang Lang Lua Cave	Northern Vietnam	Golovatch et al. 2009a
21	*E. armatus* (Miyosi, 1951)	Japan, Ehime Prefecture, Kaminada-Mati, Yosihuzi-Mura (Shikoku Island)	South-western & Southern Japan; Taiwan	Miyosi 1951; Golovatch et al. 2010; Wang 1958; Karasawa et al. 2008
22	*E. basalis* Golovatch et al., 2009	Vietnam, Vinh Ha Long Province (Southwest), Dao Bo Hon, Hang Bo Nau Cave	North-eastern Vietnam	Golovatch et al. 2009a
23	*E. cambodiensis* sp. nov.	Cambodia, Kampot Province, Banteay Meas District, Prasat Phnom Totong	Southern Cambodia	This study
24	*E. communicans* Golovatch et al., 2009	Vanuatu, Espirito Santo, Malo Island, Avorani	Melanesia	Golovatch et al. 2009a
25	*E. curticornis* Golovatch et al., 2009	Vietnam, Nghê An Province, Anh Son: Hoi Son, Hang Lung Bo Cave	North-central Vietnam	Golovatch et al. 2009b
26	*E. demangei* Silvestri, 1910	Vietnam, Hanam Province, Phu-Ly	Northern Vietnam	Silvestri 1910; Enghoff et al. 2004; Golovatch et al. 2009a, 2009b

No.	Species	Type locality	Distribution	References
27	*E. digitatus* Liu & Tian, 2013	China, Guangdong Province, Qingyuan City, Jintan Town, Cave Mi Dong	Southern China	Liu and Tian 2013; Golovatch et al. 2015
28	*E. distinctus* Golovatch et al., 2009	China, Guangxi Province, Fushui, Bapen, Cave 4	Southern China	Golovatch et al. 2009b, 2015
29	*E. elegans* (Miyosi, 1956)	Japan, Enosima, Mizonokuti, Aoga-Sima (Idzu-Inseln) (Aogashima island)	Eastern Japan	Miyosi 1956; Golovatch et al. 2009a, 2010
30	*E. filisetiger* Golovatch et al., 2009	Vietnam, Thanh Hoa Province, Th anh Son: Lang Kho Muong, Hang Doi Cave	Northern Vietnam	Golovatch et al. 2009b
31	*E. gremialis* (Hoffman, 1982)	Thailand, Chiang Mai Province, Chiang Dao District, Chiang Dao caves	Northern Thailand	Hoffman 1982a; Golovatch et al. 2009a, 2009b
32	*E. griseus* Golovatch et al., 2009	Vietnam, Kien Giang Province, Kien Luong: Hon Chong, Nui Hon Chong, outside Cave 2 near Hang Hai Côt	Southern Vietnam	Golovatch et al. 2009b
33	*E. incisus* Golovatch et al., 2009	China, Guizhou Province, Qianxi County, Hong Lin Village, Tiao Shuz Dong Cave	South-western China	Golovatch et al. 2009a, 2015
34	*E. jianjia* Liu & Wynne, 2019	China, Guangxi Zhuang Autonomous Region, Yangshuo County, Guanshan No. 4 Cave	Southern China	Liu and Wynne 2019
35	*E. latellai* Golovatch et al., 2015	China, Guizhou Province, Zhen Feng County, Bei Pan Jiang Town, Cave Shui Chi Dong (Water Pool Cave)	South-western China	Golovatch et al. 2015
36	*E. latus* Golovatch et al., 2009	China, Guangxi Province, Yachang Nature Reserve, Yan Wu Dong Cave	Southern China	Golovatch et al. 2009a, 2015
37	*E. monodentus* (Zhang *in* Zhang & Wang, 1993)	China, Yunnan Province, Mengla County, Caiyun Cave	South-western China	Zhang and Wang 1993; Golovatch et al. 2009a, 2009b, 2015
38	*E. multilobatus* Golovatch et al., 2009	Laos, Luang Prabang Province, Nong Kiaw: Tham Pha Kouang, Cave B	Northern Laos	Golovatch et al. 2009b
39	*E. nadan* Golovatch et al., 2016	Laos, Khammouane Province, Ban Nadan, Cave Tham Nadan	Central Laos	Golovatch et al. 2016
40	*E. obliteratus* Golovatch et al., 2015	China, Guizhou Province, Guanling County, Huajiang Town, Cave Huashiban Dong (Slippery Cave)	South-western China	Golovatch et al. 2015
41	*E. parvus* Liu & Wesener, 2017	Laos, Huaphan Province, Cave Tham Nam Long	Eastern Laos	Liu et al. 2017
42	*E. peculiaris* (Murakami, 1966)	Japan, Shikoku, Ehime Prefecture, Niihama, Oshima	Southwestern Japan	Murakami 1966; Golovatch et al. 2009a, 2010
43	*E. planatus* Liu & Tian, 2013	China, Guangxi Zhuang Autonomous Region, Hechi City, Liujia Town, Cave Zhenzhuyan	Southern China	Liu and Tian 2013; Golovatch et al. 2015
44	*E. reductus* Golovatch et al., 2009	Indonesia, Sulawesi Selatan, kab. Maros: Samanggi, Gua Saripa Cave	Eastern Indonesia: Sulawesi	Golovatch et al. 2009b
45	*E. regularis* Golovatch et al., 2009	Vietnam, Lao Cai Province, Sa Pa, Hang Ta Phin Cave	North-western Vietnam	Golovatch et al. 2009b
46	*E. silvaticus* (Haga, 1968)	Japan, Kyushu Island, Fukuoka Prefecture, Tagawa City, Hojoo-machi, Gooya	South-western Japan	Haga 1968; Golovatch et al. 2010
47	*E. similis* Golovatch et al., 2009	China, Guangxi Province, Mulun Nature Reserve, Gui Dong 2 Cave	Southern China	Golovatch et al. 2009a, 2015; Liu and Tian 2013
48	*E. simplex* Liu & Tian, 2013	China, Jiangxi Province, Fenyi County, Cave Taoyuan Dong	East-central China	Liu and Tian 2013; Golovatch et al. 2015
49	*E. sketi* Golovatch et al., 2015	China, Hunan Province, Longshan County, Huaoyan, Cave Feihu Dong	Central China	Golovatch et al. 2015
50	*E. spinatus* Liu & Tian, 2013	China, Hunan Province, Sidu Town, Sidu Caves	Central China	Liu and Tian 2013; Golovatch et al. 2015
51	*E. taiwanensis* Golovatch et al., 2010	Taiwan, Taipei City, Wenshan District, Chih-Nan Temple	All parts of Taiwan	Golovatch et al. 2010, 2011
52	*E. tenuis* Golovatch et al., 2015	China, Guizhou Province, Guanling County, Yong Ning Town, Cave Yun Dong (Cloud Cave)	South-western China	Golovatch et al. 2015
53	*E. triangularis* Golovatch et al., 2015	China, Sichuan Province, Beichuan County, Cave Yuan Dong	South-western China	Golovatch et al. 2015
54	*E. troglobius* Golovatch et al., 2015	China, Guizhou Province, Kaiyang, Cave Xianyan Dong	South-western China	Golovatch et al. 2015
55	*E. trontelji* Golovatch et al., 2015	China, Guizhou Province, Libo County, Libo, Cave Feng Dong	South-western China	Golovatch et al. 2015

ally long and slender; basal half of telopodite (= prefemoral part) densely setose; often with a distofemoral process, conspicuous, located laterally on femorite, sometimes absent. Acropodite well-developed, conspicuous. Solenomere often completely fused to acropodite (solenomere = acropodite), rarely separated and forming a lobe. Seminal groove running on mesal side of prefemur, usually terminating at about halfway of acropodite to distal region; with or without hairpad.

Description of the new species

Eutrichodesmus cambodiensis **Srisonchai & Panha, sp. nov.**
http://zoobank.org/10A8DC52-D01C-4892-8B20-88D9F0EBB009
Figures 1–4, 5W, 7T, 9, 10

Material examined. ***Holotype*** male (CUMZ–hpd0001), CAMBODIA, Kampot Province, Dang Tong District, near Wat Phnom Small, limestone hills, 10°42'12"N, 104°31'30"E, ca. 47 m AMSL, leg. C. Sutcharit, W. Siriwut, E. Jerutthitikul, P. Trach, S. Chuoy & R. Srisonchai (locatily no. C041), 16 September 2019. ***Paratypes.*** Twenty-three males, fifteen females (CUMZ–hpd0002), same data as holotype. Six males and six females (CUMZ–hpd0002) CAMBODIA, Kampot Province, Banteay Meas District, Prasat Phnom Totong, 10°41'49"N, 104°31'23"E, ca. 31 m AMSL, leg. C. Sutcharit, W. Siriwut, E. Jerutthitikul, P. Trach, S. Chuoy & R. Srisonchai (locatily no. C042), 16 September 2019. One male, one female (CIFI), same data as holotype. One male (ZRC_ENT00014160), one female (ZRC_ENT00014161), same data as holotype. ***Further specimens, non-types.*** Two broken males, two broken females, one male without gonopods, eight juveniles, two males and two females prepared for DNA extraction (CUMZ–hpd0002), same data as for holotype.

Etymology. The specific epithet reflects the name of the country "*Cambodia*" where all specimens were collected and to which the new species appears to be endemic; adjective.

Diagnosis. Body with incomplete volvation; metaterga with three transverse rows of regular and round tubercles, but no mid-dorsal projection (outgrowth) on metaterga; distofemoral process on gonopod telopodite very short, inconspicuous. Similar in all these characters to *E. griseus* Golovatch et al., 2009, but differs in having (1) live specimens and freshly preserved material pale greyish-brown or pale brown in colour; (2) the limbus crenulate, but not spinulate, crenulations being slightly longer than broad; (3) the acropodite curved and long, unciform, attenuated near tip; with a free solenomere starting from about midway; and (4) the solenomere digitiform, papillate, without hairpad.

Description. Body length 5–7 mm (male) or 6–8 mm (female); width of midbody metazonae ca. 0.9 mm (male) or ca. 1.2 mm (female). In width, head < collum < 2 = 3 < 4 < 5–17, thereafter body gradually tapering towards telson. Females apparently longer and larger than males.

Colour (Fig. 1). Live specimens pallid greyish-brown or brown: head grey; antennae pale brown; collum, metaterga and paraterga greyish-brown; surface below

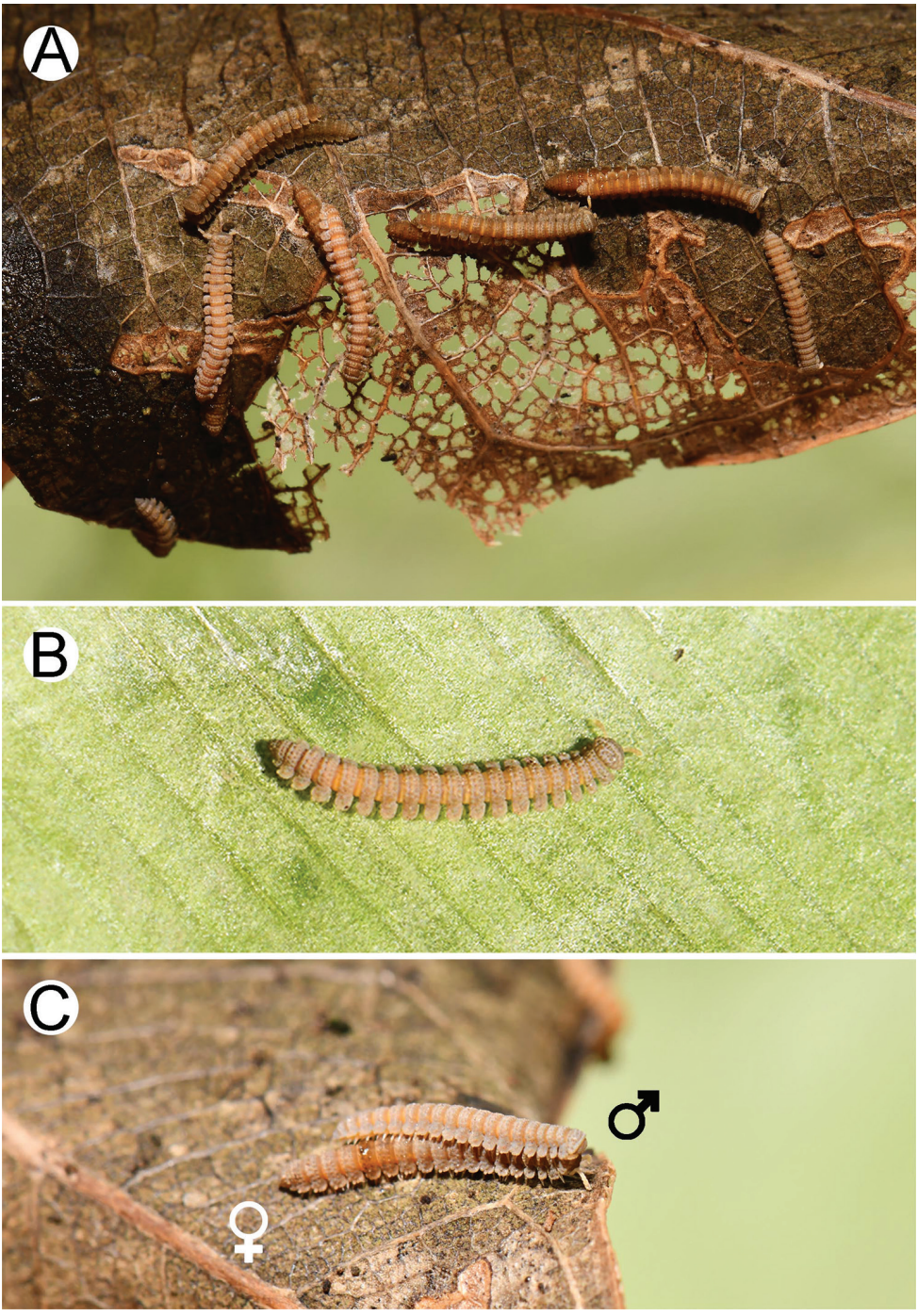

Figure 1. Photographs of live *Eutrichodesmus cambodiensis* sp. nov., paratypes (CUMZ–hapld00002) **A** pairs of mating couples **B** male and **C** mating couple. Not to scale.

paraterga, prozonae, sterna and legs brown. Specimens in alcohol after six months of presevration nearly the same in colour as in life.

Body (Fig. 2A). General appearance as in Fig. 2A. Body long and slender. Adults with 20 rings. Volvation incomplete because of a slender body and short paraterga.

Head (Fig. 2B, C). Slightly transverse, wider than high, densely pilose, not covered with collum from above. Vertex microvillose and microgranulate. A pair of small, poorly separated, paramedian knobs above antennal sockets. Isthmus between antennae ca. 1.3 times as wide as diameter of antennal socket. Epicranial suture deep and conspicuous. Labrum and genae sparsely setose.

Antennae (Fig. 2B, D). Short and stout, clavate, densely setose, setae being long.

Antennomere 6 longest, with a group of bacilliform sensilla located inside a shallow distolateral pit near tip of each of antennomeres 5 and 6. Antennomere 8 with four sensory cones apically.

Collum (Figs 2A, C, E; 3A). Large, nearly semi-circular, a little broader than head, with regular and rounded tubercles arranged in five transverse rows: usually 7+7 tubercles in anterior (first) row, followed by 4+4, 1(0)+1(0), 3+3 and 4+4 tubercles in rows 2–5, respectively. Anterior margin truncate, slightly elevated, resembling that in *E. griseus* or some species of Pyrgodesmidae. Posterior margin round. Lateral margin narrow, directed laterad.

Tegument. Overall quite dull, some specimens encrusted with dirt. Head mostly microgranulate (labrum and clypeus smooth). Collum microvillose. Prozonae finely alveolate.

Suture between pro- and metazonae quite shallow and broad, more strongly alveolate and microgranulate than prozonae. Metaterga, paraterga, surface below paraterga, sterna, epiproct and hypoproct microgranulate and microvillose. Legs smooth.

Metaterga (Figs 2A, E–G; 3A–C). Metaterga 2–19 each with three transverse rows of undiffentiated tubercles, pattern isostictic (arrangement regular in axial position). Anterior, intermediate and posterior rows each with 4+4 tubercles; those in second row on body rings 5–19 larger than in other rows. Each tubercle anteriorly with a short, spatulate, bisegmented seta. Mid-dorsal (axial) line missing.

Limbus (Fig. 3F). Crenulate, each lobulation being slightly longer than broad, tip round.

Paraterga (Figs 2A, E–F; 3A–C, E; 5W). Broad, slightly sloping down. Tip round and directed ventrolaterad. Paraterga 2 enlarged, *in situ* more strongly sloping down than on other rings, with four or five conspicuous lobules. Paraterga 3 and 4 shorter, narrower than others; each with four conspicuous lobules. Paraterga 5–18 mostly with four lobules, some rings with five ones.

Ozopores. Inconspicuous when seen in dorsal view. Pores small, oval in shape, lacking a porostele, opening laterally near rear margin of paraterga above it. Pore formula normal (5, 7, 9, 10, 12, 13, 15–19).

Pleurosternal ridges. Absent.

Epiproct (Fig. 3D, G, I). Very short, flattened dorsoventrally; knob-like apically, with two pairs of inconspicuous setae (spinnerets), each spinneret located inside a tube-like structure, both dorsal and ventral spinnerets arranged inside a circular shallow depression.

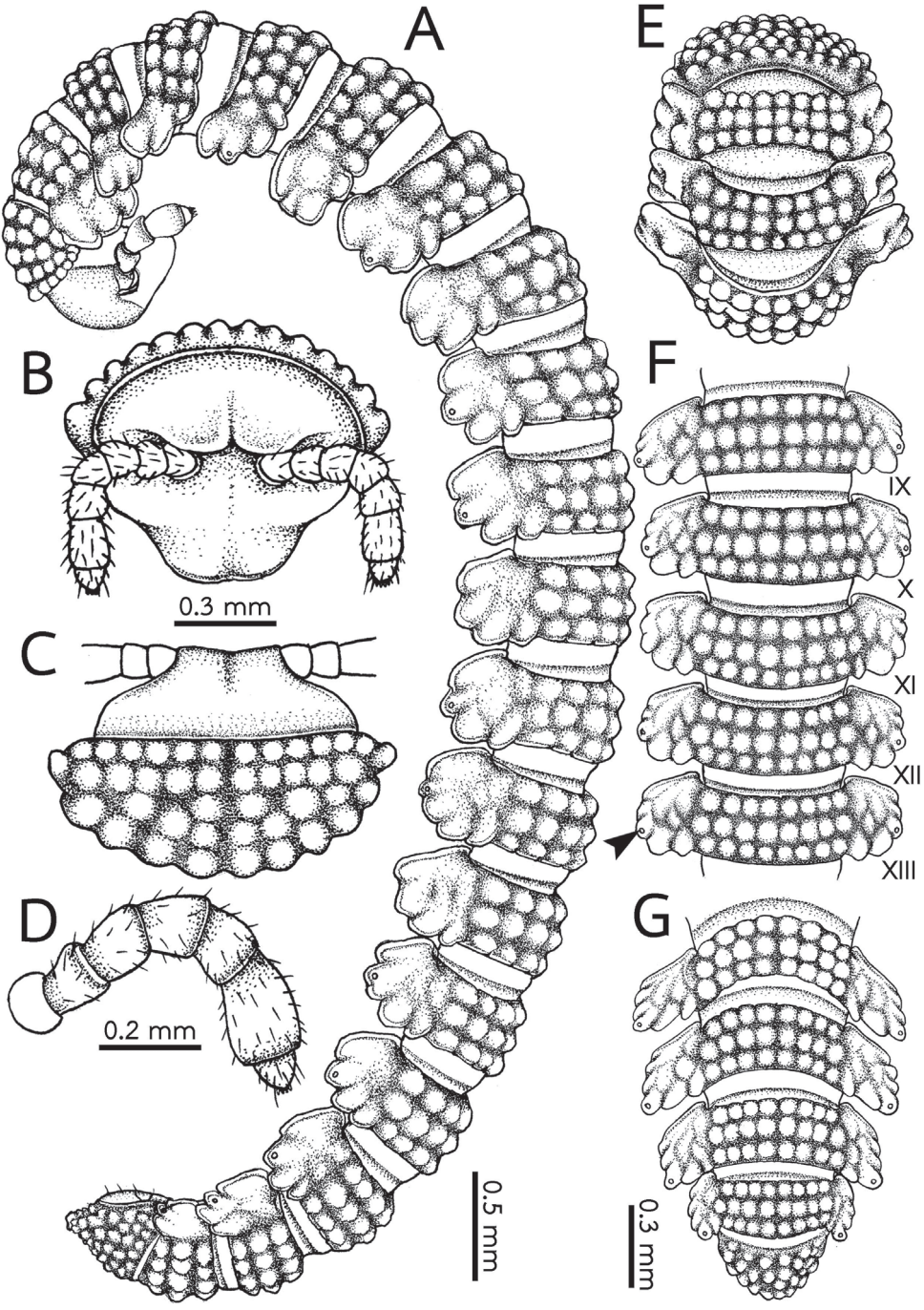

Figure 2. *Eutrichodesmus cambodiensis* sp. nov., male paratype (CUMZ–hpd0002) **A** whole body part **B** head and antenna **C** head and collum **D** antenna **E** anterior body part **F** body rings 9–13 (arrowhead points to ozopore) **G** posteriormost body rings and telson **A** lateral view **B** anterior view **C, E–G** dorsal view. Scale bars: 0.3 mm (**B, C**), 0.3 mm (**E–G**).

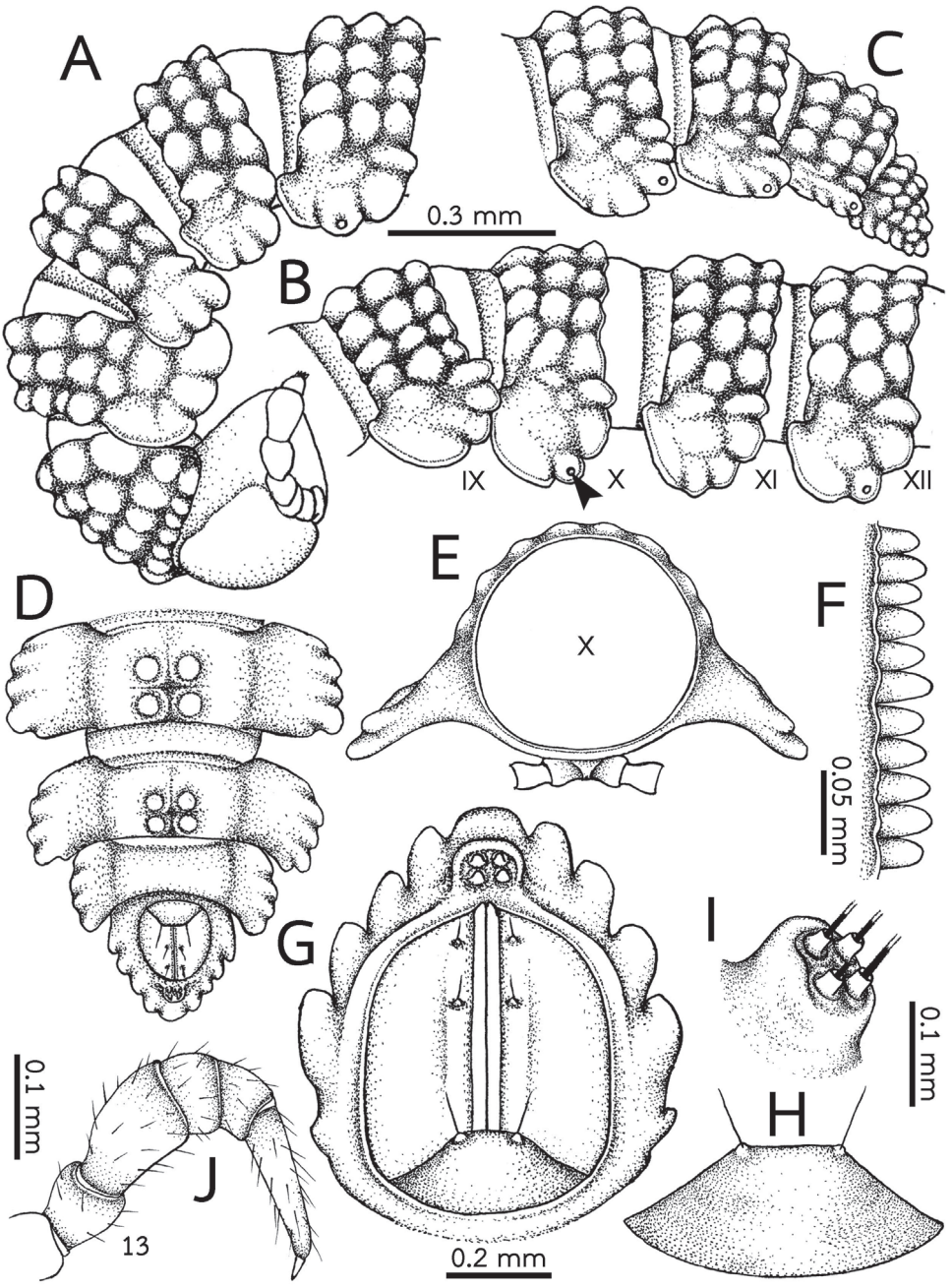

Figure 3. *Eutrichodesmus cambodiensis* sp. nov., male paratype (CUMZ–hpd0002) **A** anterior body part **B** body rings 9–12 (arrowhead points to ozopore) **C, D** posteriormost body rings and telson, **E** mid-body ring **F** limbus of body ring 10 **G** last ring and telson **H** hypoproct **I** two pairs of apical setae (spinnerets) **J** leg 13 **A–C, I** lateral view **D, G, H** ventral view. Scale bars: 0.5 mm (**A–E**), 0.1 mm (**H, I**).

Paraproct (Fig. 3G). Normal, with two pairs of small setae.

Hypoproct (Fig. 3G, H). Subtrapeziform, caudal margin truncate, with two small, inconspicuous, setiferous tubercles.

Spiracle. Simple, located above anterior and slightly before posterior legs.

Legs (Fig. 3J). Quite short and stout, in situ almost reaching the tip of paraterga. Relative length of podomeres: tarsus > femur > (prefemur ≥ coxa) = postfemur = tibia > claw.

Sterna (Fig. 3D). Narrow. Longitudinal depression between coxae in most body rings deep and narrow, only in ring 7 quite deep and wide for accommodating the shafts of gonopods. Transverse depression deep and wide.

Gonopod aperture. Very large, transversely ovoid, subequal to width of prozonite.

Gonopods (Figs 4; 7T). Shafts when retracted reaching the anterior part of sternum 7 (base of legs 8). Coxa (cx) large and stout, subquadrate, microgranulate, with a few short setae distolaterally. Cannula (cn) simple, conspicuous, curved and slender, swollen at base, inserted into a small depression at base of telopodite on posteromedial side. Telopodite suberect; basal half (= prefemoral part) nearly straight; distal half curved. Distofemoral process (dp) very short, located at about midway of telopodite, triangular, dentate. Acropodite conspicuous, with neither a lobe nor a process, distally slightly attenuated and forming a hook-like tip, directed and curved mesad. Solenomere partially separated from acropodite, conspicuous, digitiform, papillate, originating at ca. 3/4 height of telopodite beyond distofemoral process; rather short, tip *in situ* directed anteriad, apically with a large papilla which is more conspicuous than other papillae. Seminal groove (sg) conspicuous, thick, running entirely on mesal surface of telopodite, terminating without hairpad by opening on the large papilla of solonomere.

Remarks. Although the genital characters of females have not been used for taxonomic purposes in the present study, all females were examined. In all cases, the female non-genital characters were found similar to those found in males. The only difference which can be clearly seen using both live and preserved material is that females are apparently broader and longer than males (Fig. 1C).

The general colouration does not show any variability and the paratypes do not differ significantly from the holotype. Across the type series of the new species, there was little intrapopulational variation in the number of tubercles on the collum and of lobes on the paraterga: an intermediate row (third or middle row) of the collum usually showed 1+1 tubercles, only sometimes 0+1 or 1+0 tubercles; paraterga of most specimens usually had four conspicuous lobes, only sometimes five. However, all these variations in most of the non-gonopodal characters were minor, neither significant nor consistent enough to be useful for taxonomic purposes, at least in the species under consideration. Little can be said about interpopulational variation in the new species because no variation has been noted between the two examined populations and no other specimens living at and around these two locations have been found.

Notably, *E. cambodiensis* sp. nov. shows a slightly elevated anterior margin of the collum (Figs 2A, 3A). As this can easily be seen also in *E. griseus*, it is consistent with

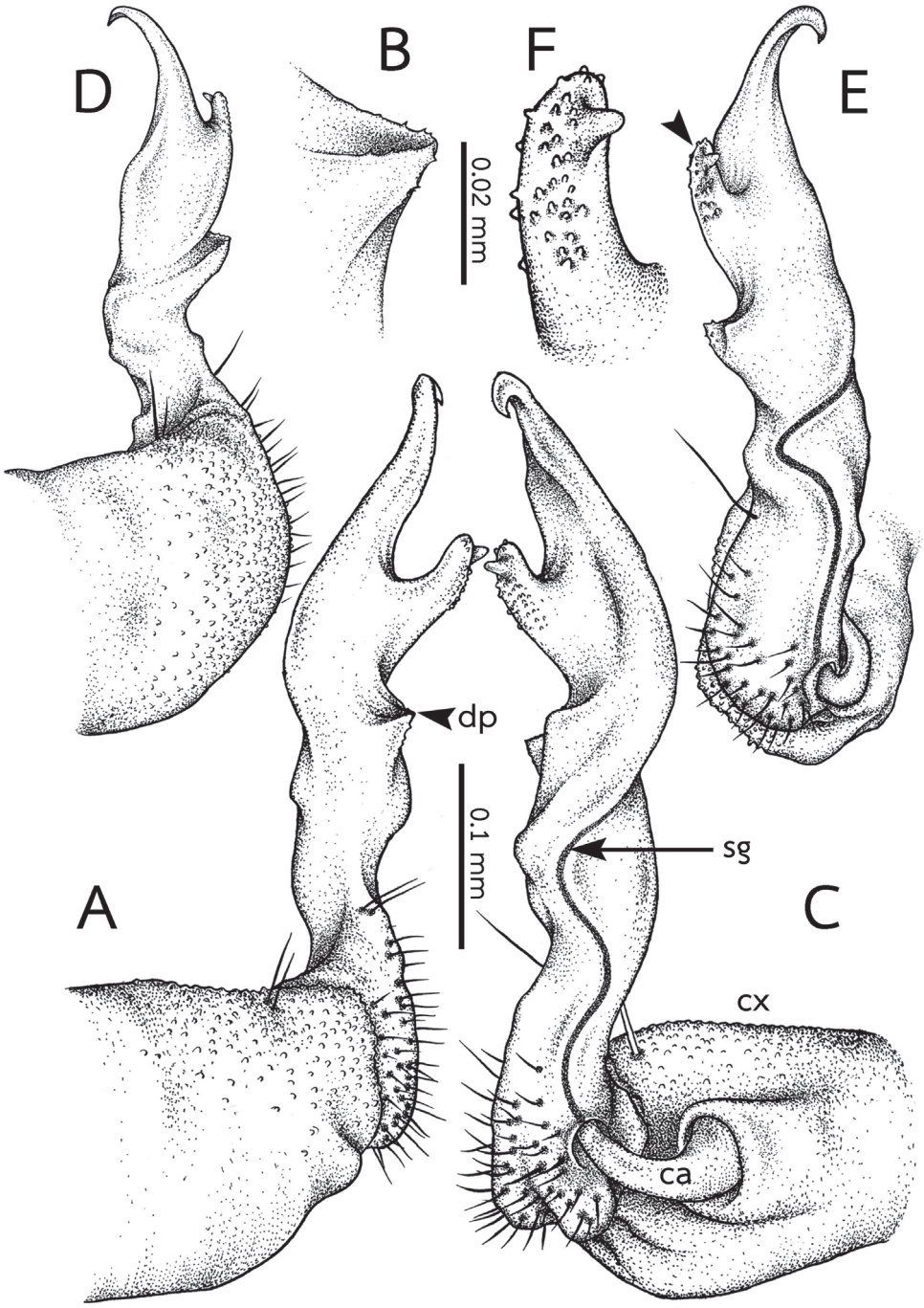

Figure 4. *Eutrichodesmus cambodiensis* sp. nov., right gonopod, male paratype (CUMZ–hpd0002) **A** lateral view (dp = distofemoral process) **B** distofemoral process **C** mesal view (cx = coxa, cn = cannula, sg = seminal groove) **D** dorsal view **E** ventral view (arrowhead points to solenomere) **F** digitiform solenomere. Scale bars: 0.1 mm (**A, C–E**), 0.02 mm (**B, F**).

what Golovatch et al. (2009b) found. Currently, only these two *Eutrichodesmus* species have the collum elevated in the anterior part, this strongly resembling the typical condition in the micropolydesmoid family Pyrgodesmidae.

The new species has the same characters as found in a bunch of congeners and shares the combination: adults with 20 body rings; body with incomplete volvation; metaterga without mid-dorsal projections, with three transverse rows of tubercles; and gonopod telopodite with a distofemoral process. All above characters are present in *E. basalis* Golovatch et al., 2009; *E. curticornis* Golovatch et al., 2009; *E. demangei* Silvestri, 1910; *E. filisetiger* Golovatch et al., 2009; *E. gremialis* (Hoffman, 1982); *E. griseus*, *E. multilobatus* Golovatch et al., 2009; *E. nadan* Golovatch et al., 2016; *E. parvus* Liu & Wesener, 2017 and *E. regularis* Golovatch et al., 2009 (see also Key and Table 2). Even though some traits have been observed, shared, especially in the gonopodal telopodite, between-species differences are always marked. With respect to the most relevant feature which lies in certain details of gonopodal structure, *E. cambodiensis* sp. nov. seems to be morphologically more similar to *E. griseus* than to any other congener, in particular in having a very short distofemoral process and the solenomere partly separated from the acropodite by forming a conspicuous lobe.

Distribution and habitat. It is worth noting that the new species was found only at the two sites. Surveys of other limestone and sandstone habitats surrounding the type locality (Kampong Trach) over a period of approximately two years have revealed no further specimens (Fig. 10). In showing a distribution of only two locations in a small and isolated limestone area, the new species can be suggested as being not only endemic to Cambodia, but also indigenous in Kampong Trach.

All specimens of the new species were hand-collected and found walking on humid rock walls of limestone caves (Fig. 9A). The vast majority of millipedes were seen crawling on humid rocks, whereas only a minor part was found slowly walking on vegetation, shaded holes and rock crevices during the daytime (Fig. 9B, C, E). It is important to note that specimens were commonly found under herb patches in a slightly shaded moist rock where the plant genus *Epithema* Blume, 1826 (family Gesneriaceae) created a mass of roots and thin litter layer on the soil in the hole (Fig. 9C). This is probably a particular microhabitat for *E. cambodiensis* sp. nov. Furthermore, we noted a co-occurrence between *E. cambodiensis* sp. nov. and the abundant *Hypselostoma cambodjense* Benthem Jutting, 1962, a microsnail (Fig. 9D), within a portion of the moist rock walls, as well as in rock crevices, but without being sympatric with other millipedes in the same microhabitats.

The habitat preferred by the new species clearly appears to be limestone, especially near caves, although all specimens were found outside the caves, near the entrance zones. No material was collected at twilight, transition or deep zones inside the cave [for a characterisation of the zonal environment in caves, see Liu and Wynne (2019)]. Many of the small holes/caves at the type locality where *E. cambodiensis* occurs are highly humid and have diminished light, owing to the shade from large trees in the area.

A large concern would be the ongoing habitat destruction very close to the type locality, where a cement factory is located on the opposite side of the mountain. Many

Table 2. Morphological comparison of some congeners with *E. cambodiensis* sp. nov. and distribution.

Characters	*E. cambodiensis* sp. nov.	*E. curticornis* Golovatch et al., 2009	*E. filisetiger* Golovatch et al., 2009	*E. griseus* Golovatch et al., 2009	*E. nadan* Golovatch et al., 2016	*E. parvus* Liu & Wesener, 2017	*E. regularis* Golovatch et al., 2009
Colour of living specimens	greyish-brown or pallid brown	uniformly pallid (probably greyish-brown)	uniformly pallid (probably light brown)	grey to blackish	uniformly light creamy-brown	uniformly light yellow-brown (probably light brown)	uniformly pallid (probably light brown)
Rows of tubercles on collum	5, regular tubercles	~5, regular tubercles	~5, irregular tubercles	5, regular tubercles	4–5?, very flat & round tubercles	5, round tubercles	5, regular tubercles
Rows of tubercles on metaterga	3 (isostictic), with inconspicuous setae	3 (mixostictic), with inconspicuous setae	3 (mixostictic), with filiform setae	3 (isostictic), with inconspicuous setae	3 (mixostictic), with inconspicuous setae	3 (mixostictic), with inconspicuous setae	3 (isostictic), with inconspicuous setae
Limbus	with round lobes, longer than broad (crenulate)	crenulate	spiculate	spinulate	microcrenulate	microcrenulate	crenulate
Paraterga	very high	low	very high	very high	very low	moderately high	moderately high
Distofemoral process (dp)	short, inconspicuous, triangular, dentate	extremely long, denticulate	very short, inconspicuous, triangular	short, inconspicuous, triangular	very long, denticulate	extremely, denticulate	long, digitiform, papillate
Acropodite	very long, without lobe	long, with a small lobe (tooth-like)	very long, with a bifid lobe	long, without lobe	Quite short, with a small lobe subapically	very long, subapically with a tooth & a lobe	with 2 lobes (small denticles)
Solenomere	long lobe, digitiform with papillate (no hairpad)	completely fused with acropodite (no hairpad)	completely fused with acropodite, with hairpad	long lobe, digitiform, with hairpad	completely fused with acropodite, with conspicuous hairy pulvillus	completely fused with acropodite (no hairpad)	lamelliform, fused with acropodite, with pilose-spinulate pulvillus
Distribution	Southern Cambodia	North-central Vietnam	Northern Vietnam	Southern Vietnam	Central Laos	Eastern Laos	North-western Vietnam

outcrops in the area appear to have been quarried and it seems plausible that the existence of the type locality would be threatened in the near future.

Observation of mating behaviour. Interestingly, all specimens of the new species collected around moist organic material and plants near the caves were pairs of several mating couples (Figs 1C, 9E). No single males or females were found separately. One presumption would be that individual millipedes were perhaps hidden in rock crevices during the daytime. The pairs of the new species mated during the rainy season when the rate of annual rainfall amount is quite high, which may imply the peak in mating occurring around September. The initial observations of the courtship were made by separating seven pairs into individual airflow plastic vials without human disturbance and we found that males appeared to initiate copulation by approaching the female from behind and then slightly reaching to the head region. The male took at least five hours grasping onto a female by its legs before it entwined and finally inserted its gonopod shaft into the female's vulva.

Notes on species groups in *Eutrichodesmus*

Table 3 summarises some significant characters across *Eutrichodesmus* species.

The genus *Eutrichodesmus* was recently revised by Golovatch et al. (2009a, 2009b), who also refined the family and its generic classification, where many remarkable species were also described. Later, Golovatch et al. (2010) reported some sharable characters that can be used for more clearly delimiting species groups. The first and until now only species group, named the "*peculiaris*-group", was proposed by Golovatch et al. (2010) and it currently encompasses seven species, viz; *E. anisodentus*, *E. nodulosus*, *E. pectinatidentis*, *E. peculiaris*, *E. silvaticus*, *E. soesilae* and *E. taiwanensis*, all sharing two rows of tubercles on the metaterga, having a broad and flattened epiproct, lacking a distofemoral process and with complete body volvation. Not only do these morphological traits strongly support this group, but their distribution is also likely to be coherent since most of the species inhabit the same region (southern part of Japan, Taiwan and mainland China).

The discovery of a new species from Cambodia not only represents the first record of the genus, but also of the entire family Haplodesmidae from that country. In this study, we do not only describe a new species, but we also update and compare the morphological characters of all currently known congeners, based on our scrutiny of all relevant original literature sources (Figs 5–8). The comparison, which relies mainly on details of gonopodal structure, body volvation patterns, the number and arrangement of the rows of tubercles and mid-dorsal projections on the metaterga, revealed an adequate delimitation for all 48 remaining species into another group for some coherent assemblages. We assemble 46 species into a second species group, here named the "*demangei*-group" and the remaining two species which are left ungrouped (see Table 3). Notably, these 46 species share some possibly related characters: metaterga usually with three rows of tubercles (except *E. armatus* and *E. digitatus* which have four or more rows); gonopod telopodite

Table 3. Species groups of *Eutrichodesmus* Silvestri, 1910 and their main morphological characters.

Group name	Species	Morphological characters				Distribution
		Body volvation	Rows of tubercles on metaterga	Mid-dorsal projection on metaterga	Distofemoral process on telopodite	
***peculiaris*-group** (7 spp.) (established by Golovatch et al. 2010)	*E. anisodentus*	complete	2	present	absent	Japan, Taiwan, and China
	E. nodulosus			present		
	E. pectinatidentis			present		
	E. peculiaris			absent		
	E. silvaticus			present		
	E. soesilae			present		
	E. taiwanensis			absent		
***demangei*-group** (46 spp.)	*E. apicalis*, *E. arcicollaris*, *E. armatocaudatus*, *E. armatus*, *E. aster*, *E. asteroides*, *E. astriproximus*, *E. astrisimilis*, *E. basalis*, *E. cambodiensis* sp. nov., *E. cavernicola*, *E. curticornis*, *E. demangei*, *E. deporatus*, *E. digitatus*, *E. distinctus*, *E. dorsiangulatus*, *E. elegans*, *E. filisetiger*, *E. gremialis*, *E. griseus*, *E. incisus*, *E. jianjia*, *E. latellai*, *E. latus*, *E. lipsae*, *E. macclurei*, *E. monodentus*, *E. multilobatus*, *E. nadan*, *E. obliteratus*, *E. paraster*, *E. parvus*, *E. planatus*, *E. reclinatus*, *E. regularis*, *E. similis*, *E. simplex*, *E. sketi*, *E. spinatus*, *E. steineri*, *E. subasteroides*, *E. tenuis*, *E. triangularis*, *E. troglobius*, *E. trontelji*	complete/ incomplete	mostly 3 (rarely 4 or more, in *E. armatus* and *E. digitatus*)	present (17 spp.)/ absent (29 spp.)	present (absent in *E. astriproximus*)	Japan China and Mainland Southeast Asia
Ungrouped (2 spp.)	*E. communicans*	complete	numerous setae (no tubercle)	absent	present (broad lobe)	Vanuatu
	E. reductus	incomplete	numerous setae (no tubercle)		present (broad lobe)	Indonesia

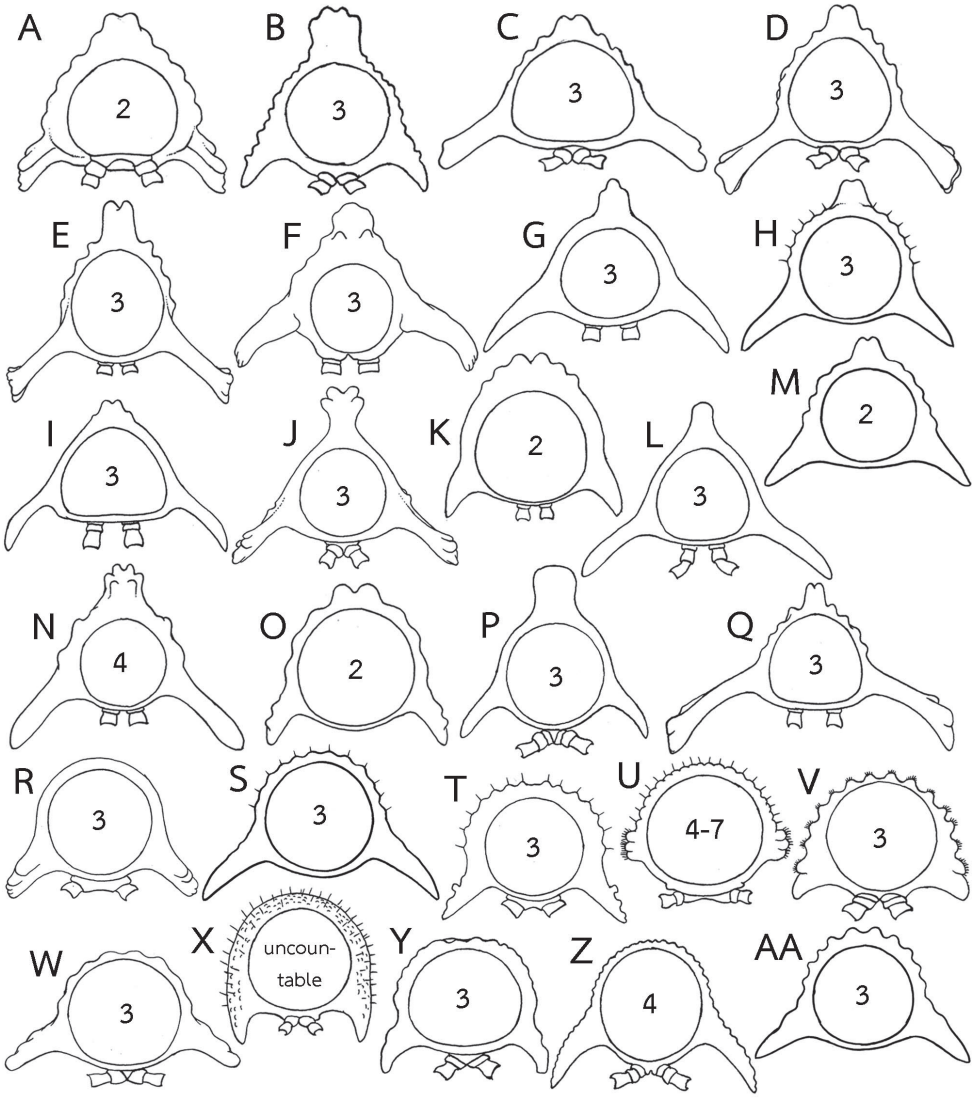

Figure 5. Body ring (posterior view) in several *Eutrichodesmus* species, number inside ring indicated rows of tubercles on metaterga. **A–Q** Species with mid-dorsal projections on metaterga. **A** *E. anisodentus* **B** *E. aster* **C** *E. asteroides* **D** *E. astriproximus* **E** *E. astrisimilis* **F** *E. cavernicola* **G** *E. deporatus* **H** *E. dorsiangulatus* **I** *E. lipsae* **J** *E. macclurei* **K** *E. nodulosus* **L** *E. paraster* **M** *E. pectinatidentis* **N** *E. reclinatus* **O** *E. soesilae* **P** *E. steineri* and **Q** *E. subasteroides* **R–AA** Species without mid-dorsal projections on metaterga **R** *E. apicalis* **S** *E. arcicollaris* **T** *E. armatocaudatus* **U** *E. armatus* **V** *E. basalis* **W** *E. cambodiensis* sp. nov. **X** *E. communicans* **Y** *E. curticornis* **Z** *E. digitatus* and **AA** *E. distinctus.* Not to scale. Figures modified from **A, M** Zhang (1995) **B, C, Y, AA** Golovatch et al. (2009b) **D, E, Q** Golovatch et al. (2016) **F** Sinclair (1901) **E, L, P** Liu and Wesener (2017) **H, S** Zhang in Zhang and Wang (1993) **I, R** Golovatch et al. (2015) **J, N** Hoffman (1977) **K** Verhoeff (1939) **O** Makhan (2010) **T, V, X,** Golovatch et al. (2009a) **U** Miyosi (1951) and **Z** Liu and Tian (2013).

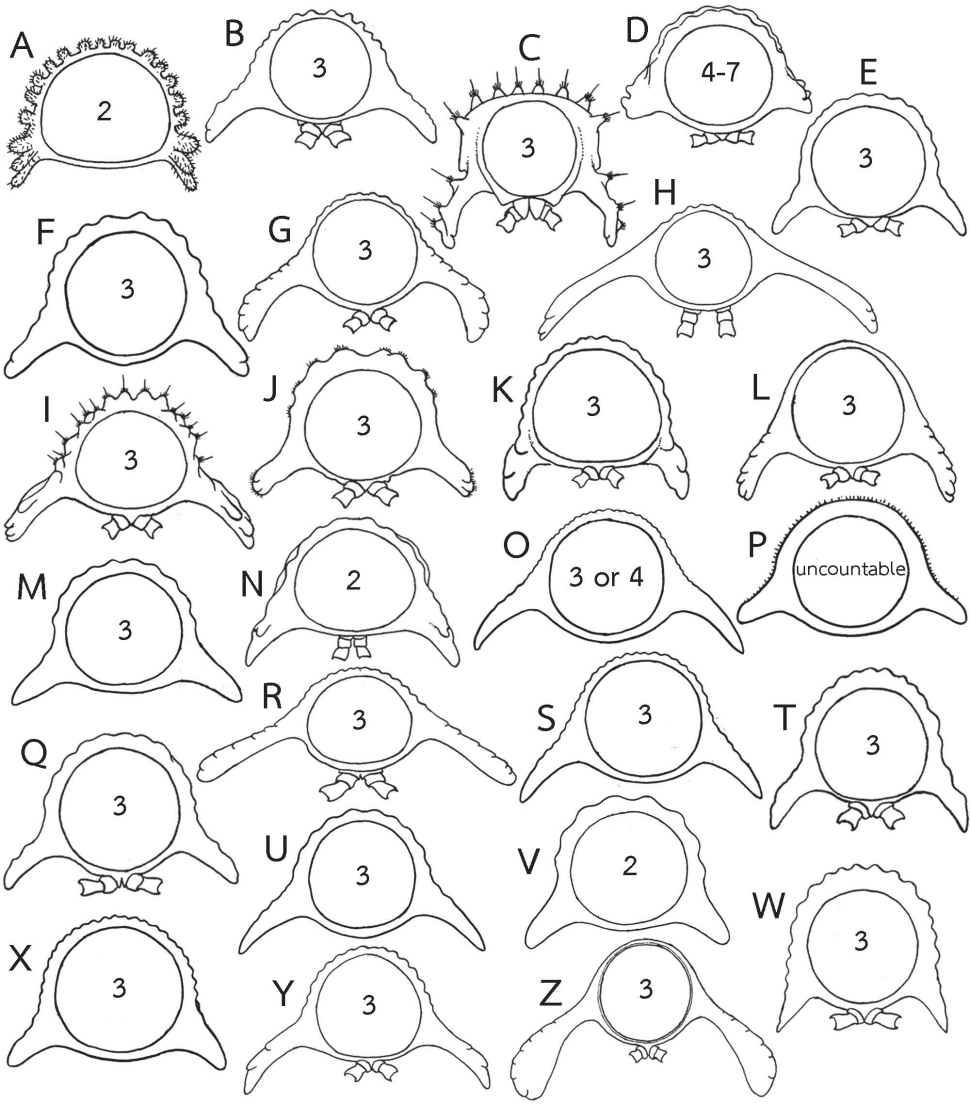

Figure 6. Body ring (posterior view) in several *Eutrichodesmus* species, number inside ring indicates rows of tubercles on metaterga. All species without mid-dorsal projections on metaterga **A** *E. elegans* **B** *E. filisetiger* **C** *E. gremialis* **D** *E. griseus* **E** *E. incisus* **F** *E. jianjia* **G** *E. latellai* **H** *E. latus* **I** *E. monodentus* **J** *E. multilobatus* **K** *E. nadan* **L** *E. obliteratus* **M** *E. parvus* **N** *E. peculiaris* **O** *E. planatus* **P** *E. reductus* **Q** *E. regularis* **R** *E. similis* **S** *E. simplex* **T** *E. sketi* **U** *E. spinatus* **V** *E. taiwanensis* **W** *E. tenuis* **X** *E. triangularis* **Y** *E. troglobius* and **Z** *E. trontelji*. Not to scale. Figures modified from **A** Miyosi (1956) **B, D, J, P, Q** Golovatch et al. (2009b) **C** Hoffman (1982) **E, H, R** Golovatch et al. (2009a) **F** Liu and Wynne (2019) **G, L, T, W, X, Y, Z** Golovatch et al. (2015) **I** Zhang *in* Zhang and Wang (1993) **K** Golovatch et al. (2016) **M** Liu and Wesener (2017) **N** Murakami (1966) **O, S, U** Liu and Tian (2013) and **V** Golovatch et al. (2010).

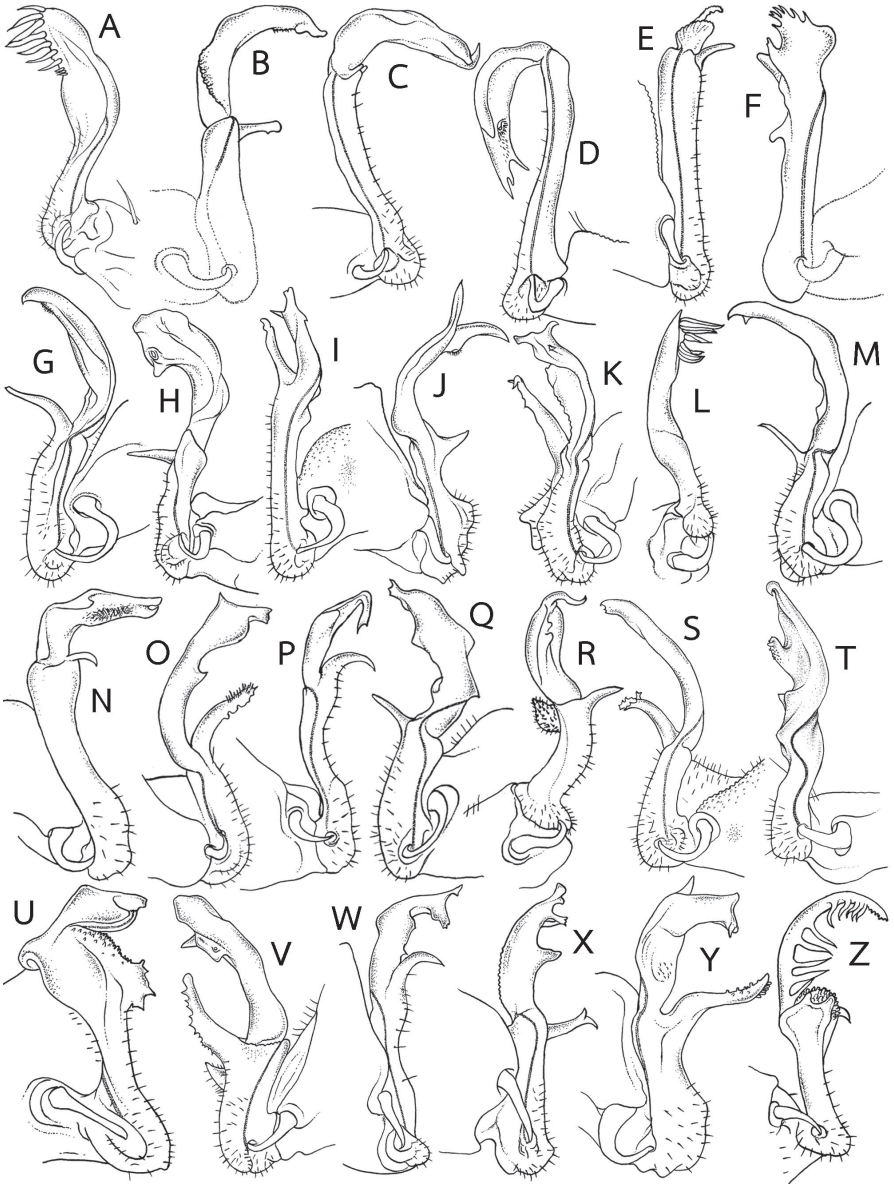

Figure 7. Gonopod outline (mesal view of left and right gonopod) in several *Eutrichodesmus* species. **A–N** Gonopods of species with mid-dorsal projections on metaterga **A** *E. anisodentus* **B** *E. aster* **C** *E. asteroides* **D** *E. astriproximus* **E** *E. astrisimilis* **F** *E. cavernicola* **G** *E. deporatus* **H** *E. dorsiangulatus* **I** *E. lipsae* **J** *E. macclurei* **K** *E. paraster* **L** *E. pectinatidentis* **M** *E. steineri* and **N** *E. subasteroides* **O–Z** Gonopods of species without mid-dorsal projections on metaterga **O** *E. apicalis* **P** *E. arcicollaris* **Q** *E. armatocaudatus* **R** *E. armatus* **S** *E. basalis* **T** *E. cambodiensis* sp. nov. **U** *E. communicans* **V** *E. curticornis* **W** *E. demangei* **X** *E. digitatus* **Y** *E. distinctus* and **Z** *E. elegans*. Not to scale. Figures modified from **A, L** Zhang (1995) **B, C, V, Y** Golovatch et al. (2009b) **D, E, N** Golovatch et al. (2016) **F** Sinclair (1901) **G, K, M** Liu and Wesener (2017) **H, P** Zhang in Zhang and Wang (1993) **I, O** Golovatch et al. (2015) **J** Hoffman (1977) **Q, S, U** Golovatch et al. (2009a) **R** Miyosi (1951) **W** Silvestri (1910) **X** Liu and Tian (2013) and **Z** Miyosi (1951).

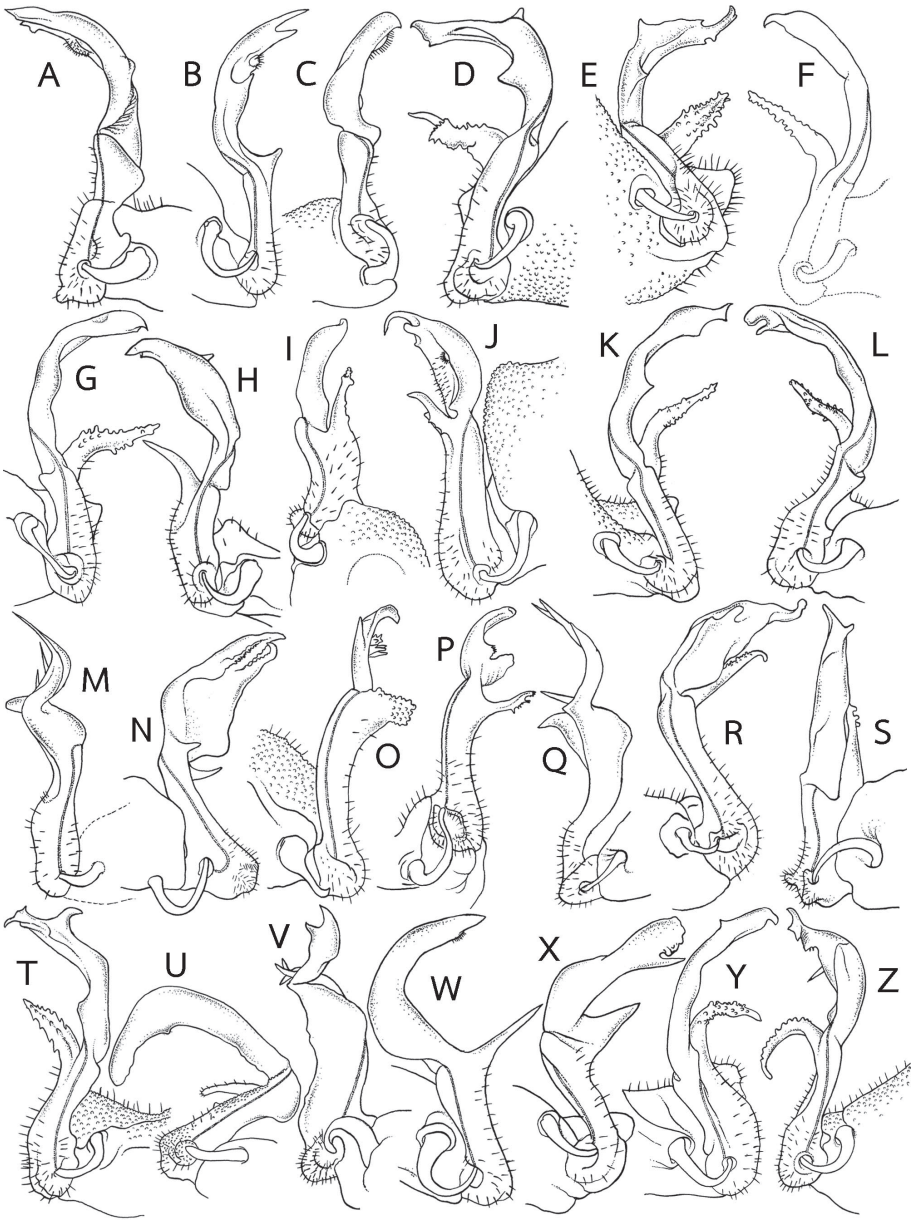

Figure 8. Gonopod outline (mesal view of left and right gonopod) in several *Eutrichodesmus* species. All species without mid-dorsal projections on metaterga. **A** *E. filisetiger* **B** *E. gremialis* **C** *E. griseus* **D** *E. incisus* **E** *E. jianjia* **F** *E. latellai* **G** *E. latus* **H** *E. monodentus* **I** *E. multilobatus* **J** *E. nadan* **K** *E. obliteratus* **L** *E. parvus* **M** *E. peculiaris* **N** *E. planatus* **O** *E. reductus* **P** *E. regularis* **Q** *E. silvaticus* **R** *E. similis* **S** *E. simplex* **T** *E. sketi* **U** *E. spinatus* **V** *E. taiwanensis* **W** *E. tenuis* **X** *E. triangularis* **Y** *E. troglobius* and **Z** *E. trontelji*. Not to scale. Figures modified from **D, G, R** Golovatch et al. (2009a) **A, C, I, O, P** Golovatch et al. (2009b) **B** Hoffman (1982) **E** Liu and Wynne (2019) **F, K, T, W, X, Y, Z** Golovatch et al. (2015) **H** Zhang in Zhang and Wang (1993) **J** Golovatch et al. (2016) **L** Liu and Wesener (2017) **M** Murakami (1966) **N, S, U** Liu and Tian (2013) **Q** Haga (1968) and **V** Golovatch et al. (2010).

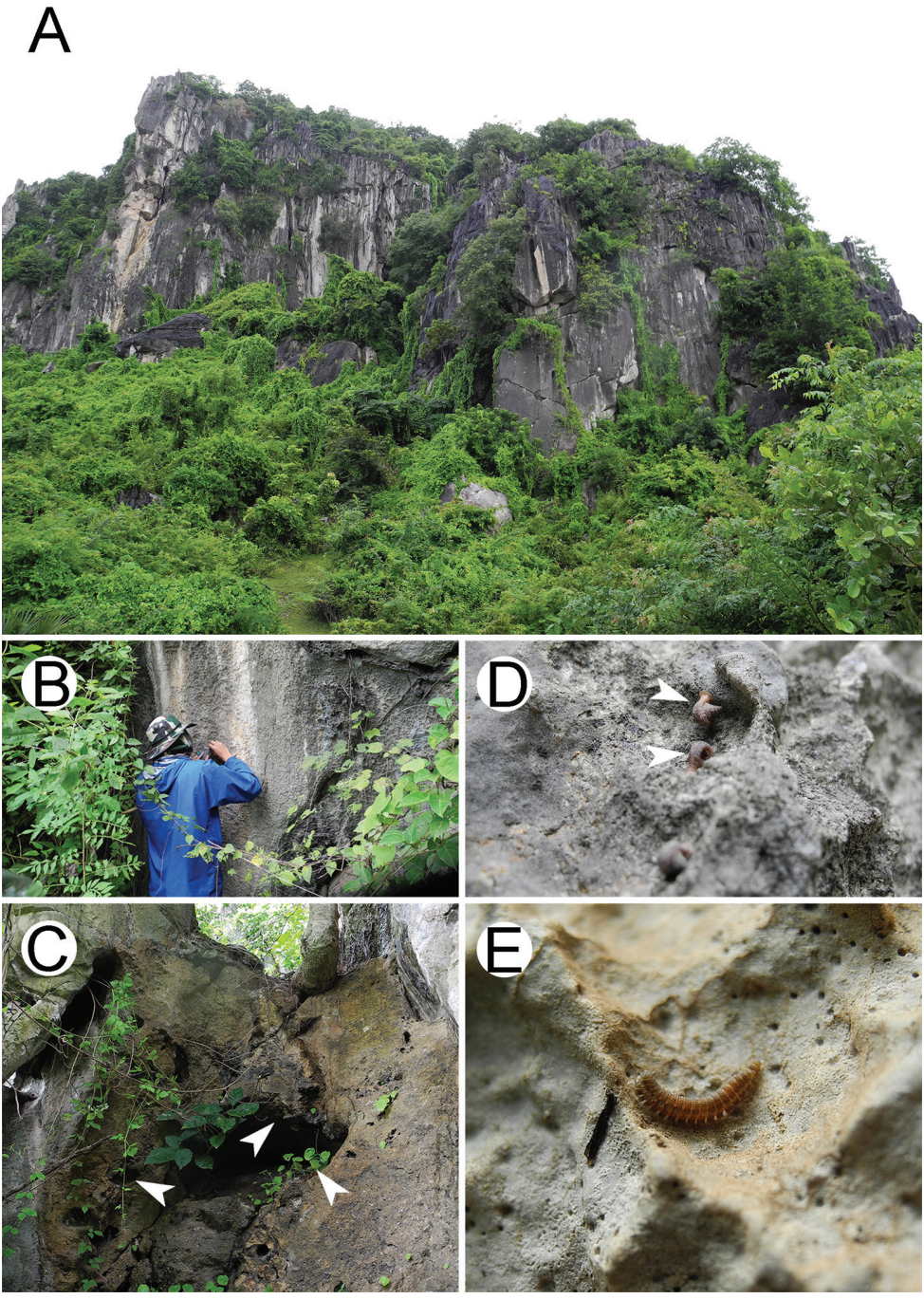

Figure 9. Habitat at the type locality of *Eutrichodesmus cambodiensis* sp. nov. **A** limestone outcrop **B, C** humid rock wall, sinkholes and crevices **D** co-occurrence of the new species with microsnail, *Hypselostoma cambodjense* Benthem Jutting, 1962 and **E** mating couple (male on top).

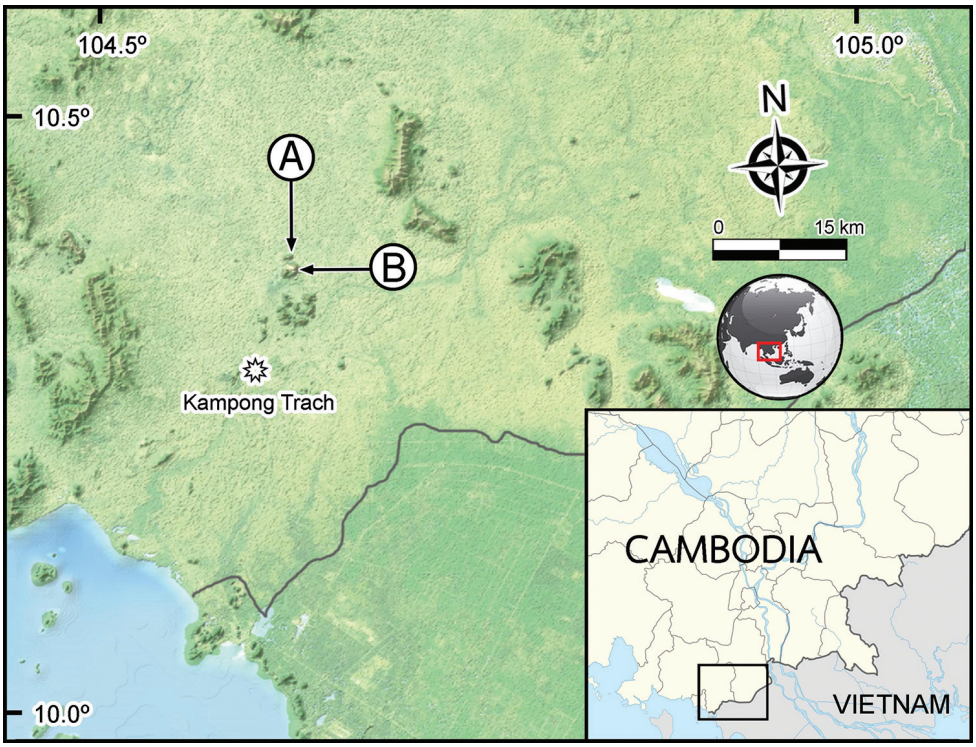

Figure 10. Known distribution of the *Eutrichodesmus cambodiensis* sp. nov. **A** limestone mount near Wat Phnom Small (type locality) **B** Prasat Phnom Totong.

with a distofemoral process (absent from *E. astriproximus*). All constituent species of *Eutrichodesmus* are presented in Table 3.

The gonopod might be a reliable tool for natural species group delimitations and quite often the assignment of many haplodesmid groups has been based on these characters. Our discrimination has also found the gonopodal structure to be useful in providing several satisfactory characters for sorting out amongst *Eutrichodesmus* species. Figures 7, 8 clearly show that all species of the "*demangei*-group" show the same pattern of such gonopodal characters as the existence of a distofemoral process on the telopodite, combined with most species showing three rows of tubercles on the metaterga, while the mid-dorsal projection and body volvation seem to be variable across *Eutrichodesmus* (Figs 5, 6). In accordance, the distribution of the "*demangei*-group", which all inhabit Japan, China and mainland Southeast Asia, corresponds to the morphological characters, although their distribution area is obviously larger. The other congeners, *E. nodulosus* and *E. reclinatus*, both lack gonopodal information yet, because they were originally described from females only. In spite of their gonopodal structure being unknown, their other morphological traits seem to fit in and serve to place these species in the "*demangei*-group" much more than to any other group.

Whereas the remaining 46 species agree in most respects with the definition of the "*demangei*-group" given above, there is a strong difference in the structural details of the gonopod, the presence of mid-dorsal projections and the number of the rows of tubercles on metaterga observed in two species, *E. communicans* and *E. reductus*. These can be assigned to neither the "*peculiaris*-group" nor the "*demangei*-group" due to the remarkable numerous setae without tubercles on the metaterga and the broad distofemoral process on the gonopod femorite, as well as their geographical distribution (*E. communicans* from Vanuatu and *E. reductus* from Indonesia) which quite clearly makes them separated from all other congeneric species. Thus, we leave *E. communicans* and *E. reductus* amongst ungrouped species as circumscribed above, since they fail to match the definition of the new or other previously-described species groups (see also Table 3).

Key to species of *Eutrichodesmus* occurring in mainland Southeast Asia

From the previous records and including the new species described here, the genus *Eutrichodesmus* contains 55 known species from Japan (5), Taiwan (1), China (24), Vietnam (12), Laos (6), Cambodia (1), Thailand (2), Malaysia (2), Indonesia (1) and Vanautu (1), as detailed in Table 1. The new species shares most of the morphological characters to a bunch of species that are known to exist in Malaysia, Laos, Thailand and Vietnam. Here, we present an identification key, updated from the key of Golovacth et al. (2009b), for species of *Eutrichodesmus* occurring in mainland Southeast Asia (= 23 species).

1 Ozopores visible, either absent or reduced (if present, appearing only on ring 17) **2**

– Ozopores normal, present at rings 5, 7, 9, 10, 12, 13 and 15–19 ..... **4**

2 Body length ca. 6.0 mm. Metaterga with conspicuous and remarkable conical tubercles, each tubercle with several bacilliform setae and a long macroseta (Fig. 6C). Distofemoral process of gonopod telopodite quite short, lamelliform, triangular (Fig. 8B) ..... ***E. gremialis***

– Body length 7.5–9.0 mm. Metaterga with flattened or regular tubercles. Distofemoral process of gonopodal telopodite very long, digitiform or tube-like (Fig. 7G, K) **3**

3 Gonopodal telopodite: distofemoral process bare; acropodite micropapillate at base, distally with two small teeth (Fig. 7G). Limbus crenulate... ***E. deporatus***

– Gonopodal telopodite: distofemoral process denticulate; acropodite not micropapillae at base, distally with one small tooth and a long digitiform lobe (Fig. 7K). Limbus microcrenulate ..... ***E. paraster***

4 Metaterga with mid-dorsal projections or crests, conspicuous, present in mid-body or posteriormost body rings **5**

– Metaterga either with only slightly elevated and inconspicuous mid-dorsal tubercles in the last two rings or lacking conspicuous mid-dorsal projections or crests **14**

5 Adult with 20 body rings **6**
– Adult with 19 body rings **11**
6 Mid-dorsal projections on metaterga 16–19 or 17–19. Ozopores opening on evident porosteles in most body rings ..... ***E. armatocaudatus***
– Mid-dorsal projections on metaterga 3–19 or 4–19 or 5–19. Ozopores opening on a lobe of paraterga either without porosteles or porosteles appearing on posteriormost rings **7**
7 Mid-dorsal projection on ring 5 inclined anteriorly at about 45°, directed anteriad or anterodorsad, not subvertical ..... ***E. reclinatus***
– Mid-dorsal projection on ring 5 nearly vertical (straight), directed dorsad or dorsoposteriad **8**
8 Metaterga 3–19 with mid-dorsal projections. Acropodite quite short, less than one-third the length of telopodite (Fig. 7F)..... ***E. cavernicola***
– Metaterga 4–19 or 5–19 with mid-dorsal projections. Acopodite quite long, almost half the length of telopodite (Fig. 7B, J, M)..... **9**
9 Body length 12.0–14.0 mm. Acropodite without lobe; tip simple, unbranched (Fig. 7B)..... ***E. aster***
– Body length 8.0–10.0 mm. Acropodite with a lobe or flange or micropapillate processes, forming a trifid or bifid tip (Fig. 7J, M)..... **10**
10 Paraterga quite short (Fig. 5P). Distofemoral process longer, curved down. Tip of acropodite bifid (Fig. 7M)..... ***E. steineri***
– Paraterga very long (Fig. 5J). Distofemoral process shorter, curved upwards. Tip of acropodite trifid (Fig. 7J)..... ***E. macclurei***
11 Distofemoral process absent (Fig. 7D) ..... ***E. astriproximus***
– Distofemoral precess present, short or long (Figs 7C, E, N)..... **12**
12 Distofemoral process shorter, rudimentary and prong-shaped; acropodite with neither a hairpad nor a hairy pulvillus (Fig. 7C). Limbus clearly crenulate..... ***E. asteroides***
– Distofemoral process quite long and slender, a digitiform; acropodite with a hairpad or a hairy pulvillus (Fig. 7E, N). Limbus microcrenulate..... **13**
13 Acropodite quite short, less than half the length of prefemur; without lobe at about midway; base enlarged, fringed, velum-like (Fig. 7E) ..... ***E. astrisimilis***
– Acropodite long, about half the length of prefemur; lamelliform; with a mesal lobe at about midway; base normal, neither enlarged nor fringed (Fig. 7N) ... ***E. subasteroides***
14 Distofemoral process of telopodite short, inconspicuous, apparent and visible only in mesal view (Figs 7T; 8A, C) **15**
– Distofemoral process of telopodite very long, conspicuous, easily seen in many views (Figs 7I, S, V, W; 8J, L, P)..... **17**
15 Body with complete volvation, larger, length 12.0–13.0 mm. Metaterga with three rows of tubercles, mixostictic; with slightly elevated mid-dorsal tuber-

cles in last two rings. Tip of acropodite branched, forming a bifid tip and a lamella. Solenomere fused with acropodite (Fig. 8A).....***E. filisetiger***

– Body with incomplete volvation, smaller, length 5.5–8.0 mm. Metaterga with three rows of tubercles, isostictic or nearly so; without a little elevated mid-dorsal tubercles in last two rings. Tip of acropodite unbranched, terminating in a dentiform tip. Solenomere not fused with acropodite, conspicuous, digitiform (Figs 7T; 8C) **16**

16 Body grey to blackish. Paraterga shorter (Fig. 6D). Ozopores opening on evident porosteles. Limbus spinulate (comb-like), spinicles sharp and very much (more than twice) longer than broad. Solenomere not papillate, with a hairpad (Fig. 8C) .....***E. griseus***

– Body greyish-brown or light brown. Paraterga quite longer (Fig. 5W). Ozopores opening on a lobe on paraterga without porostele. Limbus crenulate, lobules slightly (less than twice) longer than broad, tip of each lobule round. Solenomere papillate, without hairpad (Figs 4; 7T).....
.....***E. cambodiensis* sp. nov.**

17 Mid-dorsal tubercles on metaterga 18 and 19 slightly elevated and particularly evident.....***E. multilobatus***

– Mid-dorsal tubercles on metaterga 18 and 19 normal, neither elevated nor evident (e.g. Figs 2A, G; 3C) **18**

18 Distofemoral process bare, surface smooth (Fig. 7W).....***E. demangei***

– Distofemoral process denticulate (Figs 7S, V; 8J, L, P).....**19**

19 Body larger, length 9.0–10.0 mm. Rows of tubercles on metaterga isostictic in both longitudinal and transverse directions. Acropodite with a lobe at base.....***E. regularis***

– Body smaller, length 5.0–5.3 mm. Rows of tubercles on metaterga mixostictic. Acropodite without lobe at base.....**20**

20 Gonopod: telopodite very simple; tip of acropodite with neither a conspicuous lobe nor a tooth (Fig. 7S). Paraterga very small (Fig. 5V).....***E. basalis***

– Gonopod: telopodite not so simple; tip of acropodite with a conspicuous lobe or tooth (Figs 7V; 8J, L). Paraterga large (Figs 5Y; 6K, M).....**21**

21 Body volvation incomplete. Distal region of acropodite with a tooth and a lobe (Fig. 8L) .....***E. parvus***

– Body volvation complete. Distal region of acropodite with either a tooth or a lobe (Figs 7V; 8J) **22**

22 Tip of acropodite unciform, slender. Seminal groove opening at about midway of acropodite; with neither a hairpad nor a hairy pulvillus (Fig. 8J). Limbus clearly microcrenulate.....***E. nadan***

– Tip of acropodite neither unciform nor slender. Seminal groove opening near tip of acropodite; with a hairy pulvillus (Fig. 7V). Limbus irregularly crenulate.....***E. curticornis***

Discussion

Prior to this study, the millipede fauna of Cambodia consisted of only 23 species, over half of which were described, based on a few specimens from just a handful of locations (Attems 1938, 1953; Likhitrakarn et al. 2015, 2020; Golovatch 2018). Amongst these, only the polydesmidan families Paradoxosomatidae and Cryptodesmidae have been known to occur in that country (Likhitrakarn et al. 2015; Golovatch 2018). No micropolydesmoid representative of the family Haplodesmidae has hitherto been reported from Cambodia. This situation is partly remedied herewith by the discovery and description of *E. cambodiensis* sp. nov.

Eutrichodesmus cambodiensis sp. nov. was exclusively found in isolated limestone habitats at or around caves. Based on its apparently highly restricted distribution, the new species can soundly be considered as endemic not only to Cambodia, but also to the Kampong Trach karst. As it is evident from Table 3, almost all *Eutrichodesmus* species have been found and collected from just one or a few locations confined to small areas. This strongly suggests that they are likely to be endemic to the respective areas and that further micropolydesmoids are most likely to be found in Cambodia.

The new species seems to have partial associations with caves, but it does not tend to show a troglomorphy syndrome because it is pigmented, has no hypertrophied appendages and no specimens have been found living inside the deep cave. Accordingly, this is no troglobite. Nevertheless, certain troglomorphic traits have been suggested in several species of *Eutrichodesmus*. For example, of the 55 currently known species, 24 are endemic to China alone and over half of these as troglobites, which is definitely a strong concentration of species in the region (Liu and Wynne 2019; Golovatch and Liu 2020). The same tendency to troglomorphy is also marked in most species known from other countries (Hoffman 1977a, 1977b, 1982a; Golovatch et al. 2009a, 2016; Liu et al. 2017).

The mostly thorough work by previous authors has provided sufficiently detailed information on important taxonomic characters that have allowed for species comparisons across *Eutrichodesmus* to be conducted (Golovatch et al. 2009a, 2009b, 2010, 2015, 2016; Liu et al. 2017). Two species groups of *Eutrichodesmus* are recognisable to account for the wide variety of morphological traits. The "*peculiaris*-group" was established by Golovatch et al. (2010) and currently accommodates seven species, while 46 species are harboured together in the second, "*demangei*-group" proposed in this study. Remarkably, the details of gonopodal conformation and the number and arrangement of the rows of tubercles on metaterga support the species assignments to either group. However, although these traits tend to be reliable, two species (*E. communicans* and *E. reductus*) could not satisfactorily be assigned into either group and thus remain ungrouped (see Table 3). The new species, *E. cambodiensis* sp. nov., shows all of its unique characters that are in agreement with its placement in the *demangei*-group.

In addition to gonopodal morphology, many families of the order Polydesmida prove the great utility of certain surface structures and some other peripheral characters for family- or genus-level classifications (Simonsen 1990; Shear 2008; Mesibov 2009; Akkari and Enghoff 2011). Within *Eutrichodesmus*, the basic knowledge of periperhal characters for a few old species is very scarce, with no available SEM images. Hence, this

requires special attention in the future. With its 55 described species widely distributed in many countries, *Eutrichodesmus* seems to be the largest group of the micropolydesmoid family Haplodesmidae, but their phylogenetic relationships still remain unknown. Very little can be said about the presumed relationship between the Haplodesmidae and its recent synonym Doratodesmidae, as this synonymy is based solely on a few morphological characters (Hoffman 1982a, 1982b; Simonsen 1990; Golovatch 2009a). The further cladistic analysis and a molecular study are the obvious choices to improve the taxonomy by shedding further light on the group's diversity in these millipedes.

The finding of a new *Eutrichodesmus* species in Cambodia fills in the gap in the distribution of the group across the eastern part of mainland Southeast Asia. As demonstrated recently by the discoveries of micropolydesmoids and other millipedes in the adjacent areas (Likhitrakarn et al. 2010, 2011, 2019; Golovatch et al. 2016, Liu et al. 2014, 2016, 2017; Golovatch 2018; Srisonchai et al. 2018) with respect to the unexplored and isolated limestone in Cambodia, Malaysia, Myanmar, Laos and Thailand, no doubt further new species remain to be discovered. It is hoped that this work will be a useful contribution to the ongoing process of documenting the diversity of Diplopoda in Cambodia and promote further studies on these remarkable creatures.

Acknowledgements

This work was part of the contribution between Thai universities and the Inland Fisheries Research and Development Institute (IFReDI, Cambodia). The main funding for this research was the TRF Strategic Basic Research DBG 6080011 (2017–2019) and the Center of Excellence on Biodiversity BDC-PG2-1610001. Funding was also supported and provided in part by Ratchadapisek Somphot Fund for Postdoctoral Fellowship, Chulalongkorn University. The authors would like to thank the members of the Animal Systematics Research Unit, Chulalongkorn University, Thailand (ASRU) and IFReDI members for any kind assistance. We also thank again the Inland Fisheries Research and Development Institute (IFReDI, Cambodia) for the permission documents and specimens collecting in Cambodia. Special thanks are due to Dr. Ting Hui Ng (ZRC) for English revision and Dr. Jiroat Sangrattanaprasert (Mahidol Wittayanusorn School) for plant identifications. The subject editor (Pavel Stoev) and all reviewers (including Sergei I. Golovatch, Henrik Enghoff and Piyatida Pimvichai) are cordially thanked for great advice, very helpful suggestions and English improvement that enormously benefitted the manuscript.

References

Akkari N, Enghoff H (2011) On some surface structures of potential taxonomic importance in families of the suborders Polydesmidea and Dalodesmidea (Polydesmida, Diplopoda). ZooKeys 156: 1–24. https://doi.org/10.3897/zookeys.156.2134

Attems C (1938) Die von Dr. C. Dawydoff in französisch Indochina gesammelten Myriopoden. Mémoires du Muséum national d'Histoire naturelle. New Series 6(2): 187–353.

Attems C (1953) Myriopoden von Indochina. Expedition von Dr. C. Dawydoff (1938–1939). Mémoires du Muséum national d'Histoire naturelle (New Series), Série A 5: 133–230.

American Veterinary Medical Association (2020) AVMA Guidelines for the Euthanasia of Animals: 2020 edition. https://www.avma.org/sites/default/files/2020-01/2020-Euthanasia-Final-1-17-20.pdf

Enghoff H, Golovatch SI, Anh ND (2004) A review of the millipede fauna of Vietnam (Diplopoda). Arthropoda Selecta 13: 29–43.

Golovatch SI (2018) Further notes on the millipede family Cryptodesmidae in Southeast Asia, with descriptions of a new genus and two new species from Indochina (Diplopoda: Polydesmida). Raffles Bulletin of Zoology 66: 361–370.

Golovatch SI, Geoffroy J-J, Mauriès J-P, VandenSpiegel D (2009a) Review of the millipede family Haplodesmidae, with descriptions of some new or poorly-known species (Diplopoda, Polydesmida). In: Golovatch SI, Mesibov R (Eds) Advances in the Systematics of Diplopoda I. ZooKeys 7: 1–53. https://doi.org/10.3897/zookeys.7.117

Golovatch SI, Geoffroy J-J, Mauriès J-P, VandenSpiegel D (2009b) Review of the millipede genus *Eutrichodesmus* Silvestri, 1910 (Diplopoda, Polydesmida, Haplodesmidae), with descriptions of new species. In: Golovatch SI, Mesibov R (Eds) Advances in the Systematics of Diplopoda II. ZooKeys 12: 1–46. https://doi.org/10.3897/zookeys.12.167

Golovatch SI, Mikhaljova EV, Korsós Z, Chang H-W (2010) The millipede family Haplodesmidae recorded in Taiwan for the first time, with the description of a new species. Tropical Natural History 10: 27–36. https://li01.tci-thaijo.org/index.php/tnh/article/view/102938/82482

Golovatch SI, Mikhaljova EV, Chang H-W (2011) The millipede family Cryptodesmidae, Pyrgodesmidae, Opisotretidae and Xystodesmidae in Taiwan (Diplopoda, Polydesmida). Tropical Natural History 11: 119–134. https://li01.tci-thaijo.org/index.php/tnh/article/view/102999/82543

Golovatch SI, Geoffroy JJ, Mauriès JP, VandenSpiegel DV (2015) Review of the millipede genus *Eutrichodesmus* Silvestri, 1910, in China, with descriptions of new cavernicolous species (Diplopoda, Polydesmida, Haplodesmidae). ZooKeys 505: 1–46. https://doi.org/10.3897/zookeys.505.9862

Golovatch, SI, Akkari N (2016) Identity of the millipede, *Pseudoniponiella kometis* (Attems, 1938) (Diplopoda: Polydesmida: Cryptodesmidae). Tropical Natural History 16(1): 1–6. https://li01.tci-thaijo.org/index.php/tnh/article/view/103069

Golovatch SI, Geoffroy JJ, Mauriès JP, VandenSpiegel D (2016) Four new species of the millipede genus *Eutrichodesmus* Silvestri, 1910, from caves in Indochina (Diplopoda: Polydesmida: Haplodesmidae). Arthropoda Selecta 25: 247–256. https://doi.org/10.15298/arthsel.25.3.03

Golovatch SI, Liu W (2020) Diversity, distribution patterns, and fauno-genesis of the millipedes (Diplopoda) of mainland China. In: Korsós Z, Dányi L (Eds) Proceedings of the 18th International Congress of Myriapodology, Budapest, Hungary. ZooKeys 930: 153–198. https://doi.org/10.3897/zookeys.930.47513

Haga A (1968) Japanese Millipedes. Private publication, 11 pp. [6 pls., In Japanese]

Hoffman RL (1977a) The systematic position of the diplopod family Doratodesmidae, and description of a new genus from Malaya (Polydesmida). Pacific Insects 17: 247–255. https://pdfs.semanticscholar.org/c555/b4d3e834a208e5efce70a7082a5c72214833.pdf?_ga=2.53039848.1933375208.1589724031-587478136.1565937391

Hoffman RL (1977b) Diplopoda from Malayan caves collected by M. Pierre Strinati. Revue suisse de Zoologie 84: 699–719. https://doi.org/10.5962/bhl.part.91419

Hoffman RL (1982a) A new genus and species of doratodesmid millipede from Thailand. Archives des Sciences 35: 87–93.

Hoffman RL (1982b) Diplopoda. In: Parker SP (Ed.) Synopsis and Classification of Living Organisms. McGraw-Hill Book Company, New York & St. Louis, 2: 689–724.

Huber BA, Petcharad B, Bumrungsri S (2015) Revision of the enigmatic Southeast Asian spider genus *Savarna* (Araneae, Pholcidae). European Journal of Taxonomy 160: 1–23. https://doi.org/10.5852/ejt.2015.160

Karasawa S, Beaulieu F, Sasaki T, Bonato L, Hagino Y, Hayashi M, Itoh R, Kishimoto T, Nakamura O, Nomura S, Nunomura N, Sakayori H, Sawada Y, Suwa Y, Tanaka S, Tanabe T, Tanikawa A, Hijii N (2008) Bird's nest ferns as reservoirs of soil arthropod biodiversity in a Japanese subtropical rainforest. Edaphologia 83: 11–30. https://pdfs.semanticscholar.org/afaf/d3e99835f579fa685cbb689861041db015dc.pdf?_ga=2.219724761.1933375208.1589724031-587478136.1565937391

Likhitrakarn N, Golovatch SI, Prateepasen R, Panha S (2010) Review of the genus *Tylopus* Jeekel, 1968, with descriptions of five new species from Thailand (Diplopoda, Polydesmida, Paradoxosomatidae). ZooKeys 72: 23–68. https://doi.org/10.3897/zookeys.72.744

Likhitrakarn N, Golovatch SI, Panha S (2011) Revision of the Southeast Asian millipede genus *Orthomorpha* Bollman, 1893, with the proposal of a new genus (Diplopoda, Polydesmida, Paradoxosomatidae). ZooKeys 131: 1–161. https://doi.org/10.3897/zookeys.131.1921

Likhitrakarn N, Golovatch SI, Panha S (2015) A checklist of the millipedes (Diplopoda) of Cambodia. Zootaxa 3973: 175–184. https://doi.org/10.11646/zootaxa.3973.1.7

Likhitrakarn N, Golovatch SI, Srisonchai R, Sutcharit C, Panha S (2019) A new species of the millipede genus *Cryptocorypha* Attems, 1907, from northern Thailand (Polydesmida, Pyrgodesmidae). ZooKeys 833: 121–132. https://doi.org/10.3897/zookeys.833.32413

Likhitrakarn N, Golovatch SI, Thach P, Chhuoy S, Ngor PB, Srisonchai R, Sutcharit C, Panha S (2020) Two new species of the millipede genus *Plusioglyphiulus* Silvestri, 1923 from Cambodia (Diplopoda, Spirostreptida). ZooKeys 938: 137–151. https://doi.org/10.3897/zookeys.938.51234

Liu W, Tian M (2013) Four new cavernicolous species of the millipede genus *Eutrichodesmus* Silvestri, 1910 from southern China (Diplopoda: Polydesmida: Haplodesmidae). Zootaxa 3734: 281–291. https://doi.org/10.11646/zootaxa.3734.2.11

Liu W, Golovatch S, Tian M (2014) A review of the dragon millipede genus *Desmoxytes* Chamberlin, 1923 in China, with descriptions of four new species (Diplopoda, Polydesmida, Paradoxosomatidae). ZooKeys 448: 9–26. https://doi.org/10.3897/zookeys.448.8081

Liu W, Golovatch SI, Tian MY (2016) Six new species of dragon millipedes, genus *Desmoxytes* Chamberlin, 1923, mostly from caves in China (Diplopoda, Polydesmida, Paradoxosomatidae). ZooKeys 577: 1–24. https://doi.org/10.3897/zookeys.577.7825

Liu W, Golovatch SI, Wesener T (2017) Four new species of the millipede genus *Eutrichodesmus* Silvestri, 1910 from Laos, including two with reduced ozopores (Diplopoda, Polydesmida, Haplodesmidae). ZooKeys 660: 43–65. https://doi.org/10.3897/zookeys.660.11780

Liu W, Wynne JJ (2019) Cave millipede diversity with the description of six new species from Guangxi, China 30: 57–94. https://doi.org/10.3897/subtbiol.30.35559.figure10

Makhan D (2010) *Eutrichodesmus soesilae* sp. nov., a new millipede from Mt. Jinyun, Beibei, Chongqing, China (Diplopoda, Polydesmida, Haplodesmidae). Calodema 110: 1–5.

Mesibov (2009) New and little-used morphological characters in Polydesmida (Diplopoda). Soil Organisms 81: 531–542. https://pdfs.semanticscholar.org/d854/8165c210cdf0e3390be3a36a0260633a4a2a.pdf?_ga=2.228244573.1933375208.1589724031-587478136.1565937391

Miyosi Y (1951) Beiträge zur Kenntniss japanischer Myriopoden. 1. Aufsatz: Ueber eine Gattung von Leptodesmidae. Zoological Magazine 60: 149–150.

Miyosi Y (1956) Beiträge zur Kenntnis japanischer Myriopoden. 17. Aufsatz: Über eine neue Gattung von Oniscodesmidae und eine neue Art von Monotarsobius. Zoological Magazine 65: 311–314.

Murakami Y (1966) Postembryonic development of the common Myriapoda in Japan XXI. A new genus of the family Oniscodesmidae and a new species of the genus *Arachandrodesmus* (Cryptodesmidae). Zoological Magazine 75: 30–33.

Omine T (1982) Preliminary survey of soil fauna in the center of Iriomote-Island (riverside of the Itarashiki and Urauchi rivers). Main collection of Cryptostigmata, Myriapoda and Formicidae. Journal of Okinawa University [Okinawa Daigaku Kiyo] 2: 83–139. [In Japanese]

Omine T, Ito Y (1998) Abundance and diversity of soil macrofauna of forests of Yanbaru, northern montane part of Okinawa Island, with special reference to removal of undergrowth. Journal of Okinawa University [Okidai Ronso] 15: 131–159.

Shear WA (2008) Spinnerets in the milliped order Polydesmida, and the phylogenetic significance of spinnerets in millipeds (Diplopoda). International Journal of Myriapodology 2: 123–146. https://doi.org/10.1163/187525408X395904

Sierwald P, Spelda J (2019) MilliBase. *Eutrichodesmus* Silvestri, 1910. http://www.millibase.org/aphia.php?p=taxdetails&id=891572

Silvestri F (1910) Descrizione preliminari di nuovi generi di Diplopodi. Zoologischer Anzeiger 35: 357–364.

Simonsen A (1990) Phylogeny and biogeography of the millipede order Polydesmida, with special emphasis on the suborder Polydesmidea. Museum of Zoology, University of Bergen, 114 pp.

Sinclair FG (1901) On the myriapods collected during the "Skeat Expedition" to the Malay Peninsula, 1899–1900. Proceedings of the Zoological Society of London 71(2): 505–533. https://doi.org/10.1111/j.1469-7998.1902.tb08186.x

Srisonchai R, Enghoff H, Likhitrakarn N, Panha S (2018) A revision of dragon millipedes I: genus *Desmoxytes* Chamberlin, 1923, with the description of eight new species (Diplop-

oda, Polydesmida, Paradoxosomatidae). ZooKeys 761: 1–177. https://doi.org/10.3897/zookeys.761.24214

Verhoeff KW (1939) Zur Kenntnis ostasiatischer Diplopoden IV. Zoologischer Anzeiger 127: 273–285.

Wang YM (1958) Serica 1i: On Diplopoda from Taiwan with a new strongylosomid. Quarterly Journal of the Taiwan Museum 11: 340–344.

Willett W, Jenny B, Isenberg T, Dragicevic P (2015) Lightweight relief shearing for enhanced terrain perception on interactive maps. In: Proceedings of the 33rd ACM Conference on Human Factors in Computing Systems (CHI 2015), Seoul, South Korea, 3563–3572. https://doi.org/10.1145/2702123.2702172

Zhang C (1995a) Small Myriapoda in soil from China II. A new genus and species of the family Doratodesmidae from Zhejiang Province (Diplopoda: Polydesmida). Acta Zootaxonomica Sinica 20: 411–415.

Zhang C (1995b) Small Myriapoda in soil from China III. A new species of the milliped genus Nanocondylodesmus Zhang (Diplopoda: Polydesmida: Doratodesmidae). Acta Zootaxonomica Sinica 20: 416–419.

Zhang C, Wang D (1993) Diplopoda in caves of Yunnan – 1. A study of new genera and species of the millipede family Doratodesmidae (Diplopoda: Polydesmida). In: Linhua S, Huaiyuan T (Eds) Karst Landscape and Cave Tourism. China Environmental Science Press, Beijing, 205–220.

ZooKeys 996: 93–105 (2020)
doi: 10.3897/zookeys.996.59075
https://zookeys.pensoft.net

RESEARCH ARTICLE

A peer-reviewed open-access journal
ZooKeys
Launched to accelerate biodiversity research

Two new species and distribution records for the genus *Bohayella* Belokobylskij, 1987 from Costa Rica (Hymenoptera, Braconidae, Cardiochilinae)

Ilgoo Kang[1], Scott R. Shaw[2], Nathan P. Lord[1]

1 *Department of Entomology, Louisiana State University Agricultural Center, 404 Life Sciences Building, Baton Rouge, LA, 70803, USA* **2** *UW Insect Museum, Department of Ecosystem Science and Management (3354), University of Wyoming, 1000 E. University Avenue, Laramie, WY 82071, USA*

Corresponding author: Ilgoo Kang (ikang1@lsu.edu)

Academic editor: J. Fernandez-Triana | Received 28 September 2020 | Accepted 3 November 2020 | Published 24 November 2020

http://zoobank.org/2550092B-AC75-48F1-AEDF-84E3F30DC4EC

Citation: Kang I, Shaw SR, Lord NP (2020) Two new species and distribution records for the genus *Bohayella* Belokobylskij, 1987 from Costa Rica (Hymenoptera, Braconidae, Cardiochilinae). ZooKeys 996: 93–105. https://doi.org/10.3897/zookeys.996.59075

Abstract

Two new species of *Bohayella* Belokobylskij, 1987 from Costa Rica are described: *Bohayella geraldinae* Kang, **sp. nov**. and *Bohayella hansoni* Kang, **sp. nov.** These are new distribution records for the genus in the Neotropical region. In addition, a key to species of the genus *Bohayella* of Costa Rica is presented. The current work elevates the number of species included in *Bohayella* from nine to eleven.

Keywords

Morphology, New World, parasitoid wasp, taxonomy

Introduction

Costa Rica is one of the biodiversity hotspots, and a total estimated hymenopteran fauna in the country is ~ 20,000 species, including ~ 2,000 estimated species of braconid wasps (Gaston et al. 1996). Cardiochilinae is a subfamily of Braconidae,

containing 17 genera and 220+ species (Yu et al. 2012; Kang et al. 2020). *Bohayella* Belokobylskij, 1987 (Belokobylskij 1987) is an unusual genus of the subfamily, with nine previously described species that are only known from the Old World, including Afrotropical, Australasian, Oriental, and southern central Palearctic regions (Dangerfield et al. 1999; Mercado and Wharton 2003; Yu et al. 2012). Among the nine Old World species of *Bohayella*, two species, *B. adina* (Wilkinson, 1930) and *B. exiguurus* (Huddleston & Walker, 1988), have rearing records (Huddleston and Walker 1988). *B. adina* was reared from larvae of *Phazaca theclata* (Guenée, 1857) (Lepidoptera: Uraniidae) in India, (Beeson and Chatterjee 1935; Dangerfield 1995; Dangerfield et al. 1999), and *B. exiguurus* was reared from larvae of the citrus looper *Cleora tulbaghata* (Felder & Rogenhofer, 1875) (Lepidoptera: Geometridae) South Africa (Dangerfield et al. 1999).

Cardiochiles nigricans Mao, 1949 (Mao 1949) was transferred into *Bohayella* by Dangerfield et al. (1999) and recorded as the first species of *Bohayella* in the New World. Mercado and Wharton (2003) transferred the species into *Toxoneuron* Say, 1836 because the first metasomal tergite (T1) of the species is different from T1 of other members of *Bohayella*. Subsequently, members of *Bohayella* have been restricted to the Old World and new species of the genus have not been reported from the New World.

The first author (IK) had the opportunity to examine Costa Rican cardiochiline specimens housed in University of Wyoming Insect Museum (UWIM). Using the key to world genera of the subfamily Cardiochilinae and other diagnostic characters of *Bohayella* (Dangerfield et al. 1999), nine *Bohayella* specimens were identified. The characters of New World *Bohayella* are discussed in detail in diagnosis and discussion sections of this paper. Other Costa Rican cardiochiline specimens borrowed from several institutions were examined, but no more specimens of *Bohayella* were discovered. As a result, the nine specimens of *Bohayella* were confirmed as two species based on morphological data. Herein, we describe two new species and present a key to species of the genus *Bohayella* of Costa Rica. Distribution maps for both species are included.

Materials and methods

Specimens for this project were provided by **UWIM** (University of Wyoming Insect Museum; 1000 East University Avenue, University of Wyoming, Laramie, Wyoming 82071-3354, USA). We conducted morphological analyses using a Leica MZ75 stereomicroscope. The morphological terms and terms of wings mostly follow Dangerfield (1995) and Dangerfield et al. (1999). Morphological terminology can be checked at the Hymenoptera Ontology website (http://portal.hymao.org/projects/32/public/ontology/) as well. Terms for sculpturing are based on Harris (1979). Color habitus images were taken using a Visionary Digital BK Plus imaging system (Dun, Inc.), equipped with a Canon EOS 5DS DSLR camera. Images were stacked *via* Zerene Stacker v.1.04 (Zerene Systems LLC.). All images were edited using Adobe Photoshop CS 6 (Adobe

Systems, Inc). Body parts of each species were measured via Adobe Photoshop CS 6 (Adobe Systems, Inc). Each number in parentheses in species descriptions indicate 0.01 times the actual length, width, or height of each body part. For example, 42 and 124 in parentheses (42:124) indicate 0.42 mm and 1.24 mm, respectively. Distribution maps of two *Bohayella* species were produced using QGIS 3.10.0 (QGIS Development Team 2019). Google satellite maps were downloaded using the QuickMapServices plugin. The following abbreviations are used throughout the current paper: POL: distance between posterior ocelli, T1, T2 (second metasomal tergite), T3 (third metasomal tergite), T5 (fifth metasomal tergite), T6 (sixth metasomal tergite), T7 (seventh metasomal tergite), and T8 (eight metasomal tergite). Holotypes and paratypes are deposited in the UWIM.

Results

Bohayella Belokobylskij, 1987

Type species. *Bohayella tobiasi* Belokobylskij, 1987.

Diagnosis (based on Dangerfield et al. (1999) with modifications and additions). Diagnostic characters of *Bohayella* based on Old World members were described in Belokobylskij (1987) (in Russian) and Dangerfield et al. (1999) (in English). The following are re-described or additional characters based on morphological characters of both Old World and New World members.

Members of the genus can be identified by setose compound eyes (length and density variable); ventro-posteriorly moderately extended gena (Fig. 3F).broad clypeus without clypeal tubercles (Figs 3B, 4C); absence of occipital carina; uni- or bi-dentate mandible; 5- or 6-segmented maxillary palpus; 4-segmented labial palpus; short mouthparts (galea and glossa); deep and broad notauli and scutellar sulcus (Figs 3C, F, 4B, D); scutellum with apical cup-like pit (Figs 3C, F, 4B, D); fully developed propodeal areola (Figs 3D, F, 4B, E); moderately to strongly sculptured pronotum and mesopleuron; presence of epicnemial carina (Figs 3A, 4A); well-defined and crenulate precoxal sulcus (Figs 3A, 4A); absence of apical cup-like projection of hind tibia (Figs 3A, 4A); cylindrical or antero-posteriorly slightly expanded hind basitarsus (but never expanded like hind basitarsi found in members of *Hartemita* Cameron, 1910) (Figs 3A, 4A); pectinate tarsal claw with sharp or obtuse apical tooth; entirely or apically infuscate forewing; absence of 1r vein of forewing; absence of 3r vein of forewing; basally angled or smoothly curved Rs vein; absence of 2-1A vein of hind wing; narrow and elongate T1 (median length of T1 4.0–6.3× longer than its apical width) (Figs 3D, F, 4B, E); short T2; a medio-basal ball-like projection of T2 (Figs 3D, F, 4B, E); short and truncate hypopygium (Figs 3A, 4A); short ovipositor (if protruded, strongly downcurved); short ovipositor sheath (< ~0.2× longer than hind tibia) (Figs 3A, 4A).

Key to species of the genus *Bohayella* of Costa Rica

1 Median crenula of notauli as long as median crenula of scutellar sulcus (A); scutellar sulcus with one median crenula (A); T3–T8 mostly pale (AA) .... ***B. geraldinae* sp. nov.**

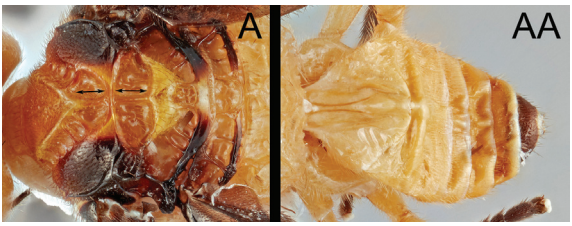

– Median crenula of notauli shorter than median crenula of scutellar sulcus (B); scutellar sulcus with three crenulae (B); T3–T8 mostly melanistic (BB) .... ***B. hansoni* sp. nov.**

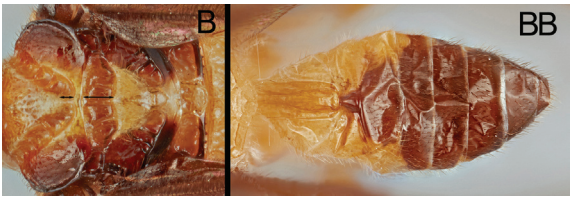

***Bohayella geraldinae* Kang, sp. nov.**
http://zoobank.org/FC39B76A-3AC3-41D7-9420-7148410F6D2C
Figure 3

Material examined. ***Holotype*** Costa Rica • ♀; female, Heredia, 3 km S. Puerto Viejo OTS, La Selva; 100 m; x.1992; P. Hanson; huertos Malaise trap set by G. Wright. ***Paratypes*** Costa Rica • 1 ♀; same data as for holotype; xi.1992 • 1 ♂; male; same collecting data as for preceding; 10°26'N, 84°01'W; 4. iv. 1987; H. A. Hespenheide.

Diagnosis. *Bohayella geraldinae* sp. nov. can be recognized by the following combination of characters: apical maxillary palpomere as long as fifth maxillary palpomere; median crenula of notauli as long as median crenula of scutellar sulcus; scutellar sulcus with one median crenula; hind basitarsus antero-posteriorly slightly expanded; dorsal metasoma mostly pale.

Description. Female. Body 4.6–4.8 mm. Forewing length: ~ 4.2 mm Antenna length: ~ 4.8 mm. ***Head.*** Antenna 34-segmented. Interantennal space with well-developed median carina. POL ~ 1.38× longer than diameter of anterior ocellus (11:8) (Fig. 3F). Eye sparsely setose with short setae; median width of eye 0.75× longer than median width of gena in lateral view (36:48). Width of clypeus ~ 2.07× longer than

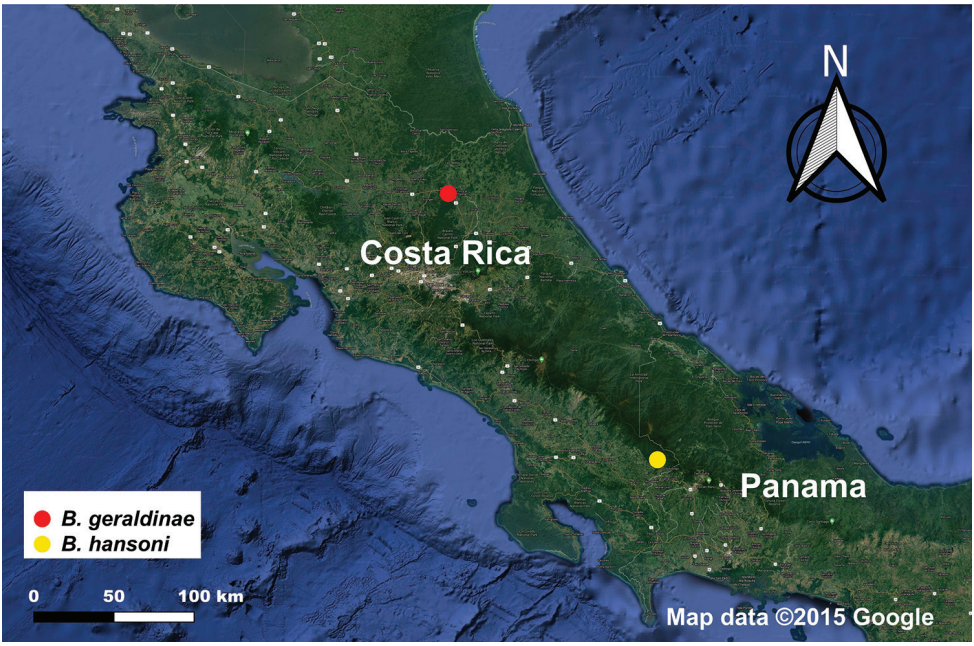

Figure 1. Distribution map of the species of *Bohayella* in Costa Rica. Map data 2020 Google.

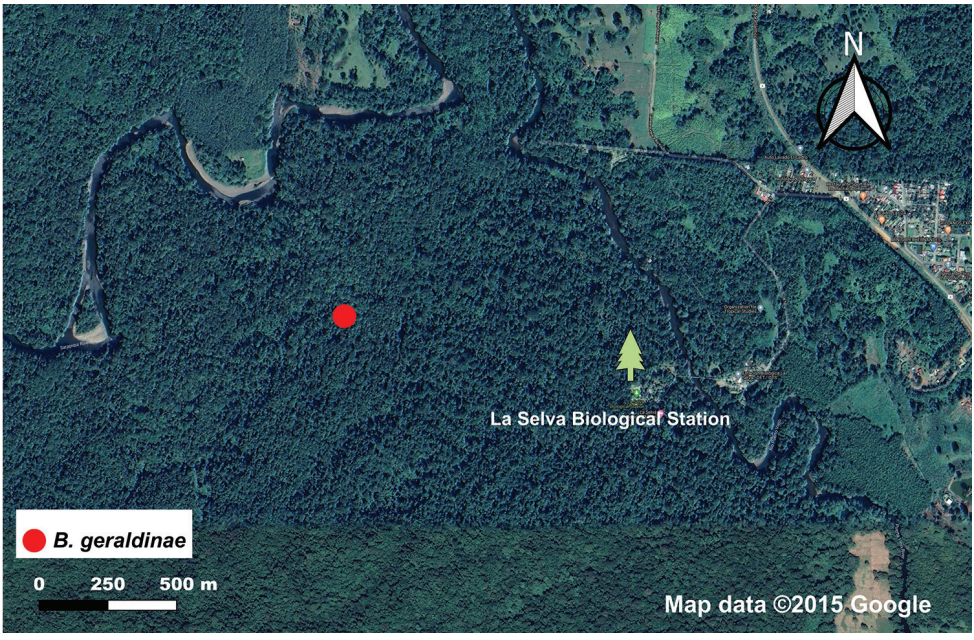

Figure 2. Distribution map of *B. geraldinae* sp. nov. in La Selva Biological Station in Costa Rica. Map data 2020 Google.

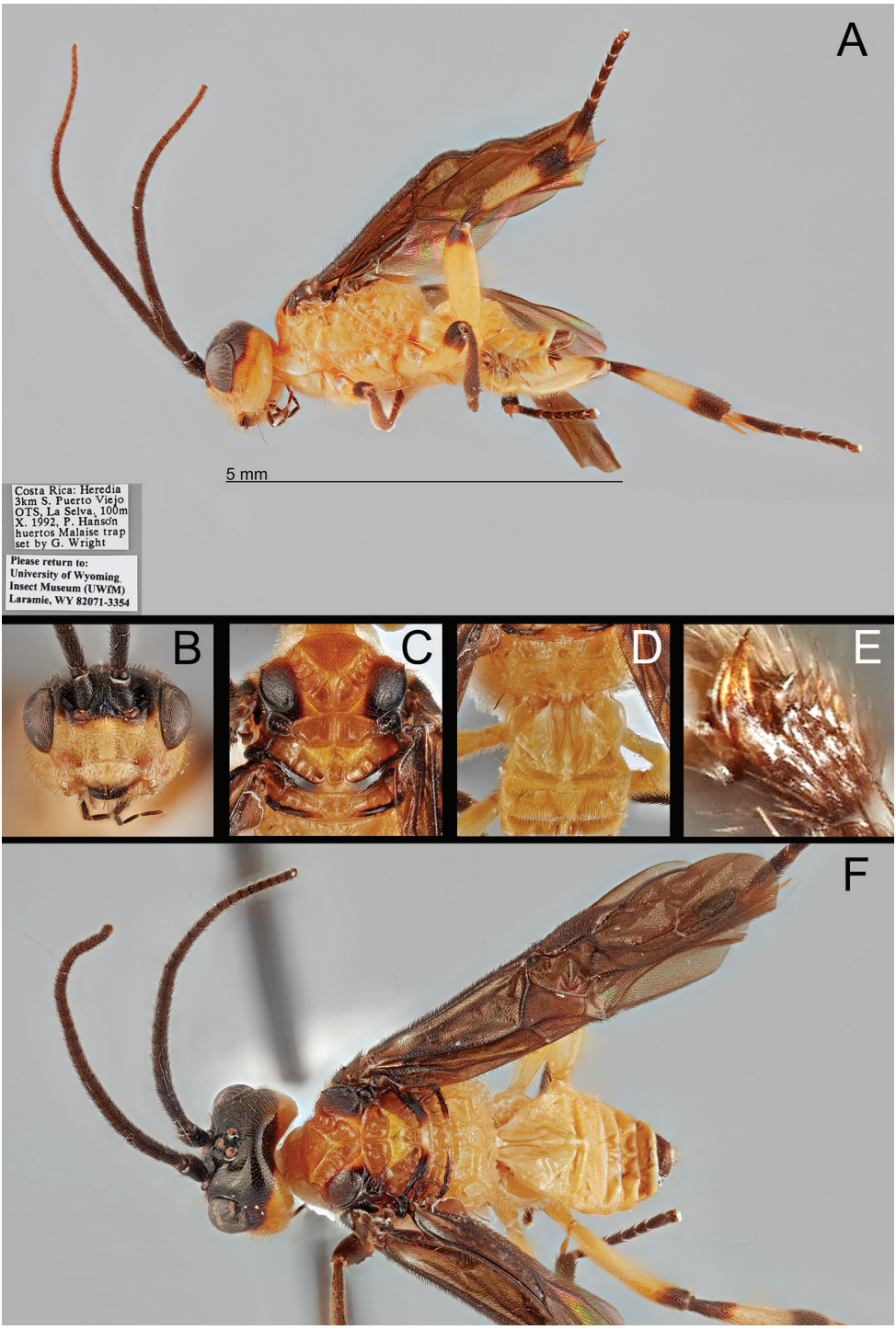

Figure 3. *B. geraldinae* sp. nov., holotype **A** lateral habitus **B** anterior head **C** dorsal mesonotum **D** dorsal propodeum and T1–T3 **E** hind tarsal claw **F** dorsal habitus.

height (60:29) (Fig. 3B). Malar space ~ 2.62× longer than basal width of mandible (34:13) (Fig. 3B). Mandible bidentate. Maxillary palpus 6-segmented; apical maxillary palpomere as long as fifth maxillary palpomere. ***Mesosoma.*** Mesoscutum with sharp margin (Fig. 3C, F). Notauli broadly converging at base, with 11 crenulae; median crenula of notauli as long as median crenula of scutellar sulcus (Fig. 3C, F). Scutellar sulcus with one median crenula (Fig. 3C, F). Postscutellar depression present (Fig. 3C, F). Propodeum rugulose with well-defined median areola; median transverse carina on propodeum reaching lateral margin (Fig. 3D, F). Pronotum dorso-posteriorly crenulate and antero-ventrally smooth. Mesopleuron dorsally and posteriorly with crenulate margin (Fig. 3A). Mesosternal sulcus broad and crenulate. Metapleuron rugulose. ***Legs.*** Basal spur on fore tibia ~ 0.86× longer than basitarsus (30:35). Width of hind femur ~ 0.34× longer than its length (42:124). Basal spur on hind tibia ~ 0.76× longer than basitarsus (58:76). Hind tarsal claw pectinate, with four sharp teeth (Fig. 3E). ***Wings.*** Forewing second submarginal cell trapezoidal, ~ 0.35× longer than maximum width (30:85); 3r absent (Note: one specimen has basally present 3r vein in particular angle); Rs sharply angled at basal third; stigma ~ 2.67× longer than medial width (80:30). 1CUa short, 0.23× longer than 1CUb (12:52). Hind wing 2-1A absent. ***Metasoma.*** T1 with a pair of lateral sutures posteriorly reduced, median length of T1 ~ 5.07× longer than apical width (71:14) (Fig. 3D, F). T2 with a ball-like projection, medially 0.21× longer than T1 (15:71) (Fig. 3D, F). T3 ~ 2.13× longer than T2 medially (32:15) (Fig. 3D, F). Protruded ovipositor sheath ~ 0.13× longer than hind tibia and apically setose (20:154) (Fig. 3A).

Male. Body ~ 5.0 mm. Same as female except for the following characters: antenna 32-segmented, melanistic color does not reach the dorsal margin of foramen magnum.

Color. Body mostly pale; the following areas are melanistic: antenna, vertex, frons, dorsal occiput, maxillary palpus, labial palpus, lateral mesonotal lobe (pale basally), lateral scutellum, margin of metanotum, apical fore femur, fore tibia, apical fore tarsus, apical mid femur, mid tibia, apical mid tarsus, apical hind femur, basal and apical hind tibia, apical hind tarsus, posterior T5 and T6 (weakly), entire T7 and T8, ovipositor sheath. Wings entirely infuscate, stigma entirely melanistic.

Host. Unknown.

Distribution. *Bohayella geraldinae* sp. nov. is known only from the La Selva Biological Station owned and managed by Organization for Tropical Studies (OTS) in Heredia, Costa Rica at an elevation of 100 m (Figs 1, 2). The station is located in the Caribbean lowlands, at a confluence of the Sarapiquí river and Puerto Viejo (McDade and Hartshorn 1994). According to Holdridge's life zone system (Holdridge 1967), the station is in the tropical wet forest region (Hartshorn and Peralta 1987), and the average annual precipitation in the area is ~ 4,000 mm (Sanford et al. 1994).

Etymology. This species is named in honor of Dr Geraldine Wright, a former student of the second author (SRS), Rhodes Scholar, professor in the Department of Zoology in the University of Oxford (United Kingdom), and the person who set the trap that collected the specimens.

***Bohayella hansoni* Kang, sp. nov.**
http://zoobank.org/7749425B-2B7F-4E69-A115-B65ED9CAD0CF
Figure 4

Material examined. ***Holotype*** Costa Rica • ♀; female, Puntarenas, San Vito, Estac. Biol., Las Alturas; 1,500 m; vi.1992; Paul Hanson; traps #1 + #2, Malaise. ***Paratypes*** Costa Rica • 2 ♀; same data as for holotype • 2 ♀; same collecting data as for preceding • 1 ♀; female; same collecting data as for preceding; 1,700 m; 11.iv.1993.

Diagnosis. *Bohayella hansoni* sp. nov. can be distinguished from *B. geraldinae* sp. nov. by the following characters: apical maxillary palpomere slightly longer than fifth maxillary palpomere; median crenula of notauli ~ 0.38× longer than median crenula of scutellar sulcus; scutellar sulcus with three crenulae; hind basitarsus cylindrical; dorsal metasoma mostly melanistic.

Description. Female. Body 3.9–4.1 mm. Forewing length: 3.9–4.1 mm Antenna length: 4.1–4.5 mm. ***Head.*** Antenna 32–34-segmented. Interantennal space with well-developed median carina. POL 1.22× longer than diameter of anterior ocellus (11:9) (Fig. 4B). Eye sparsely setose with short eye setae; length of eye ~ 0.86× longer than median width of gena in lateral view (31:36). Width of clypeus 2.00× longer than height (56:28) (Fig. 4C). Malar space 1.80× longer than basal width of mandible (36:20) (Fig.4C). Mandible bidentate. Maxillary palpus 6-segmented; apical maxillary palpomere 1.31× longer than fifth maxillary palpomere (17:13). ***Mesosoma.*** Mesoscutum with sharp margin (Fig. 4B, D). Notauli broadly converging at base, with 11 crenulae; median crenula of notauli ~ 0.38× longer than median crenula of scutellar sulcus (6:16) (Fig. 4B, D). Scutellar sulcus with three crenulae (Fig. 4B, D). Postscutellar depression present (Fig. 4B, D). Propodeum rugulose, with well-defined median areola; median transverse carina on the propodeum reaching lateral margin (Fig. 4B, E). Pronotum dorso-posteriorly crenulate and antero-ventrally smooth. Mesopleuron dorsally and posteriorly with crenulate margin (Fig. 4A). Mesosternal sulcus broad and crenulate. Metapleuron rugulose. ***Legs.*** Basal spur on fore tibia ~ 0.87× longer than basitarsus (26:30). Width of hind femur ~ 0.30× longer than its length (33:111). Basal spur on hind tibia ~ 0.81× longer than basitarsus (58:72). Hind tarsal claw pectinate with four acute teeth. ***Wings.*** Forewing second submarginal cell trapezoidal, ~ 0.34× longer than its maximum width (26:77); 3r absent; Rs sharply angled at basal third; stigma ~ 2.82× longer than medial width (79:28). 1CUa short, 0.23× longer than 1Cub (11:47) (Fig. 4A). Hind wing 2-1A absent. ***Metasoma.*** T1 with a pair of lateral sutures posteriorly reduced, median length of T1 4.00× longer than apical width (56:14) (Fig. 4B, E). T2 with a ball-like projection, medially ~ 0.20× longer than T1 (11:56) (Fig. 4B, E). T3 ~ 2.55× longer than T2 medially (28:11) (Fig. 4B). Protruded ovipositor sheath ~ 0.20× longer than hind tibia and apically setose (26:129) (Fig. 4A).

Color. Body mostly pale; the following areas melanistic: antenna, vertex, frons, dorsal occiput, maxillary palpus, labial palpus, lateral mesonotal lobe (basally pale), lateral scutellum, margin of metanotum, apical fore femur, fore tibia, apical fore tarsus,

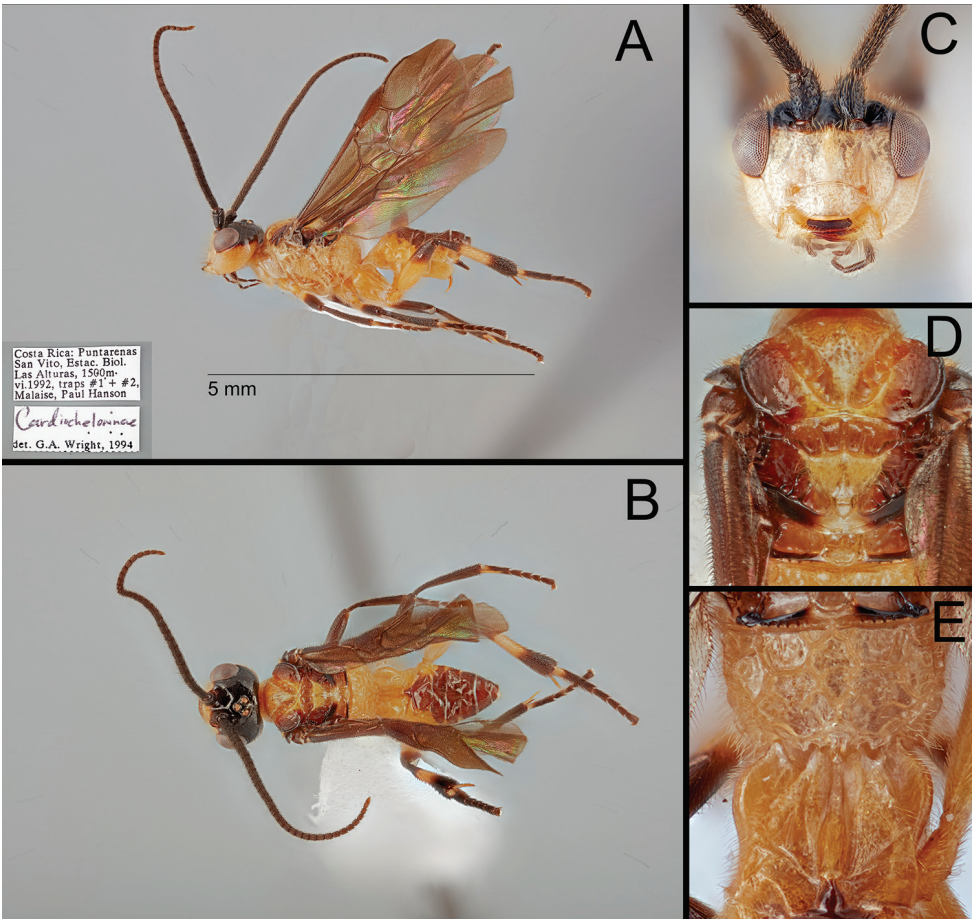

Figure 4. *B. hansoni* sp. nov., holotype. **A** lateral habitus **B** dorsal habitus **C** anterior head **D** dorsal mesonotum **E** dorsal propodeum and anterior metasoma.

apical mid femur, mid tibia, apical mid tarsus, apical hind femur, basal and apical hind tibia, apical hind tarsus, T2–T8, ovipositor sheath. Wings entirely infuscate, stigma entirely melanistic.

Male. Unknown.

Host. Unknown.

Distribution. *Bohayella hansoni* sp. nov. is known only from the Las Alturas Biological research station owned and operated by Stanford University in Las Alturas, San Vito, Costa Rica at the elevations of 1,500 m and 1,700 m (Figs 1, 5).

Etymology. This species is named in honor of Dr Paul Hanson, collaborator and professor at the Escuela de Biología, Universidad de Costa Rica. He worked tirelessly for many years collecting and sorting Costa Rican braconids from Malaise samples. SRS is very grateful for his dedication to Hymenoptera studies.

Figure 5. Distribution map of *B. hansoni* sp. nov. from Las Alturas Biological Research Station. Map data 2020 Google.

Discussion

Most genus-level diagnostic characters are shared by both Old World and New World members (*B. geraldinae* sp. nov. and *B. hansoni* sp. nov.). None of the New World members have a mostly black body, 5-segmented maxillary palpi, or apically infuscate forewings. The following characters are only shared by New World members: angled Rs vein of forewing (Figs 3F, 4A), pectinate hind tarsal claw with sharp apical tooth (Fig. 3E), and antero-posteriorly slightly expanded hind basitarsus (Fig. 3A).

Specimens of *B. hansoni* sp. nov. collected at altitudes above 1,500 m have more melanistic metasoma than specimens of *B. geraldinae* sp. nov. collected at a low altitude of 100 m (Figs 3F, 4B). The melanism associated with high elevation was confirmed not only in braconid wasps such as members of the genus *Sendaphne* Nixon, 1965 (Nixon 1965) (Fernandez-Triana et al. 2014) and *Meteorus pulchricornis* (Wesmael, 1835) (Abe et al. 2013), but also in other hymenopteran insects such as members of a vespid species, *Agelaia pallipes* (Olivier, 1792) (de Souza et al. 2020) as well as an undescribed scelionid species of *Lapitha* Ashmead, 1893 (Mora and Hanson 2019). According to Abe et al. (2013), emerged adults of *M. pulchricornis* were more melanistic when cocoons were reared at lower temperatures, and the effects of the melanism resulted in increasing body temperatures and improved flight ability of adult *M. pulchricornis*. Melanism of *B. hansoni* sp. nov. at high elevations may induce similar outcomes as in *M. pulchricornis*. Further research is needed when enough live samples are available to confirm this.

The elevation of Costa Rica ranges from sea level to 3,819 m (Hanson and Gauld 1995). If additional sampling is conducted across the country and more species of *Bohayella* are discovered, altitudinal distribution patterns of members of Costa Rican *Bohayella* can be investigated in the future (e.g., Aguirre et al. 2018).

Acknowledgements

The first author is grateful to all members of Louisiana State Arthropod Museum and the Department of Entomology as well as LSU Agricultural Center for financial support. We thank Drs Michael Sharkey and James Whitfield for their invaluable help and advice. We also thank Dr Paul Hanson in the Universidad de Costa Rica for the loan of specimens. This study was partially supported by NSF DEB #1841704 to NPL. Research support for SRS was partly provided by National Science Foundation grant DEB 14-42110 (Dimensions of Biodiversity Program). This work was also supported by Wyoming Agricultural Experiment Station funding to SRS provided through the USDA National Institute of Food and Agriculture, McIntire-Stennis project 1021111. Any opinions, findings, and conclusions expressed are those of the authors and do not necessarily reflect the views of the National Science Foundation.

References

Abe Y, Nishimura T, Maeto K (2013) Causes of polymorphic melanism and its thermoregulatory function in a parasitoid wasp *Meteorus pulchricornis* (Hymenoptera: Braconidae). European Journal of Entomology 110(4): 627–632. https://doi.org/10.14411/eje.2013.085

Aguirre H, Shaw SR, Rodríguez-Jiménez A (2018) Contrasting patterns of altitudinal distribution between parasitoid wasps of the subfamilies Braconinae and Doryctinae (Hymenoptera: Braconidae). Insect Conservation and Diversity 11(3): 219–229. https://doi.org/10.1111/icad.12265

Beeson CF, Chatterjee SN (1935) On the biology of the Braconidae (Hymenoptera). Indian Forest Records 1: 105–138.

Belokobylskij SA (1987) A new genus of the subfamily Cardiochilinae (Hymenoptera, Braconidae) from the USSR Far East. Zoologicheskiy Zhurnal 66(2): 302–304.

Cameron P (1910) On some Asiatic species of the subfamilies Spathiinae, Doryctinae, Rhogadinae, Cardiochilinae and Macrocentrinae in the Royal Berlin Zoological Museum. Wiener Entomologische Zeitschrift 29: 93–100. https://doi.org/10.5962/bhl.part.23337

Dangerfield PC (1995) The systematics of the genera of Cardiochilinae (Hymenoptera: Braconidae) with a revision of Australasian species. PhD Thesis. Adelaide, Australia: University of Adelaide, 343 pp. http://hdl.handle.net/2440/18664

Dangerfield PC, Austin AD, Whitfield JB (1999) Systematics of the world genera of Cardiochilinae (Hymenoptera: Braconidae). Invertebrate Systematics 13(6): 917–976. https://doi.org/10.1071/IT98020

de Souza AR, Mayorquin AZ, Sarmiento CE (2020) Paper wasps are darker at high elevation. Journal of Thermal Biology 89: 102535. https://doi.org/10.1016/j.jtherbio.2020.102535

Fernandez-Triana JL, Whitfield JB, Smith MA, Hallwachs W, Janzen DH (2014) Revision of the neotropical genus *Sendaphne* Nixon (Hymenoptera, Braconidae, Microgastrinae). Journal of Hymenoptera Research 41: 1–29. https://doi.org/10.3897/JHR.41.8586

Gaston K, Gauld I, Hanson P (1996) The size and composition of the hymenopteran fauna of Costa Rica. Journal of Biogeography 23(1): 105–113. https://doi.org/10.1046/j.1365-2699.1996.00978.x

Hanson PE, Gauld ID (1995) The Hymenoptera of Costa Rica. Oxford University Press, Oxford, 893 pp.

Hartshorn GS, Peralta R (1987) Preliminary description of primary forests along the La Selva-Volcan Barva altitudinal transect, Costa Rica. In: Almeda F, Pringle CM (Eds) Tropical Rainforests: Diversity and Conservation. California Academy of Science, San Francisco, 281–295.

Harris RA (1979) Glossary of surface sculpturing. Occasional Papers in Entomology 28: 1–31.

Holdridge LR (1967) Life zone ecology. Tropical science center. San Jose, Costa Rica. 266 pp.

Huddleston T, Walker AK (1988) *Cardiochiles* (Hymenoptera: Braconidae), a parasitoid of lepidopterous larvae, in the Sahel of Africa, with a review of the biology and host relationships of the genus. Bulletin of entomological research 78(3): 435–461. https://doi.org/10.1017/S0007485300013201

Kang I, Long KD, Sharkey MJ, Whitfield JB, Lord NP (2020) *Orientocardiochiles*, a new genus of Cardiochilinae (Hymenoptera, Braconidae), with descriptions of two new species from Malaysia and Vietnam. ZooKeys 971: 1–15. https://doi.org/10.3897/zookeys.971.56571

Mao YT (1949) The species of ichneumon-flies of the genus *Cardiochiles* occurring in America north of Mexico. Proceedings of the United States National Museum 99: 229–266. https://doi.org/10.5479/si.00963801.99-3237.229

McDade LA, Hartshorn GS (1994) La Selva Biological Station. In: McDade LA, Bawa KS, Hespenheide HA, Hartshorn GS (Eds) La Selva: ecology and natural history of a neotropical rain forest. University of Chicago Press, Chicago, 6–14.

Mercado I, Wharton RA (2003) Mexican cardiochiline genera (Hymenoptera: Braconidae), including a preliminary assessment of species-groups in *Toxoneuron* Say and *Retusigaster* Dangerfield, Austin and Whitfield. Journal of Natural History 37(7): 845–902. https://doi.org/10.1080/00222930110097167

Mora R, Hanson PE (2019) Widespread Occurrence of Black-Orange-Black Color Pattern in Hymenoptera. Journal of Insect Science 19(2): 1–12. https://doi.org/10.1093/jisesa/iez021

Nixon G (1965) A reclassification of the tribe Microgasterini (Hymenoptera: Braconidae). Bulletin of the British Museum (Natural History) Entomology series 2: 1–284.

Sanford Jr RL, Paaby P, Luvall JC, Phillips E (1994) Climate, Geomorphology, and Aquatic systems. In: McDade LA, Bawa KS, Hespenheide HA, Hartshorn GS (Eds) La Selva: ecology and natural history of a neotropical rain forest. University of Chicago Press, Chicago, 19–33.

QGIS Development Team (2019) QGIS Geographic Information System. Open Source Geospatial Foundation Project. http://qgis.osgeo.org

Wesmael C (1835) Monographie des Braconides de Belgique. Nouveaux Mémoires de l'Academie Royale des Sciences et Belles-lettres Bruxelles 9: 1–252.

Wilkinson DS (1930) New species and host records of Braconidae. Bulletin of Entomological Research 21(4): 481–487. https://doi.org/10.1017/S0007485300024822

Yu DS, Achterberg C van, Horstmann K (2012) Taxapad 2012, Ichneumonoidea 2011. Database on USB Flash drive. Ottawa, Ontario. http://www.taxapad.com

ZooKeys 996: 107–119 (2020)
doi: 10.3897/zookeys.996.56562
https://zookeys.pensoft.net

RESEARCH ARTICLE

A peer-reviewed open-access journal
ZooKeys
Launched to accelerate biodiversity research

First record of the genus *Trispinaria* Quicke, 1986 (Hymenoptera, Braconidae, Braconinae) in Vietnam, with descriptions of two new species

Nguyen Thi Oanh[1], Khuat Dang Long[2], Pham Quynh Mai[2], Nguyen Van Dzuong[3]

1 *Dong Thap University, Cao Lanh City, Dong Thap, Vietnam* **2** *Institute of Ecology & Biological Resources, Vietnam Academy of Science & Technology, 18 Hoang Quoc Viet Road, Cau Giay, Ha Noi, Vietnam* **3** *Tay Bac University, Son La City, Vietnam*

Corresponding author: Khuat Dang Long (khuatdanglong@gmail.com)

Academic editor: K. van Achterberg | Received 15 July 2020 | Accepted 4 November 2020 | Published 24 November 2020

http://zoobank.org/219F3EC2-D2C5-4B4A-B63E-C5FA420E33FE

Citation: Oanh NT, Long KD, Mai PQ, Dzuong NV (2020) First record of the genus *Trispinaria* Quicke, 1986 (Hymenoptera, Braconidae, Braconinae) in Vietnam, with descriptions of two new species. ZooKeys 996: 107–119. https://doi.org/10.3897/zookeys.996.56562

Abstract

Two new species of the genus *Trispinaria* Quicke, 1986, from Vietnam, viz. *T. seminigra* Long, **sp. nov.** and *T. vietnamica* Long, **sp. nov.**, are described and fully illustrated. Additionally, this is the first record of the genus *Trispinaria* in Vietnam. A checklist with distributions of previously described species of the genus *Trispinaria* is given. Comparative characters of the Vietnamese species are provided and modified key couplets are provided to facilitate their identification.

Keywords

Australasian region, Ichneumonoidea, new record, Oriental region, parasitoid, taxonomy, wasp

Introduction

Trispinaria was described by Quicke (1986) from SW Sulawesi, including only the type-species *Trispinaria priscicolorus* Quicke,1986. *Trispinaria* is an aberrant and rather uniform genus of the subfamily Braconinae. *Trispinaria* species occur over the Oriental

and Australasian regions; van Achterberg (1991) listed and keyed the eight species. Subsequently, Wang et al. (2003) described one new species from China, resulting in eight species described from the Oriental region. A ninth species is recorded from the Australasian region.

Quicke (1988) placed *Trispinaria* as sister group of *Physaraia* Shenefelt, 1978, because of the fused first and second metasomal tergites and propodeal sculpture. However, van Achterberg (1991) reported that more likely the genus is closely related to the Oriental genus *Pseudospinaria* Enderlein, 1920. Van Achterberg based his conclusion on the following suit of characters: long and curved vein 1r-m of the hind wing; protruding median carina of metanotum; united dorsal carinae of the first tergite; pair of converging grooves of the second tergite, the third-fifth metasomal tergites possess spines; the first subdiscal cell of the fore wing is more slender; the second tergite has a pair of converging grooves; and the propleuron is concave ventrally. *Pseudospinaria* differs from *Trispinaria* by having both basal segments of the metasoma movably jointed, a large fore wing second submarginal cell, bifurcate tarsal claws, and reduced scutellar sulcus. A detailed diagnosis of the genus *Trispinaria* was given by van Achterberg (1991).

The biology of *Trispinaria* is unknown but based on the united and heavily sclerotised basal metasomal tergites, van Achterberg (1991) suggested the ovipositor could insert into a hard substrate. Following the points of van Achterberg (1991), the colouration of the wasps corroborates the idea that they occur in open, sunny, and dry types of forest. In tropical rain forests most of the large braconid wasps possess a dark reddish brown and black colour pattern.

Materials and methods

The specimens studied, including holotypes and some paratypes, are housed in the Institute of Ecology & Biological Resources (**IEBR**) at Ha Noi; other paratypes have been donated to and are deposited in the American Museum of Natural History (**AMNH**), New York, USA, and the Vietnam National Museum of Nature (**VNMN**), Ha Noi, Vietnam.

Morphology

For terminology used in this paper, see van Achterberg (1993), sculpture terms are based on Harris (1979), and vein terminology follows the modified Comstock-Needham system (van Achterberg 1993). For a key to the Old World genera of the subfamily Braconinae, see Quicke (1987).

We used an Olympus SZ61 binocular microscope together with fluorescent lamps for sorting, identification and descriptions. The key to species and the descriptions of species are based on females. Measurements are taken under an Olympus SZ40

binocular microscope. The scale-lines of the plates (habitus and fore wing) represent 1.0 mm. The photographs were made with a Sony 5000 digital camera attached to a Nikon SMZ 800N binocular microscope connected to a PC at IEBR and processed with Adobe Photoshop CS5 to adjust the size and background. A distribution map of two new species of *Trispinaria* was made using Paraview (https://paraview.org).

Abbreviations used in this paper are as follows:

POL minimum postocellar line;
OOL minimum ocular-ocellar line;
OD maximum diameter of posterior ocellus;
'Bracn. + number' code number indexing for Braconinae specimens in the collection at IEBR and VNMN;
MT Malaise trap;
N north;
NC north central;
NE northeastern;
NP National Park;
NW northwestern;
S south.

Institutional abbreviations are as follows:

AMNH American Museum of Natural History, New York, USA;
IEBR Institute of Ecology & Biological Resources, Vietnam Academy of Science and Technology, Ha Noi, Vietnam;
STCT Department of Insect Ecology at IEBR;
VNMN Vietnam National Museum of Nature, Vietnam Academy of Science and Technology, Ha Noi, Vietnam.

In Vietnam, the distribution of the species is given in order of areas and provinces from north to south, and outside Vietnam, distribution of species follows an alphabetical order.

Results

Class Hexapoda Blainville, 1816
Order Hymenoptera Linnaeus, 1758
Superfamily Ichneumonoidea Latreille, 1802
Family Braconidae Nees, 1811
Subfamily Braconinae Nees, 1811
Tribe Braconini Nees, 1811

Genus *Trispinaria* Quicke, 1986

Trispinaria Quicke, 1986a: 10 & 1987: 134.

Type-species. *Trispinaria priscicolorus* Quicke, 1986 (monobasic and original designation).

Checklist and distribution of *Trispinaria* species.

T. albibasis van Achterberg, 1991: figs 33, 34, 36/ Oriental: Malaysia (Peninsular).
T. betremi van Achterberg, 1991: figs 31, 32, 35/ Oriental: Indonesia (Java).
T. chinensis Wang, Chen & He, 2003: figs 1–9/ Oriental: China (Guangxi).
T. maculata van Achterberg, 1991: figs 41–44/ Oriental: China-Taiwan; India; Malaysia (Peninsular); Singapore; Sri Lanka.
T. priscicolorus Quicke, 1986a: figs 1–11/ Australasian: Indonesia (Sulawesi).
T. sannio (Enderlein, 1920): figs 37–40/ Oriental: Indonesia; Singapore
T. setosa van Achterberg, 1991: figs 26–30/ Oriental: Indonesia (Bali)
T. seminigra Long, sp. nov./ Oriental: NE Vietnam (Tuyen Quang), N Vietnam (Ninh Binh), NC Vietnam (Ha Tinh).
T. sulcata van Achterberg, 1991: figs 22–25/ Oriental: Philippines (Mindanao, Mindoro).
T. unicolor van Achterberg, 1991: figs 17–20/ Oriental: Philippines.
T. vietnamica Long, sp. nov./ Oriental: N Vietnam (Thai Nguyen), NW Vietnam (Son La, Hoa Binh), S Vietnam (Pleicu).

Trispinaria seminigra Long, sp. nov.

http://zoobank.org/C6F2CE0E-C33C-48E8-95D2-F2BE2D120B7D
Figs 1–12

Material. ***Holotype***, ♀, "Bracn.1503" (IEBR), NE Vietnam: Tuyen Quang, Na Hang NP, Son Phu, forest, MT, 22°17'34"N, 105°28'19"E, 561 m, 15.iv.2018, KD Long. ***Paratypes***, 3 ♀, "Bracn.**768**" (IEBR), N Vietnam: Ninh Binh, Cuc Phuong NP, forest, 20°19'N, 105°35'E, 180 m, sweeping, 9.v.2002, KD Long, "Bracn.1411" (VNMN), NE Vietnam: Tuyen Quang, Na Hang, Thanh Tuong, forest, MT, 22°19'01"N, 105°24'02"E, 162 m, 5.xi.2016, KD Long; "Bracn.**710"** (AMNH), NC Vietnam: Ha Tinh, Huong Son, forest, 18°13'N, 105°24'E, 900 m, 20–28.iv.1998, AMNH, K. Long.

Description. Holotype, female, body length 6.2 mm, fore wing length 5.7 mm, antenna 7.3 mm, ovipositor sheath 1.5 mm (Fig. 1).

Head. Antenna with 58 antennomeres; length of third and fourth antennomere 1.75 (7 : 4) and 1.5× their width (6 : 4); length of subapical antennomere 1.3× its width (4 : 3); in frontal view, width of face 1.9× its length (25 : 13) (Fig. 2); length of maxillary palp 0.7× height of head (25 : 37); face flattened, transversely rugose, triangular area upper clypeus smooth (Fig. 2); malar space as long as basal width of mandible (8 : 8); clypeus convex medially, depressed laterally, its apical margin concave and

Figure 1. *Trispinaria seminigra* Long, sp. nov., holotype, female, habitus, lateral view.

with distinct carina (Fig. 2); distance between tentorial pits 1.7× distance from pit to eye margin (10 : 6); in lateral view, eye 3.0× temple (18 : 6); in dorsal view, head 1.7× as wide as long (49 : 29); in dorsal view, width of head 1.7× median length (49 : 29); eye 3.0× as long as temple (21 : 7); POL : OD : OOL = 3 : 5 : 10; eye 3.0× temple (21 : 7); frons flat, smooth, with fine median groove (Fig. 3).

Mesosoma. Length of mesosoma 1.65× its height (78 : 47); propleuron shallow, finely crenulate medially (Fig. 5); middle lobe of mesoscutum without impressions anteriorly; notauli deeper anteriorly, wider and flat posteriorly, almost smooth with faint median carina (Fig. 6); median lobe of mesoscutum without groove; mesoscutal lobes shiny, sparsely finely punctate; prescutellar sulcus narrow, crenulate; scutellum sparsely punctate; mesopleuron largely smooth, with large sparse punctures dorsally (Fig. 5); metapleuron punctate; propodeum with distinct V-shaped carina posteriorly (Fig. 4); median depression sparsely crenulate anteriorly, almost sooth posteriorly; lateral areola-like areas almost coriaceous.

Wings. Length of fore wing 3.2× its maximum width (240 : 75); length of pterostigma 3.8× its width (42 : 11); fore wing vein SR1 4.8× as long as vein 3-SR (67 : 14); r : 3-SR : SR1 = 13 : 14 : 67; cu-a interstitial, weakly inclivous (Fig. 11), cu-a : 2-CU1 = 7 : 26; 2-SR : 3-SR : r-m = 15 : 14 : 11; second submarginal cell of fore wing less robust (Fig. 11); hind wing vein 1-M weakly curved basally (Fig. 12); vein 1r-m of hind wing largely united with 1-SC+R.

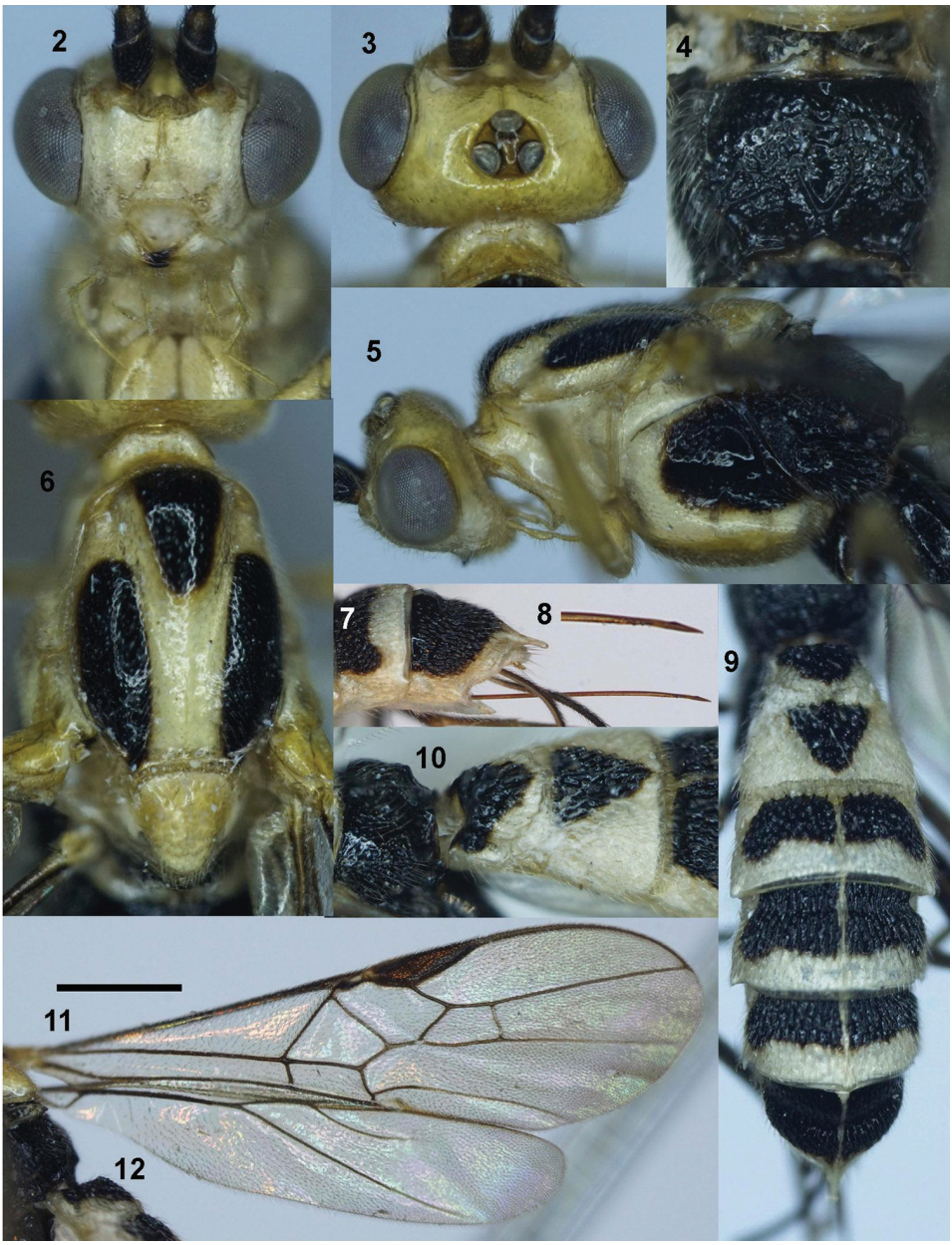

Figures 2–12. *Trispinaria seminigra* Long, sp. nov., holotype, female. **2** head, frontal view **3** head, dorsal view **4** propodeum **5** mesopleuron **6** mesonotum **7** fifth and sixth metasomal tergites, lateral view **8** apex of ovipositor **9** metasoma **10** first and second metasomal tergites, lateral view **11** fore wing **12** hind wing.

Legs. Hind coxa sparsely setose; length of femur, tibia and basitarsus of hind leg 4.9×, 10.6× and 8.0× their width, respectively; length of hind inner and outer tibial spurs 0.5× and 0.4× hind basitarsus (16 : 32)(13 : 32), respectively; length of hind

basitarsus 0.4× hind tibia (32 : 74) and 0.7× second-fifth tarsus (32 : 44); hind tarsal claw with large lobe.

Metasoma. Length of first tergite 0.9× its apical width (27 : 30), with basal excavation narrow and deep (Fig. 10); antero-lateral groove shallow, sparsely crenulate; median length of second tergite 0.9× third tergite (25 : 27; first metasomal tergite posteriorly, second-sixth metasomal tergites entirely coarsely reticulate (Fig. 9); tooth of sixth tergite developed (Fig. 7); latero-apical groove narrow, crenulate (Fig. 7); length of ovipositor sheath 0.26× fore wing (15 : 57); ovipositor with dorsal nodus; subapical ventral margin of ovipositor underneath nodus with serrations, but apico-ventrally without serrations (Fig. 8).

Colour. Head yellow; mesosoma and metasoma pale yellow; scapus brown; twenty middle antennomeres yellow; palpi and stemmaticum brownish yellow; mesoscutal lobes black, except median lobe laterally and posteriorly, lateral lobes anteriorly pale yellow; mesopleuron yellow ventrally, black dorsally; metapleuron black; scutellum pale yellow; metanotum and propodeum black; fore legs pale yellow; middle coxa, trochanter and trochantellus brown; middle femur brown, except outer side yellow; middle tibia and tarsus yellowish brown; hind legs black; hind tibial spurs pale yellow; pterostigma and veins brown; wing membrane subhyaline basally and medially, except fore wing membrane yellowish brown apically; first and second metasomal tergites black medio-basally, pale yellow laterally and apically; third-fifth metasomal tergites black basally, pale yellow apically; sixth metasomal tergite black, yellow apically; ovipositor sheath brown; ovipositor brownish yellow.

Variations. Length of body 5.8–7.7 mm, of fore wing 5.3–6.7 mm; antenna with 57–65 antennomeres; 16–26 middle antennomeres yellow or antenna brown entirely; stemmaticum brownish yellow; vein SR1 of fore wing 4.0–4.9× vein 3-SR; length of ovipositor sheath 0.22–0.25× fore wing; middle coxa and tarsus brownish yellow; middle femur and tibia yellow; ovipositor yellow.

Male. Unknown.

Biology. Unknown.

Etymology. From *semi* (Latin for half) and *niger* (Latin for black), because the mesopleuron is black dorsally in contrast to the yellow ventral half.

Distribution. N Vietnam: Tuyen Quang, Ninh Binh; NC Vietnam: Ha Tinh.

Notes. *Trispinaria seminigra* sp. nov. differs from *T. vietnamica* sp. nov. by having: median length of first metasomal tergite 0.9× as long as its apical width; propleuron shallow, finely rugose; fore wing vein cu-a slightly postfurcal and distinctly inclivous; hind wing vein 1-M almost straight basally; middle coxa dark brown; mesopleuron black dorsally; ovipositor apico-ventrally without serrations, except pre-apical ventral margin underneath with serrations.

The new species, *T. seminigra* sp. nov., is close to *T. sannio* (Enderlein), from Indonesia and Singapore by sharing the following characters: vein 1r-m of hind wing nearly united with vein 1-SC+R; apical half of subbasal cell of fore wing largely glabrous; and frons smooth. The new species can be inserted into the key by van Achterberg (1991) as follows:

7a. Whole antenna black; face coarsely punctate, at most with some rugae dorsally; second submarginal cell of fore wing comparatively robust (cf. fig. 37 in van Achterberg 1991); vein cu-a of fore wing distinctly inclivous, more than vein 3-CU1 (cf. figs 37, 40 in van Achterberg 1991); length of ovipositor sheath 0.5× fore wing; length of vein SR1 of fore wing 3.9–4.4× vein 3-SR; metapleuron with small black patch; propodeum with pair of two large black patches. Indonesia, Singapore ..... ***T. sannio*** **(Enderlein, 1920)**

a'. Antenna dark brown basally and apically, yellowish medially; face transversely rugose, except triangular area upper clypeus smooth; second submarginal cell of fore wing slender (Fig. 11); vein cu-a of fore wing less inclivous (Fig. 11); length of ovipositor sheath 0.3× fore wing; length of vein SR1 of fore wing 4.0–4.9× vein 3-SR; mesopleuron dorsally, metapleuron and propodeum entirely black (Figs 4, 5). Vietnam ..... ***T. seminigra*** **Long, sp. nov.**

Trispinaria vietnamica **Long, sp. nov.**
http://zoobank.org/4F51C7EE-573E-4186-9F42-ACCC78B59BB1
Figures 13–24

Material. ***Holotype***, ♀, "Bracn.376" (IEBR), S Vietnam: Pleicu, Dak Do, Ha Bau, > 800 m, bushes, 08.vi.2005, KD Long. ***Paratypes***: 6 ♀, "Bracn.377" (IEBR), data as holotype; "Bracn.708" (IEBR), NE Vietnam: Thai Nguyen, Dai Tu, Cat Ne, MT, orchard, 21°31'24"N, 105°29'39"E, 302 m, 30.xi.2006, KD Long; "Bracn.708" (VNMN), ibid. but 5.xi.2006, KD Long; "Bracn.747" (IEBR), ibid, but 25.xii.2006, KD Long; "Bracn.1481" (IEBR), NW Vietnam: Son La, coffee orchard, MT, 21°18'06"N, 103°55'36"E, 663 m, 10.iii.2018, KD Long, NV Dzuong; "Bracn.1491" (IEBR), NW Vietnam: Hoa Binh, Luong Son, Thanh Lap, fruit orchard, MT, 20°48'46"N, 105°37'58"E, 20 m, 5.ii.2018, STCT.

Description. Holotype, female, body length 8.3 mm, fore wing length 7.2 mm, antenna 7.7 mm, ovipositor sheath 1.8 mm (Fig. 13).

Head. Antenna with 74 antennomeres; length of third and fourth antennomeres 1.6× and 1.4× their width, respectively (8 : 5) (7 : 5); length of subapical antennomere as long as wide (3 : 3); in frontal view, width of face 0.5× its length (33 : 16) (Fig. 14); length of maxillary palp 0.8× height of head (36 : 45); malar space 0.8× as long as basal width of mandible (10 : 13); face flattened, punctate-coriaceous and rather matt; clypeus convex medially, depressed laterally, its apical margin concave and with distinct carina (Fig. 14); distance between tentorial pits 1.6× distance from pit to eye margin (13 : 8); in lateral view, eye 2.5× temple (20 : 8); in dorsal view, width of head 1.9× median length (62 : 33); POL : OD : OOL = 6 : 4 : 13 (Fig. 15); eye 3.4× temple (24 : 7); frons smooth, weakly concave.

Mesosoma. Length of mesosoma 1.6× its height (85 : 54); propleuron wide, deep and crenulate medially (Fig. 17); middle lobe of mesoscutum without impressions anteriorly; notauli deeper anteriorly, wider and flat posteriorly, with median longitudinal carina and transversely rugose posteriorly (Fig. 16); prescutellar sulcus narrow,

Figure 13. *Trispinaria vietnamica* Long, sp. nov., holotype, female, habitus, lateral view.

crenulate; mesoscutal lobes sparsely punctate; mesopleuron rugose-punctate anteriorly, coriaceous medially, punctate ventrally (Fig. 17); metapleuron rugose-punctate; propodeum with deep crenulate depression, posterior V-shaped carina indistinct (Fig. 22); surface of propodeum rugose-punctate on anterior 0.7 of propodeum, almost smooth latero-posteriorly.

Wings. Length of fore wing 3.1× its maximum width (225 : 72); length of pterostigma 3.2× its width (48 : 15); fore wing vein SR1 5.1× as long as vein 3-SR (76 : 15); r : 3-SR : SR1 = 15 : 15 : 76; cu-a slightly reclivous (Fig. 18); cu-a : 2-CU1 = 12 : 34; 2-SR : 3-SR : r-m = 17 : 15 : 16; second submarginal cell of fore wing rather robust (Fig. 18); hind wing vein 1-M thick and evenly curved basally (Fig. 21); vein 1r-m of hind wing largely united with 1-SC+R (Fig. 21).

Legs. Hind coxa densely setose latero-ventrally, but without setae dorso-apically; length of femur, tibia and basitarsus of hind leg 4.0×, 9.4× and 6.7× their width, respectively; length of hind inner and outer tibial spurs 0.5× and 0.4× hind basitarsus, respectively; length of hind basitarsus 0.4× hind tibia (40 : 94) and 0.7× second-fifth tarsus (40 : 55); tarsal claw with large acute lobe (Fig. 19).

Metasoma. Length of first tergite 0.7× its apical width (31 : 45), with wide and deep basal excavation (Fig. 23); antero-lateral groove wide and deep, crenulate; median length of second tergite 0.85× third tergite (28 : 33); first metasomal tergite posteriorly, second-sixth metasomal tergites entirely coarsely reticulate; medio-apical tooth of sixth tergite developed; latero-apical groove of sixth metasomal tergite wide, crenulate (Fig. 24); length of ovipositor sheath 0.25× fore wing (18 : 72); ovipositor with dorsal nodus and apico-ventrally with serrations (Fig. 20).

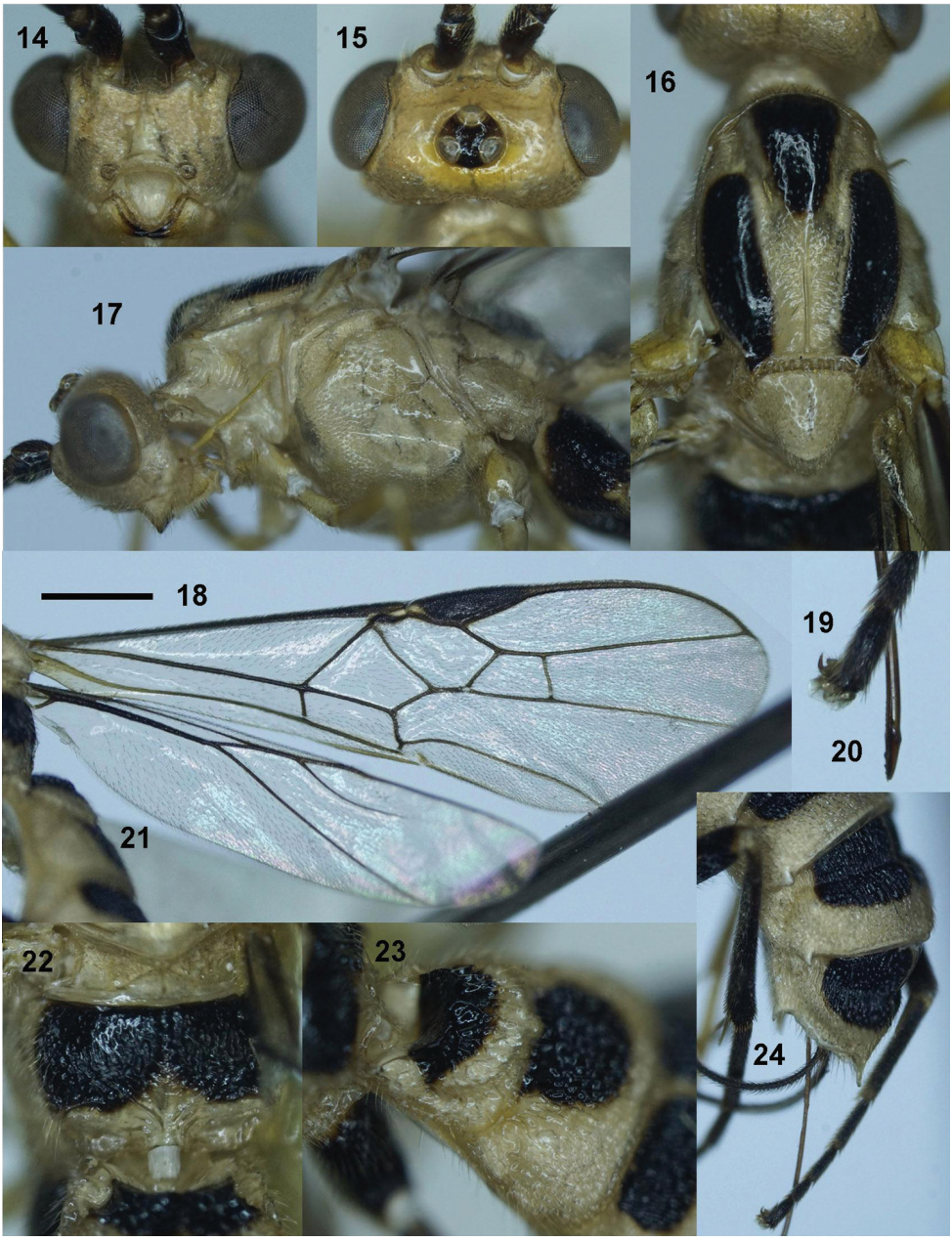

Figures 14–24. *Trispinaria vietnamica* Long, sp. nov., holotype, female **14** head, frontal view **15** head, dorsal view **16** mesonotum **17** mesopleuron **18** Fore wing **19** hind telotarsus and tarsal claw **20** apex of ovipositor **21** hind wing **22** propodeum **23** first and second metasomal tergites, lateral view **24** fifth and sixth metasomal tergites, lateral view.

Colour. Pale yellow; scapus dark brown; twenty four middle antennomeres yellow; palpi yellow; stemmaticum brown; mesoscutal lobes black, except median lobe

posteriorly and lateral lobes anteriorly pale yellow; scutellum and metanotum, fore and middle legs pale yellow; hind leg dark brown to black, except coxa basally, trochantellus and lateral strip on hind femur yellow; hind tibial spurs pale yellow; propodeum largely black, pale yellow apically; pterostigma and veins brown; wing membrane subhyaline; large patches of six basal metasomal tergites black; ovipositor sheath brown; ovipositor reddish yellow.

Variations. Length of body 5.4–8.4 mm, of fore wing 4.9–7.1 mm; antennae 65–70 antennomeres; 18–34 middle antennomeres yellow or antennae brown entirely; stemmaticum yellow; vein SR1 of fore wing 4.0–6.2× vein 3-SR; length of ovipositor sheath 0.22–0.3× fore wing; middle tarsus brownish yellow; hind tibial spurs brown.

Male. Unknown.

Biology. Unknown.

Etymology. The name of the species originates from the name of the country, where the holotype was collected.

Distribution. N Vietnam: Son La, Thai Nguyen, Hoa Binh; S Vietnam: Pleicu.

Notes. *Trispinaria vietnamica* sp. nov. differs from *T. seminigra* sp. nov. by having: first metasomal tergite with wide and deep basal excavation (narrow and deep in *T. seminigra*); median length of first metasomal tergite 0.7× as long as its apical width (0.9× in *T. seminigra*); propleuron wide and deep, crenulate (propleuron with distinct V-shaped carina posteriorly in *T. seminigra*); fore wing vein cu-a interstitial and weakly inclivous (vein cu-a vertical in *T. seminigra*); hind wing vein 1-M thick and curved basally (vein 1-M weakly curved basally in *T. seminigra*); middle coxa and mesopleuron pale yellow (black in *T. seminigra*); ovipositor apico-ventrally with serrations (apico-ventrally without serrations in *T. seminigra*).

The new species, *T. vietnamica* sp. nov., is similar to *T. maculata* van Achterberg, from India, Singapore, Sri Lanka, and Taiwan by sharing the following characters: vein 1r-m of hind wing nearly united with vein 1-SC+R; apical half of subbasal cell of fore wing largely glabrous; and frons smooth. The new species can be inserted into the key by van Achterberg (1991) as follows:

7b. Surroundings of stemmaticum of female yellowish brown; antenna near its apical 0.4 brown; face transversely rugose; fore wing vein r distinctly longer vein 3-SR (cf. fig. 42 in van Achterberg 1991); vein cu-a of fore wing vertical or nearly so, less inclivous than vein 3-CU1 (cf. figs 41 and 42 in van Achterberg 1991); length of ovipositor sheath 0.29–0.37× fore wing (fig. 42 in van Achterberg 1991). India, Singapore, Sri Lanka, Taiwan..... ..... ***T. maculata*** **van Achterberg, 1991**

b'. Surroundings of stemmaticum of female brownish yellow (Fig. 15); antenna dark brown basally and apically, near its apical 0.4 yellow; face punctate-coriaceous, except triangular area upper clypeus smooth; fore wing vein r as long as vein 3-SR (Fig. 18); vein cu-a of fore wing more or less inclivous than vein 3-CU1 (Fig. 18); length of ovipositor sheath 0.22–0.30× fore wing. Vietnam..... ***T. vietnamica*** **Long, sp. nov.**

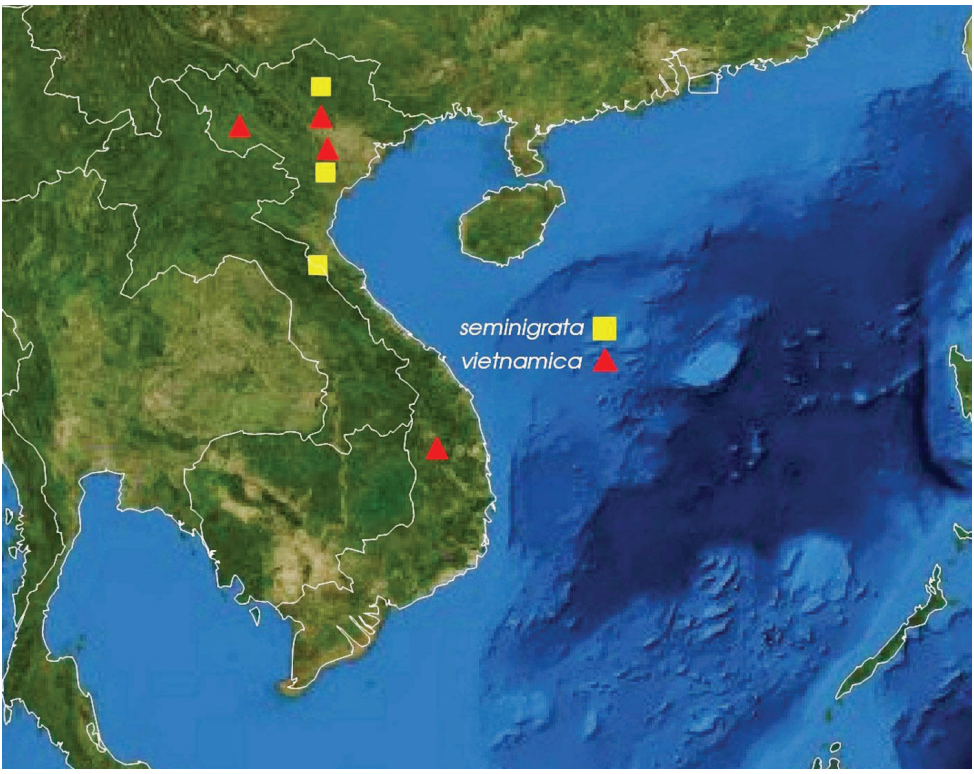

Figure 25. Distribution map of the two newly described species of *Trispinaria* in Vietnam.

Discussion

The limitations in our paper are that the type specimens of nine species described by van Achterberg (1991) and one species by Wang et al. (2003) could not be examined. However, checking the original descriptions of all the known species revealed that two new species from Vietnam could be distinguished from the other *Trispinaria* species by their bicoloured antennae, except for two paratype specimens of *T. vietnamica* sp. nov. which have their antennae dark brown entirely. Comparisons of *Trispinaria* species from Vietnam show that they are distinguishable from two similar species from the Oriental region, i.e., *T. seminigra* sp. nov. vs. *T. sannio* (Enderlein, 1920) from Indonesia and Singapore; and *T. vietnamica* sp. nov. vs. *T. maculata* van Achterberg, 1991 from India, Singapore, Sri Lanka, and Taiwan.

The colour patterns of wasps seem to be one of the characters for distinguishing between *Trispinaria* species, including the two new ones from Vietnam. Apart from the bicoloured antennae, most specimens of *T. seminigra* sp. nov. that possess a black mesopleuron dorsally and metanotum were collected by using sweep nets in the forest understorey and by the Malaise traps set under the canopy forest in the northern and north central parts of Vietnam (Fig. 25). On the contrary, all the specimens of *T. vietnamica* sp. nov. were widely collected in the more open habitats, i.e., by Malaise trap(s) set in fruit orchards and by using sweep nets above bushes. The colour

differences of the two new species discovered from Vietnam support van Achterberg's argument, that in the tropical rain forests most of the large braconid wasps possess a dark(er) colour pattern than those from outside the forest (van Achterberg 1991).

Acknowledgements

This research was funded by the Vietnam National Foundation for Science and Technology Development (NAFOSTED), grant No. 106-NN.05-2016.08. The authors wish to thank Mr Nguyen Hoang Vu, Indochina Institute of Biological and Environmental Sciences, Ha Noi, Vietnam, for his help in making the distribution map.

References

Harris RA (1979) A glossary of surface sculpturing. Occasional Papers in Entomology, California Department of Food and Agriculture 28: 1–33.

Long KD, Belokobylskij SA (2003) A preliminary list of the Braconidae (Hymenoptera) of Vietnam. Russian Entomological Journal 12(4): 385–398.

Long KD, van Achterberg C (2014) An additional list with new records of braconid wasps of the family Braconidae (Hymenoptera) from Vietnam. Tap chi Sinh hoc [Journal of Biology] 36(4): 397–415. https://doi.org/10.15625/0866-7160/v36n4.5979

Quicke DLJ (1986) Seven new genera and species of Braconinae (Hym., Braconidae) from Australasia and Indonesia. Entomologist's monthly Magazine 122: 9–29.

Quicke DLJ (1987) The Old World genera of the braconine wasps (Hymenoptera: Braconidae). Journal of Natural History 21: 43–157. https://doi.org/10.1080/00222938700770031

Quicke DLJ (1988) Higher classification, biogeography and biology of the Braconinae (Hymenoptera: Braconidae). In: VK Gupta (Ed.) Advances in Parasitic Hymenoptera Research: 117–138.

Quicke DLJ, van Achterberg C (1990) The type specimens of Enderlein's Braconinae (Hymenoptera: Braconidae) housed in Warsaw. Tijdschrift voor Entomologie 133: 251–264.

van Achterberg C (1991) Revision of the genus *Trispinaria* Quicke (Hymenoptera: Braconidae). Zoologische Verhandelingen Leiden 65(12): 181–198.

van Achterberg C (1993) Illustrated key to the subfamilies of the Braconidae (Hymenoptera: Ichneumonoidea). Zoologische Verhandelingen Leiden 283: 1–189.

van Achterberg C (1984) Revision of the genera of Braconini with first and second metasomal tergites immovably joined (Hymenoptera, Braconidae, Braconinae). Tijdschrift voor Entomologie 127: 137–164.

Wang Y-P, Chen X-X, He J-H (2003) First Chinese record of the genus *Trispinaria* Quicke (Hymenoptera, Braconidae, Braconinae) and a description of a new species. Acta Zootaxonomica Sinica 28(2): 333–335.

Yu DSK, van Achterberg C, Horstmann K (2005) World Ichneumonoidea 2004. Taxonomy, Biology, Morphology and Distribution. CD/DVD. Taxapad, Vancouver.

Yu DSK, van Achterberg C, Horstmann K (2012) Taxapad 2012, Ichneumonoidea 2011. Ottawa, Ontario. [database on flash-drive]

ZooKeys 996: 121–145 (2020)
doi: 10.3897/zookeys.996.53958
https://zookeys.pensoft.net

RESEARCH ARTICLE

A peer-reviewed open-access journal
ZooKeys
Launched to accelerate biodiversity research

Phyllocnistis furcata sp. nov.: a new species of leaf-miner associated with *Baccharis* (Asteraceae) from Southern Peru (Lepidoptera, Gracillariidae)

José Cerdeña[1,2], Jackie Farfán[1,2], Héctor A. Vargas[3], Rosângela Brito[4,5], Gislene L. Gonçalves[3], Ana Lazo[6], Gilson R. P. Moreira[5]

1 *PPG Biologia Animal, Departamento de Zoologia, Instituto de Biociências, Universidade Federal do Rio Grande do Sul, Av. Bento Gonçalves, 9500, Porto Alegre, RS 91501-970, Brazil* **2** *Universidad Nacional de San Agustín de Arequipa, Museo de Historia Natural, Av. Alcides Carrión s/n, Arequipa, Peru* **3** *Departamento de Recursos Ambientales, Facultad de Ciencias Agronómicas, Universidad de Tarapacá, Casilla 6-D, Arica, Chile* **4** *Embrapa Cerrados, Planaltina, Distrito Federal, Brazil* **5** *Departamento de Zoologia, Instituto de Biociências, Universidade Federal do Rio Grande do Sul, Av. Bento Gonçalves 9500, Porto Alegre RS, 91501-970, Brazil* **6** *Universidad Nacional de San Agustín de Arequipa, Laboratorio Fisiologia Animal, Av. Alcides Carrión s/n, Arequipa, Peru*

Corresponding author: José Cerdeña (cerdenajoseal@yahoo.es)

Academic editor: E. van Nieukerken | Received 6 May 2020 | Accepted 24 August 2020 | Published 24 November 2020

http://zoobank.org/F1EA1AA7-2A01-4DBF-A03B-49A1131704D4

Citation: Cerdeña J, Farfán J, Vargas HA, Brito R, Gonçalves GL, Lazo A, Moreira GRP (2020) *Phyllocnistis furcata* sp. nov.: a new species of leaf-miner associated with *Baccharis* (Asteraceae) from Southern Peru (Lepidoptera, Gracillariidae). ZooKeys 996: 121–145. https://doi.org/10.3897/zookeys.996.53958

Abstract

The southwestern Andes of Peru harbors a hidden taxonomic diversity of Lepidoptera. Here a new leaf-mining species of Gracillariidae (Lepidoptera) is described, *Phyllocnistis furcata* Vargas & Cerdeña, **sp. nov.,** from a dry Andean valley of southern Peru, at 2400 m above sea level. The morphological aspects of adults (male and female) and the immature stages associated with *Baccharis alnifolia* Meyen & Walp. (Asteraceae) are given, under optical microscopy and scanning electron microscopy. DNA barcodes show that its nearest neighbor is the Atlantic Forest species *Phyllocnistis ourea* Brito & Moreira, 2017 that feeds on *Baccharis anomala* DC. The importance of morphological characters from immature stages for diagnosis among congeneric species is also discussed. *Phyllocnistis furcata* represents the fourth species of *Phyllocnistis* Zeller for Peru, and first record from the south of Peru for the genus.

Keywords

Andes, Arequipa, barcoding, immature stages, Phyllocnistinae

Introduction

The Andes region of Peru contains hotspots of biodiversity for plants and animals (Myers et al. 2000). It includes global record highs of species richness and endemism rates for many taxa of Lepidoptera, particularly along the eastern slopes of the Andes (Lamas 2003; Pyrcz 2004; Hall 2005; Ignatov et al. 2011; Willmott et al. 2011; Pyrcz et al. 2014; Sublett et al. 2019). On the other hand, the level of knowledge of the lepidopteran fauna on the southwestern slopes of the Peruvian Andes is poor, based on a small number of studies of butterflies (Lamas 1977; Cerdeña et al. 2014; Farfán 2018; Farfán et al. 2020b), and with recent records of moths (Cerdeña et al. 2019; Farfán et al. 2020a), including the first record of a Gracillariidae species for this region (Davis et al. 2020).

Gracillariidae represents one of the most diverse families of micromoths with 1995 recognized species distributed in more than 100 genera (van Nieukerken et al. 2011; De Prins and De Prins 2020). Larvae are predominantly leaf-miners although some species mine stems or fruits (Guillén et al. 2001), and others bore into flowers (Vargas and Landry 2005), fruits (Hu et al. 2011) or stems (Davis et al. 1991), and may also be leaf-rollers or gall inducers (Hanson et al. 2014; Kawakita and Kato 2016; Vargas-Ortiz et al. 2019). In the Neotropics, more intense taxonomic work has been performed in the last decade, resulting in 28 newly described species (De Prins and De Prins 2020). Despite this effort of documenting the fauna, currently numbering 204 Neotropical species, there are gaps in information for gracillariids in several biodiversity hotspots, such as the Andes. Particularly in Peru, currently only 28 species of gracillariids are known (Kawakita et al. 2019; Davis et al. 2020; De Prins and De Prins 2020). From these, one is a non-native species introduced in the coastal area (Castillo and Cornejo 1996), two species were recently reported from southwestern Peru (Vargas 2010; Davis et al. 2020), five were described from northern Peru (Kawakita et al. 2019), and 19 species were described in the early last century by Edward Meyrick (Meyrick 1915, 1921) from material collected by Herbert Simpson Parish from the central Peruvian coast (Lima), central Andes (Matucana, Oroya, Huancayo, Jauja), and northeastern Peruvian Amazon (Iquitos, Yurimaguas) during two collecting trips to the tropics in 1914 and 1920 (Alexander 1916, 1921). These species in particular remain only known from the type specimens, some of which have deteriorated (Brito et al. 2017; De Prins et al. 2019).

Phyllocnistis Zeller, 1848 is a genus of Gracillariidae with 112 named species distributed in all biogeographic regions except Antarctica (Brito et al. 2016, 2017; Fochezato et al. 2018; Kirichenko et al. 2018; De Prins and De Prins 2020). A total of 28 species has been reported for the Neotropical region (De Prins et al. 2019), with 16 species recorded in the last ten years (Kawahara et al. 2009; Davis and Wagner 2011; Brito et al. 2012, 2017, 2019; Fochezato et al. 2018). However, only three species were registered from Peru: *Phyllocnistis sciophanta* Meyrick, 1915, *P. sexangula* Meyrick, 1915, and *P. citrella* Stainton, 1856; the first two species, collected from the center of Peru (Department of Lima) more than 100 years ago, remain with their host plant and immature stages unknown (Brito et al. 2017; De Prins et al. 2019). The third

species, with a worldwide distribution, known to be a pest in citrus fruits, is a native from Asia (Castillo and Cornejo 1996; De Prins et al. 2019). This lack of data is mainly due to two conditions that prevailed for a long time, not only in Peru but also in other countries of the Neotropical region (Brito et al. 2016): low collection intensity and scarce taxonomy activity on Gracillariidae and Microlepidoptera in general.

The hypermetamorphic development of the larvae of *Phyllocnistis* typically comprises two endophytic forms (e.g., Fochezato et al. 2018; Brito et al. 2019). The early, sap-feeding larva actively mines specific host tissues; later, the spinning larva does not feed and has most of the buccal apparatus atrophied, but has a functional spinneret that is used to expel silk to construct the pupal cocoon.

A variety of host plants are associated with *Phyllocnistis* in the Neotropical region, including 15 genera from 13 different plant families (Brito et al. 2017). Three species are known to be associated with the genus *Baccharis* (Asteraceae): *P. baccharidis* Hering, 1958, *P. ourea* Brito & Moreira, 2017, and an undescribed species associated with *Baccharis trimera* (Brito et al. 2017), the first from Argentina and other two from Brazil. This Neotropical plant genus is characterized by the tufted indumentum of leaves and stems, and by the unisexual florets generally in separate specimens (Müller 2006), currently comprising 440 species (Heiden et al. 2019).

Recently, as part of an ongoing study on the diversity of microlepidopterans in the Andes in southern Peru, we found a leaf-mining species of *Phyllocnistis* associated with *Baccharis*. Comparison at both morphological and molecular levels showed that it does not conform to any known *Phyllocnistis* species. The morphological description of adults (male and female) and immature stages of this new species is herein given. We also present a preliminary analysis of mitochondrial (COI) DNA sequences including congeneric Neotropical species.

Materials and methods

Larvae and pupae found in mines on leaves of *Baccharis alnifolia* Meyen & Walp. (Asteraceae) in the locality of Characato (16°27'S, 71°28'W), 2400 m, Characato Municipality, Arequipa Department, Peru, were collected and reared in plastic cups, at constant abiotic conditions (20 ± 2 °C, 13:11 h photoperiod) in the laboratory of Area de Entomología, Museo de Historia Natural, Universidad Nacional de San Agustin, Arequipa city, Peru, during September 2018, April 2019, and November 2019.

In total, 58 specimens have been studied: 23 adults, 17 larvae, 20 pupae. Adults that emerged from the mines were pinned and dried, and immature stages were fixed with Dietrich´s fluid and preserved in 70% ethanol. Genitalia were cleared by heating in hot 10% KOH for ~ 15 minutes. They were subsequently stained with Chlorazol black and Eosin, and then slide-mounted with Euparal.

Morphological observations were performed with the aid of a Zeiss Stemi305, and structures selected to be illustrated were photographed with a Nikon SMZ25 stereomicroscope. Vectorized line drawings were then made with the software CorelDraw X4, using

the corresponding digitalized images as a guide. The terminology used for descriptions of adult wing pattern, genitalia and immature stages follows Brito et al. (2017, 2019).

For scanning electron microscope analyses, specimens were dehydrated in a Baltec CPD030 critical-point dryer, mounted with double-sided tape on metal stubs, and coated with gold in a Bal-tec SCD050 sputter coater. They were then examined and photographed in a JEOL JSM6060 scanning electron microscope at the Centro de Microscopia Eletrônica (CME) of Federal University of Rio Grande do Sul (UFRGS).

For plant anatomical descriptions, field-collected leaf portions (approx. 0.3 cm^2) of *B. alnifolia* containing mines of *P. furcata* were fixed in FAA (37% formaldehyde, glacial acetic acid, and 50% ethanol, 1:1:18, v/v) for 24 h. They were then dehydrated in a series of ethanol (40%, 70%, 90%, 96%); embedded in paraffin and sectioned transversely (7 μm) on a rotary microtome. The sections were adhered to a microscope slide glass, then observed and photographed without staining, by using a Nikon SMZ25 stereomicroscope.

Total genomic DNA was extracted from larval tissue (last sap-feeding instar) of five specimens (H86–H90), using the CTAB method (Doyle and Doyle 1987), to support the hypothesis that the morphologically distinct specimens studied confirm a new *Phyllocnistis* species, and explore the phylogenetic placement among Neotropical congeners. We amplified part of the mitochondrial gene cytochrome oxidase I (COI – 639 bp) using primers and conditions described by Folmer et al. (1994). PCR products were purified using Exonuclease I (GE Healthcare Inc.) and Shrimp Alkaline Phosphatase (SAP), sequenced with forward and reverse primers using a BigDye kit, and analyzed on an ABI3730XL (Applied Biosystems Inc.). Chromatograms obtained from the automatic sequencer were read and sequences were assembled using the software CodonCode Aligner (CodonCode Corporation). The new sequences obtained in this study are publicly available in GenBank and BOLD (DS-GRANEO) databases (Table 1). To explore the phylogenetic position of the new taxon and its specific classification we combined our COI data with a published dataset of ten species and 13 undescribed lineages of Neotropical *Phyllocnistis* (Davis and Wagner 2011; Brito et al. 2012, 2017, 2019; Lees et al. 2013) (Table 1). This includes *P. ourea* that feeds on *Baccharis anomala*, and *Phyllocnistis* sp. 12 (Brito et al. 2017) associated to *Baccharis trimera* (Less) DC. *Angelabella tecomae* Vargas & Parra, 2005 (Oecophyllembiinae) and *Marmara arbutiella* Busck, [1904] (Marmarinae) were used as outgroups as they represent subfamilies closely related to Phyllocnistinae (Kawahara et al. 2017). A distance tree based on Neighbor-joining (NJ) method was generated from 31 nucleotide sequences using Kimura 2-parameters (K2P) model in MEGA X (Kumar et al. 2018). The evolutionary history was inferred by using the Maximum Parsimony (MP) analysis using the Tree-Bisection-Regrafting (TBR) algorithm with search level 1, with initial trees obtained by random addition of sequences (10 replicates) also in MEGA X. A Maximum Likelihood (ML) analysis was also performed, with the substitution model GTR+G+I according to the Akaike Information Criterion (AIC) estimated by JMODELTEST (Posada 2008), using PHYML 3.0 (Guindon et al. 2010). Initial trees for the heuristic search were obtained automati-

Table 1. Specimens used for molecular analyses of *Phyllocnistis furcata* sp. nov. Both the Sample ID and Process ID codes are unique identifiers linking the record in the BOLD database and the voucher specimen from which the sequence is derived. The asterisk(s) indicates those specimens associated with the *Baccharis* as host plant: **B. alnifolia*, ***B. anomala*, ****B. trimera*.

Species	Sample ID	Process ID	GenBank accession	Reference
Phyllocnistis furcata sp. nov.*	H86	MISA051-20	MT832361	This study
Phyllocnistis furcata sp. nov.*	H87	MISA052-20	MT832362	This study
Phyllocnistis furcata sp. nov.*	H88	MISA053-20	MT832363	This study
Phyllocnistis furcata sp. nov.*	H89	MISA054-20	MT832364	This study
Phyllocnistis furcata sp. nov.*	H90	MISA055-20	MT832365	This study
Phyllocnistis hemera	LMCI 292-25C	MISA019-17	MG264519	Fochezato et al. 2018
Phyllocnistis kawakitai	AK0105	GRANO105-11	KF460801	Lees et al. 2014
Phyllocnistis norak	CLV1381	LNOUC318-10	JN276191	Lees et al. 2014
Phyllocnistis ohshimai	CLV1367	LNOUC304-10	JN276189	Lees et al. 2014
*Phyllocnistis ourea***	LMCI 297-15B	MISA013-16	KY006927	Brito et al. 2016
Phyllocnistis petronellii	IO0536	LEPPC2394-16	KY682706	Brito et al. 2017
Phyllocnistis perseafolia	DDAV-D555	RDOPO393-10	HM382096	Davis and Wagner 2011
Phyllocnistis phoebus	LMCI 263-9	MISA014-16	KY006929	Brito et al. 2016
Phyllocnistis selene	LMCI 263-22	MISA015-16	KY006928	Brito et al. 2016
Phyllocnistis tethys	LMCI 174-55-1	GBMIN15477-13	JX272049	Brito et al. 2012
Phyllocnistis sp. 2	AK0198	LNOUD2290-12	KF460914	Lees et al. 2014
Phyllocnistis sp. 3	AK0210	LNOUD2302-12	KF460586	Lees et al. 2014
Phyllocnistis sp. 4	AYK-FG10-135	LNOUC1229-11	KF460667	Lees et al. 2014
Phyllocnistis sp. 5	CLV1284	LNOUD1191-12	KF460613	Lees et al. 2014
Phyllocnistis sp. 7	CLV1368	LNOUC305-10	JN276190	Lees et al. 2014
Phyllocnistis sp. 9	CLV2993	LNOUD336-11	KF460927	Lees et al. 2014
Phyllocnistis sp. 10	CLV3313	LNOUD489-11	KF460904	Lees et al. 2014
Phyllocnistis sp. 11	CLV4347	LNOUD776-12	KF460865	Lees et al. 2014
Phyllocnistis sp. 12***	CLV5900 and CLV5901	GRPAL1220-13 and GRPAL1221-13	KY682713 and KF460659	Lees et al. 2014
Phyllocnistis sp. 13	CLV5902	GRPAL1222-13	KY682713	Lees et al. 2014
Phyllocnistis sp. 15	LEAFMINE2015-0006	LEPPC1378-15	KY682712	Brito et al. 2017
Phyllocnistis sp. 16	LEAFMINE2015-0008	LEPPC1380-15	KY682711	Brito et al. 2017
Phyllocnistis sp. 17	LEAFMINE2015-0010	LEPPC1382-15	KY682704	Brito et al. 2017

cally with BioNJ algorithm to a matrix of pairwise distances. Monophyly-confidence limits of all analysis were assessed with the bootstrap (BS) method after 1000 bootstrap iterations. Sequence divergences were quantified using K2P model for (i) the genus *Phyllocnistis* (using 35 named species deposited in BOLD; Table 1), (ii) the Neotropical *Phyllocnistis* (10 described + 13 undescribed species, Table 1), and (iii) the new species vs. *Baccharis*-feeding lineages.

Abbreviations for the museum collections and institutions from which specimens were examined are:

LMCI Laboratório de Morfologia e Comportamento de Insetos, Universidade Federal do Rio Grande do Sul, Porto Alegre, Rio Grande do Sul, Brazil.

MUSA Museo de Historia Natural, Universidad Nacional de San Agustín de Arequipa, Arequipa, Perú.

MUSM Museo de Historia Natural, Universidad Nacional Mayor San Marcos, Lima, Peru.

Results

***Phyllocnistis furcata* Vargas & Cerdeña, sp. nov.**
http://zoobank.org/F54378EF-7ADF-425D-9FDD-B8F2223D1381
Figs 1–7

Type locality. Peru, Arequipa, Characato [16°27'S, 71°28'W], 2400 m.

Specimens examined. *Holotype*: Peru • ♂; Arequipa, Characato; 16°27'S, 71°28'W; 2400 m a.s.l.; VIII–IX.2018; J. Cerdeña, H. Vargas & J. Farfan leg.; reared from pupae collected on *Baccharis alnifolia* (Asteraceae); MUSM. ***Paratypes***: same data as for holotype • 1 ♂, 1 ♀; MUSM; • 1 ♂, 1 ♀; MUSA_ENT 015142, 015143; • 2 ♂, 2 ♀; LMCI.

Other material. Adults, pinned and dried, 5 ♂, 8 ♀, same data as for holotype, MUSA_ENT 015144, 015145, 015146, 015147, 015148, 015149, 015150, 015151, 015152, 015153, 015154, 015155, 015156. Genitalia preparations (MUSA_Gent_015142, 015143, 015146, 015147, 015148), mounted on slides, with the same collection data. Immature stages (11 sap-feeding larvae, 06 spinning larvae, 20 pupae) preserved in 70% ethanol, with the same collection data, but with dates VIII–IX.2018, IV.2019 or XI.2019, MUSA.

Diagnosis. Adults of *P. furcata* can be distinguished from all other known species of Neotropical *Phyllocnistis* in the forewing pattern by a combination of the following characters: ground color silver, four distinct transverse fasciae; transverse fasciae 1 reduced to the costal margin and mesally fused to longitudinal fascia, both not connected to transverse fascia 2; transverse fascia 3 almost reaching the middle portion of the wing. In the male abdomen, by the presence of two pairs of coremata on abdominal segment VIII, one pair consisting of wide rounded flat scales, a character not found in other Neotropical *Phyllocnistis*. In the female genitalia, by presenting a remarkable forked-shaped signum with four elongated spines on the distal margin. This species is similar to *P. wygodzinskyi* Hering, 1958 and *P. sexangula* Meyrick, 1915, in having similar patterns of fasciae. However, *P. wygodzinskyi* has a large black blotch at the inner border of the longitudinal fascia, and *P. sexangula* presents a small blotch close to the inner border of the longitudinal fascia, while *P. furcata* has no additional mark on the forewing.

Adult. (Figs 1, 2). **Description. Male:** Forewing length 3.10–3.33 mm (N = 5). Head: Vestiture silvery pale brown, completely covered with smooth, broad, scales slightly overlapping anterior margin of eyes (Fig. 1B). Antennae light brown dorsally becoming dark towards apex and silvery white ventrally, approximately equal to length of forewing (Fig. 1A, F). Labial palpus slender, ~ 0.4 mm in length, covered with light grey scales (Fig. 1F). Proboscis without scales, slightly longer than labial palpus (Fig. 1F). Thorax: Forewing ground color silvery white; with light orange longitudinal (lf) and transverse (tf) fasciae (Fig. 1A, E); if bordered by dark brown scales, extending 2/3 length of wing from base of costa, and connected with tf1 apically; tf1 not reach the inner margin, restricted between the costal margin and lf; tf2 separate from tf1,

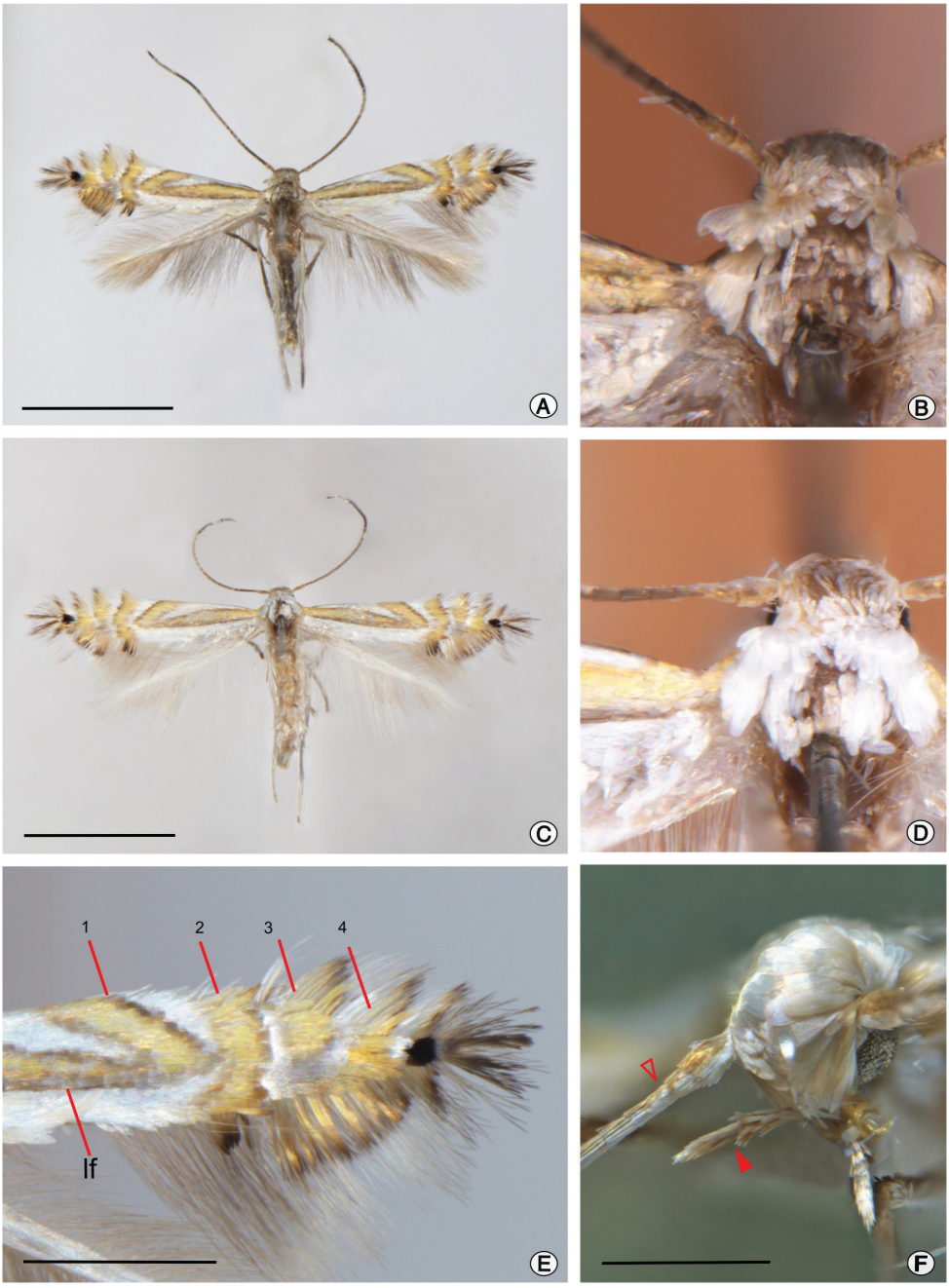

Figure 1. *Phyllocnistis furcata* sp. nov. adult morphology **A, B** holotype of *P. furcata*, male, with head in detail, dorsal view (MUSM) **C, D** paratype of *P. furcata*, female, with head in detail, dorsal (MUSA_ENT 015143) **E** detail of right forewing with terminologies adopted, lf: longitudinal fascia; tf (1–4) transverse fascia(e) **F** lateral view of a male head with labial palpus (indicated by closed arrow head) and antenna (indicated by open arrow head). Scale bars: 2 mm (**A, C**), 1 mm (**E**), 0.4 mm (**F**).

lightly convex, crossing the wing entirely; tf3 separate from tf2, but not reach the inner margin; tf4 separate from tf3, crossing the wing entirely. Apex of forewing with a well-marked black spot. Costal strigulae, light orange, emerge from the base of transverse fasciae. Apical strigulae, dark brown, emerge from black spot. Inner marginal fringe varies from orange to dark brown. Hindwings light pale brown gray, with long light brown fringes. Legs light gray except dark brown over dorsal surface of femur, tibia, and tarsus of foreleg. Abdomen length ~2.0 mm, dark grey covered with silvery pale brown scales, two pairs of coremata present laterally on segment VIII (Fig. 2A), one pair consisting of a set of flat and long scales and the other pair consisting of wide rounded flat scales (Fig. 2D). Whether the wide rounded flat scales function as coremata by themselves or appendages of the long ones remains unknown.

***Male genitalia*:** Uncus absent. Tegumen membranous, approximately equal to length of the valva, with spines arranged laterally from the base to the medial region. Saccus V-shaped, well developed, ~0.8 × the size of valva. Valvae digitiform and slightly convergent from the base to the apex, apex with small spine, setae randomly arranged along the valva getting shorter in the distal part (Fig. 2C). Phallus slender and with a slightly convex apex, weakly sclerotized, wrinkled cylinder, lightly longer than valva; cornuti absent (Fig. 2B).

Female: Forewing length 3.30–3.41 mm (N = 5). Color and pattern very similar to that of male, but head vestiture with light silvery scales (Fig. 1D). Hindwings light silvery gray with long silvery fringes and abdomen color light brown covered with silvery scales (Fig. 1C). VII abdominal sternum trapezoid, anterior margin thickened.

***Female genitalia*:** Papillae anales slightly sclerotized, covered with hair-like setae. Posterior apophyses ~2.4 × length of anterior apophyses (Fig. 2F). Ostium bursae posterior to sternum 7. Ductus bursae completely membranous, slender, elongate, over 6.0× length of posterior apophyses (Fig. 2E). Corpus bursae slightly elongated, ~0.3 × length of ductus bursae, mainly membranous with three signa; a prominent fork-shaped signum on basis, resembling a garden fork, that occupies ~0.5 × length of corpus bursae with four elongated spines distally projected, and two small signa irregular in shape with minute dark spots on distal portion and also scattered sclerotized pellets on the bursa wall (Fig. 2G). Ductus seminalis membranous, narrow, inserted in base of corpus bursae.

Immature stages. The number of larval instars was not determined, with three sap-feeding instars suspected and one spinning instar.

Egg. (Fig. 7C). Flat, slightly ellipsoid; ~0.4 × 0.25 mm; chorion translucent; aeropyles, micropyles, and external ornamentation not observed.

Sap-feeding larva. (Figs 3A, 4, 7E). Body flattened dorsoventrally, yellowish translucent (Fig. 7E). Length of largest larva examined ~ 4.5 mm. Head brown, prognathous, setae absent (Fig. 4A–C). Two pairs of small stemmata located in the lateral region (Fig. 4F). Antenna 3-segmented, with four sensilla, two stout ones located on the second segment and two on the distal segment, one spiniform and other stout (Fig. 4F). Labrum slightly bilobed with small epipharyngeal spines, which are of greater size in the lateral region (Fig. 4D). Labium slightly bilobed with small spines near distal margin (Fig. 4E). Spinneret present, in the form of a transverse slit. Maxillary

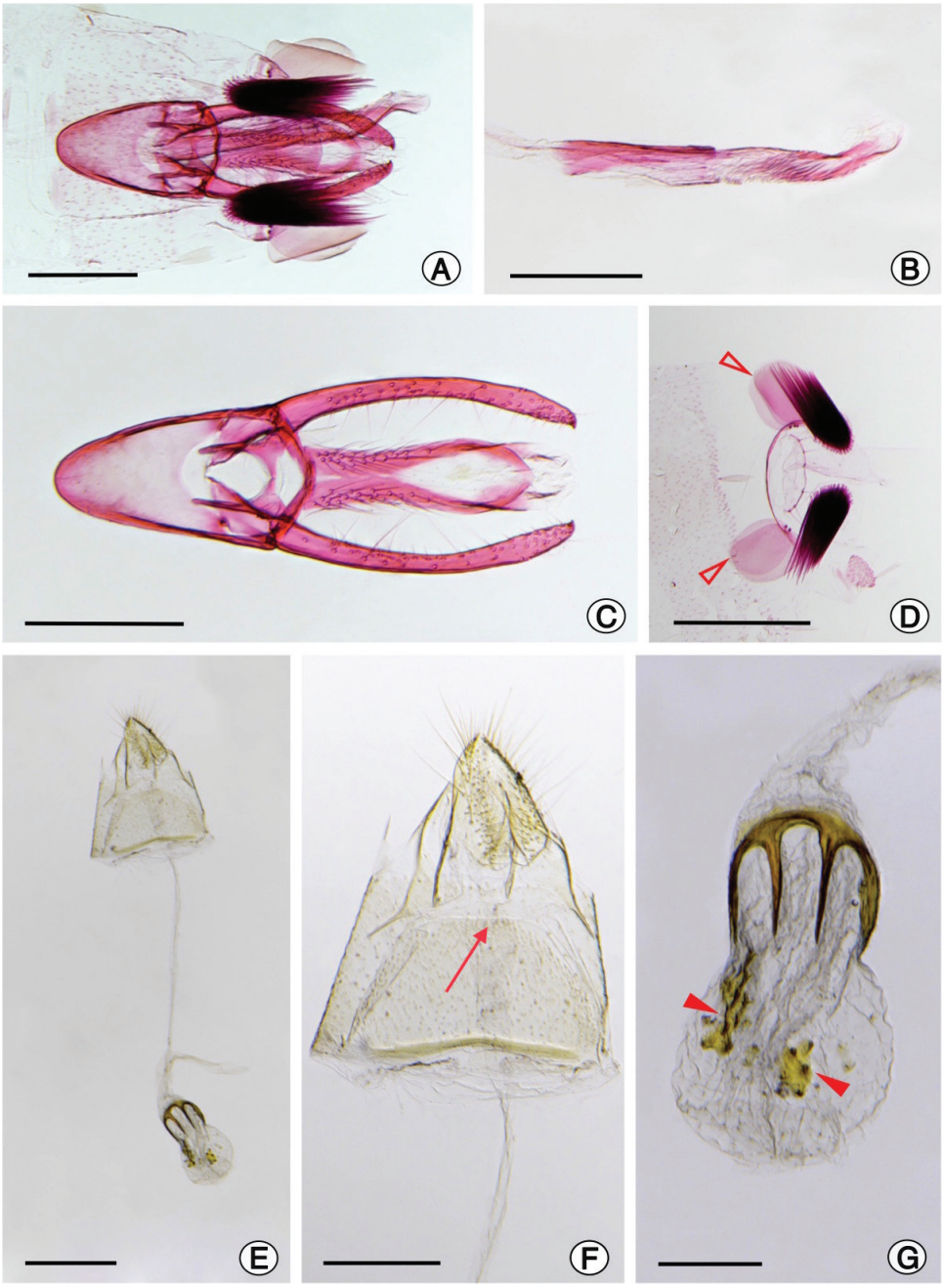

Figure 2. *Phyllocnistis furcata* sp. nov. genital morphology under light microscopy **A** male genital segments, ventral view **B** phallus, lateral **C** male genitalia with phallus removed, ventral **D** coremata (open arrows indicate wide rounded flat scales) **E** female genitalia, ventral **F** female last abdominal segments, in detail (seta points to ostium bursae) **G** corpus bursae in detail (closed arrows indicate two small signa with minute dark spots). Scale bars: 0.2 mm (**A–C, F, G**), 0.3 mm (**D**), 0.4 mm (**E**). Genitalia slides: MUSA_Gent_015142 (A), MUSA_Gent_015146 (**B–D**), MUSA_Gent_015148 (**E–G**).

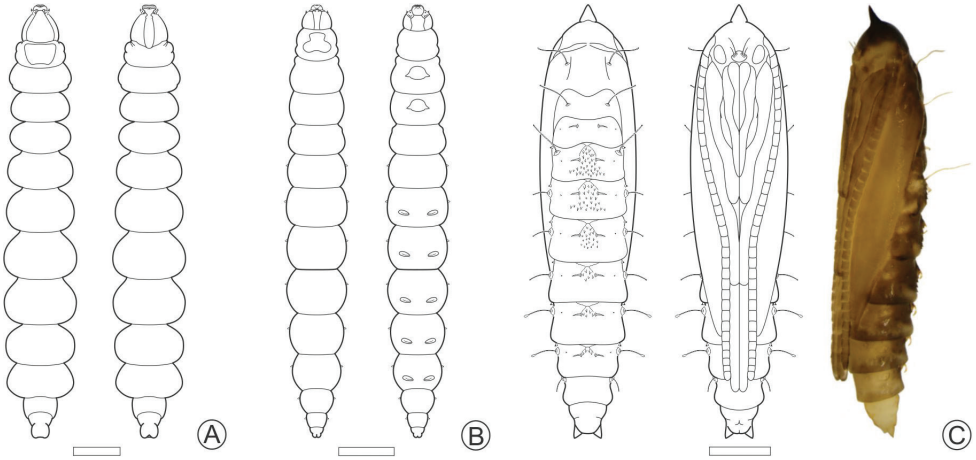

Figure 3. Larval and pupal morphology of *P. furcata* sp. nov. under light microscopy **A** sap-feeding larva, dorsal and ventral view **B** spinning larva, dorsal and ventral **C** pupa, dorsal, ventral, and lateral, respectively. Scale bars: 500 μm.

and labial palpi absent. Legs and prolegs absent (Fig. 3A). Thorax with prothoracic light-brown dorsal shield in the form of a trapezoid (Figs 3A, 4G). Thoracic and abdominal segments without setae. Circular spiracle laterally on segments T1 and A1–A8 (Fig. 4H). Caudal abdominal segment slightly bilobed distally (Fig. 4I).

Spinning larva. (Figs 3B, 5, 7F). Body yellowish, cylindrical, wider along the thorax and first abdominal segments, narrowing towards the posterior region, covered with microtrichia (Figs 3B, 7F). Approx. 5.00 mm maximum length. Head capsule weakly sclerotized, with anteriorly pronounced trophic lobe (Figs 3B, 5A–C). Stemmata absent. Antenna short, three-segmented, with five sensilla (Fig. 5F). Clypeal region with three pairs of setae (Fig. 5D). Maxillary palpi, represented by a pair of short sensilla. Spinneret short (Fig. 5E). Thorax with slightly pronounced prothoracic dorsal shield (Fig. 3B). Legs and prolegs absent. A single ambulatory callus ventrally on center of meso- and metathorax (Figs 3B, 5G). One pair of smaller ambulatory calli ventrally on A3–A7 (Figs 3B, 5I, J). One pair of lateral campaniform sensilla on A2–A9 (Fig. 5K). Caudal abdominal segment slightly bilobed distally (Fig. 5L).

Pupa. (Figs 3C, 6, 7I). 1 Coloration changing from light yellowish during early stage of pupation to yellowish brown later in development (Fig. 7I). Approx. 5.00 mm maximum length. Cocoon-cutter triangular, concave dorsally (Fig. 6A–C) with serrated lateral edges (Fig. 6D). Frons with two pairs of large frontal setae close labrum (Fig. 6E). Labrum ellipsoidal (Fig. 6B). Antenna long and straight, extending to abdominal segment A7; forewing extending to A6 (Fig. 3C); prothoracic, mesothoracic and metathoracic legs reaching segments A3, A5 and A8, respectively (Fig. 3C). A pair of long setae, latero-dorsally on meso-, metathorax and A2 (Figs 3C, 6F). Lateral setae on abdominal segments A3–A7 (Fig. 3C); those of meso-, metathorax, A2–5 with dentate apex (Fig. 6I), those of A6–7 with clavate apex (Fig. 6H). A8 segment with a

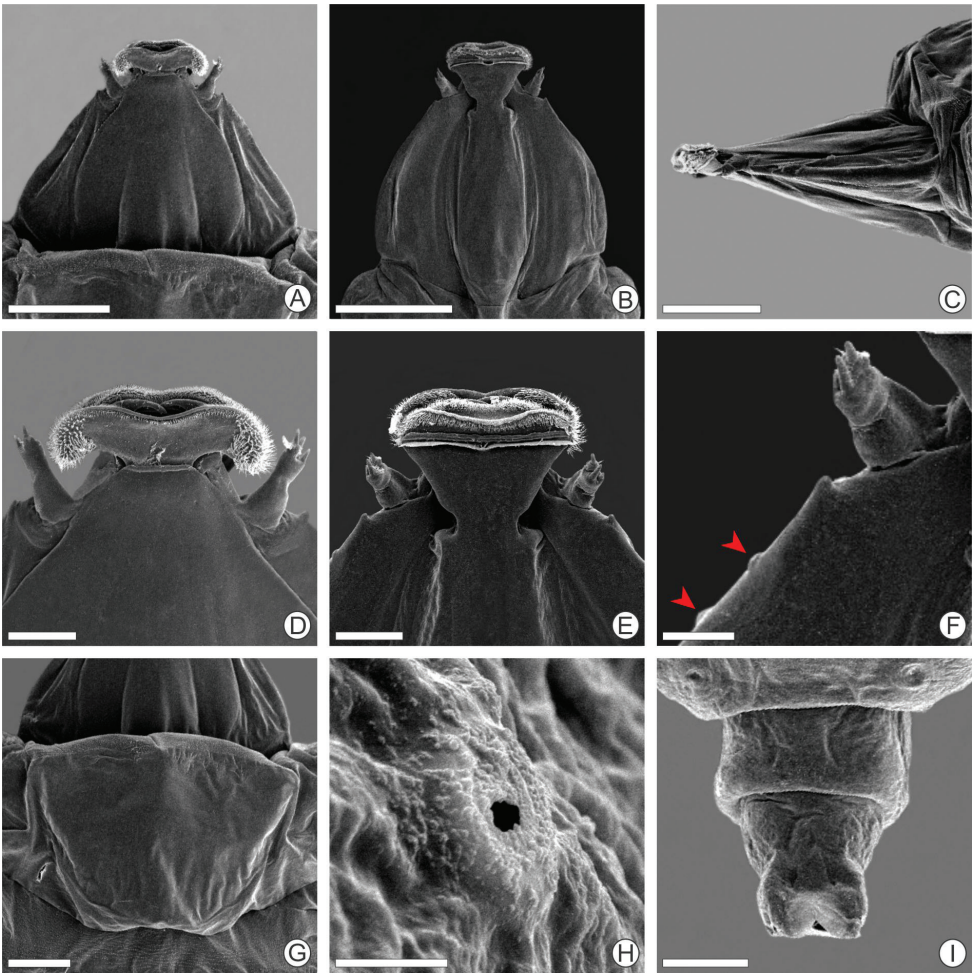

Figure 4. Scanning electron micrographs of *P. furcata* sp. nov. sap-feeding larva **A–C** head under dorsal, ventral, and lateral views **D** labrum, dorsal **E** labium, ventral **F** antenna and stemmata (indicated by arrow), ventral **G** prothoracic shield, dorsal **H** abdominal spiracle, lateral **I** last abdominal segment, ventral. Scale bars: 200 μm (**A, B**), 150 μm (**C**), 50 μm (**D, E**), 25 μm (**F**), 100 μm (**G, I**), 5 μm (**H**).

pair of acute setae latero-dorsally directed posteriorly (Fig 6K). One pair of conspicuous spiracles up to A2–A7 (Fig. 6J). Dorsum of A1–A7 with a pair of curved, large spines, projecting laterally, from A2 to A7 with a variable sized patch of smaller spines projecting posteriorly between them (Fig. 6G). One pair of small lateral spines on the pleural region from A1 to A7 (Fig 6H). Pleural region of body and last four abdominal segments covered by microtrichia (Fig. 6K, L). A pair of slightly divergent acute processes from caudal apex on last abdominal segment (Fig. 6K, L).

Etymology. The species name *furcata*, from the Latin adjective *furcatus*, *furca* meaning fork, alludes to the large and prominent form of the signum present in the female genitalia, resembling a garden fork.

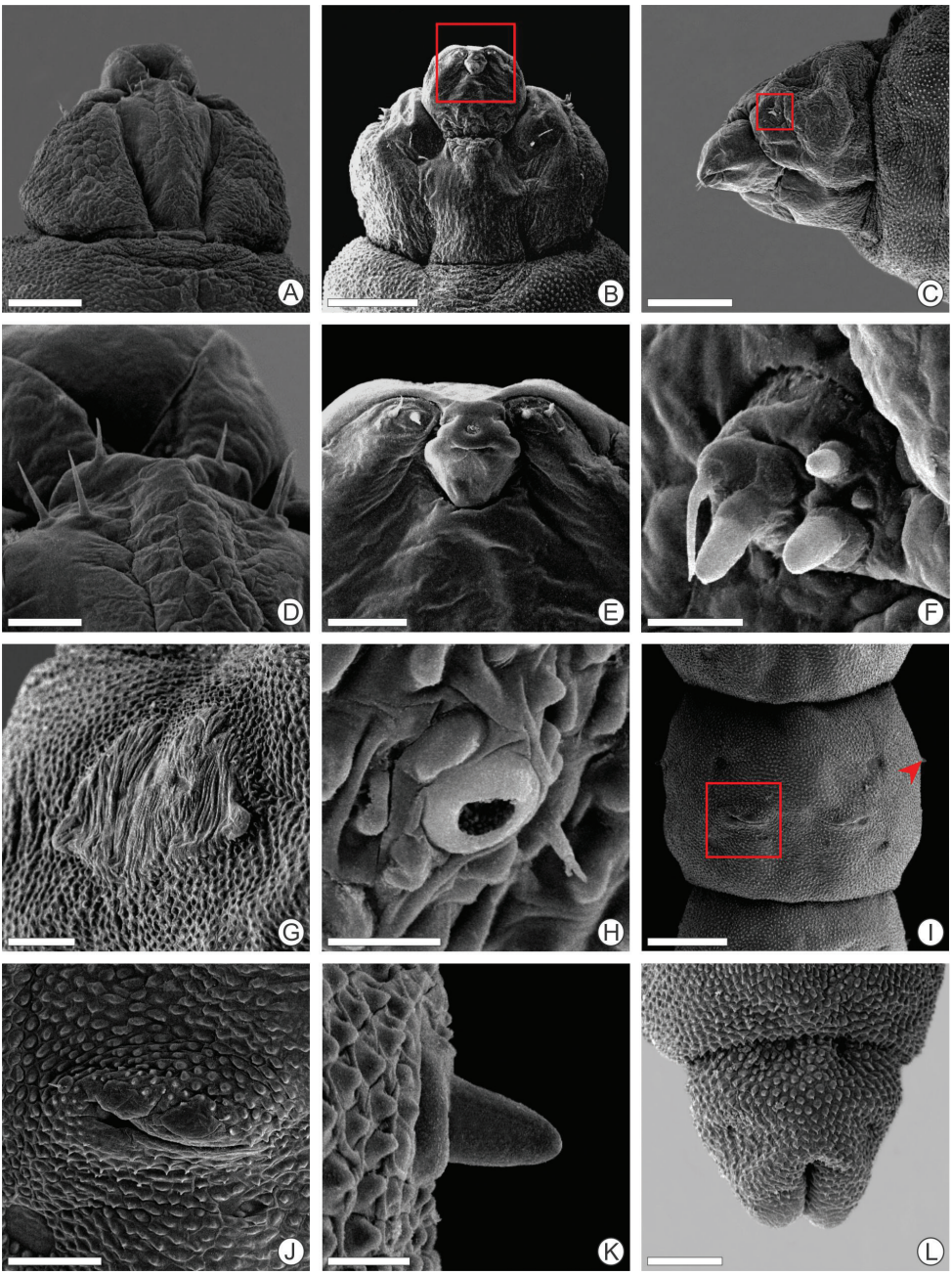

Figure 5. Scanning electron micrographs of *P. furcata* sp. nov. spinning larva **A–C** head under dorsal, ventral, and lateral views respectively **D** detail of trophic lobe and clypeal region, dorsal **E** spinneret, (indicated by square in B) **F** antenna, lateral (indicated by square in C) **G** mesothoracic ambulatory callus in detail, ventral **H** abdominal spiracle, lateral **I** abdominal segment A6, ventral (campaniform sensilla indicated by arrow) **J** abdominal ambulatory callus in detail, ventral (indicated by square in I) **K** campaniform sensilla in detail, ventral (indicated by arrow in I) **L** last abdominal segment, dorsal. Scale bars: 100 μm (**A, B**), 150 μm (**C, I**), 25 μm (**D, E**), 10 μm (**F, H, K**), 50 μm (**G, L**), 40 μm (**J**).

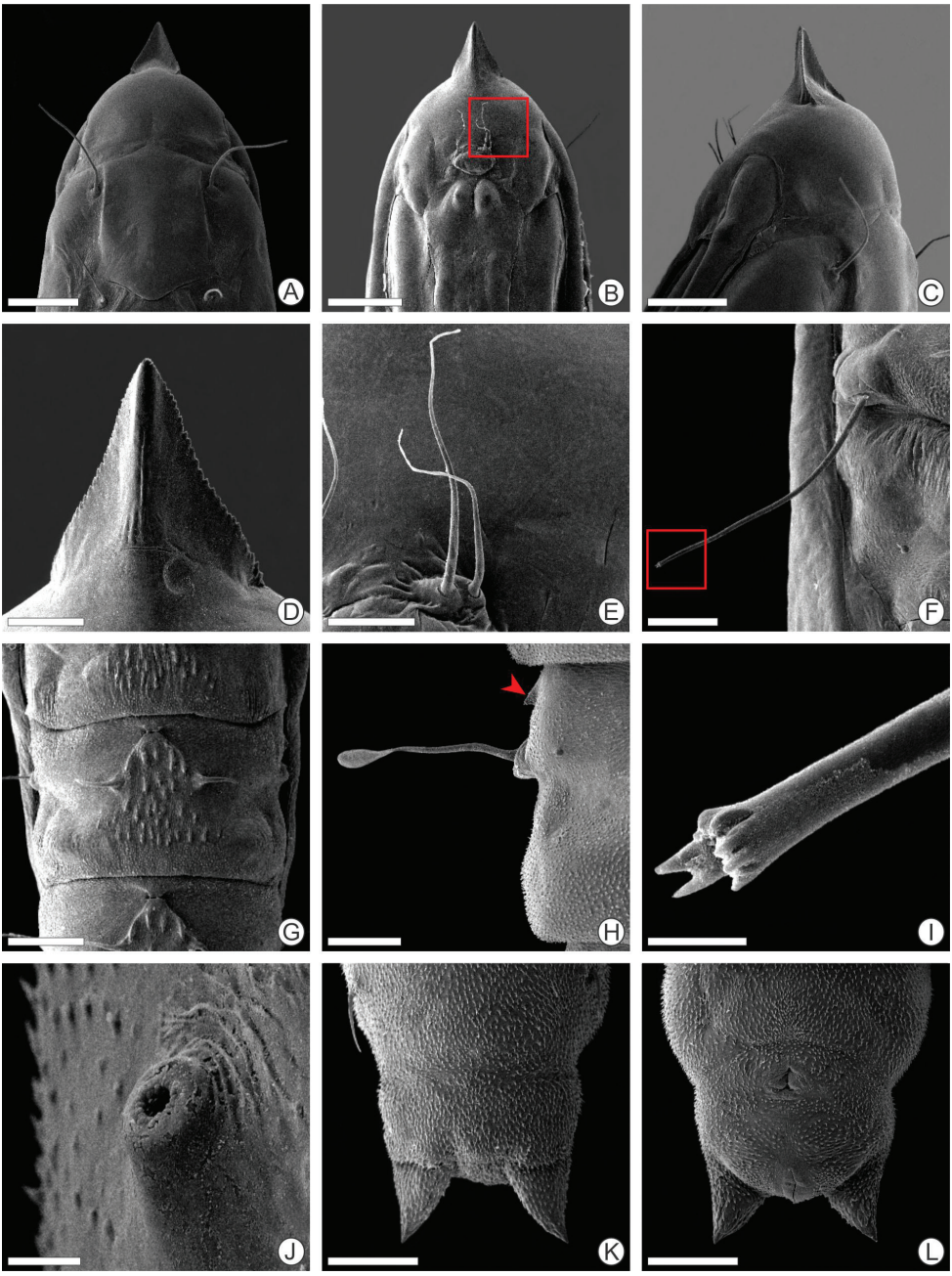

Figure 6. Scanning electron micrographs of *P. furcata* sp. nov. pupa **A–C** head under dorsal, ventral, and lateral views **D** cocoon-cutter, ventral **E** setae on clypeus, ventral (indicated by square in B) **F** lateral seta on abdominal segment A2, dorsal **G** detail of abdominal segment A3, dorsal **H** lateral seta with clavate apex, adjacent to spiracle (indicated by arrow) and close to small spine on abdominal segment A6, dorsal **I** detail of lateral seta distal portion, with dentate apex from abdominal segment A2, (indicated by square in F) **J** abdominal spiracle, lateral **K, L** last abdominal segments, dorsal and ventral, respectively. Scale bars: 200 µm (**A–C, G**), 50 µm (**D**), 40 µm (**E**), 100 µm (**F, H, K, L**), 10 µm (**I, J**).

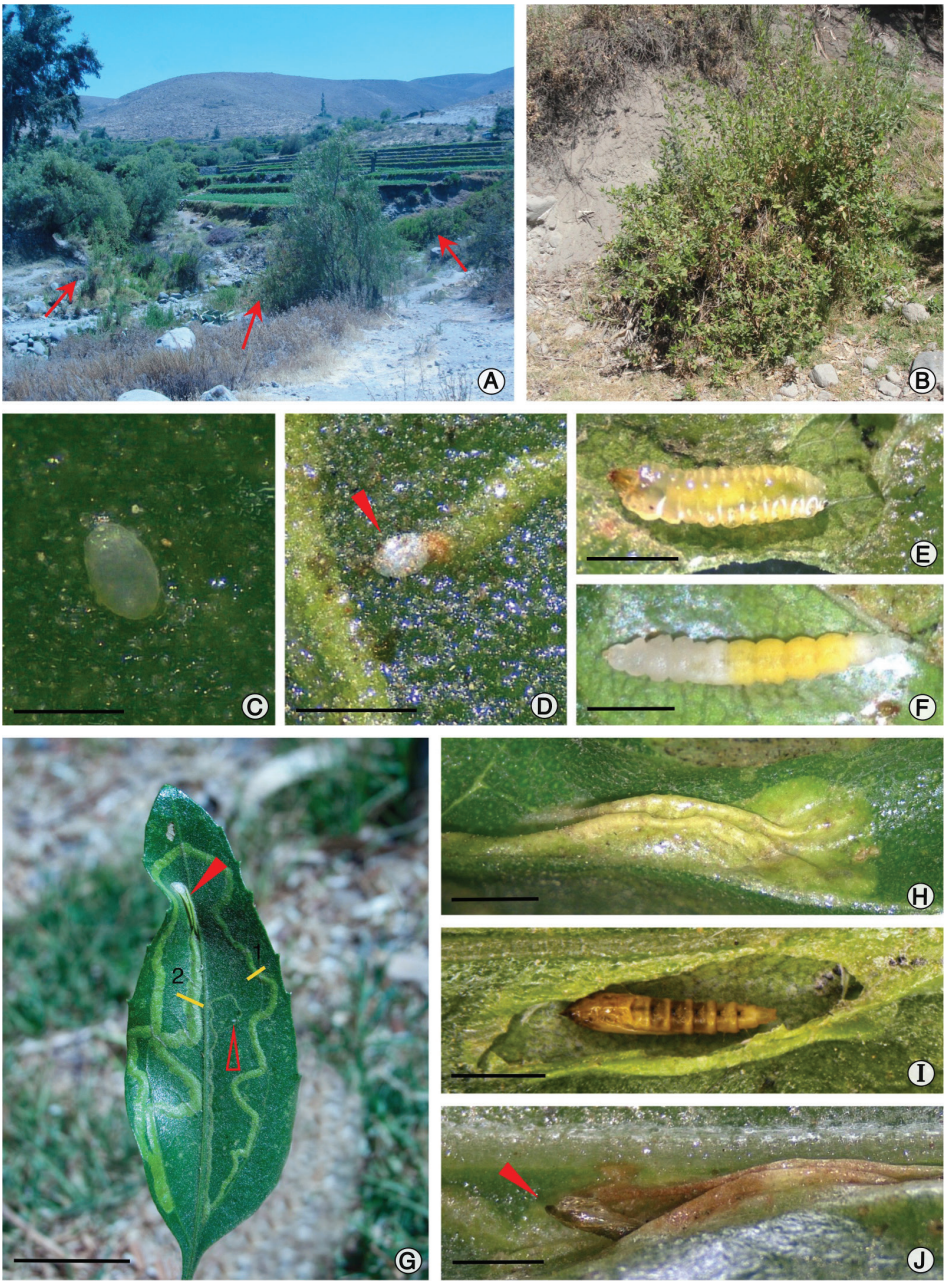

Figure 7. Natural history of *P. furcata* sp. nov. **A** type locality in Characato valley, Arequipa, southern Peru (setae point to *Baccharis* host-plants) **B** *B. alnifolia* plant, under close view **C** egg containing developing embryo **D** early mine with attached egg shell remains (pointed by arrow head) **E** sap-feeding larva, dorsal **F** spinning larva, dorsal view **G** leaf with a single *P. furcata* mine on adaxial surface (numbers indicate position of histological sections presented in Fig. 8; open and closed arrows indicated respectively the beginning and ending of the mine) **H** pupal cocoon, latero-dorsal **I** pupa, dorsal **J** pupal exuvium protruded from cocoon after adult emergence (close arrows points to pupal exuvium). Scale bars: 0.25 mm (**C**), 0.5 mm (**D**), 2 mm (**E, F**), 20 mm (G), 2.5 mm (**H–J**).

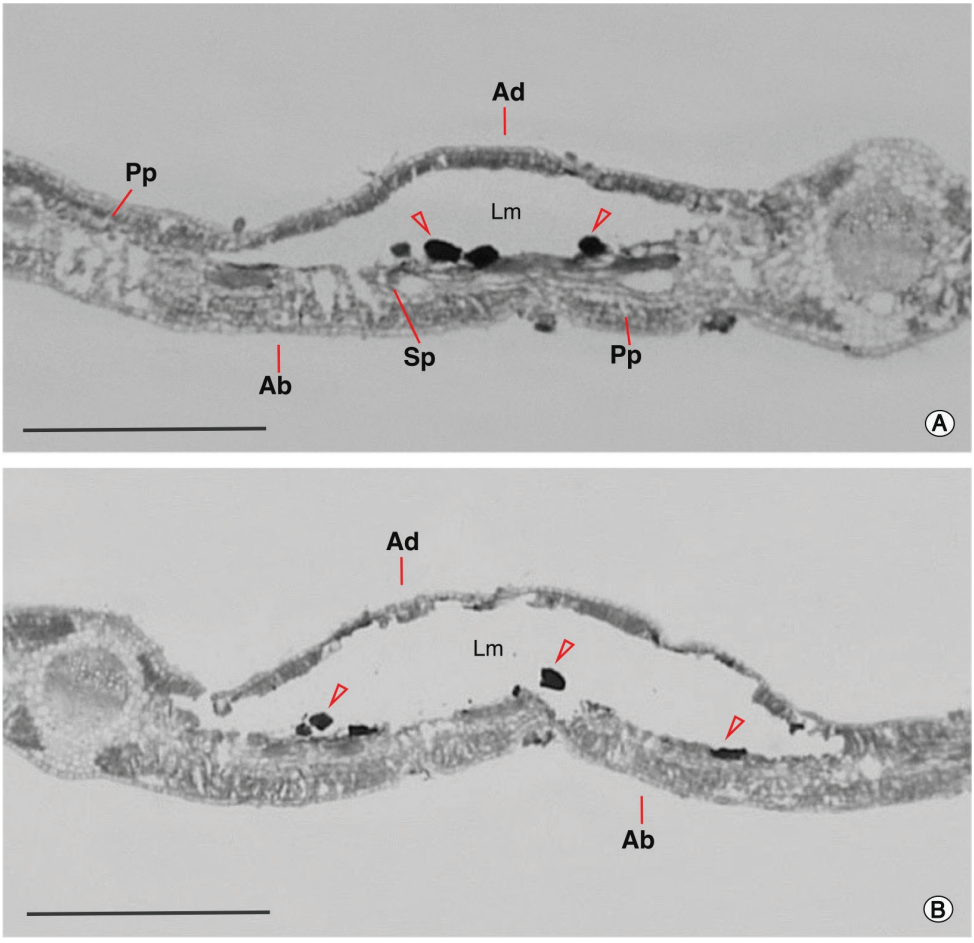

Figure 8. Transverse histological sections of *P. furcata* sp. nov. mine on *Baccharis alnifolia* Meyen & Walp. (Asteraceae) leaf **A** intermediate portion (location indicated by line 1 in Fig. 7G) **B** final portion (location indicated by line 2 in Fig. 7G). Feces are indicated by open arrows. Ab, epidermis of abaxial surface; Ad, epidermis of adaxial surface; Lm, leaf mine; Pp, palisade parenchyma; Sp, spongy parenchyma. Scale bars: 0.5 mm.

Host plant. (Fig. 7B). *Baccharis alnifolia* Meyen & Walp. (Asteraceae) is the only host plant known for the immature stages of *P. furcata*. This species is distributed from Peru to northern Chile, with an altitudinal range between 2400–3800 m (Beltran et al. 2006; Rodriguez et al. 2018). In Peru, *B. alnifolia* inhabits the western slopes of the Andes, distributed from the departments of La Libertad to Tacna (Beltran et al. 2006). It is commonly known as "chilca", a shrub that reaches a height of 1.5 to 3 meters, and grows predominately on river banks (Brako and Zarucchi 1993).

Distribution. *Phyllocnistis furcata* is known only from the type locality, Characato, Arequipa, Peru (Fig. 7A).

Life history. (Figs 7C–J, 8). *Phyllocnistis furcata* mines are serpentine throughout their length, initially narrow, increasing in width to the end of the mine, covering most of the area of the leaf (Fig. 7G). Mines were found either on young leaves un-

der development or fully expanded ones, and almost all began near the midrib and extended along it. We found the majority of mines on the abaxial side of the leaf, and fewer on the adaxial side of the leaf. Most mines were found singly on a leaf; however, sometimes mined leaves carried two mines, either two on the abaxial side or one on each side. Mature mines are light green in color (Fig. 7G). Larvae are sap-feeders during the first instars (Fig. 7E) and are specialized in the palisade parenchyma, leaving the epidermis layers and generally the spongy parenchyma intact (Fig. 8). During the last spinning instar, it does not feed, but spins a cocoon within which pupation occurs (Fig. 7F). The cocoon is endophyllous, located on the final portion of the mine, during construction leading to a fold outside the leaf typical for *Phyllocnistis* (Fig. 7H). Before adult emergence, the anterior half of the pupa (head and thorax) protrudes out, while the posterior half remains in the pupal cocoon (Fig. 7J). In the examined mines, ~20% had a living and not parasitized larva or pupa. The remaining mines (~80%) were either empty or contained larvae or pupae which were either dead or parasitized by unidentified species of Hymenoptera; the affected stages varied from early sap-feeding larvae to pupal stage. Our field collection data indicate that the species may occur all year around in the area, with higher densities found in April and November.

Molecular data. (Fig. 9). The five DNA barcodes obtained for *P. furcata* (intraspecific distance = 0%) fall within the same clade, supporting the identification of the new species (Fig. 9). The nearest neighbor (BS = 57) is *P. ourea* (Fig. 9A), a *Baccharis*-feeding species. This pattern is consistent in MP and ML analysis (Fig. 9B, C, respectively), with node support (BS = 59). The mean distance between *P. furcata* and Neotropical *Phyllocnistis* (14.8%) is near the overall divergence within the genus (15.3%) and Neotropical groups (15.3%) (Table 2). The lowest divergence was observed between *P. furcata* and *P. ourea*. However, the *Baccharis*-feeding lineage *Phyllocnistis* sp. 12 showed high divergence distance (14.7%), similar to other species from the Neotropics.

Discussion

Phyllocnistis is one of the most species-rich genera of gracillariids, in which a number of taxa were recently described in the Neotropical region, predominantly from tropical and subtropical forests (Davis and Wagner 2011; Brito et al. 2012, 2016,

Table 2. Mean genetic distance (minimum – maximum) based on COI sequences using Kimura-2 parameters method for distinct phylogenetic arrangement of *Phyllocnistis* species, with special reference to *Phyllocnistis furcata* sp. nov. N, number of specimens used in the dataset.

Group	N	Mean (minimum – maximum)
All named species of *Phyllocnistis*	35	15.4% (3.3–22.1)
Neotropical *Phyllocnistis* (described + undescribed species)	29	15.3% (8.9–21.6)
P. furcata vs Neotropical *Phyllocnistis*	29	14.8% (11.9–18.5)
P. furcata vs. *P. ourea*	6	11.9%
P. furcata vs. *Phyllocnistis* sp. 12	7	14.7%

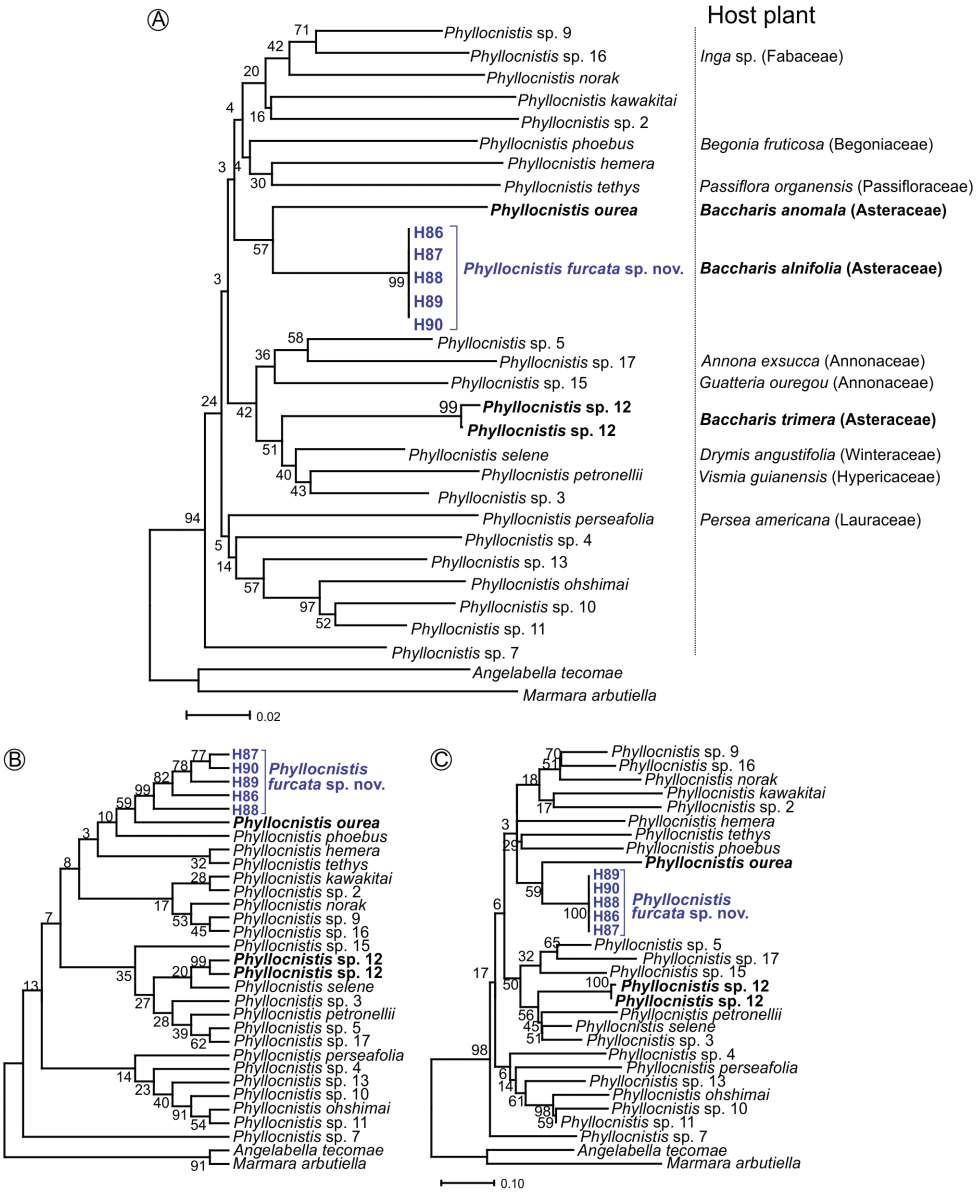

Figure 9. COI trees showing the specific classification of *Phyllocnistis furcata* sp. nov. (blue), and its position among 23 Neotropical *Phyllocnistis* lineages **A** phylogeny inferred using the Neighbor-Joining method with Kimura 2-parameter model. Host plants, when known, are indicated for each species [data were obtained from Brito et al. (2017) and BOLD database] **B** maximum parsimony consensus tree (length 1006, consistency index 0.3315, and retention index 0.4675) **C** maximum likelihood tree using the general time reversible model of sequence ecolution. –ln likelihood = 4913.93 The percentage of replicate trees in which the associated taxa clustered together in the bootstrap test (1000 replicates) are shown above the branches in A, B, and C. *Angelabella tecomae* Vargas & Parra, 2005 (Oecophyllembiinae) and *Marmara arbutiella* Busck, [1904] (Marmarinae) were used as outgroups. Bold indicates species/lineages that use *Baccharis* species as host plants.

2017; Lees et al. 2013). Herein we describe an Andean new species, *P. furcata*, based on morphological and molecular characters that clearly separate it from congeneric species. The COI tree showed a monophyletic status for the new species, and different methods of reconstruction support the inference of its sister relationship with *P. ourea* among Neotropical lineages.

Overall, adults of *P. furcata* resemble the majority of Neotropical *Phyllocnistis* in general aspects of forewing pattern (Brito et al. 2017, 2019; Fochezato et al. 2018); nevertheless, comparing *P. furcata* with *P. ourea* and *P. baccharidis*, all associated with *Baccharis* as host plants, there are no characters in the wing pattern that group them together; however, they share the presence of a small stout spine at the apex of the valva in the male genitalia. However, a high genetic distance (11.4%) is found between *P. furcata* and *P. ourea*, suggesting either an ancient divergence of these sister species or incomplete sampling of Neotropical species, taking into account that much more *Phyllocnistis* species could be expected associated with the large genus *Baccharis* (440 sp), and what could also be expected the close relationships among these micromoths.

Phyllocnistis ourea clustered in all COI analysis as the closest related to *P. furcata*, sharing the same genus of host plant (*Baccharis anomala*), which could indicate a clade which is associated only with *Baccharis*. However, the undescribed *Phyllocnistis* sp. 12 (Brito et al. 2017), which feeds on *Baccharis trimera*, did not cluster in that group. Moreover, this lineage presents a high genetic divergence (ca. 15%) from *P. furcata*, near to the mean divergence found of all *Phyllocnistis* species, suggesting a convergent evolution of host plant use. Such pattern is distinct to described for a species group of *Phyllocnistis* that feed on Salicaceae, recovered as a single evolutionary clade in a COI tree (Kirichenko et al. 2018). Further inclusion of *P. baccharidis*, and eventually more species/lineages (currently unknown) associated with *Baccharis*, together with a multilocus approach, will allow one to make more robust phylogenetic inferences and shed light on the diversification of Neotropical *Phyllocnistis* related to its host plants.

Interestingly, males of *P. furcata* possess two pairs of coremata on abdominal segment VIII. Only one pair, formed by long, slender, flattened scales is found generally in species of *Phyllocnistis* in which the coremata are described (e.g., Kawahara et al. 2009; Brito et al. 2012, 2019; Kirichenko et al. 2018). *Phyllocnistis furcata* presents one pair similar to those in other congeneric species, and a second pair formed by wide rounded flat scales, which may represent the first report of this type of structure for the genus. Furthermore, another interesting aspect is observed in females of *P. furcata*, where one of the three signa of the corpus bursae is prominent (~0.5 × length of corpus bursae) with a particular fork-shaped appearance not observed in any other species of *Phyllocnistis.* This partially resembles the only signum of *P. tropaeolicola* Kawahara, Nishida & Davis, 2009, which has the form of a narrow band with two spines projecting inwards (Kawahara et al. 2009), but the spines are more prominent in *P. furcata*. *Phyllocnistis drimiphaga* Kawahara, Nishida & Davis, 2009 is another species with one of its two signa of large size, but five short spines arise from this signum. The remaining species of this genus mostly contain a small pair of fusiform signa or a single signum that occupies less than 2/3 of corpus bursae (Kirichenko et al. 2018; De Prins

et al. 2019). Also, there is no information about the variability of coloration pattern between females and males in other species of *Phyllocnistis*, notably that males are slightly darker than females in *P. furcata.* This has not been observed in other species of the genus, and should be reviewed in detail in the future.

The knowledge of immature stages of *Phyllocnistis* is also insufficient. In the majority of the species of the genus whose pupal morphology is described, pupae are characterized by a well-developed cocoon cutter and some abdominal terga (generally A2–A7) with a pair of prominent laterally curved spines and many small spines medially (Kobayashi and Hirowatari 2011; Brito et al. 2012, 2019; Fochezato et al. 2018; Kirichenko et al. 2018; Liu et al. 2018). However, a few species do not match this pattern perfectly. For instance, *P. subpersea* Davis & Wagner, 2011 has the cocoon cutter in the form of a pair of stout conical processes with a strongly recurved subapical spine (Davis and Wagner 2011). Curved spines of the abdominal terga are absent in two Neotropical species (Brito et al. 2012, 2019) and are present only on two segments of *P. citrella* (Kobayashi et al. 2013). The pupa of *P. furcata* matches well the general pattern of the genus. In addition, the prominent curved spines are present on A1–A7, a condition also found in *P. ourea*, whose larvae also feed on *Baccharis* (Brito et al. 2019). The apex of the lateral setae of A6 and A7 is clavate in the pupae of these two *Baccharis*-feeding *Phyllocnistis*. However, this condition is also found in other species whose larvae are associated with other plant families (Kawahara et al. 2009; Davis and Wagner 2011; Brito et al. 2019). In the spinning larva, a single ambulatory callus placed ventrally at the center of the meso- and metathorax is found in *P. ourea* (Brito et al. 2019), *P. furcata*, and also in the Thymelaeaceae-feeding *P. hemera* Brito & Fochezato, 2018, while lateral sensilla on abdominal segments are found in *P. hemera* (Fochezato et al. 2018) and *P. furcata*. In the sap-feeding larva, the presence of two stemmata, like in *P. furcata*, has been described for *P. ourea* and the Winteraceae-feeding *P. selene* Brito & Moreira, 2017 (Brito et al. 2019). Certainly, the external morphology of the immature stages should be explored in additional species of *Phyllocnistis* to have a more realistic perspective of the actual variation and its relationship with ecology and evolution.

The few studies in which the damage pattern caused by leaf miner larvae of Gracillariidae has been characterized using histological sections, suggest that its feeding activity can either be restricted to specific tissues throughout the leaf miner stage or the consumed tissues can change with larval ontogeny (Brito et al. 2012; Body et al. 2015; Moreira et al. 2018; Pereira et al. 2019; Vargas-Ortiz et al. 2019). In the case of *Phyllocnistis*, the larvae of *P. citrella* feed only in the epidermis of *Citrus* (Rutaceae) (Achor et al. 1997), and those of *P. tethys* Moreira & Vargas, 2012 on the spongy parenchyma of *Passiflora organensis* Gardn. (Passifloraceae) (Brito et al. 2012). Furthermore, larvae of *P. hemera* feed initially on the epidermis and later on the palisade parenchyma of *Daphnopsis fasciculata* (Meisn) Nevelling (Thymelaeaceae) (Fochezato et al. 2018). The feeding behavior of larvae of *P. furcata* was found to be restricted to the palisade parenchyma of *B. alnifolia*.

The mines of *P. furcata* are found on adaxial and abaxial surfaces of the leaf. In contrast, those of *P. ourea*, another *Baccharis*-feeding *Phyllocnistis*, are restricted

to the adaxial surface of the leaf of its host *B. anomala* (Brito et al. 2019). Despite histological descriptions of leaves of *B. anomala* mined by *P. ourea* not being available, it appears that the remarkable difference between the distribution pattern of the mines of the two species in the leaves of their hosts could be due, at least in part, to differences in leaf anatomy of the two hosts and the ability of the larvae to feed on palisade parenchyma. The organization of the mesophyll in *B. alnifolia* is isobilateral, with two or three layers of palisade parenchyma in each side and one or two layers of spongy parenchyma in the middle, a pattern reported for several species of *Baccharis* (Budel et al. 2018; Ornellas et al. 2019), while the organization of the mesophyll of *B. anomala* is dorsoventral, with two or three layers of palisade parenchyma and approximately three layers of spongy parenchyma (Budel and Duarte 2008). Given this diversity in leaf tissue structure, additional studies are needed to better understand the ecology and evolution of herbivory in *Phyllocnistis*. Certainly, histological descriptions of leaves mined by additional species of this genus will be helpful to propose hypotheses.

The known distribution of endemic species of *Phyllocnistis* in the western slopes of Peruvian Andes was previously restricted to the type localities of the two species described at the beginning of the last century by Edward Meyrick (1915, 1921) around the Department of Lima, in central Peru. Thus, the discovery of *P. furcata* in the Arequipa Department, as a result of recent evaluations of the Microlepidoptera fauna, provides the first record of this genus from southwestern Peru, at 2400 m, where the vegetation is dominated by xeric shrublands with abundant cacti (Montesinos et al. 2012, Heim 2014). However, as already mentioned, the taxonomic diversity of gracillariid species remain poorly studied in Peru, due to the absence of local specialists and collections of micromoths in general. As discussed in Brito et al. (2016), there exists a "taxonomic impediment" for the progress of studies on Neotropical gracillariids in general. Therefore, regional revisions of micromoth faunas would represent an important advance to the knowledge of this diverse group in Peru (e.g., Davis et al. 2020), particularly in areas that are subject to the highest rates of anthropic environmental degradation, like the environments of the southern Andes of Peru.

Acknowledgements

Thanks are due to staff members of Centro de Microscopia Eletrônica (UFRGS) for assistance and use of scanning electron microscopy facilities. RB was supported by fellowships from CNPq. GRPM was supported by a CNPq grant. JC and JF were supported, respectively by CNPq and CAPES scholarships. AL was supported by a project of the Universidad Nacional de San Agustin de Arequipa (UNSA) with Contract reference IBAIB-01-2019-UNSA. We acknowledge the Subject Editor, Erik J. van Nieukerken, for his reading and corrections. Our thanks also go to the reviewers of the document for their valuable comments.

References

Achor DS, Browning H, Albrigo LG (1997) Anatomical and histochemical effects of feeding by *Citrus* leafminer larvae (*Phyllocnistis citrella* Stainton) in *Citrus* leaves. Journal of the American Society for Horticultural Science 122: 829–836. https://doi.org/10.21273/JASHS.122.6.829

Alexander CP (1916) New or little-known crane-flies from Colombia, Ecuador and Peru (Tipulidae, Diptera). Transactions of the American Entomological Society 42: 1–4.

Alexander CP (1921) New or little-known crane-flies from the Amazonian region. Proceedings of the Academy of Natural Sciences of Philadelphia 73: 39–103.

Beltran H, Granda A, León B, Sagástegui A, Sánchez I, Zapata M (2006) Asteraceae endémicas del Perú. Revista Peruana de Biología 13(2): 64–164. https://doi.org/10.15381/rpb.v13i2.1807

Body M, Burlat V, Giron D (2015) Hypermetamorphosis in a leaf-miner allows insects to cope with a confined nutritional space. Arthropod-Plant Interactions 9(1): 75–84. https://doi.org/10.1007/s11829-014-9349-5

Brako L, Zarucchi JL (1993) Catalogue of the flowering plants and gymnosperms of Peru. Monographs in Systematic Botany from the Missouri Botanical Garden 45.

Brito R, Gonçalves GL, Vargas HA, Moreira GRP (2012) A new species of *Phyllocnistis* Zeller (Lepidoptera: Gracillariidae) from southern Brazil, with life-history description and genetic comparison to congeneric species. Zootaxa 3582: 1–16. https://doi.org/10.11646/zootaxa.3582.1.1

Brito R, De Prins J, De Prins W, Mielke OHH, Gonçalves GL, Moreira GRP (2016) Extant diversity and estimate number of Gracillariidae (Lepidoptera) species yet to be discovered in the Neotropical region. Revista Brasileira de Entomologia 60(4): 275–283. https://doi.org/10.1016/j.rbe.2016.06.002

Brito R, Lopez-Vaamonde C, Gonçalves GL, Becker VO, Mielke OHH, Moreira GRP (2017) Taxonomic revision of Neotropical *Phyllocnistis* Zeller, 1848 (Lepidoptera: Gracillariidae), with descriptions of seven new species and host plant associations. Zootaxa 4341(3): 301–352. https://doi.org/10.11646/zootaxa.4341.3.1

Brito R, Mielke OHH, Gonçalves GL, Moreira GRP (2019) Description of three new species of *Phyllocnistis* Zeller, 1848 (Lepidoptera: Gracillariidae) from the Atlantic Forest, South Brazil, with notes on natural history and phylogeny. Austral Entomology 58: 27–51. https://doi.org/10.1111/aen.12298

Budel, JM, Duarte MR (2008) Estudo farmacobotanico de partes vegetativas aereas de *Baccharis anomala* DC., Asteraceae. Revista Brasileira de Farmacognosia 18: 761–768. https://doi.org/10.1590/S0102-695X2008000500022

Budel JM, Raman V, Monteiro LM, Almeida VP, Bobek VB, Heiden G, Takeda IJM, Khan IA (2018) Foliar anatomy and microscopy of six Brazilian species of *Baccharis* (Asteraceae). Microscopy Research and Technique 81(8): 832–842. https://doi.org/10.1002/jemt.23045

Castillo P, Cornejo R (1996) *Phyllocnistis citrella*, minador de las hojas de los cítricos, nuevo insecto plaga para Tumbes. Revista Peruana de Entomología 38: 105–107.

Cerdeña J, Pyrcz T, Zacca T (2014) Mariposas altoandinas del sur del Perú, I. Satyrinae de la puna xerofítica, con la descripción de dos nuevos taxones y tres nuevos registros para Perú

(Lepidoptera: Nymphalidae). Revista Peruana de Biología 21(3): 213–222. https://doi.org/10.15381/rpb.v21i3.10894

Cerdeña J, Lopez E, Parra L, Vargas HA, Farfán J (2019) First record of *Pero rodriguezi* Vargas, 2007 (Geometridae) in Peru with description of the female. Journal of the Lepidopterists' Society 73(2): 129–131. https://doi.org/10.18473/lepi.73i2.a7

Davis DR, Wagner DL (2011) Biology and systematics of the New World *Phyllocnistis* Zeller leafminers of the avocado genus *Persea* (Lepidoptera, Gracillariidae). ZooKeys 97: 39–73. https://doi.org/10.3897/zookeys.97.753

Davis DR, Kassulke RC, Harley KLS, Gillett JD (1991) Systematics, morphology, biology, and host specificity of *Neurostrota gunniella* (Busck) (Lepidoptera: Gracillariidae), an agent for the biological control of *Mimosa pigra* L. Proceedings of the Entomological Society of Washington 93(1): 16–44.

Davis DR, Farfán J, Cerdeña J, Huanca-Mamani W, Vargas HA, Vargas-Ortiz M, Gonçalves GL, Moreira GRP (2020) *Adenogasteria leguminivora* Davis & Vargas gen. et sp. nov. (Lepidoptera: Gracillariidae): a new seed-feeding micromoth associated with Fabaceae in Peru and Chile. Austral Entomology 59: 37–51. https://doi.org/10.1111/aen.12439

De Prins J, De Prins W (2020) Global Taxonomic Database of Gracillariidae (Lepidoptera). http://www.gracillariidae.net/ [accessed 20 March 2020]

De Prins J, Arévalo-Maldonado H, Davis DR, Landry B, Vargas HA, Davis MM, Brito R, Fochezato J, Oshima I, Moreira GRP (2019) An illustrated catalogue of the Neotropical Gracillariidae (Lepidoptera) with new data on primary types. Zootaxa 4575(1): 1–110. https://doi.org/10.11646/zootaxa.4575.1.1

Doyle JJ, Doyle JL (1987) A rapid DNA isolation procedure for small quantities of fresh leaf tissue. Phytochemical Bulletin 19: 11–15.

Farfán J (2018) Mariposas (Lepidoptera: Papilionoidea) de Arequipa, Perú: lista preliminar con dos nuevos registros para Perú. Revista Peruana de Biología 25(4): 357–370. https://doi.org/10.15381/rpb.v25i4.15536

Farfán J, Cerdeña J, Arivilca M, Condori-Mamani M, Huanca-Mamani W, Vargas HA (2020a) First record of *Alucita danunciae* (Lepidoptera: Alucitidae) in Peru. Studies on Neotropical Fauna and Environment 55(2): 103–108. https://doi.org/10.1080/01650521.2019.1702617

Farfán J, Lamas G, Cerdeña J (2020b) A new species of *Mathania* Oberthür, 1890 from Peru (Lepidoptera, Pieridae). Zootaxa 4758(3): 589–595. https://doi.org/10.11646/zootaxa.4758.3.11

Fochezato J, Brito R, Isaias RMS, Gonçalves GL, Moreira GRP (2018) *Phyllocnistis hemera* sp. nov. (Lepidoptera: Gracillariidae): a new species of leaf-miner associated with *Daphnopsis fasciculata* (Thymelaeaceae) in the Atlantic Forest. Revista Brasileira de Entomologia 62: 57–65. https://doi.org/10.1016/j.rbe.2017.11.001

Folmer O, Black M, Hoeh W, Lutz R, Vrijenhoek R (1994) DNA primers for amplification of mitochondrial cytochrome c oxidase subunit I from diverse metazoan invertebrates. Molecular Marine Biology and Biotechnology 3(5): 294–299.

Guillén M, Davis DR, Heraty JM (2001) Systematics and biology of a new, polyphagus species of *Marmara* (Lepidoptera: Gracillariidae) infesting grapefruit in the Southwestern United States. Proceedings of the Entomological Society of Washington 103(3): 636–654.

Guindon S, Dufayard JF, Lefort V, Anisimova M, Hordijk W, Gascuel O (2010) New Algorithms and Methods to Estimate Maximum-Likelihood Phylogenies: Assessing the Per-

formance of PhyML 3.0. Systematic Biology 59(3): 307–321. https://doi.org/10.1093/sysbio/syq010

Hall JPW (2005) Montane speciation patterns in *Ithomiola* butterflies (Lepidoptera: Riodinidae): are they consistently moving up in the world? Proceedings of the Royal Society of London B, Biological Sciences 272: 2457–2466. https://doi.org/10.1098/rspb.2005.3254

Hanson P, Nishida K, Gómez-Laurito J (2014) Insect galls of Costa Rica and their parasitoids. In: Fernandes GW, Santos JC (Eds) Neotropical Insect Galls. Springer, New York, 497–518. https://doi.org/10.1007/978-94-017-8783-3_23

Heiden G, Antonelli A, Pirani JR (2019) A novel phylogenetic infrageneric classification of *Baccharis* (Asteraceae: Astereae), a highly diversified American genus. Taxon 68(5): 1048–1081. https://doi.org/10.1002/tax.12128

Heim E (2014) Flora of Arequipa, Peru. Books on Demand, Germany, 128 pp.

Hering EM (1958) Neue Microlepidopteren von Tucuman. Acta Zoologica Lilloana 15: 303–312.

Hu B, Wang S, Zhang J, Li H (2011) Taxonomy and biology of two seed-parasitic gracillariid moths (Lepidoptera, Gracillariidae), with description of a new species. ZooKeys 83: 43–56. https://doi.org/10.3897/zookeys.83.783

Ignatov II, Centeno P, Janovec JP, Tobler MW, Grados J, Lamas G (2011) Patterns of diversity, composition, and distribution of sphingid moths along an elevational gradient in the Andes-Amazon region of southeastern Peru. Annals of the Entomological Society of America 104: 68–76. https://doi.org/10.1603/AN09083

Kawahara AY, Nishida K, Davis DR (2009) Systematics, host plants, and life histories of three new *Phyllocnistis* species from the central highlands of Costa Rica (Lepidoptera, Gracillariidae, Phyllocnistinae). ZooKeys 27: 7–30. https://doi.org/10.3897/zookeys.27.250

Kawahara AY, Plotkin D, Ohshima I, Lopez-Vaamonde C, Houlihan PR, Breinholt JW, Kawakita A, Xiao L, Regier JC, Davis DR, Kumata T, Jae-Cheon Sohn JC, De Prins J, Mitter C (2017) A molecular phylogeny and revised higher-level classification for the leaf-mining moth family Gracillariidae and its implications for larval host use evolution. Systematic Entomology 42(1): 60–81. https://doi.org/10.1111/syen.12210

Kawakita A, Kato M (2016) Revision of the Japanese species of *Epicephala* Meyrick with descriptions of seven new species (Lepidoptera, Gracillariidae). ZooKeys 568: 87–118. https://doi.org/10.3897/zookeys.568.6721

Kawakita A, Sato AAW, Salazar JRL, Kato M (2019) Leafflower – leafflower moth mutualism in the Neotropics: Successful transoceanic dispersal from the Old World to the New World by actively pollinating leafflower moths. PLoS ONE 14: e0210727. https://doi.org/10.1371/journal.pone.0210727

Kirichenko N, Triberti P, Kobayashi S, Hirowatari T, Doorenweerd C, Ohshima I, Huang G-H, Wang M, Magnoux E, Lopez-Vaamonde C (2018) Systematics of *Phyllocnistis* leaf-mining moths (Lepidoptera, Gracillariidae) feeding on dogwood (*Cornus* spp.) in Northeast Asia, with the description of three new species. ZooKeys 736: 79–118. https://doi.org/10.3897/zookeys.736.20739.figure17

Kobayashi S, Hirowatari T (2011) Two Chlorantaceae leafminers of the genus *Phyllocnistis* (Lepidoptera: Gracillariidae: Phyllocnistinae) from Japan, with descriptions of a new species and pupal morphology. Lepidoptera Science 62(4): 156–165.

Kobayashi S, Huang GH, Nakamura A, Hirowatari T (2013) Four new species of Gracillariidae (Lepidoptera) from China and Japan, and description of the pupal morphology of the genera *Corythoxestis*, *Eumetriochroa*, *Guttigera*, and *Metriochroa*. Zootaxa 3619(2): 101–129. https://doi.org/10.11646/zootaxa.3619.2.1

Kumar S, Stecher G, Li M, Knyaz C, Tamura K (2018) MEGA X: Molecular Evolutionary Genetics Analysis across Computing Platforms. Molecular Biology and Evolution 35(6): 1547–1549. https://doi.org/10.1093/molbev/msy096

Lamas G (1977) A preliminary check-list of the butterflies (Lepidoptera) of Peru west of the Andes. Revista de Ciencias (Lima) 70(1): 59–77.

Lamas G (2003) Las Mariposas de Machu Picchu. Guía ilustrada de las mariposas del Santuario Histórico Machu Picchu, Cuzco, Perú. Fondo Nacional para Areas Naturales Protegidas por el Estado, Lima, 221 pp.

Lees DC, Kawahara AY, Rougerie R, Ohshima I, Kawakita A, Bouteleux O, De Prins J, Lopez-Vaamonde C (2013) DNA barcoding reveals a largely unknown fauna of Gracillariidae leaf-mining moths in the Neotropics. Molecular Ecology Resources 14: 286–296. https://doi.org/10.1111/1755-0998.12178

Liu T, Sun J, Cai B, Wu Y (2018) *Phyllocnistis podocarpa* sp. nov. (Lepidoptera, Gracillariidae), a buddhist pine leaf-miner from Japan: taxonomy, DNA barcodes, damage and parasitoids. Zootaxa 4422(4): 558–568. https://doi.org/10.11646/zootaxa.4422.4.6

Meyrick E (1915) Descriptions of South American Micro-Lepidoptera. Transactions of the Entomological Society of London 2: 201–256. https://doi.org/10.1111/j.1365-2311.1915.tb02527.x

Meyrick E (1921) Exotic Microlepidoptera. Exotic Microlepidoptera (Marlborough) 2(15): 449–480.

Montesinos D, Cleef A, Sýkora K (2012) Andean shrublands of Moquegua, South Peru: Prepuna plant communities. Phytocoenologia 42(1–2): 29–55. https://doi.org/10.1127/0340-269X/2012/0042-0516

Moreira GRP, Pollo P, Brito R, Gonçalves GL, Vargas HA (2018) *Cactivalva nebularia*, gen. et sp. nov. (Lepidoptera: Gracillariidae): a new *Weinmannia* leaf miner from southern Brazil. Austral Entomology 57: 62–76. https://doi.org/10.1111/aen.12267

Müller J (2006) Systematics of *Baccharis* (Compositae-Astereae) in Bolivia, including an overview of the Genus. Systematic Botany Monographs 76: 1–341.

Myers N, Mittermeier RA, Mittermeier CG, Fonseca GAB da, Kent J (2000) Biodiversity hotspots for conservation priorities. Nature 403: 853–858. https://doi.org/10.1038/35002501

Nieukerken EJ van, Kaila L, Kitching IJ, Kristensen NP, Lees DC, Minet J, Mitter C, Mutanen M, Regier JC, Simonsen TJ, Wahlberg N, Yen SH, Zahiri R, Adamski D, Baixeras J, Bartsch D, Bengtsson BA, Brown JW, Bucheli SR, Davis DR, De Prins J, De Prins W, Epstein ME, Gentili-Poole P, Gielis C, Hattenschwiler P, Hausmann A, Holloway JD, Kallies A, Karsholt O, Kawahara A, Koster JC, Kozlov MV, Lafontaine JD, Lamas G, Landry JF, Lee S, Nuss M, Park KT, Penz C, Rota J, Schmidt BC, Schintlmeister A, Sohn JC, Solis MA, Tarmann GM, Warren AD, Weller S, Yakovlev RV, Zolotuhin VV, Zwick A (2011) Order Lepidoptera Linnaeus, 1758. In: Zhang ZQ (Ed.) Animal biodiversity: an outline of higher-level classification and survey of taxonomic richness. Zootaxa 3148: 212–221. https://doi.org/10.11646/zootaxa.3148.1.41

Ornellas T, Heiden G, Nunes de Luna B, Barros CF (2019) Comparative leaf anatomy of *Baccharis* (Asteraceae) from high-altitude grasslands in Brazil: taxonomic and ecological implications. Botany 97(11): 615–626. https://doi.org/10.1139/cjb-2019-0035

Pereira CM, Arévalo-Maldonado HA, Triberti P, Brito R, Isaias RMS, Gonçalves GL, Moreira GRP (2019) *Vallissiana universitaria* (Lepidoptera, Gracillariidae): a new genus and species of leaf-mining moth associated with *Erythroxylum* (Erythroxylaceae) in the Atlantic Forest of Brazil. Zootaxa 4604: 141–160. https://doi.org/10.11646/zootaxa.4604.1.5

Posada D (2008) jModelTest: Phylogenetic Model Averaging. Molecular Biology and Evolution 25: 1253–1256. https://doi.org/10.1093/molbev/msn083

Pyrcz TW (2004) Pronophiline butterflies of the highlands of Chachapoyas in northern Peru: faunal survey, diversity and distribution patterns (Lepidoptera, Nymphalidae, Satyrinae). Genus 15(4): 455–622.

Pyrcz TW, Willmott K, Garlacz R, Boyer P, Gareca Y (2014) Latitudinal gradient and spatial covariance in species richness of tropical Lepidoptera in the Andes. Insect Conservation and Diversity 7: 355–364. https://doi.org/10.1111/icad.12058

Rodriguez R, Marticorena C, Alarcón D, Baeza C, Cavieres L, Finot VL, Fuentes N, Kiessling A, Mihoc M, Pauchard A, Ruiz E, Sanchez P, Marticorena A (2018) Catálogo de las plantas vasculares de Chile. Gayana Botánica 75: 1–430. https://doi.org/10.4067/S0717-66432018000100001

Sublett CA, Cook JL, Janovec JP (2019) Species richness and community composition of sphingid moths (Lepidoptera: Sphingidae) along an elevational gradient in southeast Peru. Zoologia 36: 1–11. https://doi.org/10.3897/zoologia.36.e32938

Vargas HA (2010) *Angelabella tecomae* (Lepidoptera: Gracillariidae): an exotic hostplant in northern Chile and first record from Peru. Revista Colombiana de Entomologia 36(2): 340–341.

Vargas HA, Landry B (2005) A new genus and species of Gracillariidae (Lepidoptera) feeding on flowers of *Acacia macracantha* Willd. (Mimosaceae) in Chile. Acta Entomologica Chilena 29(1): 47–57.

Vargas-Ortiz M, Gonçalves GL, Huanca-Mamani W, Vargas HA, Moreira GRP (2019) Description, natural history and genetic variation of *Caloptilia guacanivora* sp. nov. Vargas-Ortiz & Vargas (Lepidoptera: Gracillariidae) in the Atacama Desert, Chile. Austral Entomology 58: 171–191. https://doi.org/10.1111/aen.12351

Willmott KR, Lamas G, Hall JPW (2011) Systematics of *Hypanartia* (Lepidoptera: Nymphalidae: Nymphalinae), with a test for geographical speciation mechanisms in the Andes. Systematic Entomology 26(4): 369–399. https://doi.org/10.1046/j.1365-3113.2001.00157.x

ZooKeys 996: 147–152 (2020)
doi: 10.3897/zookeys.996.55002
https://zookeys.pensoft.net

RESEARCH ARTICLE

A peer-reviewed open-access journal
ZooKeys
Launched to accelerate biodiversity research

Description of a new *Hiroshia* species (Lepidoptera, Thyatiridae) from Hubei Province, China

Hong Zheng[1], Gábor Ronkay[2], László Ronkay[2], Hui-Lin Han[1,3]

1 *School of Forestry, Northeast Forestry University, Harbin, CH-150040, China* **2** *Heterocera Ltd, H-11437 Budapest, Szt. István krt 4, Hungary* **3** *Key Laboratory of Sustainable Forest Ecosystem Management-Ministry of Education, Northeast Forestry University, Harbin, 150040, China*

Corresponding author: Hui-Lin Han (hanhuilin@aliyun.com; 1710312254@qq.com)

Academic editor: A. Hausmann | Received 2 June 2020 | Accepted 21 October 2020 | Published 24 November 2020

http://zoobank.org/1ECDA4BD-DC36-4126-AD54-48273D3A7E1F

Citation: Zheng H, Ronkay G, Ronkay L, Han H-L (2020) Description of a new *Hiroshia* species (Lepidoptera, Thyatiridae) from Hubei Province, China. ZooKeys 996: 147–152. https://doi.org/10.3897/zookeys.996.55002

Abstract

A third species of *Hiroshia* László, Ronkay & Ronkay, 2001, *H. shennongjiaensis* Ronkay, Ronkay & Han, **sp. nov.** is described from Hubei Province in China. The adult and the male genitalia of the new species are illustrated and compared with those of its congeners, *H. albinigra* László, Ronkay & Ronkay, 2001 and *H. nanlingana* Zhuang, Owada & Wang, 2014; an identification key based on the male genitalia is presented.

Keywords

False owlet moth, identification key, male genitalia, morphology, new species, taxonomy

Introduction

The genus *Hiroshia* László, Ronkay & Ronkay, 2001 was established for a single species, *H. albinigra* László, Ronkay & Ronkay, 2001 which occurs in the Mt. Fansipan, N. Vietnam. Subsequently, an allopatric sister-species, *H. nanlingana* Zhuang, Owada & Wang, 2014 was discovered and described from the Mt. Nanling in China (László et al. 2001, 2007; Zhuang et al. 2014). In this present study, a third species of the genus, *H. shennongjiaensis* Ronkay, Ronkay & Han, sp. nov. is described from Hubei Province, China, from an untouched forest area composed of broad-leaved forest, mixed coniferous woodland and shrubby undergrowth.

Materials and methods

The examined material originates from the collections of the Institute of Zoology, Chinese Academy of Sciences. Dissection of the abdomen and genitalia follows Kononenko and Han (2007). The moths were photographed using the camera Nikon D700; the genitalia slides were photographed with an Olympus photomicroscope with Helicon Focus software, further processed in Adobe Photoshop CS6. The type-specimens of the new species are deposited in the collection of the Institute of Zoology, Chinese Academy of Sciences (**IZCAS**).

Taxonomic account

Genus *Hiroshia* László, Ronkay & Ronkay, 2001

Hiroshia László, Ronkay & Ronkay, 2001, Acta Zoologica Academiae Scientiarum Hungaricae 47(1): 27–85. Type species. *Hiroshia albinigra* László, Ronkay & Ronkay, 2001 (type-locality: Vietnam, Fan-si-pan Mts. [MWM]).

***Hiroshia shennongjiaensis* Ronkay, Ronkay & Han, sp. nov.**
http://zoobank.org/24982942-1CEF-4D70-985A-AF638153D721
Figures 1–2, 6, 8–10

Material examined. *Holotype*. ♂, China, Hubei Province, Badong County, Yanduhe town, Xiaoshennongjia village, altitude 1320 m, 26. iv. 2016, leg. J Yao & KD Zhao; gen. prep. No. hhl-4220-1; coll. IZCAS. ***Paratypes*.** 2 ♂, from the same site as the holotype, 28. iv. 2016, leg. J Yao & KD Zhao; coll. IZCAS.

Diagnosis. The new species is very similar externally to *H. albinigra* (Fig. 3) and *H. nanlingana* (Fig. 4) by its size (wingspan 46–46.5 mm, those of *H. albinigra* and *H. nanlingana* are 46–51 mm and 48–51 mm, respectively), wing shape and main elements of the forewing pattern. The forewing is more unicolorous, without prominent whitish markings which are typical of the other two species of the genus. The distinguishing features are as follows: forewing ground color of *H. shennongjiaensis* rather monotonous graphite-grey, without prominent reddish or red-brown irroration (in *H. albinigra* and *H. nanlingana* with conspicuous red or reddish-brown suffusion in median area); apical patch darker, pale bluish-grey (in *H. albinigra* and *H. nanlingana* white or grey-white); submarginal area pale ochreous-brown to greyish-brown between postmedial and praeterminal lines (in *H. albinigra* and *H. nanlingana* prominently white and grey-white); orbicular stigma more visible, whitish with distinct blackish outline (in *H. albinigra* and *H. nanlingana* indistinct); and the hindwing basal area is paler, rather greyish-white (in *H. albinigra* and *H. nanlingana*, it is darker, stronger, suffused by light brown).

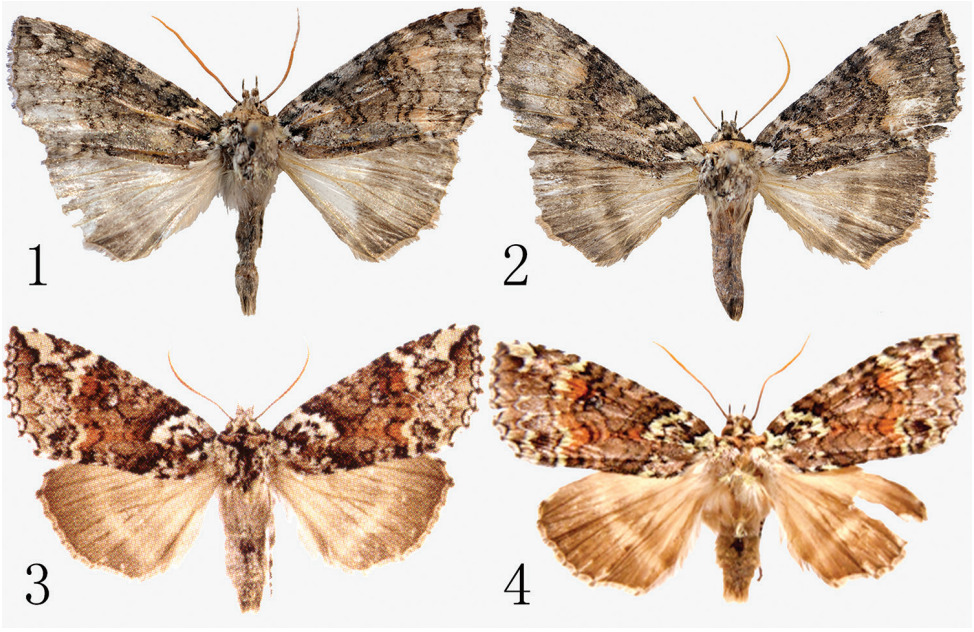

Figures 1–4. *Hiroshia* spp., adults **1** *H. shennongjiaensis* sp. nov., male, holotype **2** ditto, male, paratype **3** *H. albinigra*, male (László et al. 2007) **4** *H. nanlingana*, male (after Zhuang et al. 2014).

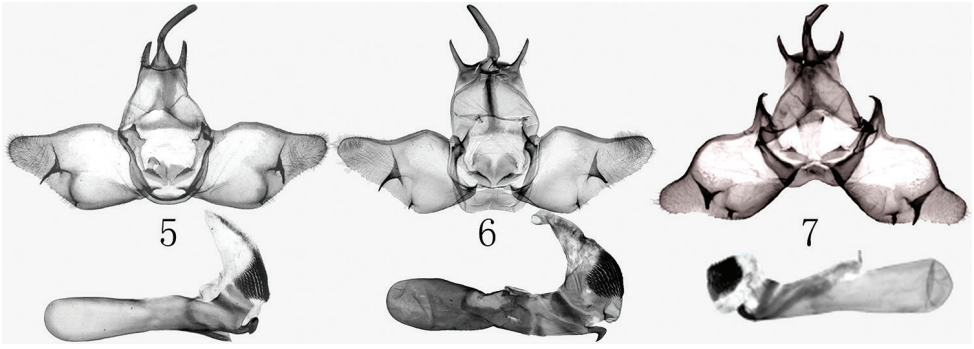

Figures 5–7. *Hiroshia* spp., male genitalia **5** *H. albinigra*, male (László et al. 2007) **6** *H. shennongjiaensis* sp. nov., male, holotype, gen. prep. No. hhl-4220-1 **7** *H. nanlingana*, male (after Zhuang et al. 2014).

Configuration of the male genitalia of *H. shennongjiaensis* (Fig. 6) is more similar to that of *H. albinigra* (Fig. 5) than to *H. nanlingana* (Fig. 7) as both species have a rudimentary subbasal costal process which is very large and acutely pointed in *H. nanlingana*. The new species can be distinguished from its congeners by its thinner and longer socii (those of *H. albinigra* and *H. nanlingana* are shorter and thicker); broader and rather quadrangular tegumen (it is dorsally tapering and more or less trapezoidal in the other two species); thinner and stronger sclerotised fultura superior

(it is broader and less strong in *H. albinigra* and *H. nanlingana*); larger dorsal sclerotised plates of the juxta and the acutely pointed and hook-like carinal tooth of the aedeagus (it is upturned and apically more or less rounded in the other two species). In addition, the basal process of the costa is smoothly arched in *H. shennongjiaensis* while it is shortly peaked in *H. albinigra*, and huge, thorn-like and apically hooked in *H. nanlingana*.

Description. Adult (Figs 1–2). Male. Wingspan 46.0–46.5 mm. Pubescence of head mixed grey and light brown; labial palpi covered by grey scales at 1st and 2nd segments, 3rd segment thin, finely scaled; antennae beige. Patagium beige; thorax covered by white and smoky black hair-scales. Abdomen dark grey, mixed with smoky black, greyish-brown and light brown scales. Ground color of forewing light graphite-grey, irrorated sparsely with smoky black and greyish-white scales; basal dash white or whitish-grey marked by blackish line; crosslines double and waved; basal line black, its inner line distinct and excurved, outer line thin and arched; antemedial line double, black, parallel and approaching, filled with white and pale grey scales; median fascia narrow, dark grey sinuous; postmedial line double, blackish-grey, incurved at cell and at veins CuA2-3A, its inner line close to outer line of median line; area between postmedial and preterminal lines pale ochreous-brown to greyish-brown; preterminal line black and discrete, arched; subterminal line finer, crenellate, weakly arched, incurved, distinct and rather broad at apex area, with light bluish-grey suffusion along its inner side; light patch of termen irregularly cuneiform, light bluish-grey; terminal line black, finely laced, incurved between veins; fringes greyish-brown and mixed darker brown; basal line area white; orbicular stigma small, round, whitish, with black frame; reniform stigma flat-cashew shaped. Hindwing basal area greyish-white, outer part of wing stronger greyish-brown to smoky grey suffused; transverse line broad and diffuse, slight incurved at CuA2-3A; discal spot obsolete; marginal area wide, dark smoky grey; fringes brown. Female unknown.

Male genitalia. (Fig. 6) Uncus finger-shaped and sclerotized, weakly smooth curved at basal part; socii separated from uncus, straight, slender cone shaped, ca 5/9 as long as uncus, apically finely pointed. Tegumen broad, quadrangular, membranous, with slender and thick ventral edge; vinculum rather shortly U-shaped, moderately sclerotized, sunken at bottom. Juxta formal hat-shaped, sclerotized, sunken at dorsal margin. Fultura superior narrow and prominently sclerotized, reversed T-shaped. Valva irregular quadrangular; costal margin slender and thick, with a bulge ca 1/5 times as long as valva, then smoothly incurved, the process of basal costa smoothly arched; sacculus broad, swollen, shorter than half of valva, process of sacculus apically tiled; cucullus blunt round, densely covered long hair; harpe asymmetrical, strongly sclerotized, flat and triangular shaped, left one slightly arched, long, extend out of ventral margin, right one shorter than left one; clasper strongly sclerotized, very short spike-shaped, and extending towards saccular margin. Aedeagus long and tubular, straight, coecum swollen, ca ½ times as long as aedeagus; carina strongly sclerotized, trapezoid ring-shaped, dorso-lateral process hook-shaped and apically acute, the subprocess plate arched; vesica broader, with short and broad basal dorsal diverticulum, a large cornuti

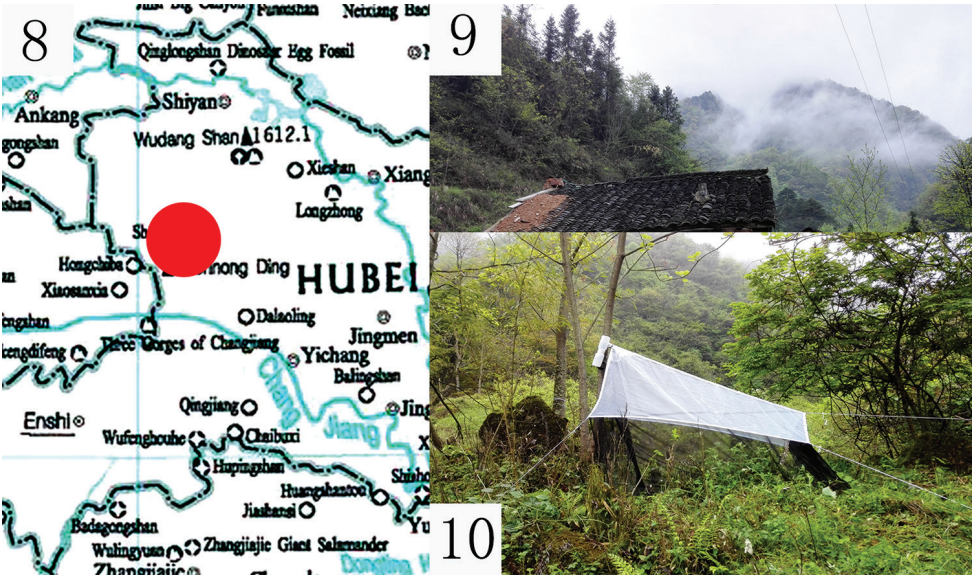

Figures 8–10. 8 Map showing collection site of *H. shennongjiaensis* sp. nov. **9–10** Both sides of the collection site composed of mainly broad-leaved forest, mixed conifers and shrubberies.

field consisting of separate, short, acute spinules, and a narrow band of minute spiculi extending towards ductus ejaculatorius.

Female genitalia. Unknown.

Distribution. China (Hubei: Badong) (Fig. 8).

Etymology. The species name "*shennongjiaensis*" refers to the type-locality in the Shennongjia National Nature Reserve in Hubei Province.

Bionomics. The new species inhabits broad-leaved forest, mixed with conifers and shrubberies, at ca 1300 m altitude in the southern part of the Shennongjia National Nature Reserve (Figs 9, 10). This area is located in the western part of Hubei Province and is close to the Dabashan National Nature Reserve. The three known specimens were collected in April.

Key to the species of the genus *Hiroshia* László, Ronkay & Ronkay, 2001 based on the male genitalia

1 Socii close to uncus; basal costal process with smaller or larger apical thorn; carinal process apically rounded **2**

– Socii separated from uncus; basal costal process small, apically rounded; carinal process acutely hooking ..... ***shennongjiaensis***

2 Basal costal process with short apical peak, vinculum evenly rounded ..... ***albinigra***

– Basal costal process with huge, apically curved thorn; vinculum medially deeply incised ..... ***nanlingana***

Acknowledgements

This study was supported by the National Natural Science Foundation of China (No. 31872261, 31572294), and the Fundamental Research Funds for the Central Universities (No. 2572019CP11). We also thank to the Institute of Zoology, Chinese Academy of Sciences for support with the materials examined.

References

Kononenko VS, Han HL (2007) Atlas Genitalia of Noctuidae in Korea (Lepidoptera). In: Park K-T (Ed.) Insects of Korea (Series 11). Junhaeng-Sa, Seoul, 464 pp.

László GM, Ronkay G, Ronkay L (2001) Taxonomic studies on the Eurasian Thyatiridae. Revision of the *Wernya* Yoshimoto, 1987 generic complex and the genus *Takapsestis* Matsumura, 1933 (Lepidoptera). Acta Zoologica Academiae Scientiarum Hungaricae 47(1): 27–85.

László GM, Ronkay G, Ronkay L, Witt ThJ (2007) The Thyatiridae of Eurasia including the Sundaland and New Guinea (Lepidoptera). Esperiana 13: 7–683.

Zhuang H, Owada M, Wang M (2014) First record of *Hiroshia* László, Ronkay & Ronkay from China, with description of a new species (Lepidoptera: Thyatiridae). Zootaxa 3794(2): 289–293. https://doi.org/10.11646/zootaxa.3794.2.7